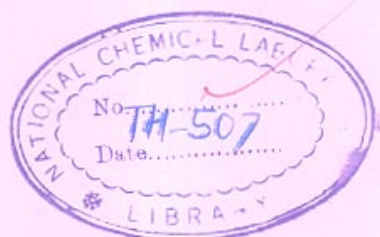


**STUDIES ON CATALYTIC HYDROGENATION
OF o-NITROPHENOL TO o-AMINOPHENOL
IN THREE PHASE SLURRY REACTOR**

COMPUTERISED

A THESIS
SUBMITTED TO THE
UNIVERSITY OF POONA
FOR THE DEGREE OF
DOCTOR OF PHILOSOPHY
(IN CHEMISTRY)



BY

MUKUND GANGADHAR SANE
M.Sc.

66.094.17:66.023(043)
SAN

NATIONAL CHEMICAL LABORATORY
PUNE 411 008 (INDIA)
NOVEMBER 1986

COMPUTERISED

DEDICATED
TO
Chi. ASHWINI
and
Chi. AMOL

COMPUTERISED

ACKNOWLEDGEMENT

I wish to place on record my deep felt gratitude to Dr. Vasant R. Choudhary, Scientist, Chemical Engineering Division, NCL for his inspiring guidance but for which the present investigation could not have been successfully completed.

I wish to express my sincere thanks to Mrs. Mayadevi and Dr. S.S. Tambe for the cooperation in computational work.

My special thanks go to Dr. N.R. Ayyangar for the encouragement and to Mr. H.G. Vadgaonkar and Dr. P.H. Brahme for useful discussions during the course of this study. I am also grateful to Dr. A.P. Singh, Dr. G.S. Pathak and Dr.(Mrs.) Mitra for their cooperation in the catalyst characterisation.

I take this opportunity to thank to all my colleagues and staff members of the Glass Blowing Section and Workshop for the cooperation and help.

I also wish to express my sincere thanks to the Director, NCL for permitting me to carry out research and allowing it to submit in the form of thesis.

PUNE
November 1986


[MUKUND G. SANE]

NOTE

The minor spacing errors that occur in some places in the thesis are due to spacing adjustments made by the electronic typewriter on which the thesis was typed.

CERTIFICATE AS PER FORM A

Certified that the work incorporated in the thesis :

*STUDIES ON CATALYTIC HYDROGENATION OF σ -NITROPHENOL TO
 σ -AMINOPHENOL IN THREE PHASE SLURRY REACTOR*

*submitted by Mr. Mukund G. Sane was carried out by the candidate under
my supervision. Such material as has been obtained from other sources
has been duly acknowledged in the thesis.*



Dr. Vasant R. Choudhary

SUPERVISOR

CONTENTS

Page No.

SUMMARY AND CONCLUSIONS

INTRODUCTION (Literature Survey,
Objective and Scope) 1

PART-I

SOLUBILITY OF HYDROGEN IN METHANOL CONTAINING REACTION COMPONENTS FOR HYDROGENATION OF o-NITROPHENOL

1.1	INTRODUCTION	15
1.2	EXPERIMENTAL	15
1.2.1	Materials	15
1.2.2	Solubility Apparatus and Experimental Procedure	16
1.2.3	Measurement of Density of Reaction Mixtures	19
1.3	RESULTS AND DISCUSSIONS	19
1.3.1	Effect of Pressure	19
1.3.2	Effect of Temperature	21
1.3.3	Influence of Reaction Species on the Solubility	21

PART-II

HYDROGENATION OF o-NITROPHENOL ON RANEY-Ni : EFFECT OF PREPARATION AND STORAGE CONDITIONS OF RANEY-Ni

2.1	INTRODUCTION	32
2.1.1	Effect of Preparation Conditions of Raney Nickel on Its Properties	32
2.1.2	Effect of Ageing of Raney Nickel on Its Properties	35
2.1.3	Present Investigation	36

		Page No.
2.2	EXPERIMENTAL	37
	2.2.1 Materials	37
	2.2.2 Preparation of Raney Nickel Catalyst	38
	2.2.3 Measurement of Properties of Raney Nickel	40
	2.2.4 Measurement of Catalytic Activity	48
2.3	EFFECT OF PREPARATION CONDITIONS OF RANEY NICKEL	52
	2.3.1 Effect of Type of Alkali	52
	2.3.2 Effect of Alkali Concentration	52
	2.3.3 Effect of Leaching Temperature	56
	2.3.4 Effect of Duration of Leaching	
	2.3.5 Effect of Washing Agent	61
	2.3.6 Optimum Conditions for Preparation of the Catalyst for the Hydrogenation of ONP to OAP	66
2.4	EFFECT OF STORAGE CONDITIONS OF RANEY-Ni	68
	2.4.1 Ageing of the Raney-Ni Catalyst Prepared Under Optimum Leaching and Washing Conditions	80
	2.4.2 Comparison of Optimum Preparation and Storage Conditions of Raney-Ni for Different Hydrogenation Processes	80
<u>PART-III</u>		
	HYDROGENATION OF o-NITROPHENOL ON Pd-CARBON	
3.1	EXPERIMENTAL	
	3.1.1 Materials	88
	3.1.2 Catalyst Preparation	89
	3.1.3 Catalyst Characterisation	90

		Page No.
3.1.4	Experimental Set up And Procedure for Carrying Out the Hydrogenation Reaction	92
3.1.5	Measurement of Adsorption of Reaction Species	96
3.1.6	Measurement of Gas-Liquid Mass Transfer Coefficient	100
3.2	EFFECT OF CONCENTRATION OF Pd IN Pd-CARBON AND SOLVENT ON THE HYDROGESATION OF o-SITROPHE SOL	104
3.2.1	Effect of Concentration of Pd in Pd-Carbon	104
3.2.2	Effect of Solvent on the Hydrogenation	107
3.3	INFLUENCE OF MASS TRANSFER ON THE HYDROGESATIOS OF o-SITROPHE SOL ON Pd-CARBON	113
3.3.1	Reaction Model	113
3.3.2	Suspension of Catalyst Particles	115
3.3.3	Gas-Liquid Mass Transfer	118
3.3.4	Liquid-Solid Mass Transfer	130
3.3.5	Intraparticle Mass Transfer	143
3.3.6	Effective Diffusivity of Catalyst (Measured During Catalysis)	145
3.4	ADSORPTIOS OF REACTION SPECIES ON Pd-CARBON FOR LIQUID PHASE HYDROGESATION OF O-SITROPHE SOL	159
3.4.1	Introduction	159
3.4.2	Single Component Adsorption	161
3.4.3	Two Component Adsorption	176
3.4.4	Influence of Solvent on the Adsorption	186

		Page No.
3.5	KINETICS OF HYDROGENATION OF o-NITROPHENOL ON Pd-CARBON IN THREE PHASE STIRRED REACTOR	191
	3.5.1 Kinetic Data	191
	3.5.2 Analysis of Initial Rate Data	193
	3.5.3 Heterogeneous Modelling of the Hydrogenation Reaction	205
3.6	POISONING OF Pd-CARBON IN SLURRY PHASE HYDROGENATION OF o-NITROPHENOL	231
	3.6.1 Introduction	231
	3.6.2 Experimental	232
	3.6.3 Results and Discussions	233

APPENDICES

SUMMARY AND CONCLUSIONS

o-Aminophenol (2-hydroxy aniline) is an important intermediate for the manufacture of dyes, drugs and pesticides. It is manufactured by catalytic liquid phase hydrogenation of *o*-nitrophenol. The most commonly used catalysts for the hydrogenation process are Raney nickel and supported palladium (mostly palladium on activated carbon).

Although, a number of studies have been reported for the hydrogenation of *o*-nitrophenol on Raney-nickel with various promoters, no detailed investigation on the effect of preparation conditions and ageing (or storage) conditions of Raney-nickel on the hydrogenation has been reported so far. It is, therefore, interesting to study the influence of preparation and ageing parameters on the hydrogenation activity of Raney-nickel in the hydrogenation of *o*-nitrophenol.

Supported palladium (particularly Pd on activated carbon) is commonly used in the low pressure hydrogenation of nitro groups in aromatic compounds. A few studies have been reported on the hydrogenation of *o*-nitrophenol on palladium catalyst. However, no detailed investigation covering the effect of reaction medium (or solvent), Pd loading on carbon and various mass transfer processes (viz. gas-liquid, liquid-solid, and intraparticle mass transfer) on the hydrogenation process has been reported. Also no studies involving detailed kinetic modelling of the hydrogenation reaction, adsorption of reaction species on Pd-carbon and catalyst poisoning have been reported so far.

The present investigation was undertaken with the following objectives:

- To study the effect of the leaching conditions (viz. type of alkali, alkali concentration, temperature and duration of leaching) and washing agent (viz. tap water, deionised distilled water, 50% ethanol, and 95% ethanol) in the preparation of Raney nickel on its surface properties and catalytic activity in the hydrogenation of o-nitrophenol.
- To study the effect of storage conditions of Raney nickel (viz. liquid medium, temperature, gas atmosphere and storage period) on the hydrogenation process.
- To study the effect of solvent (C_1 - C_3 alcohols) and concentration of Pd in Pd-activated carbon catalyst on the hydrogenation process.
- To study in details the effects of the gas-liquid, liquid-solid and intraparticle mass transfer processes on the hydrogenation on Pd-carbon.
- To collect extensive kinetic data on the hydrogenation on Pd-carbon in chemical controlled regime and develop a kinetic model which can form a basis for a rational design of the catalytic reactor for the hydrogenation process.
- To collect the data on the solubility of hydrogen in the reaction medium (used for the hydrogenation process) containing reaction species. The data is required for kinetic analysis.
- To study the adsorption of reaction species of the hydrogenation (viz. o-nitrophenol, o-aminophenol and water) on the Pd-carbon catalyst at reaction conditions.
- To study the poisoning of Pd-carbon by sulfur, chloro and heavy metal compounds in the hydrogenation of o-nitrophenol.

The H_2 -solubility measurements and the catalytic hydrogenation reaction were carried out in a high pressure stirred three phase reactor (Parr Autoclave).

The thesis has been divided into the following three parts.

PART I: SOLUBILITY OF HYDROGEN IN METHANOL CONTAINING REACTION SPECIES FOR HYDROGENATION OF o-NITROPHENOL

The solubility of hydrogen in pure methanol (which has been found to be the best reaction medium for the hydrogenation reaction) and the methanol containing the reaction species [viz. o-nitrophenol (ONP), o-aminophenol (OAP) and water], individual and their mixtures at the concentrations, H_2 -pressures (439-2143 kPa) and temperatures (293-328 K) involved in the hydrogenation has been determined. The solubility data for all the systems were found to follow the Henry's law. The dissolution of hydrogen was found to be an endothermic process.

The solubility (s) of H_2 in methanol at all pressures and temperatures was found to be decreased due to the presence of reaction species in the following order.

$s(\text{pure methanol}) > s[\text{o-nitrophenol}(0.36 \text{ mol.dm}^{-3}) \text{ in methanol}] > s[\text{o-aminophenol}(0.36 \text{ mol.dm}^{-3}) \text{ in methanol}]$.

However, the addition of water to the methanol-OAP and methanol-ONP-OAP systems causes an increase in the solubility. Nevertheless, an addition of either of the reaction species or their mixture reduces the solubility of H_2 in methanol.

PART II: HYDROGENATION OF o-NITROPHENOL ON RANEY-NICKEL

Effect of Preparation Conditions of Raney-Ni

Effect of the leaching conditions, such as type of alkali, alkali concentration, temperature and duration of leaching and the nature of the washing agent (tap water, distilled water, deionised distilled water, 50% ethanol,

95% ethanol) on the surface properties (such as surface area and crystal size) and catalytic activity (in the hydrogenation of o-nitrophenol at 308 K and H₂-pressure of 1508 kPa) of Raney-Ni has been studied and the optimum conditions for the preparation of Raney-Ni catalyst for the hydrogenation reaction have been obtained. The hydrogenation activity and surface properties of Raney-Ni are found to be strongly influenced by its preparation conditions.

The optimum preparation conditions for the Raney-Ni catalyst having the maximum activity for the hydrogenation are as follows: concentration of aqueous NaOH = 3.75 mol.dm⁻³, leaching temperature = 358 K, duration of leaching = 8 hr, washing agent = deionised distilled water.

Effect of Ageing of Raney-Ni

Effect of different storage conditions (viz. liquid medium, temperature, gas atmosphere and period) on the hydrogenation activity of Raney-Ni has been studied. It is found that the hydrogenation activity of Raney-Ni depends on the net effect produced by the above storage parameters. The effect of the various ageing conditions on the catalytic activity of Raney-Ni in the hydrogenation is as follows:

- (i) When the catalyst is stored in distilled deionised water under H₂ atmosphere either at room temperature or in the refrigerator, its hydrogenation activity increases and passes through a maximum with the increase in the storage period.
- (ii) When the catalyst is stored in 95% ethanol under H₂, its hydrogenation activity increases with the increase in the storage period.
- (iii) The catalyst stored under H₂ atmosphere and/or at room temperature have higher activity than that stored under air and/or in refrigerator.

- iv) The catalyst stored in deionised distilled water has higher activity than that stored in 95% ethanol and 5% aqueous NaOH.

The catalyst prepared at the optimum conditions gave the maximum catalytic activity when it was stored in deionised distilled water under H₂ atmosphere at room temperature for a period of 140 hr.

PART III : HYDROGENATION OF o-NITROPHENOL ON Pd-CARBON

Effect of Concentration of Pd in Pd-carbon and of Solvent on the Hydrogenation

The hydrogenation activity of Pd-carbon (measured at 308°K and H₂ pressure of 2163 kPa) was found to be increased with the increase in the concentration of Pd (which was varied from 0.2 to 4.62 wt %) on carbon. All the further studies (except the catalyst poisoning studies) were carried out using the Pd-carbon containing 4.62 wt % Pd.

The effect of reaction medium (viz. methanol, ethanol and n-propanol) on the hydrogenation of o-nitrophenol has also been studied at 308 K and H₂-pressure of 2163 kPa. The order of preference of the alcohols as a reaction medium has been found to be as follows:

Methanol > Ethanol > n-Propanol

Adsorption of Reaction Species on Pd-Carbon at Reaction Conditions

Adsorption isotherms for the single and multicomponent adsorption of the reaction species (viz. o-nitrophenol, o-aminophenol and water) from their methanol solution on the Pd-carbon have been measured at the temperature (278-308 K) at which the catalytic hydrogenation reaction is carried out. The single and binary adsorption data could be fitted to Langmuir type adsorption equations.

Influence of Mass Transfer on the Hydrogenation

In order to collect the hydrogenation rate data in a chemical control regime (which is essential for kinetic modelling of any catalytic process), the influence of gas-liquid, liquid-solid and intraparticle mass transfer processes on the hydrogenation reaction rate has been investigated in details. The occurrence of the reaction in the chemical control regime was confirmed by comparing the maximum rates of both the gas-liquid mass transfer (determined from the gas-liquid mass transfer coefficient obtained experimentally in the absence of the reaction by measuring the rate of absorption of H₂ in methanol at different stirring speeds in the reactor) and liquid-solid mass transfer (determined from the liquid-solid mass transfer coefficient estimated from the liquid-solid mass transfer correlation) with the observed maximum reaction rate, and also by studying the effect of stirring speed, catalyst loading and catalyst particle size on the reaction rate at the maximum temperature and concentration of o-nitrophenol. The hydrogenation process was found to be in the chemical control regime at the following reaction conditions: concentration of o-nitrophenol $\leq 0.36 \text{ mol.dm}^{-3}$, temperature $\leq 328 \text{ K}$, catalyst particle size $\leq 45 \mu\text{m}$, catalyst loading $\leq 1.0 \text{ g.dm}^{-3}$, stirring speed $\geq 850 \text{ rpm}$.

The effective diffusivity of the catalyst during catalysis was determined from the knowledge of the catalyst effectiveness factor measured experimentally.

Kinetic Modelling of the Hydrogenation Reaction

has been collected
 An extensive kinetic data on the hydrogenation of o-nitrophenol on Pd-carbon (4.62 wt.% Pd) in chemical control regime at different initial concentrations of o-nitrophenol (0.072-0.36 mol.dm⁻³), H₂-pressures (445-1463 kPa) and temperatures (293-328 K) using methanol as a reaction medium. The hydrogenation rate data at all the temperatures could be fitted well to the following Hougen-Watson (Langmuir type) rate model based on the mechanism involving single site molecular adsorption of all the reaction species and the overall hydrogen process controlled by the surface reaction,

$$r = \frac{k K_N K_H^3 C_N C_H^3}{(1 + K_N C_N + K_H C_H + K_A C_A + K_W C_W)^4}$$

where, r is the reaction rate; C_N, concentration of o-nitrophenol; C_H, concentration of hydrogen; K_N, o-nitrophenol adsorption constant; K_H, hydrogen adsorption constant; K_A, o-aminophenol adsorption constant; K_W, water adsorption constant; and k, surface reaction rate constant.

The activation energy for the hydrogenation reaction has been determined. Analysis of initial rate data was also done.

Poisoning of Pd-Carbon in the Hydrogenation of o-Nitrophenol

The poisoning effect of thiophene, dichloroethane, mercuric chloride and lead, zinc and mercuric acetates on the catalytic activity of carbon supported palladium in the hydrogenation of o-nitrophenol (at 308 K and H₂-pressure of 1508 kPa) has been investigated in three phase stirred slurry

reactor. Among the poisons, the mercuric acetate was found to be the most potent poison. The hydrogenation activity of the catalyst is correlated with the poison concentration by the following expressions.

For poisoning by thiophene, dichloroethane and Pb-acetate;

$$\left[\frac{r_o - r_p}{r_o \cdot r_p} \right] = \beta \left[\frac{\alpha C_p}{1 + \alpha C_p} \right]$$

For poisoning by Hg(II) acetate and chloride and Zn-acetate,

$$r_p = r_o (1 - \alpha' C_p^n)$$

where, r_o and r_p are the initial hydrogenation rates for the unpoisoned and poisoned catalysts, respectively; C_p , the concentration of poisons; and α , α' , β and n , the poisoning parameters.

INTRODUCTION

INTRODUCTION

1. COMMERCIAL APPLICATION OF o-AMINOPHENOL

Aminophenols and their derivatives are widely used in the photographic, pharmaceutical and dye industries (1). They are the intermediates leading to more complex molecules particularly for the dyestuff industry. They are amphoteric in nature possessing properties both as weak acids and bases. Certain substituted aminophenols possess desirable physiological properties and have been employed as analgetics and antipyretics.

o-Aminophenol (2-hydroxy aniline) is an important intermediate for the manufacture of dyes, drugs and pesticides. It produces dark to medium brown colour by oxidation, due to this it is used as a component of brown hair dye formulations. It occurs as a white rhombic needles or plates (melting point: 170-174°C). Nitration of *o*-aminophenol (OAP) produces 2-amino-5-nitrophenol, which is a useful dye intermediate. It is used in the manufacture of 8-hydroxyquinoline which is extensively used in analytical chemistry. ONP forms salts such as the hydrochloride, sulphate and acetate. It is a photographic developer and as an intermediate in the production of oxidation dyes especially for dyeing hair, fur and feathers.

2. COMMERCIAL PRODUCTION OF ORTHO-AMINOPHENOL

o-Aminophenol is generally produced by the following three methods:

1. Catalytic hydrogenation of orthonitrophenol (mostly in liquid phase).
2. Electrochemical reduction of ONP
3. Amination of aromatic halide compounds

o-Aminophenol is produced most readily by 'Bechamp method' of reducing *o*-nitrophenol (ONP) by means of iron and acid (2). Many other

reducing systems have also been reported such as, sodium sulphide (3), aluminium amalgam in alcohol (4), zinc dust in water (5), etc.

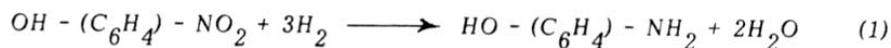
It is also manufactured by the catalytic hydrogenation of an acetic acid solution of *o*-nitrophenol (ONP) over Pd-C (6) or an alcoholic solution of ONP in the presence of Raney nickel (7). Many patents based on catalytic hydrogenation (8,9), amination (10,11) and electrochemical reduction (12,13) have been claimed for the manufacture of *o*-aminophenol.

3. CATALYTIC HYDROGENATION OF *o*-NITROPHENOL - A LITERATURE SURVEY

A summary of the literature on the catalytic slurry phase hydrogenation of *o*-nitrophenol is presented in Table-1. It can be noted from the literature (Table-1), that the most commonly used catalysts for the hydrogenation of *o*-nitrophenol are Raney nickel (without or with promoters) and palladium. The hydrogenation activity of Raney nickel is found to be increased substantially by an addition of promoters such as transitional metals [viz. MO (16-18), V (18,23,24), Nb (18,26), etc.] and platinum group metals [viz. Pd (21,27,34), Ru (20-22)]. A particular type of solvent used as a reaction medium has a strong influence on the rate of hydrogenation (22,31,43,44).

4. THERMODYNAMICS OF HYDROGENATION OF *o*-NITROPHENOL

The hydrogenation of *o*-nitrophenol (ONP) to *o*-aminophenol (OAP) can be written as



4.1 Heat of Reaction

The heat of reaction (ΔH_r) can be evaluated from the heat of

TABLE-I

SUMMARY OF LITERATURE ON CATALYTIC SLURRY PHASE HYDROGENATION OF *o*-NITROPHENOL

Catalyst (promoter)	Solvent	Temperature (K)	H ₂ -pressure (atm)	Remarks	Reference
1	2	3	4	5	6
Raney nickel	aq. KOH	-	-	The catalyst activity increased with the concentration of Ni-Al alloy	14
Raney nickel	aq. NaOH solution	333-343	1.8	Process for aminophenols described	9
Pt-Raney-nickel	aq. KOH solution	323-362	2-2.5	Catalytic activity increased by addition of Pt	15
Raney nickel (with MO)	aq. KOH solution	293-333	-	Catalytic activity increased by addition of MO	16
Raney nickel (with MO)	aq. KOH solution	353-363	-	MO acts as a promoter	17
Raney nickel (with MO V, Nb)	EtOH	-	-	Addition of optimum amount of Mo, V and Nb increased the activity of the catalyst	18
Raney nickel (with Cr)	-	-	-	Addition of Cr decreased activity of the catalyst	19
Raney nickel (with Ru)	alkali solution	-	-	Addition of Ru enhanced the activity of the catalyst	20
Raney nickel (with Pd and Ru)	C ₂ -C ₄ alcohols and water	-	-	Ethanol found to be the best solvent	21

.....

Table-1 contd.

1	2	3	4	5	6
Raney nickel (with Ru)	Water, aq. KOH, ethanol (96%)	293	-	Addition of Ru increased the catalytic activity. Ethanol found to be better solvent than water and aq. KOH	22
Raney nickel (with V)	Ethanol (96%) and aq. alkali solution	-	-	Catalyst activity effected by the type of leaching agent in the preparation of the catalyst	23
Raney nickel (with V)	-	293-365	-	Catalytic activity depends on the concentration of V_2O_3 in the catalyst	24
Raney nickel (with Zr)	-	293-333	-	The promoting action of Zr studied	25
Raney nickel (with Nb Zr and Ta)	-	-	-	The catalytic activity increases with the concentration of Nb and Ta and passes through maximum with concentration of Zr	26
Nickel-Pd	Ethanol, water, aq. NaOH	293-333	-	The catalytic activity depends strongly on the concentration of Pd	27
Pd	aq. acid and alkali solution	-	-	Effect of applied potential on the reduction of nitrophenol isomers investigated	28
Pd black	alcohol solution (50%)	-	-	Effect of substituents on reduction of nitro group studied	29
Admas Pd	-	-	-	-do-	30

.....

Table-1 contd.

1	2	3	4	5	6
Pd-polyethylene terphthalate	Weak acid, methanol, ethanol, etc.	293-333	-	The hydrogenation rate depends on the reaction medium	31
Pd-polymer catalysts	Ethanol (85%)	-	-	Mechanism of Pd activation by the polymers discussed	32
Pd-carbon	aq. NaOH solution	363	2-5	Preparation of aminophenols described	8
Pt and Pd	Mineral acid or acetic acid and water	-	-	Process for hydrogenation of nitro-phenols described	6
Ruthenium Palladium	Ethanol, water and aq. KOH	293-313	-	Kinetics of hydrogenation studied by potentiometry	33
Pd-Ni Catalyst electrode	-	293-313	-	Addition of Ni enhances the reduction rate of ONP	34
Ni	Methanol, benzene	488	15.47	-	35
Ni	Anhyd. alcohol	373	90	-	36
Ni	Absolute alcohol	373	92-96	-	37
Skeleton Ni	Alkali and ethanol (96%)	293-333	-	Reaction and hydrogen concentration on catalyst studied by potentiometry	38
Nickel with (MgO)	-	-	-	Addition of MgO causes increase in activity of Ni	39
Nickel (with Co)	Water, ethanol, isopropanol	293	-	Effect of cobalt addition on the catalytic activity studied and potential of the catalyst measured	40

.....

Table-I contd.

1	2	3	4	5	6
NiO clay (with ZnO)	aq. or alcoholic solution	-	-	-	41
Ru Pt	-	-	-	Addition of mixed Ru-Pt catalyst found to be higher than that of individual Ru and Pt	42
Ru Pd - Al ₂ O ₃	Ethanol and aq. KOH solution	293	-	Ethanol found to be better solvent than aq. KOH	43
Ru Pt - TiO ₂	Water, ethanol, aq. KOH	293-333	-	The hydrogenation rate depends on the solvent used	44
Os Pt - ThO ₂	-	-	-	Addition of Os increases the activity of Pt	45

formation (ΔH_r) of the reaction species as follows:

$$(\Delta H_r) = \sum \Delta H_{f(\text{products})} - \sum \Delta H_{f(\text{reactants})} \quad (2)$$

The standard heats of formation of water, hydrogen and ONP are available in the literature. The values of $\Delta H_{f(298K)}$ for hydrogen, water and ONP are - 68.315 (46), 0.0 (46), and - 46.4 (47) kcal.mol⁻¹, respectively.

Since the value of (ΔH_r) for OAP is not available in the literature, it is estimated by the group contribution method reported by Franklin (48, 49). The heat of formation of OAP at 298K has been estimated to be - 19.76 kcal.mol⁻¹. The calculation of the heat of formation is given in Appendix-1. The heat of the hydrogenation of *o*-nitrophenol to *o*-aminophenol is estimated to be,

$$\begin{aligned} \Delta H_r (298K) &= \Delta H_{f(\text{OAP})} + 2 \Delta H_{f(\text{water})} - \Delta H_{f(\text{ONP})} - 3 \Delta H_f (H_2) \\ &= - 19.76 + 2 (- 68.315) - (- 46.4) - 3(0) \\ &= - 109.99 \text{ kcal.mol}^{-1} \\ &= - 459.75 \text{ kJ.mol}^{-1} \end{aligned}$$

The negative sign and the value of the heat of reaction indicate that the hydrogenation reaction is highly exothermic.

4.2 Equilibrium Constant

The equilibrium constant (K) for the hydrogenation reaction can be obtained from the relation

$$- \Delta G = RT \ln K \quad (3)$$

where, ΔG , is the free energy change in the reaction; R , the gas constant and T , the temperature. ΔG can be estimated from the knowledge of the free energies of formation of products and reactants as follows.

$$\Delta G = \sum \Delta F_{(\text{products})} - \sum \Delta F_{\text{reactants}}$$

The value of K at 298K has been estimated to be of the order of 1.41×10^{73} . This fact indicates that the hydrogenation reaction is irreversible.

For the estimation of the value of ΔG , the data on the free energy of formation (at 298K) of water ($\Delta G_f = -68.315 \text{ kcal.mol}^{-1}$) (46) and hydrogen ($\Delta G_f = 0$) (46) were available in the literature. Whereas the values of the free energy of formation of OAP ($\Delta G_f = 8.873 \text{ kcal.mol}^{-1}$) and ONP ($\Delta G_f = +0.003 \text{ kcal.mol}^{-1}$) have been estimated by the group contribution method suggested by van Krevelen (50,51). The estimation of the values of ΔG_f for ONP and OAP is given in Appendix-2.

5. OBJECTIVE AND SCOPE OF PRESENT INVESTIGATION

The present work was undertaken as a part of our laboratory programme for the development of commercial catalyst and catalytic process for the hydrogenation of *o*-nitrophenol to *o*-aminophenol in an agitated three phase reactor.

From the literature survey on the catalytic hydrogenation of *o*-nitrophenol (Table-1) the following things are clear. The most commonly used catalysts for the hydrogenation process are Raney nickel and supported palladium (mostly palladium on activated carbon).

Although, a number of studies have been reported on the hydrogenation of *o*-nitrophenol on Raney nickel with various promoters, no detailed

investigation on the effect of preparation conditions and ageing (or storage) conditions of Raney nickel on the hydrogenation has been reported so far. Recently, Choudhary and co-workers (52,53) have observed a very strong influence of the preparation conditions of Raney nickel, such as leaching conditions (viz. type of alkali, alkali concentration, temperature, and duration of leaching) of Ni-Al alloy and the nature of washing agent (viz. tap water, deionised distilled water, 50% ethanol, 95% ethanol, etc.) employed in the preparation of Raney nickel, on its crystal size, hydrogen content, and catalytic activity in the slurry phase hydrogenation of *p*-nitrotoluene to *p*-toluidine. The ageing conditions of Raney nickel (viz. liquid medium, temperature, gas atmosphere and storage period) have also a strong influence on its hydrogen content and catalytic activity in the hydrogenation (53). It is, therefore, interesting to study the influence of the above preparation and ageing parameters on the hydrogenation activity of Raney nickel also in the hydrogenation of *o*-nitrophenol.

Supported palladium (particularly Pd on activated carbon) is commonly used in the low pressure hydrogenation of nitro groups in aromatic compounds (54). A few studies (Table-1) have been reported on the hydrogenation of *o*-nitrophenol on palladium catalyst. However, no detailed investigation on the effects of reaction medium (or solvent), Pd loading on carbon and various mass transfer processes (viz. gas-liquid, liquid-solid, and intraparticle mass transfer) on the hydrogenation of *o*-nitrophenol has been reported. Also, no kinetic modelling showing the controlling mechanism of the hydrogenation process has been done so far. Poisoning of Pd-carbon in the hydrogenation process has also not been investigated yet.

The present investigation was therefore undertaken with the following objectives.

1. To study the effect of the leaching conditions (viz. type of alkali, alkali concentration, temperature and duration of leaching) and washing agent (viz. tap water, deionised distilled water, 50% ethanol, and 95% ethanol) in the preparation of Raney nickel on its surface properties and catalytic activity in the hydrogenation of *o*-nitrophenol.
2. To study the effect of storage (or ageing) conditions of Raney nickel (viz. liquid medium, temperature, gas atmosphere and storage period) on its hydrogenation activity in the hydrogenation reaction.
3. To study the effect of solvent (C_1 - C_3 alcohols) and concentration of Pd in Pd-activated carbon catalyst on the hydrogenation.
4. To study in details the gas-liquid, liquid-solid, and intraparticle mass transfer effects on the hydrogenation on Pd-carbon.
5. To collect extensive kinetic data on the hydrogenation on Pd-carbon in chemical controlled regime and develop a kinetic model for the hydrogenation process.
6. To collect the data on the solubility of hydrogen in the reaction medium (used for the hydrogenation process) containing reaction species. The data is required for kinetic modelling.
7. To study the adsorption of reaction species of the hydrogenation (viz. *o*-nitrophenol, *o*-aminophenol and water) on Pd-carbon at reaction conditions.
8. To study the poisoning of Pd-carbon by sulfur, chloro and heavy metal compounds in the hydrogenation of *o*-nitrophenol.

REFERENCES

1. Kirk-Othmer 'Encyclopedia of Chemical Technology' 3rd Edn. (1978), (John Wiley and Sons Inc).
2. Bechamp, A.J., *Ann-Chim et Phys.* 42 (1854), 186.
3. Hofmann, A., *Justus Liebigs Ann. Chem.* 103 (1857) 351.
4. Wislicenus, H. and Kaufman, L., *Chem. Ber.* 28 (1895) 1326.
5. Bamberger, E., *Chem. Ber.*, 28 (1895) 251.
6. Frieifelden, N. and Robinson, R., *U.S. Patent*, 3,079,435 (1963).
7. Finked'shetion, A.V. and Kuz'mina, Z.M., *Dokl-Acad, Nauk SSSR*, 158(1) (1964) 176.
8. Joseph, L., *Fr. Patent*, 1354430 (1964).
9. Erich, T., *Ger. Patent*, 1244196 (1967).
10. Felix, K. and Robert J., *Australian Patent*, 205,525 (1957).
11. Komiyama, T. and Terada, K., *Jpn. Patent*, 79,36220 (1979).
12. Kirkhgol, G.A. and Spektor, M.O., *Russ. Patent*, 39,117 (1934).
13. Udupa, H.V. and Ananiharaman, P.N., *Indian Patent*, 143869 (1978).
14. Fasman, A.B. and Pushkarava, G.A., *Isv. Yushh. Ucheb. Zaved., Khim. Tekhnol*, 11(8) (1968) 886.
15. Fasman, A.B., Isabekov, A., Skoi'skii, D.V., Prasnyakov, A.A. and Chernosova, K.T., *Zh. Fiz. Khim.* 40(9) (1966) 2086 (Russ).
16. Kabier, T., Fasman, A.B., Molyukova, N.I. and Sokol'skii, D.V., *Dokl. Akad. Nauk. SSSR*, 159(5) (1964) 1087 (Russ).
17. Fasman, A.B., Kabier, T., Sokol'skii, D.V. and Molyukava, M.I., *Zh. Fiz. Khim.* 40(1) (1966) 114 (Russ).

18. Omarov, A.K., Bizhanov, F.B., Sokol'skii, D.M., Popov, N.I., Omitrieva, Yu. P. and Khisumeltdinov, A.M., *Met. Obogashch* 4, (1969) 205 (Russ).
19. Fasman, A.B., Molyuhova, N.I., Kabier, T., Sokol'skii, D.V. and Chernosova, K.T., *Zh. Fiz. Khim.* 48(8) (1966) 1758 (Russ).
20. Fasman, A.B., Isabekov, A. and Almasher, B.K., *Zh. Fiz. Khim.* 42(4) (1968) 903 (Russ).
21. Bizhanov, F.B., Sokol'skii, D.V., Popov, D.V., Malkine, N.I. and Khisamefemov, A.M., *Katal. Vosatanov Gidrirov. Zhidk Fage* (1970), 80.
22. Sokol'skii, D.V., Sarmuzina, A.G., Dzhardamalieva, K.K., Khisame-t-dinov, A.M. and Bizhanov, F.B., *Izv. Akad. Nauk Kaz. SSR Ser. Khim.* 17(4) (1967) 49 (Russ).
23. Bizhanov, F.B., Sokol'skii, D.V., Popov, N.I. and Dmitrieva, Yu.P. (U.S.S.R.) *Khim. Khim. Tekhnol (Alma-Ata)* (1971) 50 (Russ).
24. Molyukora, N.I., Petrov, B.F., Fasman, A.B. and Sokol'skii, D.V., *Zh. Fiz. Khim.* 41(6) (1967) 1411 (Russ).
25. Kabiy, T., Fasman, A.B., Sokol'skii, D.V. and Atmashev, B., *Dokl. Akad. Nauk SSSR* 166(4) (1966) 877 (Russ).
26. Fasman, A.B., Kabier, T. and Yagudeev, T.A., *Zh. Fiz. Khim.* 41(11) (1967) 2809, (Russ).
27. Bizhanov, F.B., Sokol'skii, D.V., Popov, N.I. and Malkina, N. Vu., *Izv. Akal. Nauk Kaz. SSR Ser. Khim.* 17(6) (1967) 27 (Russ).
28. Andreeva, A.A. and Zakarina, N.A., *Tr. Inst. Org. Katal. Elektro-khim. Akad. Nauk. Kaz. SSR*, 5 (1973) 75 (Russ).
29. Shmonina, V.P. and Abdrakhmanova, R.M., *Katal Vosstunov. Gidrirov. Zhidk Faze* (1970) 51 (Russ).
30. Taya, K. and Takagi, Y., *Tokyo Gokagei Daigaku Kiyo, Dai-4-Bu*, 24 (1972) 142 (Japan).
31. Sokol'skii, D.V., Lankin, S.F. and Tyurankau, O.A., *Zh. Fiz. Khim.* 40(3) (1966) 732 (Russ).
32. Tyurenkova, O.A., *Zh. Fiz. Khim.* 43(8) (1969) 2088 (Russ).

33. Sokol'skii, D.V., Surmurzina, A.G. and Dzhardamaliera, K.K., *Tr. Inst. Khim. Nauk. Akad. Nauk Kaz. SSR*, 17 (1967) 100 (Russ).
34. Sokol'skii, D.V., Omarova, S.R. and Seitzhknov, A., *Izv. Akad. Nauk. Kaz. SSR, Ser. Khim.* 23(5) (1973) 16 (Russ).
35. Brown, O.B., Eizel, G. and Henke, C.O., *J. Phys. Chem.*, 32 (1928), 631.
36. Sinzaburo, H., *J. Chem. Soc. (Japan)* 60 (1939) 729.
37. Shinzaburo, F., *Mem. Coll. Kyoto Imp. Univ.* 23A (1942) 431.
38. Sokol'skii, D.V. and Bezverkhova, S.T., *Doklady Akad. Nauk SSSR* 94 (1954) 493.
39. Kashimova, G.I., Bizhanov, F.B., Sokol'skii, D.V., Popov, N.I. and Khisametdinov, Z.M., *Izv. Akad. Nauk Kaz. SSR, Ser. Khim.* 20(2), (1970) 20 (Russ).
40. Kashimova, G.I., Bizhanov, F.B., Popov, N.I., *Khim. Khim. Tekhnol.* 7-8 (1968) 138 (Russ).
41. Sokol'skii, D.V. and Kashimova, G.I., *Khim. Khim. Tekhnol.* 21(1), (1978) 82 (Russ).
42. Sokol'skii, D.V., Dzhardamalieva, K.K., Surmurzina, A.G. and Tommanov, T., *Dokl. Akad. Nauk SSSR*, 176(ls) (1967) 1093 (Russ).
43. Sokol'skii, D.V., Kazora, T.V. and Dzhardamlieva, K.K., *Izv. Akad. Nauk Kaz. SSR, Ser. Khim.* 20(6) (1970) 72 (Russ).
44. Kyzora, T.V., Sokol'skii, D.V. and Dzhardamlieva, K.K., *Izv. Akad. Nauk Kaz. SSR, Ser. Khim.* 21(6) (1971) 14 (Russ).
45. Sokol'skii, D.V., Dilmagamhetov, S.N. and Dzhardamalieva, K.K., *Izv. Vych. Uchebn. Zaved. Khim. Khim. Tekhnol.* 19(6) (1976), 869.
46. Dean, J.A., *Lange's Handbook of Chemistry*, 13th Edition (1985), McGraw Hill Book Co.
47. Shull, D., *'The Chemical Thermodynamics of Organic Compounds'*, (1969) John Wiley and Sons, Inc.

48. Franklin, J.L., *Ind. Eng. Chemistry*, 41 (1949) 1070.
49. Franklin, J.L., *J. Chem. Phys.*, 21 (1953) 2029.
50. van Krevelen, D.W. and Chermin, H.A.G., *Chem. Eng. Sci.* 1 (1951), 66.
51. van Krevelen, D.W. and Chermin, H.A.G., *Chem. Eng. Sci.*, 1, (1952) 238.
52. Choudhary, V.R., Chaudhari, S.K. and Sane, M.G., in *Advances in Catalysis Science and Technology*, Ed. T.S.R. Prasad Rao, Wiley Eastern Ltd., New Delhi (1985) 171.
53. Choudhary, V.R. and Chaudhari, S.K., *J. Chem. Tech. Biotechnol.*, 32 (1982) 925.
54. Thomas, C.L., *Catalytic Processes and Proven Catalysts*, Academic Press, New York (1970).

PART-I

SOLUBILITY OF HYDROGEN IN METHANOL CONTAINING
REACTION COMPONENTS FOR HYDROGENATION OF σ -NITROPHENOL

1.1 INTRODUCTION

Precise data on the solubility of a gas, which is one of the reactant, is required in interpreting the kinetics of gas-liquid and gas-liquid-solid (catalytic or non-catalytic) reactions. However, it is necessary to know not only the solubility of a gas in the solvent used as a reaction medium, but also the solubility of the gas in the presence of reaction species in the medium. It is not easy to estimate the solubility of a gas in the reaction mixture directly from the solubility data for the gas-solvent system and hence it must be measured experimentally.

The solubility of hydrogen in methanol at different pressures and temperatures has already been studied in detail (1-6). Recent studies (7,8,9) have shown that the solubility of hydrogen in methanol is strongly affected by the presence of *o*-nitroanisol (7), nitrobenzene (8) and *p*-nitrotoluene (9). The solubility of hydrogen in methanol containing reaction species for the hydrogenation of *o*-nitrophenol has, however not been reported so far.

The present study was undertaken to determine the solubility of hydrogen in methanol in the presence of *o*-nitrophenol, *o*-aminophenol and water at the different H_2 pressures (439-2145 kPa) and temperatures (293-328K). The data were essential for obtaining hydrogen concentrations required for the kinetic modelling of the hydrogenation process.

1.2 EXPERIMENTAL

1.2.1 Materials

The following high purity materials are used.

Methanol (AR BDH) : Freshly distilled and degassed before use.

o-Nitrophenol (AR German repacked) : Recrystallised before use

o-Aminophenol (LR BDH) : Recrystallised before use

Hydrogen (IOLARI) : Obtained from M/s. Indian Oxygen Ltd., Bombay

1.2.2 Solubility Apparatus and Experimental Procedure

The gas solubility apparatus, which is similar to that described earlier by Choudhary et al. (10), is shown in the Fig. 1.1. It consists essentially of two parts: one, the sample burette in which the desorption of the dissolved gas occurs at atmospheric pressure and the volume of liquid sample is measured quantitatively; and the second, the gas collecting and measuring unit. The liquid sample collecting burette and the gas collector are provided with water jackets for keeping the temperature constant during the measurement. Flexible teflon tubes were used to connect the movable parts with the main body of the apparatus. All stopcocks were grease free.

Degassed methanol (1000 cm^3) with or without containing reaction species was charged to a Parr autoclave (made of 316 stainless steel, capacity: 2000 cm^3 , inside dia: 10 cm, inside depth 26.7 cm, provided with thermowell cooling coil and stirrer). The autoclave is shown later in Fig. 2.4 (Part - II). The empty space and the methanol in the autoclave were flushed with the high purity hydrogen. The methanol was then equilibrated with hydrogen at a known pressure and temperature for 1 hr. The reaction medium was stirred at a stirring speed of 760 rpm using a three blade stirrer (dia: 5.5. cm, situated at a distance of 2.8 cm from the bottom of the autoclave) while maintaining the pressure of hydrogen constant.

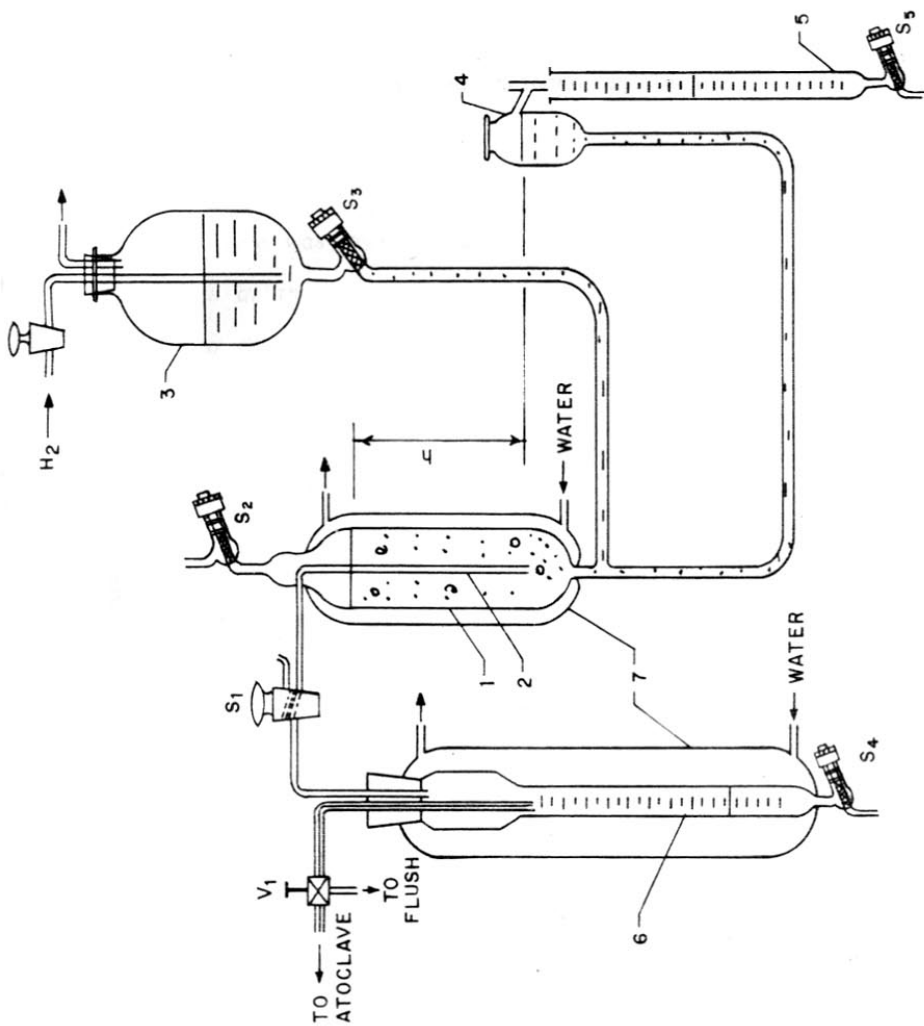


FIG.1.1: SOLUBILITY APPARATUS

(1) GAS COLLECTOR; (2) GAS INLET TUBE; (3) METHANOL RESERVOIR; (4) PRESSURE ADJUSTING DEVICE; (5) GRADUATED BURETTE; (6) SAMPLE BURETTE; (7) WATER JACKET; (S₁) THREE WAY STOP-COCK (S₂, S₃, S₄ and S₅) ROTAFLOW STOP-COCK.

66.094.17:66.023(043) TH-507
SAN

The saturation was carried out for a period of 1 hr.

The gas solubility apparatus was connected to the autoclave and the sample collecting burette was flushed with hydrogen and stopcocks S_1 and S_2 were closed. The methanol in the gas collector and the reservoir was then saturated with hydrogen. The gas collector was completely filled with the H_2 -saturated methanol by raising the pressure adjusting device above the methanol level in the methanol reservoir, and opening stopcocks S_2 and S_3 . Stopcocks S_2 and S_3 were then closed. The pressure adjusting device was lowered and methanol level in it was brought to the same level as at the tip of the gas inlet tube. The sample burette was connected to the gas collector by turning stopcock S_1 . The methanol level in the gas inlet tube was adjusted very close to that at the tip of the tube by lowering or raising the pressure adjusting device. Thus the system was made ready for the solubility measurement.

Before the solubility was measured, stirring was stopped and the liquid inlet tube of the autoclave was flushed with about 10-12 ml of the solution using three way valve V1. After flushing, valve V1 was opened carefully and the liquid sample about 15-20 (cm^3) was introduced into the sample burette at a slow rate. The desorbed hydrogen [(ranging from 10-20 cm^3 (STP))] determined by measuring quantitatively the volume of methanol displaced from the gas collector into the graduated burette. Sufficient time was allowed for the complete desorption of hydrogen at 300K and at atmospheric pressure. The solubility experiments were carried out at least three times to ensure reproducibility of the data.

Calculation

The volume of the gas desorbed was calculated by the relation:

$$x = \left(\frac{V - v}{v} \right) \left(\frac{273}{T_w} \right) \left[\frac{P_A - P_{(\text{MeOH})} - (h \rho_{\text{MeOH}} / 13.6)}{760} \right] \quad (1.1)$$

where

- x = amount of gas desorbed (at NTP) per cm^3 of liquid sample
- V = volume of methanol displaced
- v = volume of the liquid sample
- P_A = atmospheric pressure
- $P_{(\text{MeOH})}$ = vapor pressure of methanol at T_w temperature
- T_w = temperature of the gas collector
- h = height of the methanol column (as shown in Fig. 1.1)
- ρ_{MeOH} = density of methanol

1.2.3 Measurement of Density of Reaction Mixtures

Density of methanol containing the reaction species at different concentrations (i.e. system I-VI) at 293-328K was measured by the usual procedure.

1.3 RESULTS AND DISCUSSION

The experimental data on solubility of hydrogen in pure methanol and in the methanol containing *o*-nitrophenol (ONP), *o*-aminophenol (OAP) and water at different pressures and temperatures are presented in Table 1.1. The solubility value was taken as an average of the three replicated data.

1.3.1 Effect of Pressure

The solubility data (Table-1.1) were found to follow the Henry's law:

$$S = \alpha P \quad (1.2)$$

TABLE-1.1

DATA ON SOLUBILITY OF HYDROGEN IN METHANOL CONTAINING THE REACTION SPECIES AT DIFFERENT CONCENTRATIONS

Temperature (K)	Pressure (kPa)	Solubility, S ($\mu\text{mol.cm}^{-3}$, kPa^{-1}) System					
		I	II	III	IV	V	VI
293	2145	78.32	75.88	76.53			72.21
	1457	52.85	50.12	50.30			49.20
	907	32.66	31.37	31.61			28.12
	494	14.48	17.18	17.22			13.75
308	2130	79.51	76.87	79.20	78.83	75.55	74.47
	1442	57.95	54.63	55.85	54.99	54.52	53.17
	892	33.92	32.58	33.09	32.93	32.38	30.75
	480	18.54	18.00	18.28	18.23	15.56	15.35
318	2113	100.62	88.65	88.81			78.02
	1425	66.05	57.69	57.90			55.63
	875	40.80	35.09	35.75			32.32
	463	24.60	18.64	19.39			18.52
328	2089	109.08	90.18	92.81			84.42
	1401	70.64	59.35	60.16			59.15
	852	45.15	37.63	38.75			34.14
	439	27.61	20.45	21.03			20.31

I - Pure methanol,

II - Methanol containing o-nitrophenol ($0.36 \text{ mmol.cm}^{-3}$),

III - Methanol containing o-nitrophenol ($0.18 \text{ mmol.cm}^{-3}$) + o-aminophenol ($0.18 \text{ mmol.cm}^{-3}$) + water ($0.36 \text{ mmol.cm}^{-3}$)

IV - Methanol containing o-aminophenol ($0.36 \text{ mmol.cm}^{-3}$) + water ($0.72 \text{ mmol.cm}^{-3}$),

V - Methanol containing o-nitrophenol ($0.18 \text{ mmol.cm}^{-3}$) + o-aminophenol ($0.18 \text{ mmol.cm}^{-3}$) and

VI - Methanol containing o-aminophenol ($0.36 \text{ mmol.cm}^{-3}$).

where S is the solubility of gas; α , the Henry's constant; and p , the gas pressure. The H_2 -solubility (S) vs. pressure plots are shown in Figs. 1.2-1.4. The values of the Henry's constant, which represents the solubility of H_2 at the pressure of 1 kPa, for the different systems are given in Table 1.2.

The data on the density and vapor pressures of the mixed solvents are presented in Tables 1.3 and 1.4, respectively. The former data are measured experimentally. The latter data were obtained from the knowledge of vapor pressures of pure components by applying the Raoult's law.

1.3.2 Effect of Temperature

The results in Tables 1.1 and 1.2 show that, for all the systems, the solubility increases with the increase in the temperature. Figure 1.5 shows the temperature dependence of the Henry's constant for the different systems, according to the expression:

$$= A \exp(-\Delta H / RT) \quad (1.3)$$

where $-\Delta H$ is the heat of dissolution of gas; R , the gas constant; T , the temperature; and A , a constant. The values of $-\Delta H$ (obtained from the slopes of the linear plots of $\log \alpha$ vs $1/T$, according to Eqn. 1.3) and A for the different systems are included in Table 1.2. The negative values of the heat of dissolution indicate that the dissolution of H_2 is endothermic for all the systems. This is consistent with the earlier observations (8,9).

1.3.3 Influence of Reaction Species on the Solubility

It is clear from the results (Tables 1.1 and 1.2) that the solubility of H_2 in methanol at all pressures and temperatures is decreased due to

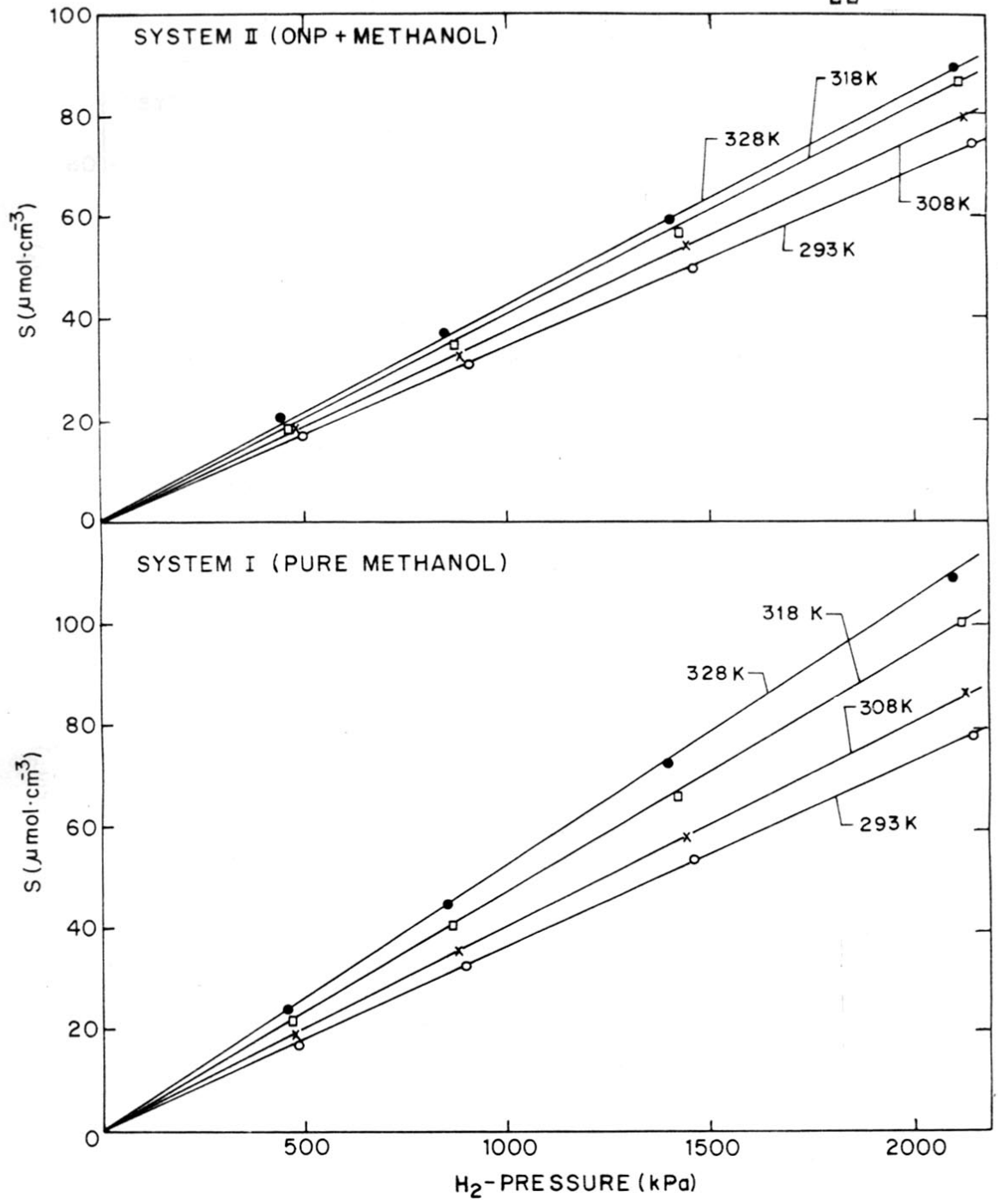


FIG.1·2: PRESSURE DEPENDENCE OF THE SOLUBILITY OF H_2 IN SYSTEM I AND II

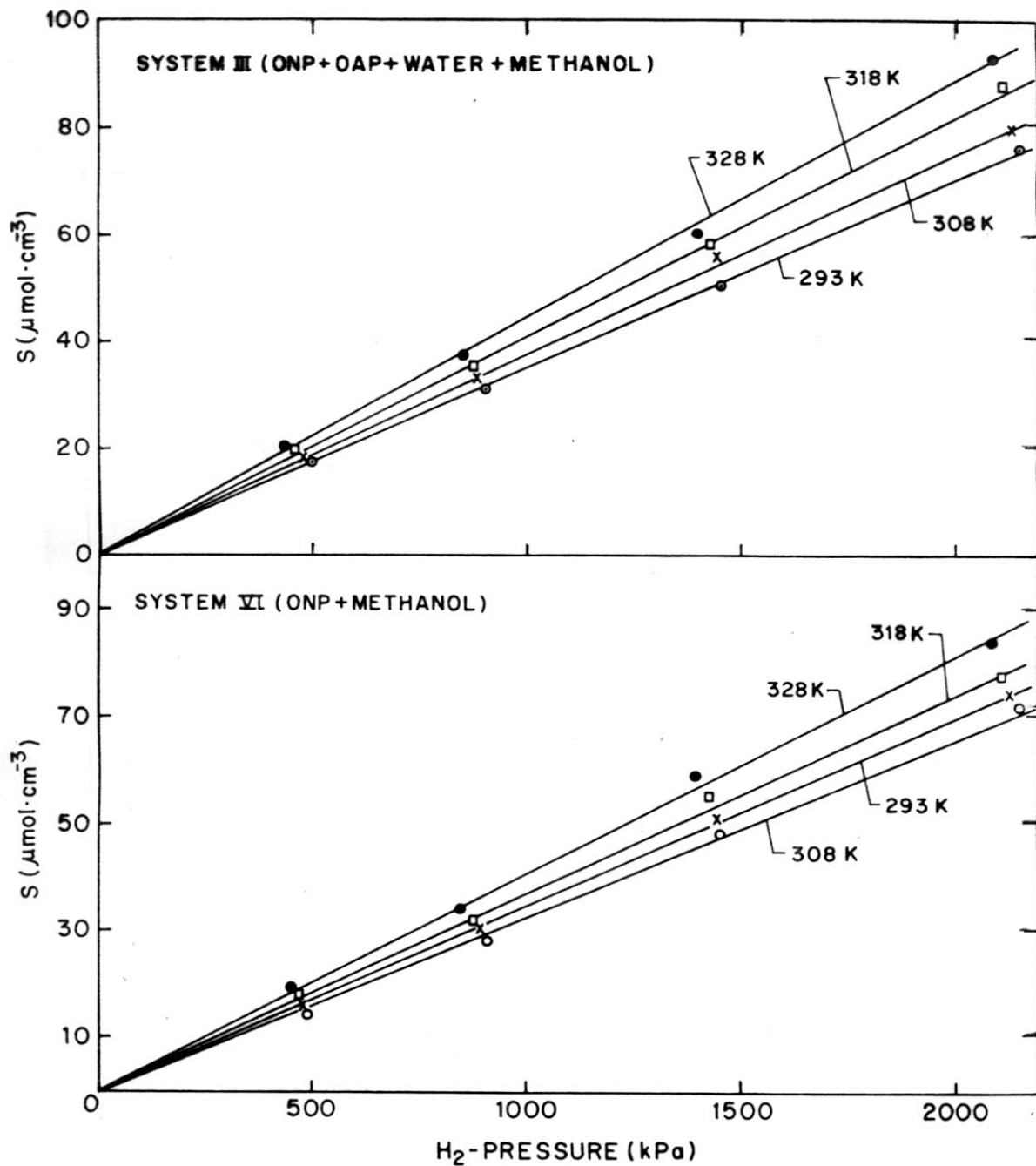


FIG.1.3: PRESSURE DEPENDENCE OF THE SOLUBILITY OF H₂ IN SYSTEM III AND VI

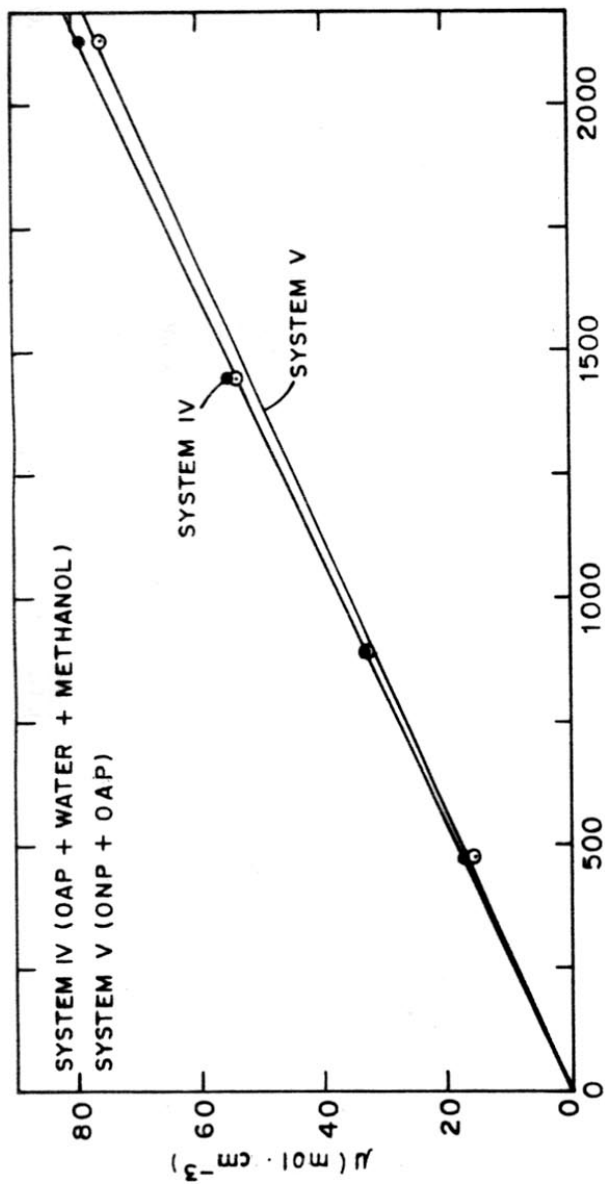


FIG. 1.4. PRESSURE DEPENDENCE OF THE SOLUBILITY OF H₂ IN SYSTEM IV AND V

TABLE-1.2

VALUES OF HENRY'S CONSTANT (α), HEAT OF DISSOLUTION (ΔH), AND A (EQN.1.3) FOR THE DISSOLUTION OF H_2

System	Henry's constant, $\alpha \times 10^3$ ($\mu\text{mol.cm}^{-3}$, kPa^{-1})			Heat of dissolution, ³ $-\Delta H \times 10^{-1}$ (J. mol^{-1})	A ($\mu\text{mol.cm}^{-3}$, kPa^{-1})	
	293K	308K	318K			
I (Pure methanol)	36.5	40.5	47.5	53.0	-5.01	0.269
II [ONP (0.36 mmol.cm^{-3}) in methanol]	35.0	38.0	41.0	42.5	-8.77	1.32
III [ONP (0.18 mmol.cm^{-3}) + OAP (0.18 mmol.cm^{-3}) + Water (0.36 mmol.cm^{-3}) in methanol]	35.0	37.5	41.0	44.25	-5.43	0.324
IV [OAP (0.36 mmol.cm^{-3}) + Water (0.72 mmol.cm^{-3}) in methanol]	-	37.0	-	-	-	-
V [ONP (0.18 mmol.cm^{-3}) + OAP (0.18 mmol.cm^{-3}) in methanol]	-	35.5	-	-	-	-
VI [OAP (0.36 mmol.cm^{-3}) in methanol]	33	35	37.25	40.75	-4.93	0.244

TABLE-1.3DATA ON DENSITY OF SYSTEMS (I-VI)

Temp. (K)	Density (g.cm ⁻³)					
	I	II	III	IV	V	VI
293	0.7915	0.8275	0.8087	0.8150	0.8050	0.8025
308	0.7775	0.8017	0.7869	0.7881	0.7835	0.7746
318	0.7696	0.7936	0.7781	0.7793	0.7746	0.7650
328	0.7605	0.7839	0.7695	0.7698	0.7661	0.7548

TABLE-I.4

DATA ON VAPOR PRESSURE OF SYSTEMS I-VI

Temp. (K)	Component	Vapour pressure (kPa)					
		System I	II	III	IV	V	VI
293	Methanol	12.96	12.77	12.57	12.39	12.77	12.77
	o-Nitrophenol	-	0.00024	0.00013	-	0.00012	-
	Water	-	-	0.0349	0.0675	-	-
308	Methanol	27.88	27.46	27.04	26.65	27.46	27.46
	o-Nitrophenol	-	0.00069	0.00035	-	0.00035	-
	Water	-	-	0.0840	0.1622	-	-
318	Methanol	44.42	43.75	43.09	42.47	43.76	43.76
	o-Nitrophenol	-	0.0013	0.00066	-	0.00067	-
	Water	-	-	0.1434	0.276	-	-
328	Methanol	68.57	67.54	66.51	65.55	67.54	67.54
	o-Nitrophenol	-	0.0032	0.0016	-	0.0015	-
	Water	-	-	0.2354	0.4548	-	-

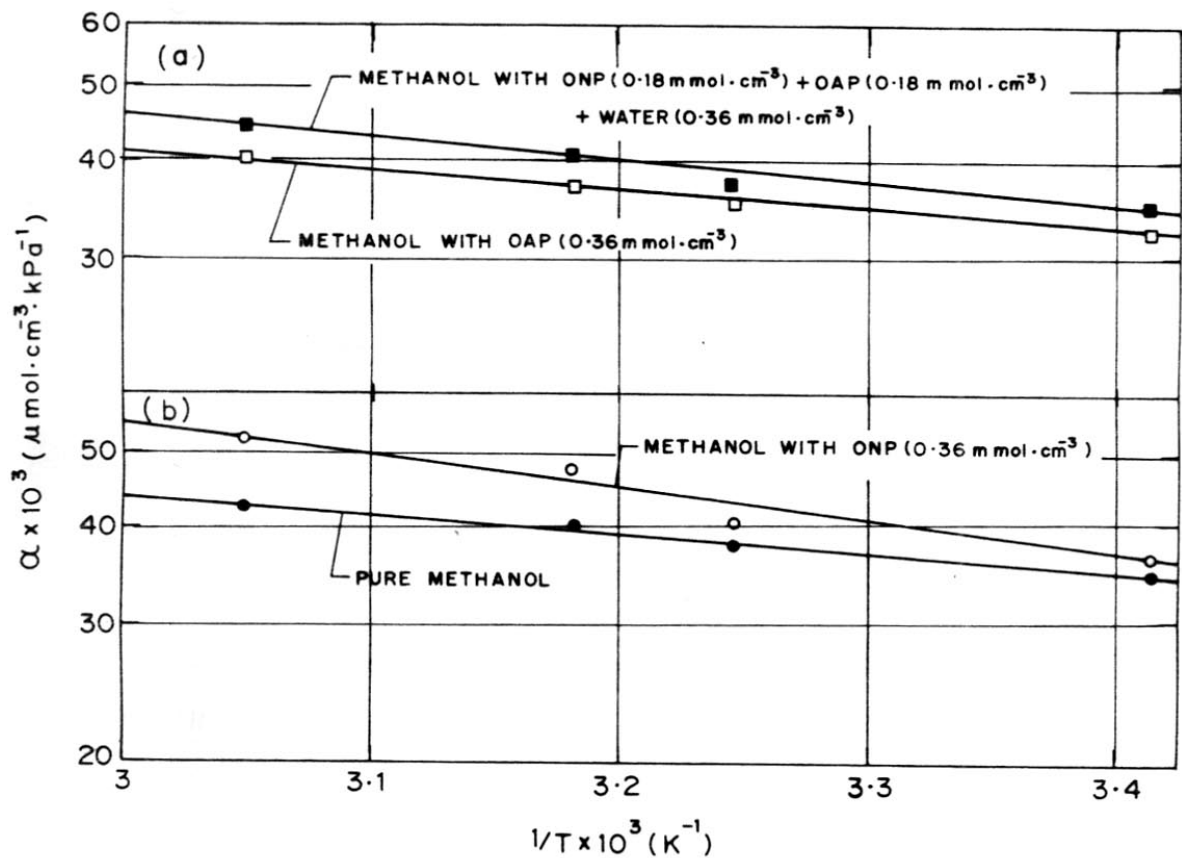


FIG 1.5. TEMPERATURE DEPENDENCE OF THE HENRY'S CONSTANT FOR THE DIFFERENT SYSTEMS.

the presence of the reaction species in the following order.

$$S (\text{pure methanol}) > S [\text{o-nitrophenol } (0.36 \text{ mmol.cm}^{-3}) \text{ in methanol}] > S [\text{o-aminophenol } (0.36 \text{ mmol.cm}^{-3}) \text{ in methanol}].$$

However, the addition of water to the methanol - OAP and methanol-ONP-OAP systems causes an increase in the solubility. Nevertheless, an addition of either of the reaction species or their mixture reduces the solubility of H_2 in methanol. The increase in the solubility due to the addition of water may probably be due to the interaction of water with the other reaction species.

The concentrations of the reaction species in methanol (Table 1.1) for the solubility measurements were chosen considering 0, 50 and 100% conversion of *o*-nitrophenol (initial concentration: $0.36 \text{ mmol.cm}^{-3}$) to *o*-aminophenol in the hydrogenation, so that the variation in the solubility of H_2 in the reaction mixture with the conversion could be followed. The systems II, III and IV represent the reaction mixture at 0, 50 and 100% conversion of *o*-nitrophenol, respectively.

NOMENCLATURE

A	constant, Eqn. (1.2) ($\mu\text{mol.cm}^{-3}$, kPa^{-1})
h	height of the methanol column (mm)
$P_{(\text{MeOH})}$	vapour pressure of methanol (torr)
p	atmospheric pressure (torr)
R	gas constant ($\text{J.mol}^{-1}.\text{K}^{-1}$)
S	solubility of gas in liquid (mol.cm^{-3})
T_w	temperature of the gas collector (K)
V	volume of methanol displaced (cm^3)
v	volume of liquid sample (cm^3)
x	amount of gas desorbed, cm^3 (at NTP) cm^{-3} (liquid)
α	Henry's constant ($\mu\text{mol.cm}^{-3}$, kPa^{-1})
ΔH	heat of dissolution (J.mol^{-1})
ρ_{MeOH}	density of methanol (g.cm^{-3})

REFERENCES

1. Stephen, H. and Stephen, T., 'Solubilities of Inorganic and Organic Compounds' Pergamon Press, Oxford, Vol.I, Part 1 (1963) 539-541.
2. Krichevskii, I.R., Zhavoronhov, N.M. and Taihlis, D.S., *J. Chem. Ind. (USSR)*, 14 (1937) 170.
3. Shenderi, E.R., Zelvenskii, Ya.D. and Ivanovskii, F.P., *Gazovaya Prom.* 6 (3) *Viz.* (1961) 42.
4. Schroeded, W., *Z. Natur-Porch.*, B. 24 (15) (1969) 800.
5. Masahiro, Y., Shozo, S., Hirokatsu, M. and Yaichi, E., *Kogyo Kagaku Zasshi*, 72 (10) (1969) 2174 (Japan).
6. Katayama, T. and Nitta, T., *J. Chem. Eng. Data*, 21 (2) (1976) 194.
7. Brahme, P.H., Vadgaonkar, H.G., Ozarde, P.S. and Parande, M.G., *J. Chem. Eng. Data*, 27 (1982) 461.
8. Radhakrishnan, K., Ramachandran, P.A., Brahme, P.H. and Chaudhari, R.V., *J. Chem. Eng. Data*, 28 (1983) 1.
9. Choudhary, V.R. and Chaudhari, S.K., *Indian J. Technol.* 22 (1984), 156.
10. Choudhary, V.R., Parande, M.G. and Brahme, P.H., *Ind. Eng. Chem. Fundam.* 21 (4) (1982) 472.

PART-II

HYDROGENATION OF o-NITROPHENOL ON RANEY-Ni :
EFFECT OF PREPARATION AND STORAGE CONDITIONS OF RANEY-Ni

2.1 INTRODUCTION

2.1.1 Effect of Preparation Conditions of Raney Nickel on Its Properties

Nickel-aluminium alloy is commonly used for the preparation of Raney-nickel. The alloy contains NiAl_3 , Ni_2Al_3 and Ni_3Al phases (1,2) and the composition of these phases depends on the alloy composition. The non-catalytic part of the alloy (i.e. Al) can be leached out by hydrolysis with water, alkali or acid. However, the leaching is most commonly done by alkali treatment. The catalytic activity of Raney nickel is affected by leaching conditions (viz. type of alkali used, alkali concentration, temperature, duration of leaching) and washing conditions (viz. washing agent, temperature, duration of washing, etc.) and, therefore, it is extremely difficult to obtain catalyst with perfectly uniform activity and also difficult to reproduce it. Yasumura (3) has presented a comprehensive review on Raney nickel, with particular emphasis on the factors affecting its catalytic activity. Csuros and Petro (4) studied the effect of different alkalies used for the extraction of aluminium from Raney nickel alloy (nickel 48% - aluminium 52%) on the hydrogenation activity of Raney nickel catalyst. Their results indicated that among the alkalies (K_2CO_3 , Na_2CO_3 and NaOH), the maximum activity of the catalyst was obtained when the alloy was leached with sodium hydroxide.

Freel et al. (2) studied the effect of alkali concentration in the preparation of Raney nickel on the leaching of aluminium from the Ni-Al alloy. In moderately concentrated aqueous alkali, the eutectic and NiAl_3 phase reacted more rapidly than the Ni_2Al_3 phase. They also found that the leaching of aluminium with dilute alkali solution is not complete and the catalyst after leaching contains a substantial amounts of aluminium.

Kagan and coworkers (5) studied the effect of leaching temperature of NiAl_3 and Ni_2Al_3 on the surface, volume fraction and size of the particles of the Raney nickel produced.

Petrov and Fasman (6) have observed the effect of leaching time in the leaching of Ni-Al alloy of different compositions on the structure and the specific activity of the Raney nickel catalyst. They observed that lengthy period of leaching leads to less effective catalysts except in the case of catalysts prepared from molten alloys.

Ishikawa (7) measured the size of the Ni crystals by X-ray analysis and found a close relationship between the composition and the leaching conditions of Ni-Al alloys on the one hand, and the size of the resulting nickel crystals on the other. When the Ni-Al alloys were leached under a definite condition, the size grew with leaching time and this trend accelerated with the increase in temperature. Further, when the Ni-Al alloys were leached under the same conditions, the size was inversely proportional to the nickel content of the Ni-Al alloys. Ishikawa (7) has also pointed that the catalyst having its maximum activity for the hydrogenation of a substance has a definite crystal size characteristic of the substance, and hence it is impossible to prepare Raney nickel catalyst which exhibits its highest activity to every substance. The effect of crystal size on catalytic activity indicated that the activity is strongly affected by the geometrical factors of the catalyst.

Freidlin and Rudneva (8) observed that the high activity of Raney nickel is not attributed to the form of the crystal lattice, the presence of impurities, the particle size or its specific surface area, but to the hydried formation on the surface due to the formation of hydrogen with

the metal surface produced during the catalyst preparation.

Yakubunok et al. (9) studied the effect of preparation conditions of Raney nickel on the distribution of hydrogen on the surface of the catalyst. The distribution of hydrogen on the surface of the catalyst was affected by the catalyst preparation conditions (viz. temperature and period of leaching). A prolonged leaching intensified a bond of adsorbed hydrogen with the catalyst surface.

Davtyan and coworkers (10) have observed a dependence of the lattice parameter of the Raney nickel catalyst on their preparation conditions. They have suggested that the activity of the catalyst is due to the lattice parameter as well as to its dispersion. They have further observed (11) that the catalyst activity of Raney nickel depends on its lattice parameter, the greater the concentration of lattice the higher its activity.

Kubomatsu (12) studied the role of residual aluminium in the Raney nickel catalyst and found that the presence of residual aluminium in the catalyst prevents the growth of Ni-crystals, and hence is indispensable for maintaining the high activity of the catalyst.

Ishikawa (13) observed that the specific surface area of Raney nickel increases with the temperature and time of leaching, whereas hydrogen content and residual aluminium in the catalyst decreases gradually with the leaching temperature.

Our recent study (14) in the hydrogenation of *p*-nitrotoluene on Raney-Ni prepared under different conditions has indicated a strong influence of leaching conditions of Ni-Al (50% Al) alloy (viz. type of alkali, concentration

of alkali, temperature and duration of leaching) and the washing agent (viz. tap water, distilled water, deionised distilled water, 50% ethanol, and 95% ethanol) used in the washing of the leached alloy on the hydrogen content and hydrogenation activity of the Raney-Ni catalyst formed.

2.1.2 Effect of Ageing of Raney Nickel on its Properties

Raney nickel is extremely pyrophoric and hence it catches fire when brought into contact with air. Its preservation in a dry state is rather difficult and hence various ways, such as keeping it always covered with liquid or sealing with harden oil have been used for its storage. A commonly used medium for storing Raney-Ni is ethanol (Adkin's method). Only a few studies (15-20) have been so far reported on the effect of storage conditions on the catalytic properties of Raney nickel and results reported in them are contradictory (17,18).

Dominguez et al. (19) observed no change in its activity after three months of storage in alcohol. Yasamura (15) found that the activity was least affected when the catalyst was stored in distilled water along hydrogen. Orito and others (18) studied the activity and the surface area of the Raney nickel catalyst stored in various liquids (viz. primary and secondary alcohols, dioxane, benzene, toluene, etc.). They observed a change in surface area of the catalyst with the storage time and liquid medium. But the change in surface area did not directly influence in the reduction of catalytic activity. This observation is in contrast to that of Smith (16).

Recently, Choudhary and Chaudhari (20) have studied the effect of different storage conditions (liquid medium, temperature, gas atmosphere, and storage period) on the H_2 content of Raney nickel and on its catalytic

activity in the hydrogenation of *p*-nitrotoluene to *p*-toluidine. Their results indicate that the effect of a particular storage condition on the activity of the catalyst cannot be isolated, the activity depends on the combined effect of the storage conditions employed.

2.1.3 Present Investigation

It can be noted from the above literature survey that the catalytic activity of Raney-Ni depends on its hydrogen and residual aluminium content, lattice parameters and crystallite size. These parameters are affected by the preparation conditions and storage conditions of the catalyst. Further, as the Raney nickel catalyst having its maximum activity for the hydrogenation of a particular substance has a definite crystal size characteristic of the substance (7), it is necessary to find out the optimum preparation and storage conditions for the Raney nickel catalyst having the maximum activity for the hydrogenation of *o*-nitrophenol to *o*-aminophenol reaction. The present investigation was therefore undertaken with the following objectives.

1. To study systematically the effect of various preparation conditions of Raney nickel (viz. the type of alkali, the concentration of alkali, the temperature, the duration of leaching and the nature of washing agent) on the catalytic activity in the liquid phase hydrogenation of *o*-nitrophenol (ONP) to *o*-aminophenol (OAP) using methanol as a reaction medium and arrive at the optimum conditions for the preparation of Raney nickel catalyst giving maximum activity for the hydrogenation process.
2. To study in details the effect of storage conditions, viz. liquid medium (deionised water, 95% ethanol, and 5% aqueous sodium hydroxide), temperature (room temperature and temperature of refrigerator), gas atmosphere (hydrogen and air), and ageing period,

on the activity of Raney nickel in the hydrogenation of *o*-nitrophenol to *o*-aminophenol in an agitated high pressure three phase slurry reactor using methanol as a reaction medium.

2.2 EXPERIMENTAL

2.2.1 Materials

Raney alloy : Composition Ni (50 wt %) and Al (50 wt %) (obtained from Fison, Philadelphia, USA).

Particle size : 250 to 500 mesh.

Chemicals

Ammonium chloride (AR)

Ammonium hydroxide (AR)

Ammonium sulphocyanide (LR)

Cyclohexane (LR)

Ethanol (95%) (distilled)

Ferric ammonium sulphate (AR)

Hydrochloric acid (AR)

Hydrofluoric acid (LR)

Hydrogen peroxide (AR BDH)

Karl Fischer reagent (BDH)

Methanol (freshly distilled)

Methyl red (BDH)

o-Nitrophenol (AR, German repacked)

Potassium hydroxide (LR BDH)

Potassium iodide (AR BDH)

Sodium hydroxide (LR BDH)

Sodium thiosulphate (AR BDH)

Starch (LR)

Succinic acid (LR)

Titanous chloride (30%) (LR BDH)

Urea (LR)

Gases

Hydrogen (IOLAR II, obtained from IOL, Bombay)

Nitrogen (IOLAR II, obtained from IOL, Bombay)

2.2.2 Preparation of Raney Nickel Catalyst

The experimental setup for the preparation of Raney nickel is shown in Fig. 2.1. It consisted of a stirred jacketed reactor (made of stainless steel 15 cm dia. and 35 cm height), provided with a cooling coil, a thermometer, H_2 inlet tube and provision for the addition of the alloy.

A known volume of aqueous alkali solution (2000 cm^3) was taken in the reactor and maintained at the desired temperature by circulating a constant temperature water through the reactor jacket. The solution was stirred at 1200 rpm and hydrogen gas ($20\text{-}30\text{ cm}^3\text{.min}^{-1}$) bubbled through it in order to remove the dissolved oxygen. The hydrogen flow was continued throughout the leaching period. When temperature of the alkali solution reached the desired value, a known amount of Raney alloy [(50 g particle size : 30-60 microns)] was added to it in small portions in a period of 10 min. The reaction temperature was maintained by removing the exothermic heat of reaction by adjusting the flow of a chilled water through the cooling coil.

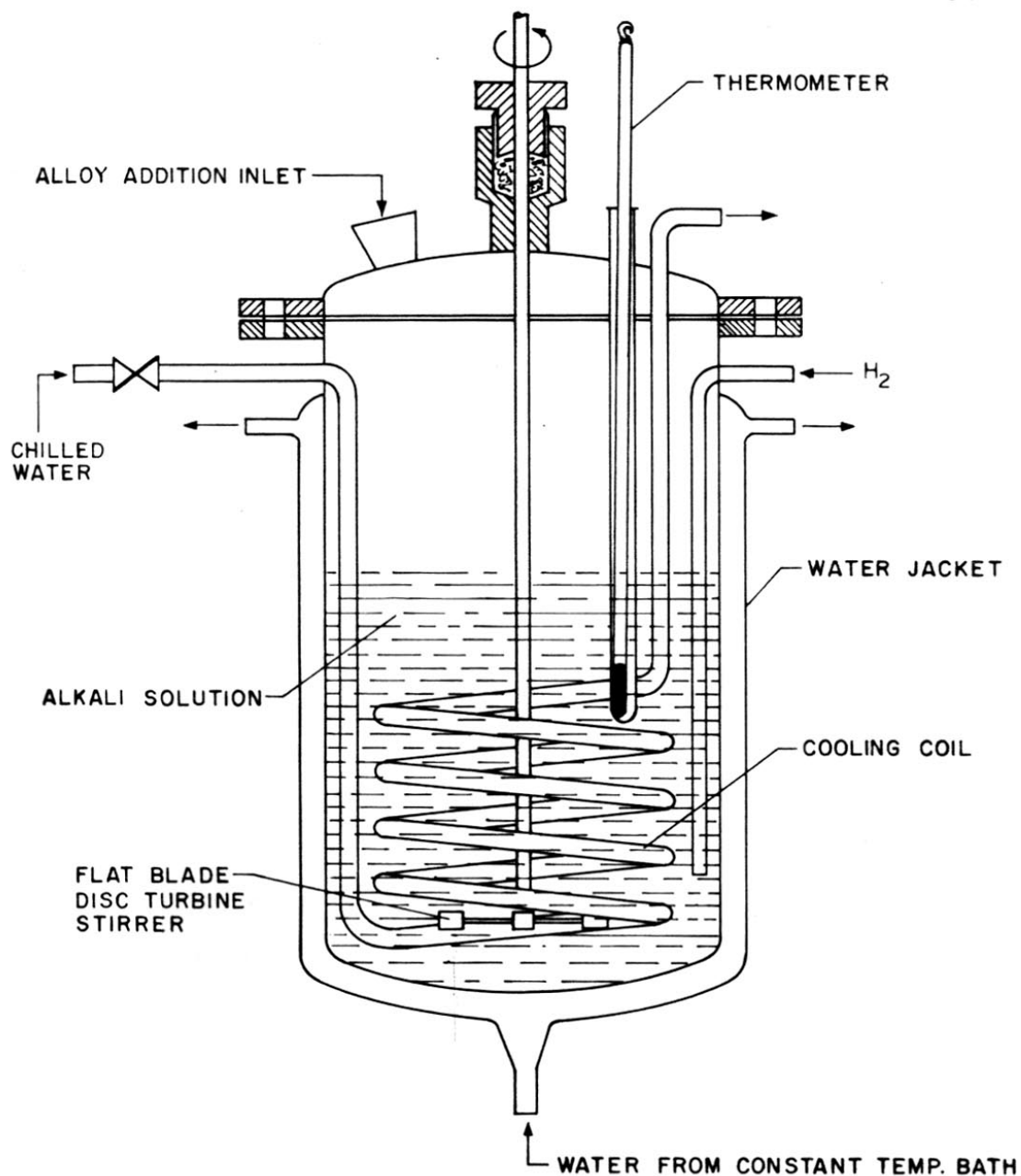


FIG.2-1: EXPERIMENTAL SET-UP FOR PREPARATION OF RANEY NICKEL

After the alloy was leached for the desired period, the stirring was stopped, the catalyst particles allowed to settle, the supernatant solution removed by suction and the catalyst particles washed with the desired washing agent (presaturated with hydrogen) at 303-308K till free from alkali (as shown by litmus test). The duration of washing was 20-25 min. The catalyst was then stored under hydrogen atmosphere in the same liquid medium as that used for the washing.

The catalyst was subjected to the activity test after the storage period of 45-50 hr. The leaching and washing variables covered are as follows.

Type of alkali used	:	NaOH and KOH
Concentration of alkali (NaOH)	:	1.25 - 20 mol.dm ⁻³
Leaching temperature	:	283 - 358K
Leaching time	:	1-12 hr
Washing agents	:	tap water, distilled water, deionised distilled water, 50% ethanol, and 95% ethanol.

The temperature of the leaching could be controlled within $\pm 1^\circ\text{C}$.

A number of Raney nickel catalysts were prepared by systematically varying one preparation condition at a time while keeping all the other conditions the same. The catalyst prepared under different controlled conditions are listed in Table-2.1.

2.2.3 Measurement of Properties of Raney Nickel

2.2.3.1 Determination of residual aluminium in the catalyst

The residual aluminium in the Raney nickel catalysts was determined by the method similar to that used by Schnyder (22). A known amount

TABLE-2.1

PREPARATION CONDITIONS OF RANEY NICKEL CATALYSTS

Volume of alkali solution : 2000 cm³
 Composition of Raney alloy : Ni (50 wt %) - Al (50 wt %)
 Particle size of alloy (av) : 30-60 μm
 Amount of Raney alloy : 50 g
 Stirring speed (av) : 1200 rpm

Catalyst	Concentration of NaOH (mol.dm ⁻³)	Temperature of leaching (K)	Time of leaching (hr)	Washing agent	Storage conditions*
1	2	3	4	5	6

Effect of alkali

RN 1	10.00	313	6	Deionised distilled water	Stored in deionised distilled water under H ₂ at room temperature
RN 2	10.00 (KOH)	"	"	"	"

Effect of alkali concentration

RN 3	20.00	"	"	"	"
RN 4	12.50	"	"	"	"
RN 5	6.25	"	"	"	"
RN 6	3.75	"	"	"	"
RN 7	2.50	"	"	"	"
RN 8	1.25	"	"	"	"

Table-2.1 contd.

1	2	3	4	5	6
<u>Effect of temperature</u>					
RN 9	10.00	283	6	Deionised distilled water	Stored in deionised distilled water under H ₂ at room temperature
RN 10	"	298	"	"	"
RN 11	"	328	"	"	"
RN 12	"	343	"	"	"
RN 13	"	358	"	"	"
<u>Effect of leaching period</u>					
RN 14	"	313	1	"	"
RN 15	"	"	2	"	"
RN 16	"	"	4	"	"
RN 17	"	"	8	"	"
RN 18	"	"	12	"	"
<u>Effect of washing agent</u>					
RN 19	"	"	6	Filtered tap water	Filtered tap water under H ₂ at room temperature
RN 20	"	"	"	Distilled water	Distilled water under H ₂ at room temperature
RN 21	"	"	"	50% ethanol	50% ethanol under H ₂ at room temperature
RN 22	"	"	"	95% ethanol	95% ethanol under H ₂ at room temperature

* All the catalysts were stored for 45-50 hr before measuring their catalytic activity

of catalyst about 3.0 g based on wet weight was warmed with 10 cm³ of dilute hydrochloric acid (3M). After the complete dissolution of the catalyst, dilute ammonium hydroxide was added until the solution turned turbid. Diluted HCl was added until the turbidity cleared and 1 or 2 drops of the acid were added in excess. To the solution, 100 cm³ of 6% succinic acid solution, 10 g ammonium chloride and 4 g urea were added successively. The resulting solution was made up to about 400 cm³ with distilled water. It was then boiled for 2 hr and cooled to room temperature. The precipitate formed was filtered and washed with a 1% succinic acid solution neutralised by ammonium hydroxide. The precipitate along with the filter paper was ignited at 1473K in a platinum crucible and the residual alumina (Al₂O₃) was estimated gravimetrically.

The weight percent of the residual aluminium in the catalyst was obtained as;

$$\text{Residual Al (wt.\%)} = \frac{26.97 \times w}{101.04 \times (w_3 - w_4)} \times 100 \quad (2.1)$$

where, w is the amount of Al₂O₃ (g), w_3 is the weight of the wet catalyst, and w_4 is the weight of water contained in the wet catalyst as determined by the Karl Fisher method. The residual aluminium was determined in the catalyst RN-1, 14, 17 and 18 prepared at different leaching periods.

2.2.3.2 Solid phase particle density and porosity of the catalyst

These properties were determined using the apparatus shown in Fig. 2.2.

Solid phase density (ρ_s) : The Raney nickel, along with methanol, was introduced into the catalyst bulb by removing the cap of the Rotaflow

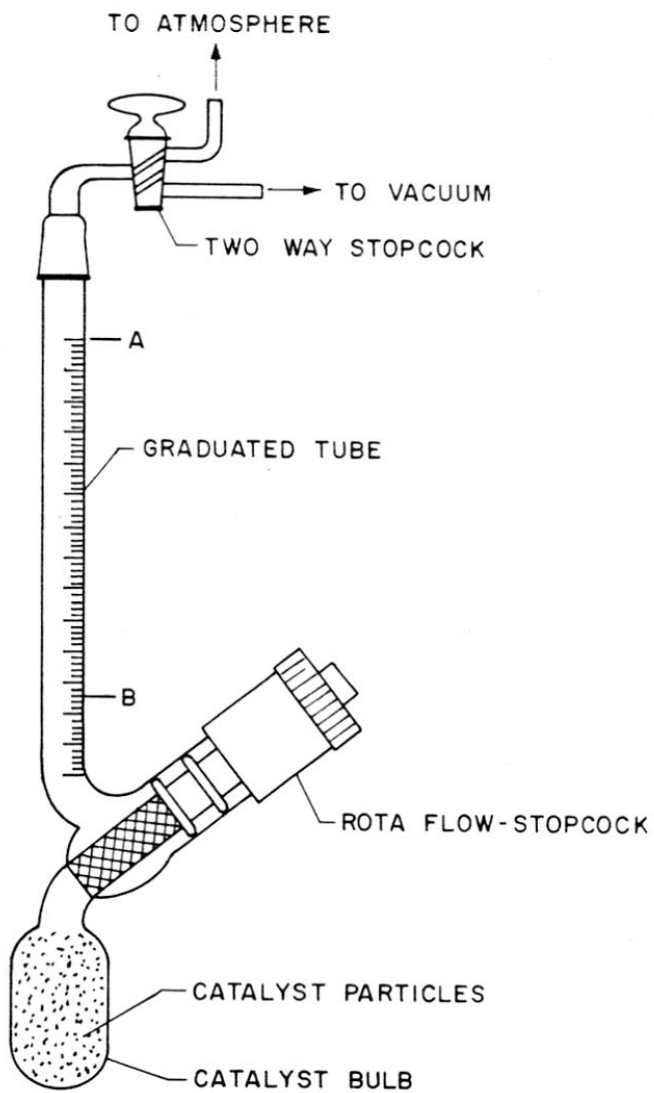


FIG.2.2 : APPARATUS FOR MEASURING SOLID PHASE AND PARTICLE DENSITIES OF RANEY NICKEL

stopcock. The cap was replaced and the methanol in the catalyst bulb was evaporated very carefully at room temperature by applying suction to the bulb. The Rotaflo stopcock was closed and the apparatus weighed. This procedure was repeated till a constant weight was obtained. The graduated tube was filled with cyclohexane upto the level marked A (Fig. 2.2) and the reading A noted. Gas bubbles, if any, present in the liquid column were removed by applying a slight suction. The system was connected to atmosphere by the two way stopcock. The liquid was introduced in the evacuated catalyst bulb, the Rotaflo stopcock closed and the reading of the liquid level B in the graduated tube noted. A similar experiment was performed without the catalyst.

The volume of the solid phase of the catalyst could be obtained as the difference between (A-B) without catalyst and (A-B) with catalyst from which the solid phase density (ρ_s) could be calculated ($\rho_s = \text{weight of the catalyst} / \text{volume of solid phase of the catalyst}$).

Particle density : For determining the particle density, mercury was used instead of cyclohexane as it does not penetrate the pores at atmospheric pressure. In this case the difference between (A-B)_{without catalyst} and (A-B)_{with catalyst} gave the volume of the particles of the catalyst. The particle density could be calculated from the catalyst weight and the volume of its particles.

Porosity : It was obtained from the particle density and the solid phase density of the catalyst.

$$\text{Porosity } (\epsilon) = 1 - (\rho_p / \rho_s)$$

Bulk density : The bulk density of the catalyst was determined by measuring the loss in weight due to evaporation of methanol under vacuum at room temperature. The evacuation was continued till a constant weight was obtained.

$$\text{Bulk density, } \rho_b \text{ (g.cm}^{-3}\text{)} = \frac{w_1 - w_2}{V_b}$$

where,

w_1 = weight of catalyst covered with methanol (g)

w_2 = weight of methanol (i.e. loss in weight due to evaporation) g.

V_b = volume of the catalyst in methanol (cm^3).

2.2.3.3 Surface area and crystallite size

The surface area of the catalysts was determined using the method described by Smith and Fuzek (23) which is based on the monomolecular adsorption of lauric acid from its benzene solution. The crystallite size of the catalysts was obtained by the X-ray diffraction line broadening method described elsewhere (24). The values of surface area and crystallite size of the catalysts are included in Table-2.2. The results indicate that the size of the Raney-Ni crystallites increases very significantly with the increase in the leaching temperature and period. However, the surface area of the catalyst is affected by the changes in the leaching parameters to a relatively small extent. The increase in the size of nickel crystallites with no significant decrease in their surface area may be because of the formation of cracks and/or crystal defects.

2.2.3.4 Morphology of the catalyst

The morphology of the particles of the Raney-Ni catalysts was studied with a Cambridge stereoscan 150 model Scanning Electron Microscope.

TABLE-2.2

PROPERTIES OF RANEY NICKEL CATALYSTS PREPARED AT DIFFERENT CONDITIONS

Catalyst*	Concn. of NaOH (mol.dm ⁻³)	Leaching temp. (K)	Leaching period (hr)	Surface area (m ² .g ⁻¹)	Crystallite size D x 10 ⁸ (cm)
<u>Effect of alkali</u>					
RN1	10.00	313	6	600	-
RN2	10.00 (KOH)	313	6	-	-
<u>Effect of alkali concentration</u>					
RN3	20.00	313	6	-	-
RN4	12.50	313	6	61	127
RN5	6.25	313	6	58	134
RN6	3.75	313	6	65	109
RN7	2.50	313	6	70	83
RN8	1.25	313	6	-	-
<u>Effect of leaching temperature</u>					
RN9	10.00	283	6	-	-
RN10	10.00	298	6	64	104
RN11	10.00	328	6	63	133
RN12	10.00	343	6	59	171
RN13	10.00	358	6	56	180
<u>Effect of leaching period</u>					
RN14	10.00	313	1	61	114
RN15	10.00	313	2	67	132
RN16	10.00	313	4	66	-
RN18	10.00	313	12	57	156

* Catalysts washed with deionised water saturated with hydrogen and stored in deionised water under hydrogen atmosphere at room temperature.

Typical scanning electron photomicrographs of the catalysts are shown in Fig. 2.3. It can be noted that the nickel particles have rod-like shape and their size increases with the increase in the alkali concentration, temperature and period of leaching employed in the catalyst preparation.

2.2.4 Measurement of Catalytic Activity

A number of Raney nickel catalysts were prepared by substantially varying one preparation condition at a time while keeping all the other conditions the same. The catalyst prepared under different controlled conditions are listed in Table 2.1. The catalyst was always kept under the liquid as it is extremely pyrophoric. The exact procedure followed for measuring the catalyst volume was as follows.

The required volume of the catalyst was removed from the catalyst container and transferred to a 10 cm^3 measuring cylinder. The catalyst was then washed with methanol till it was free from the liquid in which it was stored and allowed to settle. The measuring cylinder was tapped from time to time. The time allowed for the settling (20 min) and the tapping procedure were exactly the same for all the catalysts. All the results are based on the dry weight of the catalysts, obtained from the knowledge of bulk density and the volume of the catalyst used.

2.2.4.1 Hydrogenation reactor

The catalytic activity of Raney nickel catalyst in the hydrogenation process was determined in an agitated three phase high pressure reactor (Parr autoclave) shown in Fig. 2.4, using methanol as the reaction medium. The reactor [capacity: 2000 cm^3 , inside dia. : 10 cm and inside depth: 26.7 cm] was made up of SS 316. It was provided with a gas inlet tube,

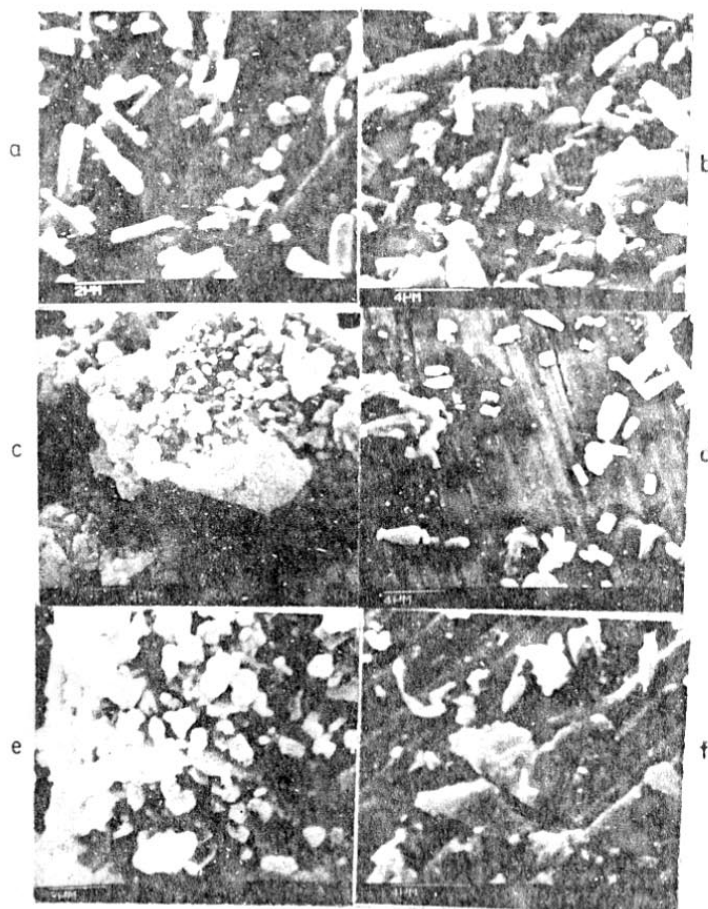


Fig. 2.3 Scanning electron micrographs of Raney-Ni prepared at different leaching conditions : (a) RN5 (conc. of NaOH: 6.25 M), (b) RN4 (conc. of NaOH:12.5M) (c) RN 14 (leaching period: 1 hr, (d) RN 17 (leaching period: 12 hr), (e) RN 1 (leaching temp.: 313K), (f) RN12 (leaching temp. : 343K)

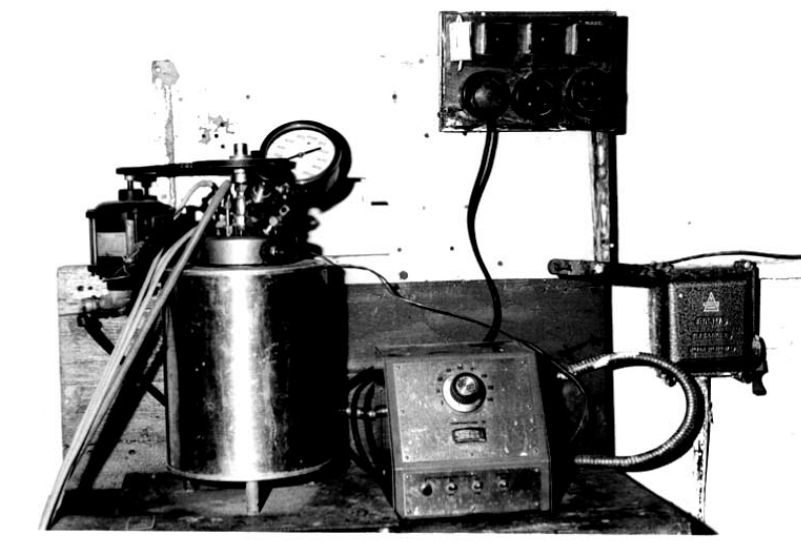


FIG. 2-4. PHOTOGRAPH OF THE PARR AUTOCLAVE USED FOR THE HYDROGENATION OF *o*-NITROPHENOL

a cooling coil, a stirrer, a thermowell, a pressure gauge and a safety valve. The reactor can be heated externally to a desired temperature by an electrically heated oven. The exothermic heat of the reaction could be removed by passing cooling water through the internal cooling coil. Stirring is achieved by a three blade stirrer situated at a distance of 2.8 cm from the bottom of the reactor.

2.2.4.2 Experimental procedure

A known amount of Raney nickel catalyst (about 1.0 cm³ in methanol) was introduced in the reactor, along with 200 cm³ of methanol. A solution of ONP [50 g in 800 cm³ of methanol] was then transferred to the reactor. The reactor was then closed by tightening the side flangens and was put into electrical oven. Nitrogen gas (free of oxygen) was then passed through the reactor to remove air from the reaction medium and from the free space in the autoclave. After driving out air from the reactor, hydrogen gas (> 99.99%) was introduced in the reactor at atmospheric pressure and the reactor was flushed with H₂. The temperature of the reaction mixture was attained to a desirable value (i.e. 308K), the reactor was pressured to 1508 kPa of hydrogen and the stirring started. The liquid samples were taken from time to time, while maintaining the H₂-pressure in the reactor constant.

All the Raney-Ni catalysts were tested for their performance in the hydrogenation at the following experimental conditions:

Volume of reaction mixture	:	1000 ± 5 cm ³
Initial concentration of o-nitrophenol	:	0.36 mmol.cm ⁻³
Catalyst loading	:	(1.03 + 0.62) x 10 ⁻³ g.cm ⁻³

Reaction temperature	:	308K
H ₂ -pressure	:	1508 kPa
Stirring speed	:	980 rpm
Reaction time	:	3 hr .

The experimental data on the catalytic activity of the Raney-Ni catalysts prepared and stored under different conditions are presented in Appendix-2.1 and 2.2, respectively.

2.3 EFFECT OF PREPARATION CONDITIONS OF RANEY NICKEL

2.3.1 Effect of type of alkali

The experimental data on the hydrogenation with the catalysts RN1 and RN2 prepared by leaching the Raney alloy with aqueous NaOH [10 M ($M = \text{g.mol.dm}^{-3}$)] and with aqueous KOH (10 M), respectively are plotted in Fig. 2.5.

The values for the initial reaction rates (r_0) for these catalysts are given in Table-2.3. The results (Table-2.3) indicate that the catalyst RN1 (prepared by the leaching with NaOH) has higher activity than the one prepared by the leaching with KOH. Figure 2.5 shows that NaOH is superior to KOH for preparing active Raney nickel catalyst by the alkali leaching process. This observation is consistent with those of Csuros and Petro (4) and Choudhary et al. (14).

2.3.2 Effect of alkali concentration

The hydrogenation activity curves (x vs t) for the catalysts prepared by the leaching with aqueous NaOH of different concentrations (1.25-20 M) are presented in Fig. 2.6. The values of initial reaction rates are included in Table-2.3. The results clearly indicate a strong dependence of the

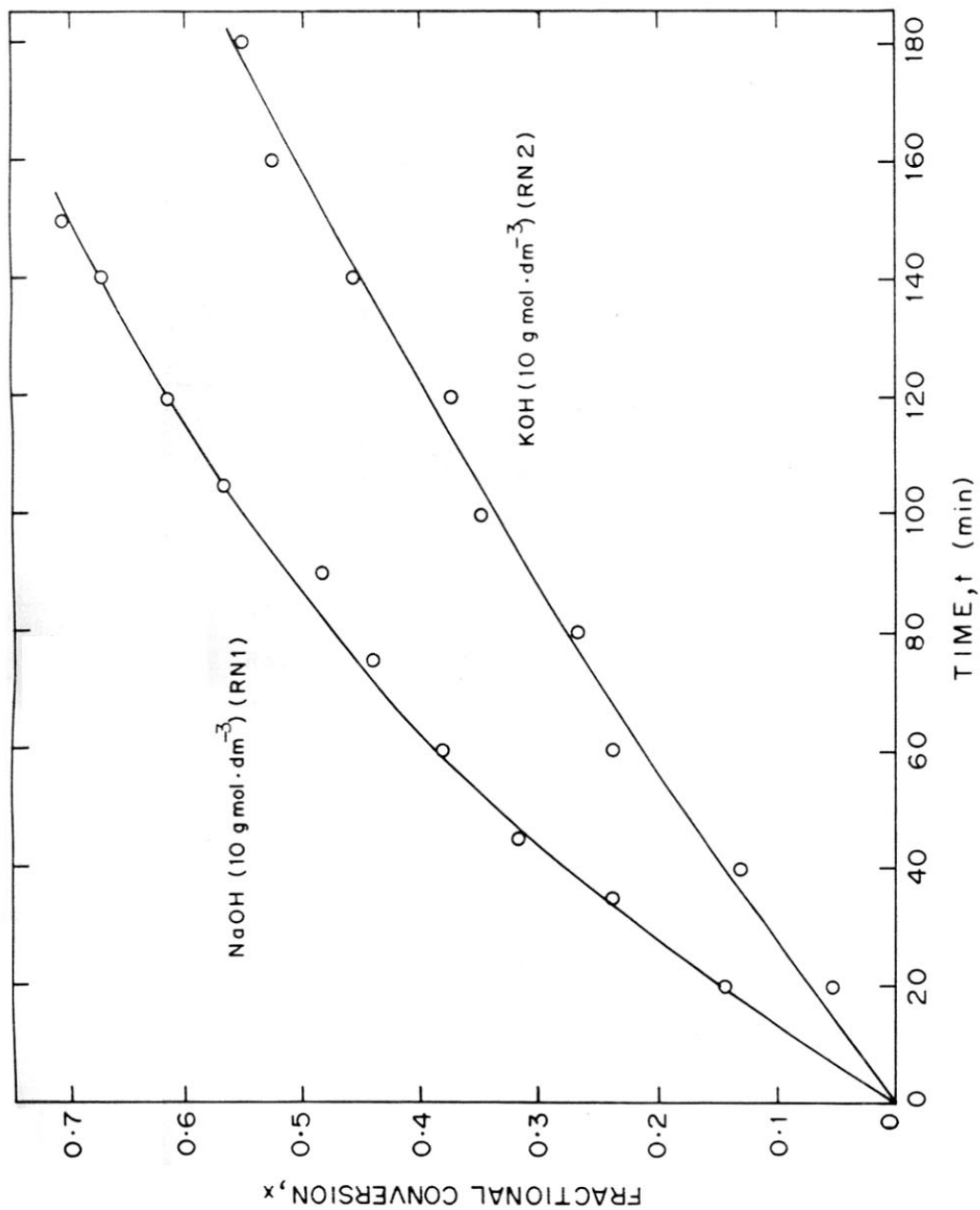


FIG. 2.5: THE ACTIVITY CURVES (x vs. t) FOR THE CATALYSTS PREPARED USING DIFFERENT ALKALIES

TABLE-2.3

INITIAL HYDROGENATION RATE DATA FOR THE CATALYSTS PREPARED
BY THE LEACHING WITH AQUEOUS ALKALI OF DIFFERENT CONCENTRATIONS

Common leaching conditions

Leaching temperature	:	313 K
Leaching period	:	6 hr
Washing solvent	:	deionised distilled water
Storage condition	:	stored in deionised distilled water under H_2 for 45-50 hr

Catalyst	Concentration of alkali (mol.dm ⁻³)	Initial reaction rate $r_0 \times 10^3$ (min. ⁻¹)
RN1	10.00 (NaOH)	7.33
RN2	10.00 (KOH)	3.80
RN3	20.00 (NaOH)	1.84
RN4	12.50 (NaOH)	2.95
RN5	6.25 (NaOH)	5.71
RN6	3.75 (NaOH)	9.80
RN7	2.50 (NaOH)	7.09
RN8	1.25 (NaOH)	8.33

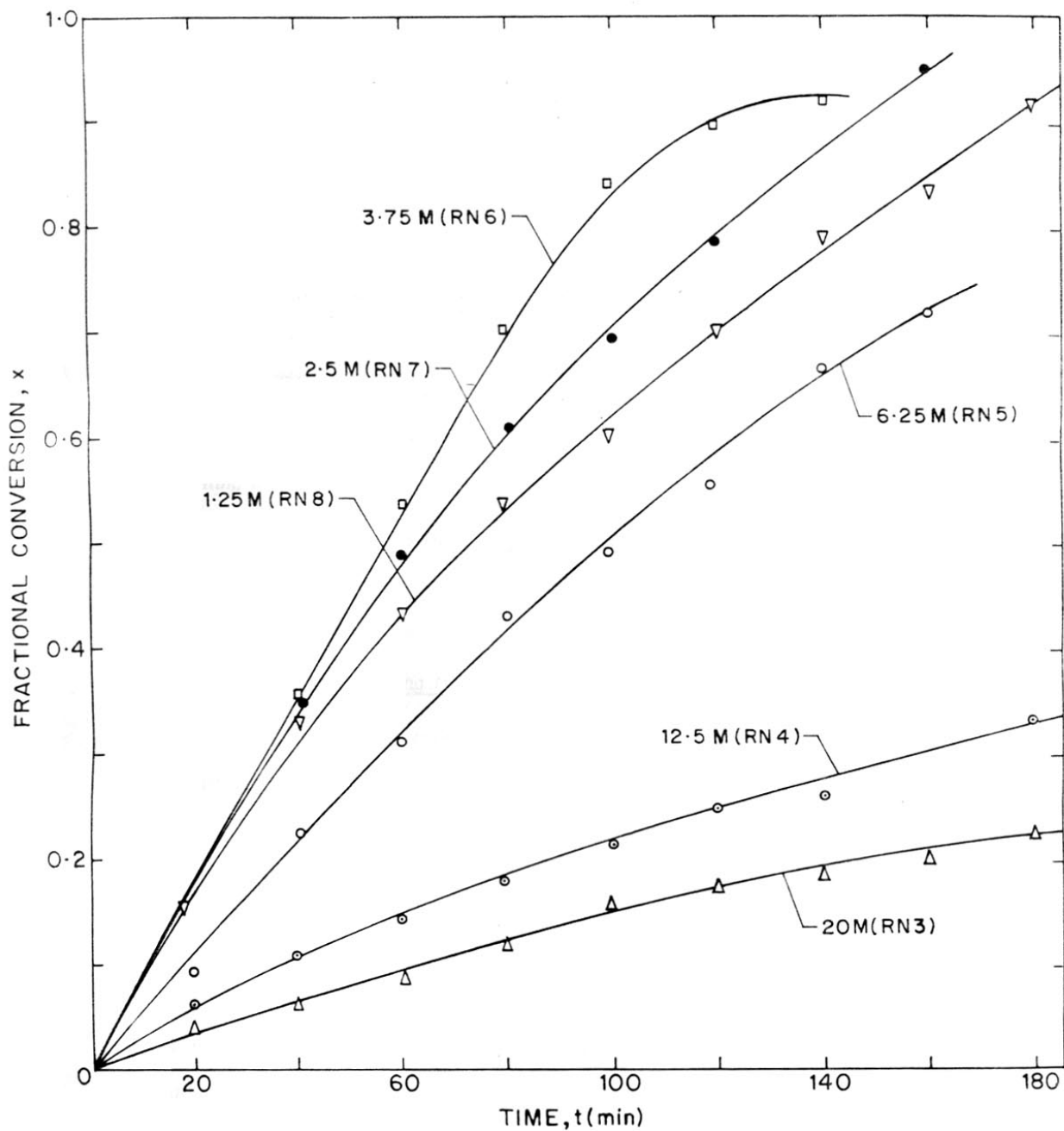


FIG.2.6: THE ACTIVITY CURVES (x vs. t) FOR THE RANEY Ni CATALYSTS PREPARED USING aq. NaOH OF DIFFERENT CONCENTRATIONS ($M = \text{mol. dm}^{-3}$)

catalytic activity of Raney-Ni on the concentration of NaOH used in its preparation.

Figure 2.7 shows that the catalytic activity passes through a maxima (at 3.75 M NaOH) and then decreases with concentration of NaOH. The variation of the catalytic activity with the alkali concentration employed in the catalyst preparation seems to be quite complex.

The results indicate that the catalyst with the maximum activity for the hydrogenation is obtained by using 3.75 M aqueous NaOH in the leaching process.

At the lower catalyst concentration (1.25 M NaOH) the catalyst produced did not settle immediately and hence the washing became difficult; the supernatant liquid was blackish.

2.3.3 Effect of leaching temperature

The x vs t curves for the catalysts prepared at different leaching temperatures (288-358 K) are presented in Fig. 2.8 and the values of the initial reaction rates are presented in Table-2.4. The variation of the initial reaction rate with the leaching temperature employed in the catalyst preparation is shown in Fig. 2.9. It can be noted from Fig. 2.9 that the initial reaction rate passes through a maximum (at 308 K) and a minimum (at 328 K) with the increase in the leaching temperature from 288 to 358 K. The catalyst prepared at the leaching temperature of 358 K showed the maximum activity in the hydrogenation.

The catalyst prepared at the lower leaching temperature (288 K) did not settle immediately and hence the washing became very difficult. However, the catalysts prepared at the higher leaching temperatures (≥ 358 K)

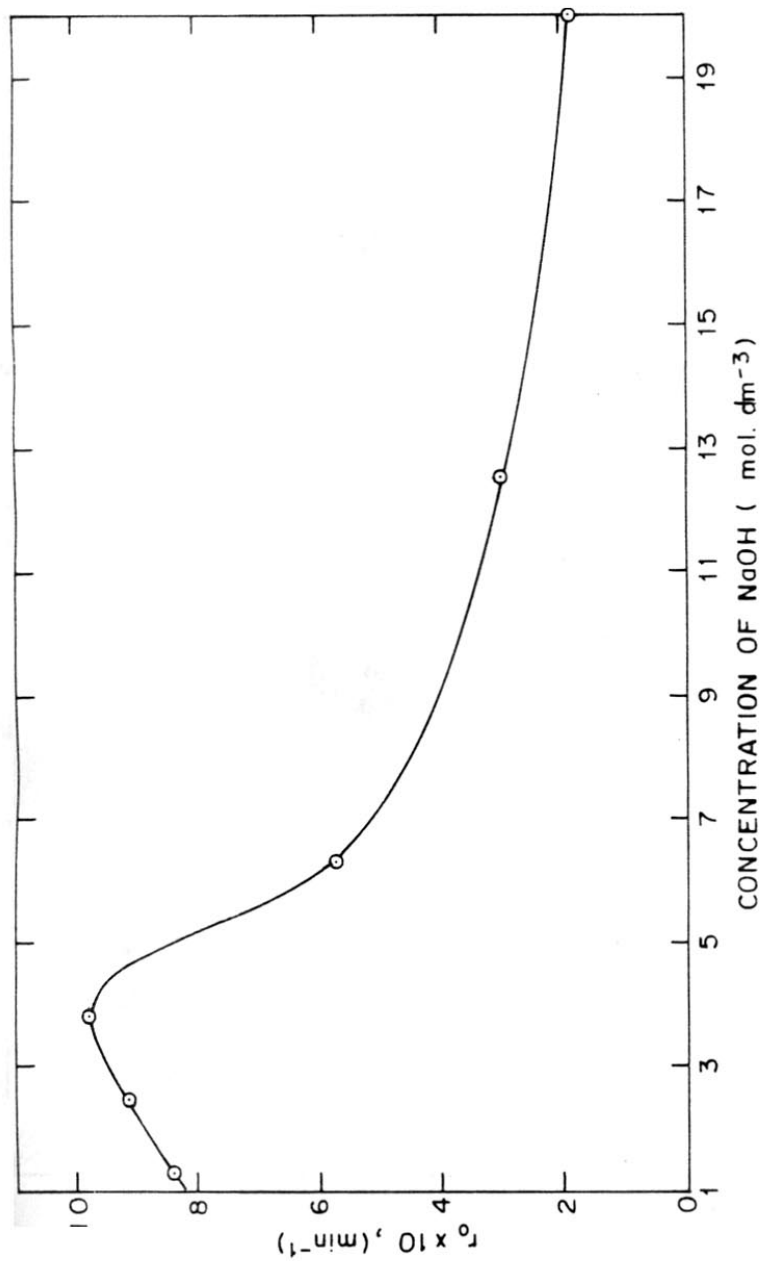


FIG. 2.7. DEPENDENCE OF THE INITIAL RATE (r_0) FOR THE HYDROGENATION OF o-NITROPHENOL ON THE CONCENTRATION OF ALKALI (NaOH) USED IN THE PREPARATION OF RANEY-Ni CATALYST

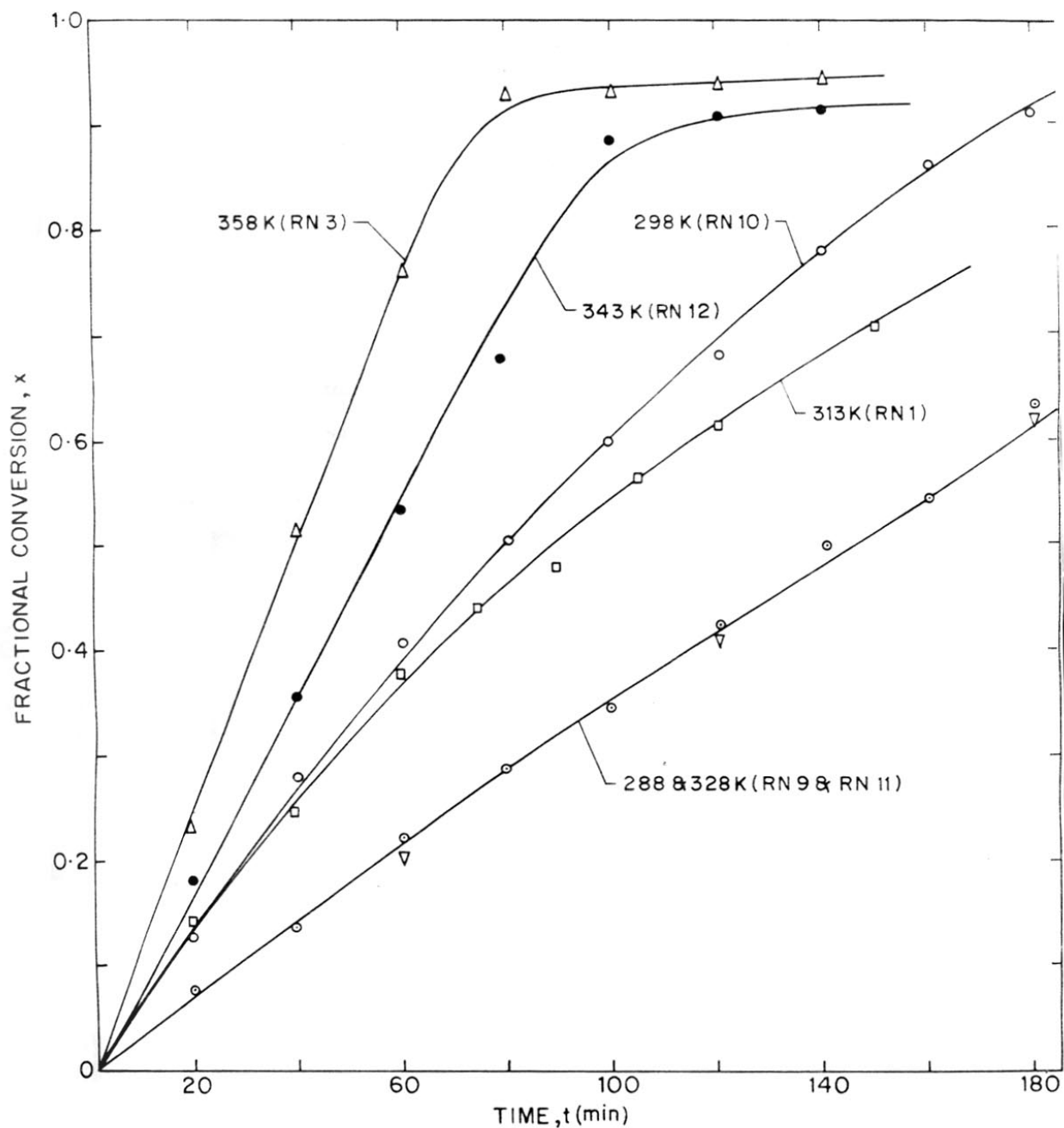


FIG.2-8: THE ACTIVITY CURVES (x vs. t) FOR THE RANEY Ni CATALYST PREPARED AT DIFFERENT LEACHING TEMPERATURE

TABLE-2.4

INITIAL HYDROGENATION RATE DATA FOR THE CATALYSTS PREPARED BY THE LEACHING AT DIFFERENT TEMPERATURES

Common leaching conditions

Concentration of NaOH	:	10.0 mol.dm ⁻³
Leaching period	:	6 hr
Washing solvent	:	deionised distilled water
Storage condition	:	stored in deionised distilled water under H ₂ for 45-50 hr

Catalyst	Leaching temperature (K)	Initial reaction rate $r_0 \times 10^3$ (min ⁻¹)
RN9	288	3.78
RN10	298	7.14
RN1	313	7.33
RN11	328	3.78
RN12	343	9.13
RN13	358	12.70

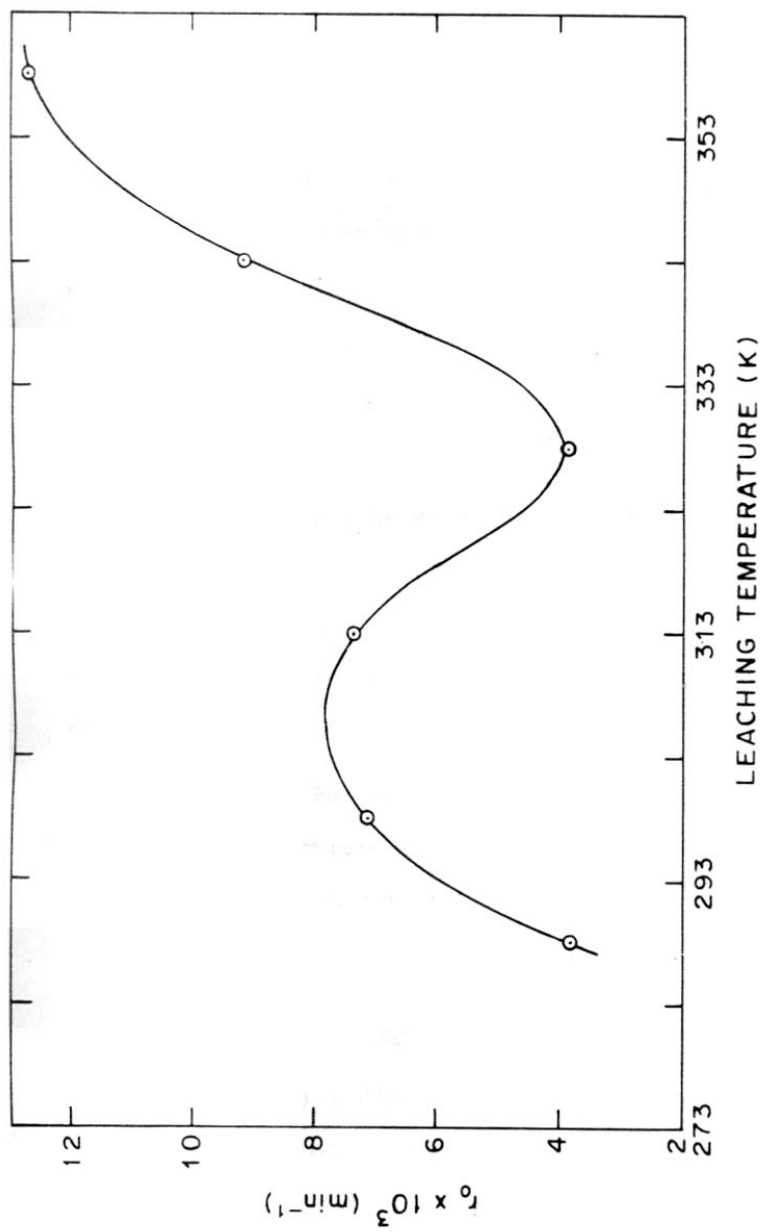


FIG. 2-9. DEPENDENCE OF THE INITIAL RATE (r_0) FOR THE HYDROGENATION OF o-NITROPHENOL ON THE LEACHING TEMPERATURE EMPLOYED IN THE PREPARATION OF RANEY NICKEL CATALYST

were found to be agglomerised to a large extent.

2.3.4 Effect of duration of leaching

The activity curves (x vs t) for the catalyst prepared by carrying out the leaching for different durations are presented in Fig. 2.10. The values of initial reaction rate and the residual aluminium content for the catalysts are given in Table 2.5.

It can be noted from the Table-2.5 that the amount of residual aluminium in the catalyst decreases with the increase in the duration of leaching.

The dependence of the initial reaction rate for the hydrogenation and the residual aluminium in the catalyst on the leaching period is shown in Fig. 2.11. When the duration of leaching was increased from 1 to 12 hr, the catalytic activity is passed through a maximum for a leaching period of 8 hr.

Petrov and Fasman (6) have also observed that prolonged leaching leads to less effective catalysts. The crystal size of the catalyst increases (7) with the leaching time, and this trend is accelerated when the temperature is increased.

2.3.5 Effect of washing agent

The activity curves (x vs t) for the catalysts prepared at the same leaching conditions but washed with different washing agents after the leaching are presented in Fig. 2.12. The values of initial reaction rate for the catalysts washed with different solvents and stored in the

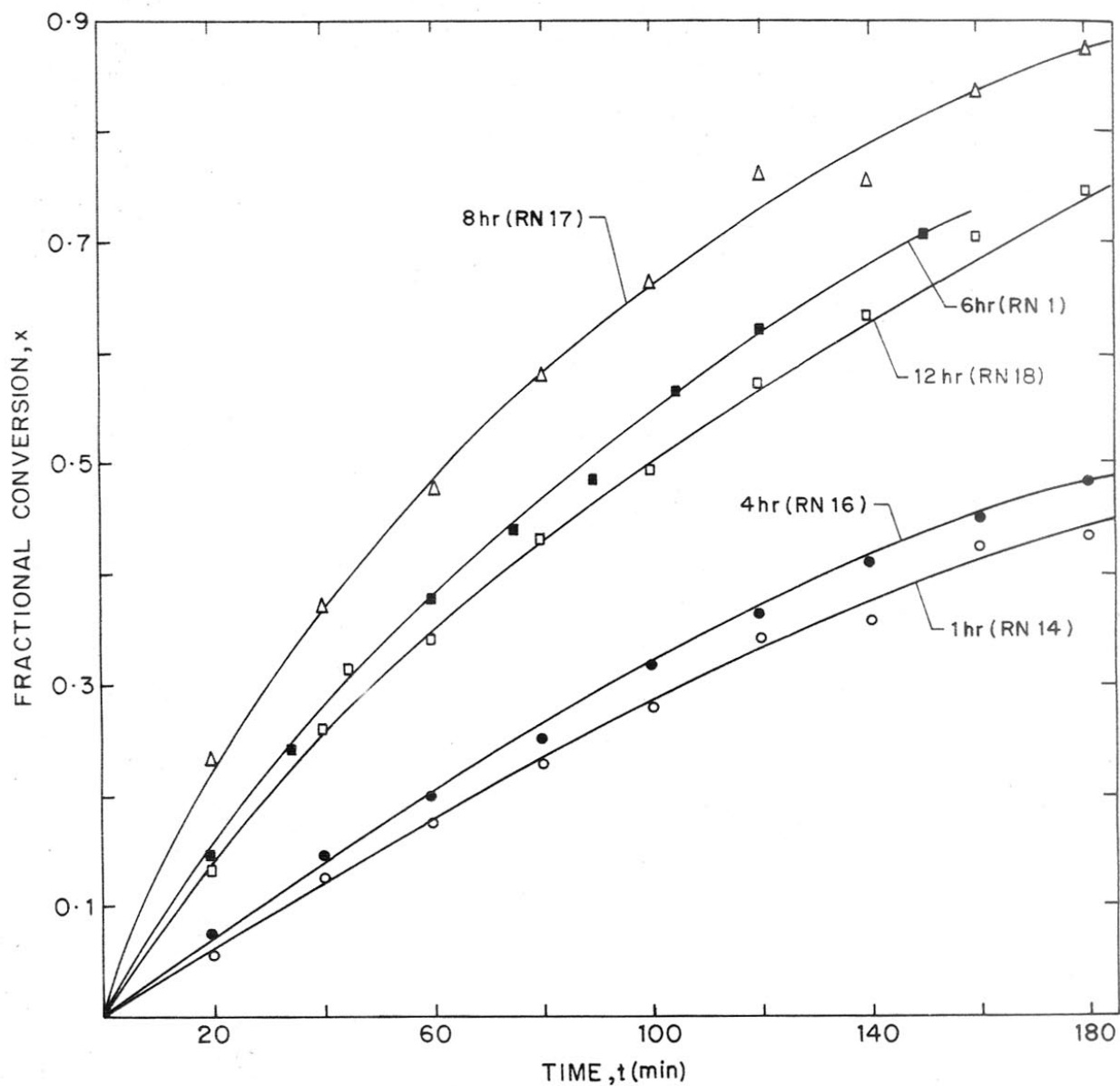


FIG.2-10: THE ACTIVITY CURVES (x vs. t) FOR THE RANEY Ni CATALYSTS PREPARED AT DIFFERENT LEACHING PERIODS

TABLE-2.5

INITIAL HYDROGENATION RATE AND RESIDUAL ALUMINIUM CONTENT OF THE CATALYSTS PREPARED BY THE LEACHING FOR DIFFERENT PERIODS

Common leaching conditions

Concentration of NaOH	:	10.0 mol.dm ⁻³
Leaching temperature	:	313 K
Washing solvent	:	deionised distilled water
Storage condition	:	stored in deionised distilled water under H ₂ for 45-50 hr

Catalyst	Leaching period (hr)	Residual aluminium content (wt %)	Initial reaction rate $r_0 \times 10^3$ (min ⁻¹)
RN14	1	4.73	3.40
RN16	4	3.73	4.05
RN1	6	3.48	7.33
RN17	8	3.36	12.70
RN18	12	3.26	7.20

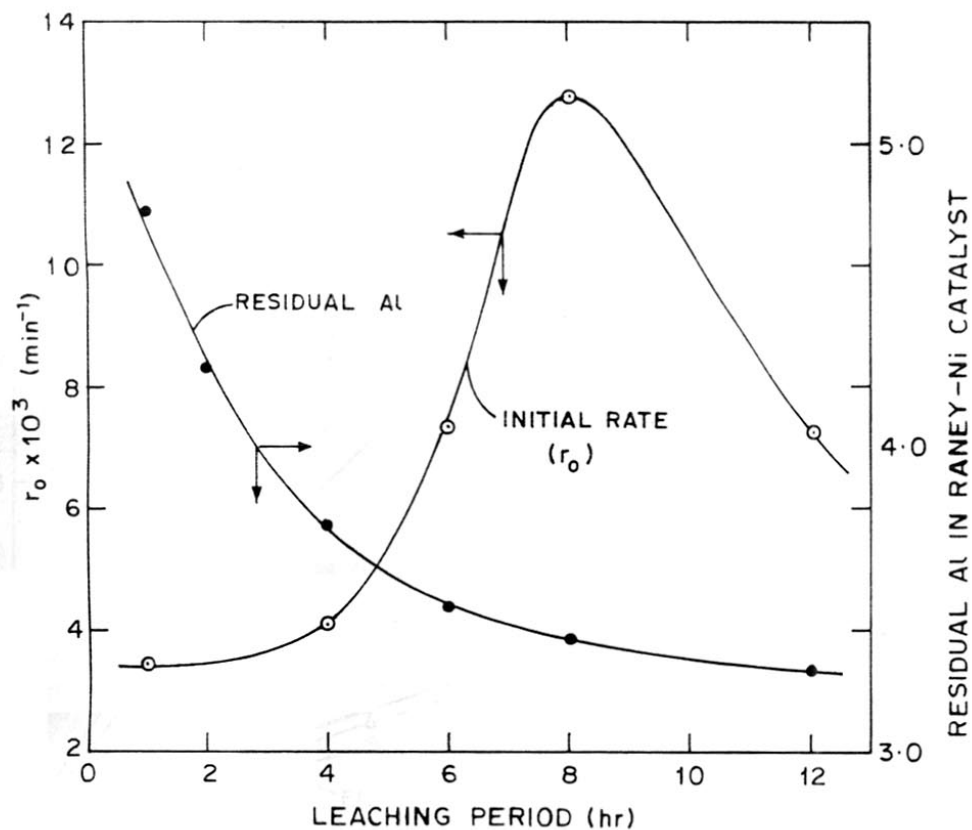


FIG. 2.11. DEPENDENCE OF THE INITIAL RATE (r_0) FOR THE HYDROGENATION OF *o*-NITROPHENOL AND THE RESIDUAL ALUMINIUM IN THE CATALYST ON THE LEACHING PERIOD EMPLOYED IN THE CATALYST PREPARATION

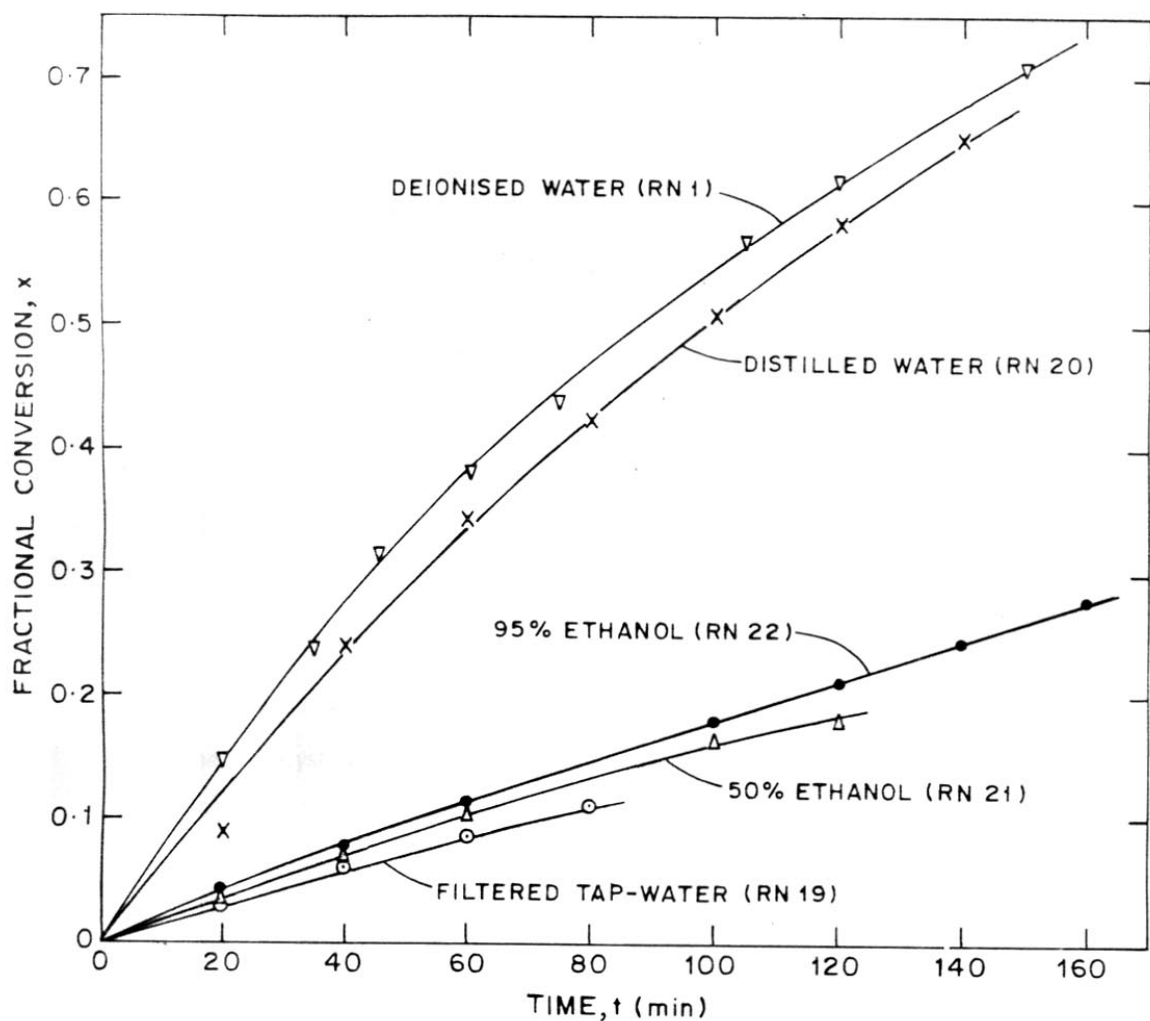


FIG. 2·12. ACTIVITY CURVES (x vs. t) FOR THE RANEY Ni CATALYST WASHED WITH DIFFERENT WASHING AGENTS AFTER THE LEACHING AT THE SAME CONDITIONS

respective solvents for 45-50 hr under H_2 atmosphere are presented in Table-2.6.

The results indicate that the activity of the Raney nickel catalysts (prepared at the same leaching conditions) depends strongly on the kind of the solvent used for its washing. Washing with deionised distilled water leads to the catalyst with the maximum activity. The activity of the catalysts obtained by using different washing agents is of the following order:

Deionised distilled water > distilled water > 95% ethanol >
50% ethanol > filtered tap water

2.3.6 Optimum conditions for preparation of the catalyst for the hydrogenation of ONP to OAP

Based on the above study the optimum conditions for the preparation of the catalyst with maximum activity [from the Raney alloy containing Ni 50 (wt %) - Al 50 (wt %)] for the hydrogenation process were found to be as follows.

Concentration of alkali	:	3.75 M NaOH
Leaching temperature	:	358 K
Duration of leaching	:	8 hr
Washing agent	:	deionised distilled water

The optimum conditions for the preparation of the catalyst are expected (7) to vary depending upon the organic compound to be hydrogenated, as the catalyst has a definite crystal size that is characteristic of the substance. In case of hydrogenation of p-nitrotoluene over a Raney nickel catalyst (14) the optimum preparation conditions for the catalyst

TABLE-2.6

INITIAL HYDROGENATION RATE DATA FOR THE CATALYSTS WASHED BY DIFFERENT SOLVENTS AFTER THEIR PREPARATION BY THE LEACHING

Common leaching conditions

Concentration of NaOH	:	10.0 mol.dm ⁻³
Leaching temperature	:	313 K
Leaching period	:	6 hr

Catalyst	Washing agent	Catalyst storage conditions	Initial reaction rate, $r_0 \times 10^3$ (min ⁻¹)
RN1	Deionised distilled water	Deionised distilled water under H ₂	7.33
RN19	Filtered tap water	Filtered tap water under H ₂	1.40
RN20	Distilled water	Distilled water under H ₂	6.00
RN21	50% Ethanol	50% Ethanol under H ₂	1.70
RN22	95% Ethanol	95% Ethanol under H ₂	1.9

* Catalysts stored for 45-50 hr

Note: The pH of the distilled water and the deionised distilled water was 5.5 and 6.7 respectively. The dilution of ethanol was done by the deionised distilled water.

giving maximum activity were found to be quite different.

Properties of the Raney nickel catalyst prepared under the above optimum conditions are given below.

Solid phase density ρ_s	:	8.10 g.cm^{-3}
Particle density ρ_p	:	332 g.cm^{-3}
Porosity (ϵ)	:	0.59
Bulk density ρ_b	:	1.04 g.cm^{-3}

The initial hydrogenation rate for the catalyst prepared under the optimum conditions was found to be $18.5 \times 10^{-3} \text{ min.}^{-1}$

2.4 EFFECT OF STORAGE CONDITIONS OF RANEY-Ni

It is well known that ageing affects the catalytic activity of Raney nickel. The ageing of the catalyst depends on the storing conditions, (viz. liquid medium, temperature and the gas atmosphere) under which it is aged or stored after its preparation by the leaching of aluminium from nickel-aluminium alloy with alkali.

Raney nickel catalysts (RN1) was prepared by leaching the nickel aluminium alloy with aqueous sodium hydroxide by the procedure described earlier under the following conditions.

Concentration of NaOH	:	$10.0 \text{ g.mol.dm}^{-3}$
Leaching temperature	:	313 K
Duration of leaching	:	6 hr
Washing agent	:	distilled deionised water

After its preparation, the catalyst was washed immediately with the solvent used for its storage and then stored in it under the desired gas atmosphere as follows. The catalyst to be stored under air was first

washed with the solvent and transferred along with the solvent to a conical flask with its side tube open to atmosphere, and the flask stoppered and kept at the room temperature or at the temperature of the refrigeration. The catalyst stored in hydrogen atmosphere was placed in a stoppered conical flask (provided with inlet and outlet for hydrogen) in the desired solvent. The air in the flask was flushed out by bubbling hydrogen through the liquid. After the flushing, the inlet was closed and a water seal was fitted to the outlet to prevent the back suction of air into the flask and any possible build-up in the pressure of hydrogen released by the reaction of residual aluminium in the catalyst with the solvent. The flask was then kept at the room temperature or at the temperature of the refrigerator. The average room temperature was about 303 K and the refrigerator temperature was 285 ± 3 K.

After the storage for the desired period the catalyst was removed from the storage vessel, washed free of the solvent with methanol and subjected to the activity measurement.

The experimental data on the measurement of the catalyst RN1 stored at different conditions are presented in Appendix-2.2.

The effect of the following catalyst storage conditions in the hydrogenation activity of Raney nickel has been studied.

1. Liquid medium (viz. deionised water, 95% ethanol and 5% aqueous NaOH).
2. Temperature (room temperature and temperature of refrigerator).
3. Gas atmosphere (H_2 and air).
4. Ageing period (0.5 - 240 days).

The results of the ageing of RN1 are given in Table-2.7.

The hydrogenation activity curves (fractional conversion vs time) for the catalyst stored in deionised distilled water under hydrogen for different period at room temperature (i.e. at 303 K) and in refrigerator (i.e. at 285 K) are shown in Fig. 2.13. The activity data for the catalyst stored in 95% ethanol under hydrogen for different periods at the room temperature and in the refrigerator are shown in Fig. 2.14. A storage time dependent activity of the catalyst (RN1) stored at the different conditions is shown in Fig. 2.15.

In case of the catalyst stored in 95% ethanol under hydrogen at room temperature or in refrigerator, the hydrogenation activity increases with the ageing period. However, when the catalyst is stored in deionised water under hydrogen at room temperature or in the refrigerator, its hydrogenation activity increases during the initial period and passes through a maximum with the increase in the ageing period. The maximum activity for the catalyst stored at the room temperature is observed at a ageing period of 30 days. While for the catalyst stored in refrigerator, its maximum activity is observed at a ageing period of 120 days. In the latter cases the observed maximum activity is much lower than that in the former case. Figure 2.16 shows the effect of the ageing temperature on the hydrogenation activity of the catalyst aged for the same period (30 days) in deionised distilled water under air and in 5% aqueous sodium hydroxide under hydrogen. In both the cases, the catalyst aged at room temperature gave better performance.

For the purpose of comparison, the initial rate data for the hydrogenation on the catalyst aged at different conditions for a period of 30 days

TABLE-2.7

DATA ON THE HYDROGENATION ACTIVITY OF RANEY-Ni (RNI) STORED AT DIFFERENT CONDITIONS

Preparation conditions of RNI

Concentration of NaOH : 10 g.mol.dm⁻³
 Temperature of leaching : 313 K
 Leaching period : 6 hr
 Washing agent : deionised distilled water

Catalyst No.	Storage conditions			Ageing periods (d)	Initial reaction rate $r_0 \times 10^3$ (min ⁻¹)
	Liquid medium	Gas atmosphere	Temperature (K)		
1	2	3	4	5	6
RNI(1)	Deionised distilled water	hydrogen	303 (av)	0.5	7.33
RNI(2)	"	"	"	7.0	6.60
RNI(3)	"	"	"	14.0	9.80
RNI(4)	"	"	"	30.0	11.70
RNI(5)	"	"	"	120.0	7.29
RNI(6)	"	"	285 (av)	30.0	4.60
RNI(7)	"	"	"	120.0	7.69
RNI(8)	"	"	"	240.0	6.85

.....

Table-2.7 contd.

1	2	3	4	5	6
RNI(9)	deionised distilled water	air	303 (av)	30	5.46
RNI(10)	"	"	285 (av)	30	4.16
RNI(11)	95% ethanol	hydrogen	303 (av)	14.0	-
RNI(12)	"	"	"	30.0	3.73
RNI(13)	"	"	"	120.0	-
RNI(14)	"	"	285 (av)	30.0	2.45
RNI(15)	"	"	"	120.0	-
RNI(16)	5% NaOH	hydrogen	303 (av)	30.0	3.30
RNI(17)	"	"	285 (av)	30.0	2.24

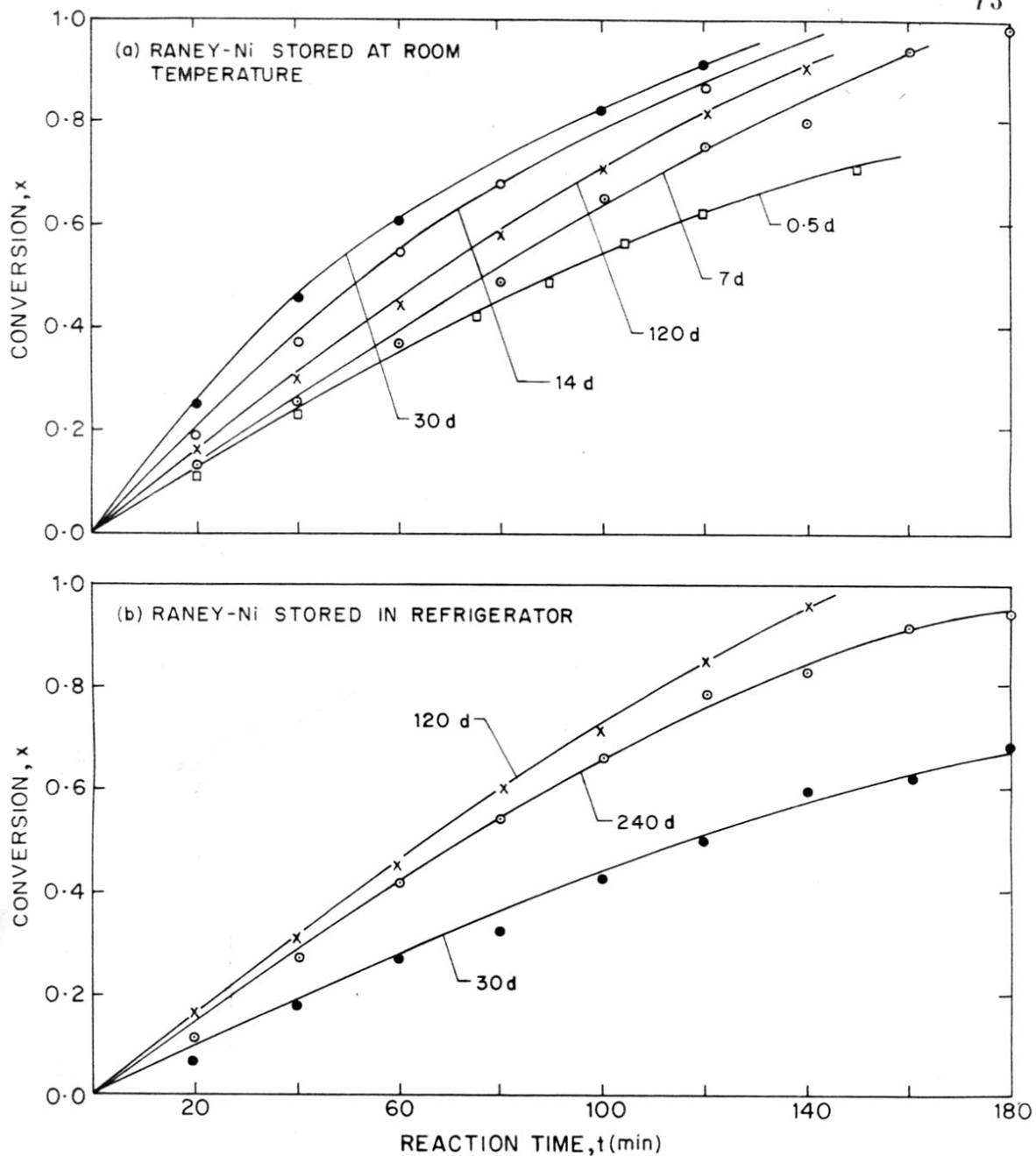


FIG.2.13: ACTIVITY CURVES (x vs. t) FOR THE RANEY-Ni STORED IN DEIONISED WATER UNDER HYDROGEN AT (a) ROOM TEMPERATURE (b) IN REFRIGERATOR FOR DIFFERENT PERIODS

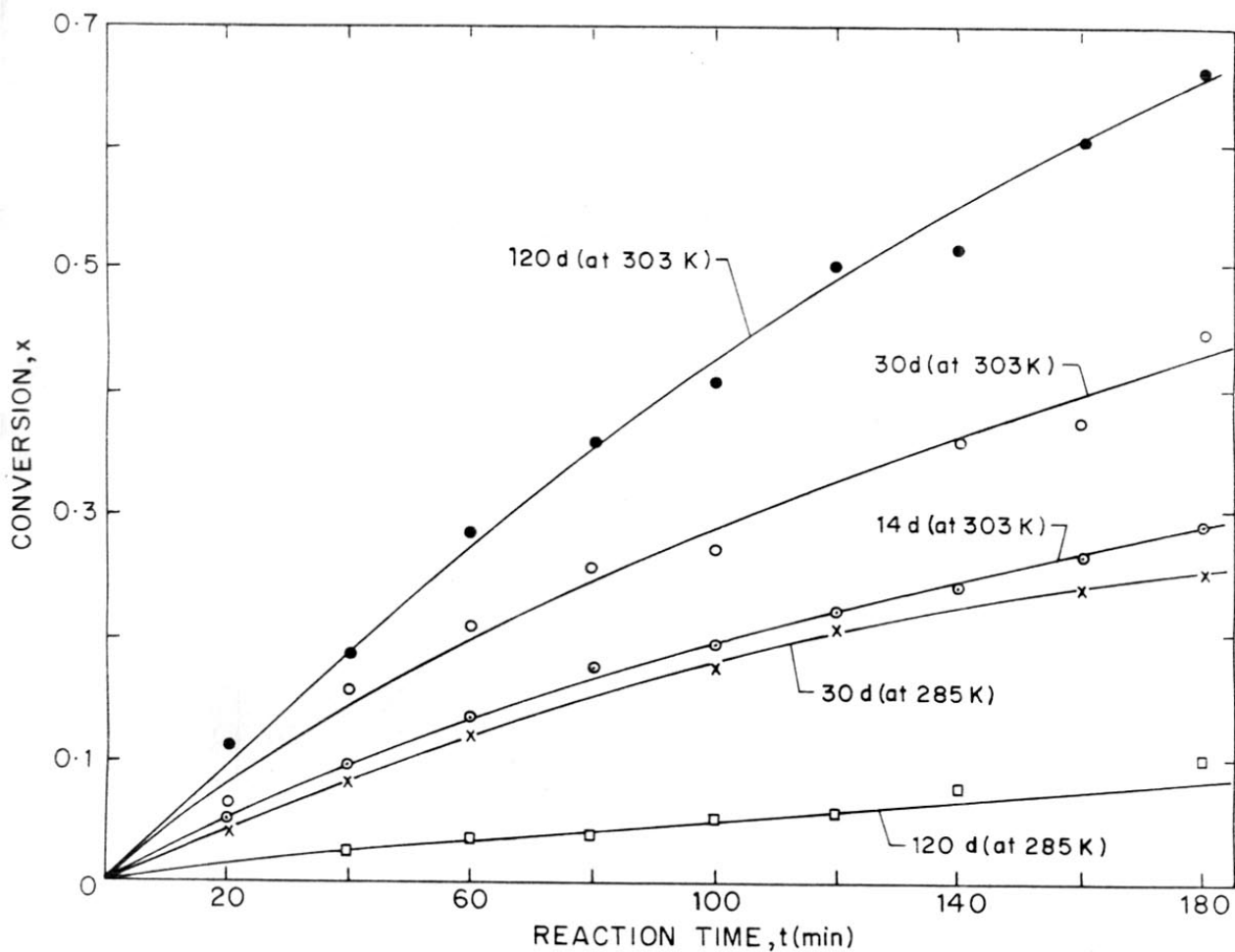


FIG.2-14: THE ACTIVITY CURVES (x vs. t) FOR RANEY-Ni STORED IN 95% ETHANOL UNDER H_2 AT DIFFERENT TEMPERATURES AND PERIODS

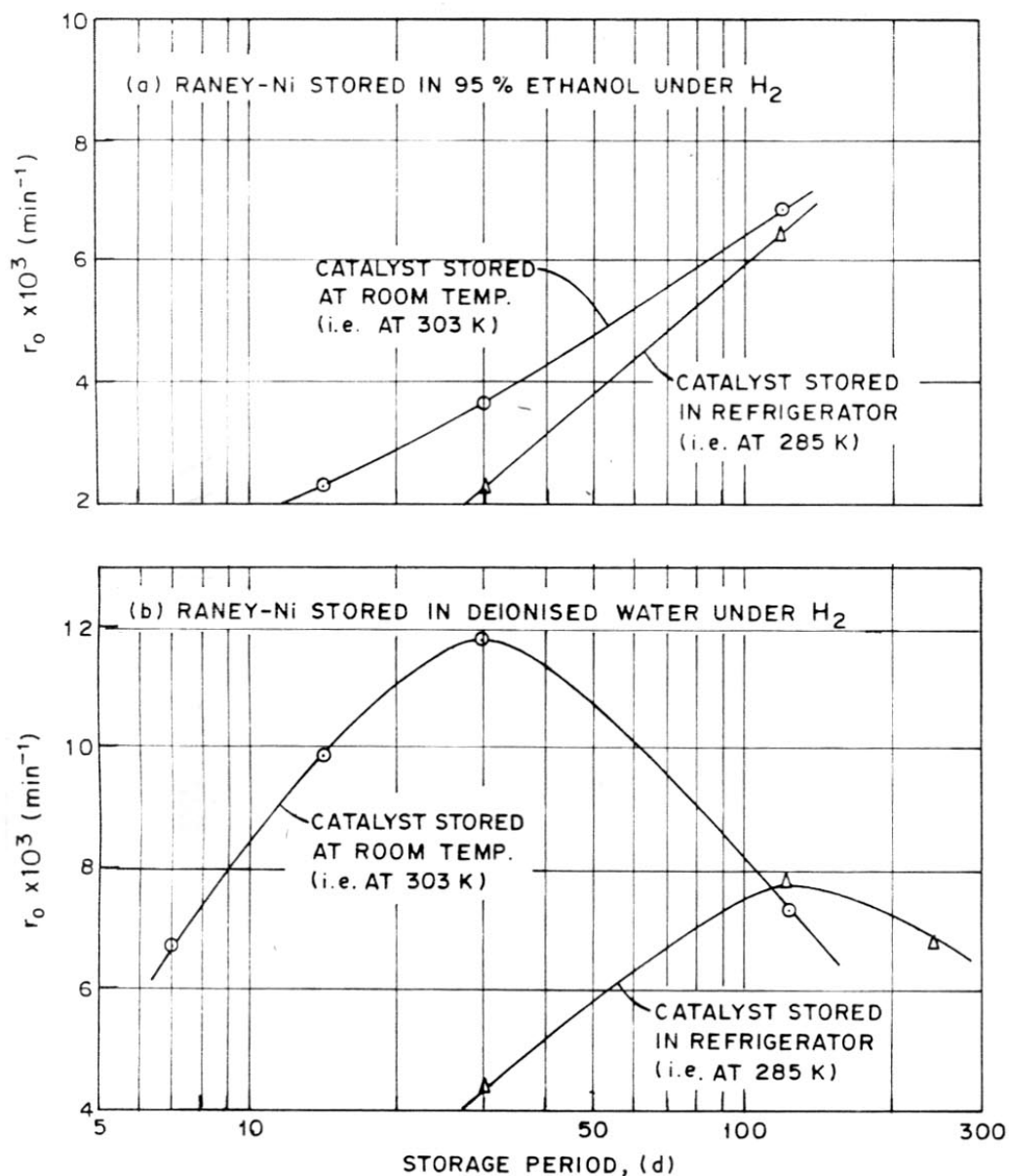


FIG. 2.15. STORAGE TIME DEPENDENCE OF THE CATALYST ACTIVITY OF RANEY-Ni (RN 1) STORED AT THE DIFFERENT CONDITIONS

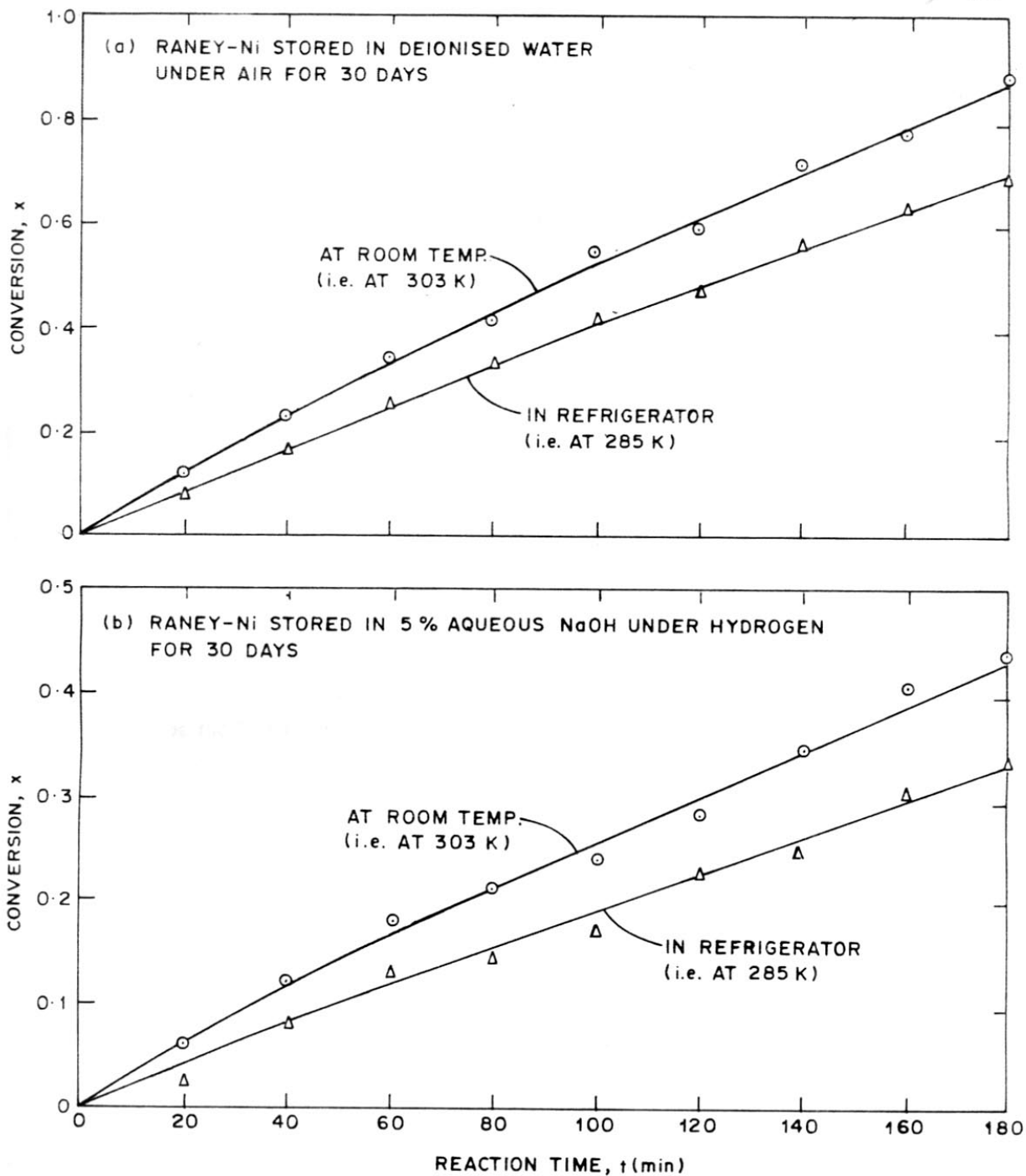


FIG. 2.16. ACTIVITY CURVES (x vs. t) FOR THE RANEY-Ni STORED IN WATER AND AQUEOUS NaOH

are presented in Table-2.8. The results indicate that the catalyst stored in deionised water under hydrogen at room temperature possess highest activity for the hydrogenation.

It can be noted from the above observations that the hydrogenation activity of the catalyst depends on the net effect produced by all the catalyst storage conditions (i.e. liquid medium, temperature, gas atmosphere and ageing period).

Based on the above results the following generalization can be made regarding the effect of the various storage conditions on the activity of the catalyst for the hydrogenation process.

Effect of storage medium

The catalyst is very strongly influenced by the liquid medium, employed for the catalyst stored. Deionised distilled water is found to be the best medium for this purpose.

The choice of medium lies in the following order.

Deionised distilled water \gg 95% ethanol $>$ 5% aqueous NaOH

This may be because of the high rate of the crystal growth of the catalyst in the presence of deionised water (26) as compared to that in the presence of the other solvents.

Effect of gas atmosphere

The catalyst stored under hydrogen atmosphere possess higher catalytic activity than that stored under air. Thus the initial reaction rate (r_0) for the catalyst stored under hydrogen atmosphere at 303 K is $11.70 \times 10^{-3} \text{ min}^{-1}$ and for the one stored under air atmosphere it is

TABLE-2.8

INITIAL REACTION RATE DATA FOR THE HYDROGENATION ON THE RANEY-Ni AGED FOR 30 DAYS AT DIFFERENT CONDITIONS

Solvent	Ageing conditions		$r_0 \times 10^3$ (min^{-1})
	Gas atmosphere	Temperature	
Deionised water	H_2	303	11.70
Deionised water	H_2	285	4.56
Deionised water	air	303	6.10
Deionised water	air	285	4.24
95% Ethanol	H_2	303	3.73
95% Ethanol	H_2	285	2.45
5% Sodium hydroxide	H_2	303	3.30
5% Sodium hydroxide	H_2	285	2.24

$6.10 \times 10^{-3} \text{ min}^{-1}$, the storage medium (deionised distilled water) being the same for both the cases. The same trend is also repeated for the catalyst stored at 285 K temperature. This is expected mostly due to the poisoning of the catalyst by the chemisorption of oxygen when it is stored under air atmosphere.

Effect of temperature

The ageing at room temperature (303 K) results in the catalyst with much higher activity than that observed for the catalyst stored in the refrigerator (285 K). Further, the ageing period required for attaining the maximum hydrogenation activity for the catalyst stored at room temperature is much smaller (30 days) than that (120 days) required when it is stored at the refrigerator temperature. This is expected because of the higher rate of the crystal growth of the catalyst at room temperature than that at the temperature of the refrigerator.

Effect of ageing period

The dependence of the catalytic activity on the ageing period (Fig. 2.15) points to the fact that (i) the effect of the ageing period on the catalytic activity depends strongly on the liquid medium and the ageing temperature and (ii) the catalyst ageing to a certain extent is advantageous.

The ageing is expected to affect the catalyst surface properties because of (i) the reaction of the liquid medium with the residual aluminium in the catalyst, thus forming new catalytic sites and (ii) the increase in the crystallite size due to the crystal growth.

Ishikawa (7) has observed that Raney nickel, having its maximum activity for the hydrogenation of a particular substance has a definite

crystal size characteristic of the substance. Thus the hydrogenation activity of the catalyst is strongly affected by its crystal size, which is controlled by the conditions employed for its storage.

2.4.1 Ageing of the Raney-Ni Catalyst Prepared Under Optimum Leaching and Washing Conditions

The activity curves (x vs t) for the catalyst prepared under optimum conditions (given earlier in Section-2.3.2.6) and stored in deionised water under hydrogen for different periods are presented in Fig. 2.17 and the values of the initial reaction rate (r_0) are given in Table-2.9. The variation of the initial reaction rate for the catalyst with its storage period is presented in Fig. 2.18.

The results indicate that the activity of the Raney nickel catalyst increases initially and passes through a maximum at a storage period of about 140 hr and then reduces sharply with the further increase in the storage period.

2.4.2 Comparison of Optimum Preparation and Storage Conditions of Raney-Ni for Different Hydrogenation Processes

The optimum preparation and storage conditions of Raney-Ni giving maximum activity in the hydrogenation of *p*-nitrotoluene (to *p*-toluidine) and *o*-nitrophenol (to *o*-aminophenol) are compared in Table-2.10. It may be noted that both the hydrogenation reactions were carried out simultaneously using Raney nickel catalyst from the same lot, when the effect of a particular catalyst preparation or storage parameter was to be studied. The data in Table-2.10 very clearly indicate that the optimum catalyst preparation conditions (except the washing agent) for the two hydrogenation reactions are quite different. As far as the optimum storage conditions

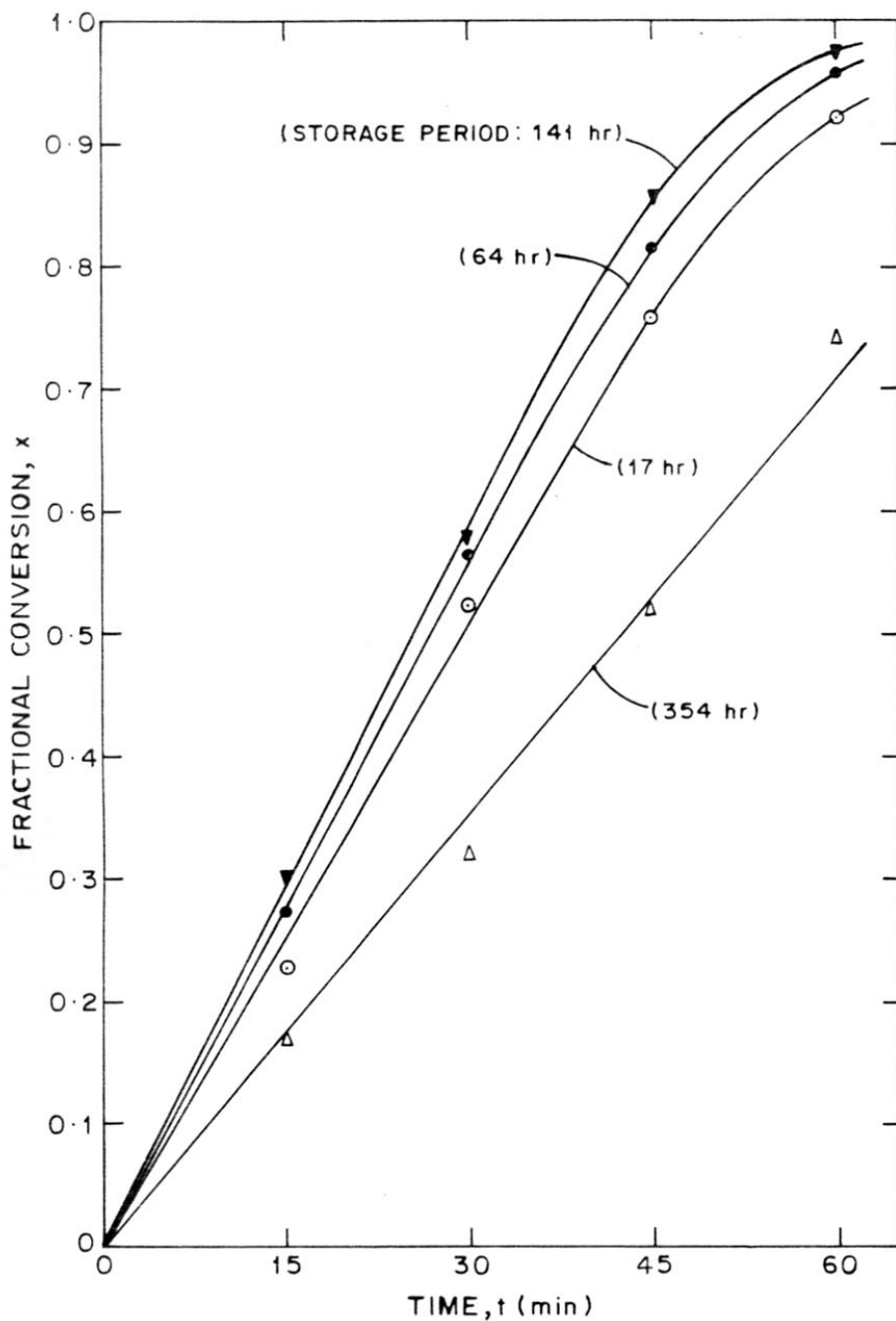


FIG. 2-17. THE ACTIVITY CURVES (x vs. t) FOR THE CATALYST RN 23 (PREPARED UNDER THE OPTIMUM CONDITIONS) SHRED IN DEIONISED WATER UNDER H_2 AT DIFFERENT PERIODS

TABLE-2.9

INITIAL HYDROGENATION RATE DATA FOR THE CATALYST PREPARED UNDER THE OPTIMUM CONDITIONS AND STORED IN DEIONISED DISTILLED WATER UNDER H_2 FOR DIFFERENT PERIODS

Optimum preparation conditions of the catalyst (RN23)

Concentration of NaOH	:	3.75 M
Leaching temperature	:	358 K
Leaching period	:	8 hr
Washing agent	:	deionised distilled water
Storage medium	:	deionised distilled water
Gas atmosphere	:	H_2

Catalyst no.	Storage period (hr)	Initial reaction rate $r_o \times 10^3$ (min^{-1})
RN23 (1)	17	17
RN23 (2)	64	19
RN23 (3)	141	20
RN23 (4)	354	12

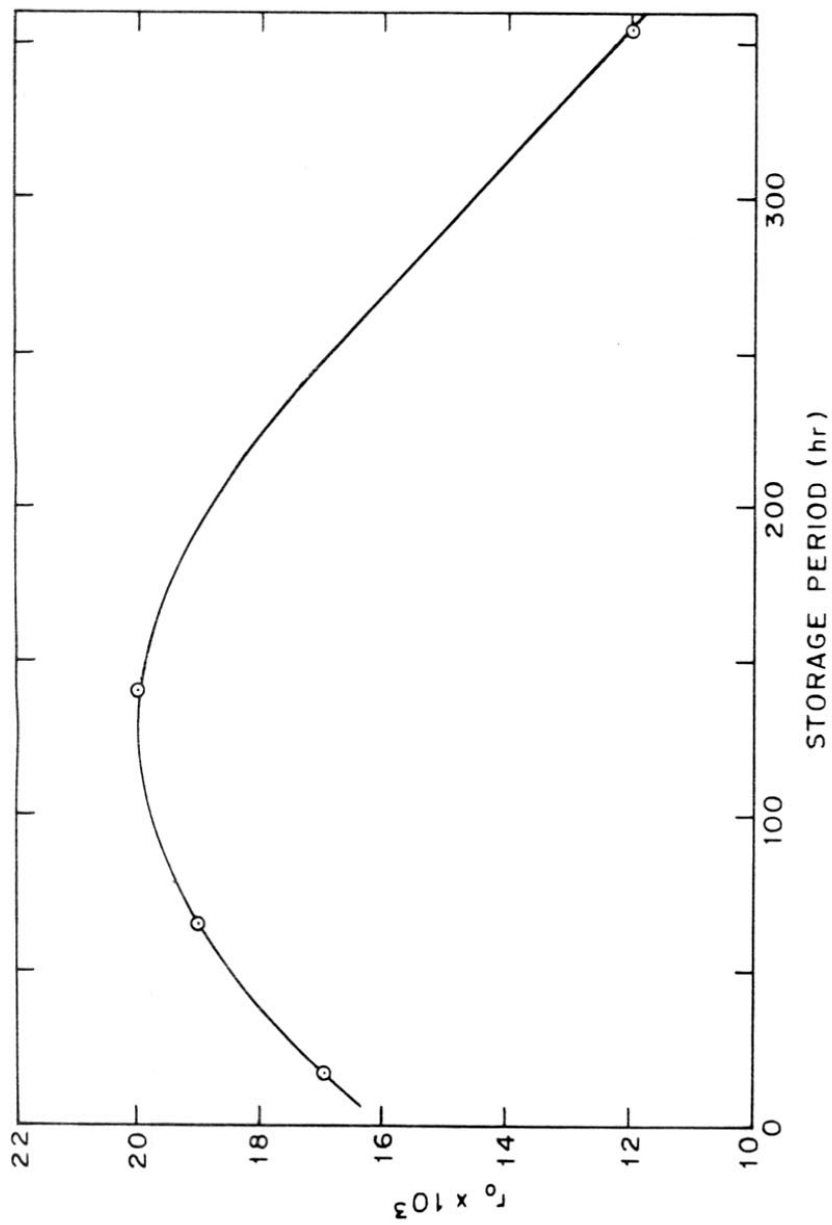


FIG. 2-18. THE VARIATION IN THE HYDROGENATION ACTIVITY (r_0) OF THE CATALYST RN 23 (PREPARED UNDER THE OPTIMUM CONDITIONS) WITH THE STORAGE PERIOD

TABLE-2.10

OPTIMUM PREPARATION AND STORAGE CONDITIONS OF RANEY NICKEL
GIVING MAXIMUM ACTIVITY IN THE HYDROGENATION OF p-NITRO-
TOLUENE AND o-NITROPHENOL

	Hydrogenation of p-nitrotoluene (14)	Hydrogenation of o-nitrophenol
<u>Optimum catalyst preparation conditions</u>		
Concentration of NaOH	6.25 mol.dm ⁻³	3.75 mol.dm ⁻³
Leaching temperature	313 K	358 K
Leaching period	2.5 hr	8 hr
Washing agent	deionised distilled water	deionised distilled water
<u>Optimum catalyst storage conditions of RN1</u>		
Liquid medium	deionised distilled water	deionised distilled water
Gas atmosphere	H ₂ atmosphere	H ₂ atmosphere
Temperature	room temperature (303 K)	room temperature (303 K)
Ageing period	2-3 days	30 days

are concerned, the liquid medium, gas atmosphere and temperature for the storage of the catalyst is same but the ageing periods required for attaining the maximum catalytic activity are different for the two hydrogen processes. These observations lead to the conclusion that the optimum preparation and storage conditions of Raney-Ni vary from a compound (which is to be hydrogenated) to compound.

REFERENCES

1. Taylor, A., Weiss, J., *Nature* 141 (1938) 1055.
2. Freel, J., Pieters, W.J.M. and Anderson, R.B., *J. Catal.* 16 (1970), 281.
3. Yasumura, J., *Kagaku No Kyoiki*, 6 (1952) 733.
4. Csuros, Z. and Petro, J., *Acta Chem. Acad. Sci. (Hung)*, 17 (1958) 289 (English).
5. Kagan, A.S. and Kagan, N.M., Ul'yomov, G.D., Mironov, L.G., (USSR), *Zh. Fiz. Khim.* 47(7) (1973) 1729.
6. Petrov, B.F. and Fasman, A.B., *Zh. Prikl. Khim.* 47(4) (1974) 496, (Russ).
7. Ishikawa, J., *Nippon Kagaku Zasshi*, 82 (1961) 135.
8. Freidlin, L.K. and Rudheva, K.G., *Vaprosy Khim. Kineti, Kalaiizai Reaktisionoi. Sposobnosti, Akad. Nauk. (USSR)* (1955), 557.
9. Yakubunok, E.F., Podvyazhin, Yu. A. and Yuekelison, I.I., *Zn. Prikl. Khim.* 42(11) (1969) 2605 (Russ).
10. Davtyan, O.K., Misyuk, E.G. and Makordei, R.I., *Elektrokhimiya*, 7 (11) (1971) 1595 (Russ).
11. Misyuk, E.G., Davtyan, O.K., Semizoroya, N.F. and Makordei, R.I., *Elektrokhimiya* 7 (11) (1971) 1601 (Russ).
12. Kubomatsu, T. and Kagaku, To, *Kogyo* 31 (1957) 190.
13. Ishikawa, J., *Nippon Kagaku Zasshi* 81 (1960) 1629.
14. Choudhary, V.R., Chaudhari, S.K. and Sane, M.G., 'Advances in Catalysis - Science and Technology, Ed. T.S.R. Prasad Rao, Wiley Eastern Ltd., New Delhi (1985) 171.
15. Yasumura, J., *Kagaku to Kogyo*, 23 (1949) 99.
16. Smith, H.A., Badoit, W.C. and Fuzek, J.F., *J. Am. Chem. Soc.*, 71 (1949) 3769.

17. Shripati Rao, H., Narsimhan, P., Chari, K.S. and Agarwal, J.S., *Indian J. Technol.* 2 (1964) 21.
18. Orito, Y., Imai, S. and Niwa, S., *Tokyo Shikensho Hokokuo*, 60, (1965) 242.
19. Dominguez, X.A., Lopex, I.C. and Franco, R., *J. Org. Chem.* 26, (1961) 1626.
20. Choudhary, V.R. and Chaudhari, S.K., *J. Chem. Tech. Biotech.* 32 (1982) 925.
21. Chaudhari, S.K., 'Studies on Raney nickel catalysts', Ph.D. Thesis, University of Poona, Pune 1981.
22. Schnyder, A., Dissertation, Polytechnique Institute of Brooklyn, (1962).
23. Smith, H.A. and Fuzek, J.E., *J. Am. Chem. Soc.*, 68 (1946) 229.
24. Klug, H.P. and Alexander, L.E., in 'X-ray Diffraction Procedures for Polycrystalline and Amorphous Materials', John Wiley and Sons, Inc., London (1954) 491.
25. Siggia, S., 'Quantitative Organic Analysis via Functional Groups' 3rd Edn. John Wiley and Sons, Inc., New York and London (1963), 526.
26. Kubomatsu, T., Kishida, S. and Kanishi, K., *Kogaku to Kogyo*, (Osaka), 37 (1963) 382.

PART-III

HYDROGENATION OF o-NITROPHENOL ON Pd-CARBON

CHAPTER-3.1

CHAPTER-3.1

EXPERIMENTAL

3.1.1 MATERIALS

Activated carbon (washed with 50% HNO_3 and then with deionised distilled water till free from acid and dried at 423 K in vacuum oven for 24 hr)

PdCl_2 (99% pure 60% Pd) (SISCO)

Formaldehyde (AR, BDH, 40% solution)

Water (deionised distilled)

HCl (AR, BDH)

KI (AR, BDH)

Methanol (AR, BDH dried over 3A molecular sieves)

Ethanol (AR, dried over 3A molecular sieves)

n-Propanol (AR, freshly distilled)

o-Nitrophenol (AR, German repacked)

o-Aminophenol (AR, Volro repacked)

Thiophene (Riedel)

Dichloroethane (E. Merck)

Mercuric chloride (AR, BDH)

Mercuric acetate (AR, BDH)

Lead acetate (AR, BDH)

Zinc acetate (LR, BDH)

Hydrogen (IOLAR II, obtained from M/s. IOL, Bombay)

Nitrogen (IOLAR, II, obtained from M/s. IOL, Bombay)

3.1.2 CATALYST PREPARATION

The activated carbon (before its use in the catalyst preparation) was pretreated with 50% HNO_3 solution and washed with deionised distilled water. The residual acidity was neutralized by sodium carbonate solution and the carbon was thoroughly washed with deionised distilled water. It was then dried at 423 K in vacuum oven for 24 hr. The pretreated carbon has the following surface properties:

Sp. surface area	:	$678 \text{ m}^2 \text{ g}^{-1}$
Particle density	:	0.82 g.cm^{-3}
Pore volume	:	$0.68 \text{ cm}^3 \text{ .g}^{-1}$
Porosity	:	0.56

The Pd-carbon catalysts containing Pd at different concentrations (0.2 - 4.62 wt % Pd on carbon) were prepared by impregnating the pretreated activated carbon with PdCl_2 from its very dilute acidic (HCl) solution at 368 K, filtering and washing the impregnated carbon with deionised distilled water and reducing the impregnated catalyst with alkaline formaldehyde solution at 368 K. The reduced catalyst is then filtered and washed thoroughly with deionised distilled water and dried in vacuum at 373 K for 4 hr.

The catalyst impregnation was carried out in a two liter beaker provided with a stirrer and a burette for adding the PdCl_2 solution. About 50 g of the activated carbon and 500 cm^3 of distilled water was introduced in the beaker and the slurry was heated on a water bath to a temperature of 368 K. Then a desired volume of 2% PdCl_2 acidic (HCl) solution was added to the slurry at a rate of about 2 cm^3 of the PdCl_2 solution per minute, while constantly stirring the slurry. After the addition of all the

PdCl_2 solution, the carbon- PdCl_2 solution system was stirred for one hr at 368 K, and then it was kept at room temperature for 24 hr for the completion of adsorption of PdCl_2 . The impregnated carbon was then filtered and washed with the water and the filtrate was analysed for Pd by the titration against standard KI solution using iodide ion selective electrode. The amount of PdCl_2 impregnated on the carbon was obtained by the material balance. The catalyst was reduced by alkaline formaldehyde at a pH of 11. After the reduction, the catalyst was washed thoroughly with the water till free from alkali, filtered, dried at 373 K for 4 hr in vacuum oven and stored in a desiccator.

3.1.3 CATALYST CHARACTERISATION

3.1.3.1 Measurement of Particle Density, Solid Phase Density, Pore Volume and Porosity

These properties were measured using the specific gravity bottle methods (1).

A known weight of the catalyst (about 2-3 g) free from adsorbed water is boiled with cyclohexane (AR, BDH) for about 30 min to remove the air trapped in the pores, cooled to room temperature and transferred quantitatively to a specific gravity bottle. Rest of the volume of the specific gravity bottle is filled with the liquid and the bottle is weighed with its contents. The liquid from the bottle is then completely drained out, care being taken to ensure that no solid is lost. The bottle with the solid with its pores filled with the liquid is weighed.

The particle density (ρ_p), solid phase density (ρ_s), and pore volume (P_v) are obtained by the use of the following expressions:

$$\rho_p = (w \rho_l) / (x_1 + x_3 - x_2 - x_0) \quad (1)$$

$$\rho_s = (w \rho_l) / (x_1 - x_2 + w) \quad (2)$$

and

$$P_v = (x_3 - x_0 - w) / (w \rho_l) \quad (3)$$

where

- x_0 = weight of empty specific gravity bottle (g)
- x_1 = weight of specific gravity bottle filled with pure liquid (g)
- x_2 = weight of specific gravity bottle + catalyst with all its pores filled with cyclohexane + the make up liquid (g)
- x_3 = weight of specific gravity bottle + catalyst with all its pores filled with cyclohexane (g)
- ρ_l = density of the cyclohexane (g.cm^{-3})
- w = weight of catalyst (g)
- P_v = pore volume ($\text{cm}^3.\text{g}^{-1}$) of the catalyst

The above methods were used for measuring ρ_p , ρ_s and P_v of the pretreated carbon (particle size : 2-3 mm). However, in case of the Pd-carbon catalysts (particle size : 30-180 μm), only their solid phase density was determined by the above method; whereas their particle density was measured using the mercury displacement method described earlier in Part-II. The porosity was determined from the knowledge of ρ_s , ρ_p and P_v as follows:

$$\epsilon = \rho_p P_v \quad (4)$$

$$\epsilon = (\rho_s / P_v) / (1 + \rho_s P_v) \quad (5)$$

and

$$\epsilon = [(1 - (\rho_p / \rho_s))] \quad (6)$$

3.1.3.2 Measurement of Surface Area

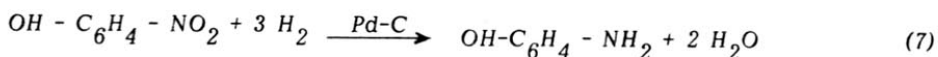
The specific surface area of the activated carbon and Pd-carbon catalysts was determined by the single point BET method by measuring adsorption of nitrogen at liquid nitrogen temperature and at a nitrogen concentration of 30 mol % (balance Helium) using a Monosorb Surface Area Analyser (Quanta Chrome Corporation, USA) based on dynamic adsorption/desorption technique. The solid samples were heated at 573 K for 1 hr *in situ* before the N₂ adsorption.

3.1.3.3 Scanning Electron Microscopy

The catalysts were examined by a Cambridge Stereoscan Model 150 Scanning Electron Microscope.

3.1.4 EXPERIMENTAL SET UP AND PROCEDURE FOR CARRYING OUT THE HYDROGENATION REACTION

The hydrogenation reaction,



was carried out in an agitated high pressure batch reactor (made up of 316 stainless steel). The experimental set up for the hydrogenation reaction is shown schematically in Fig. 3.1.1. It consists mainly of a high pressure stirred reactor (Parr Autoclave, obtained from Parr Instruments Co. USA) (capacity 2.0 dm³) and an intermediate H₂-pressure vessel (capacity: 1.27 dm³). The reactor is provided with a three blade (twisted blade type) stirrer (blade diameter: 5.5 cm; location of stirrer blades: 2.8 cm above the bottom of the reactor), a cooling coil, a thermowell, a H₂-inlet tube, a pressure gauge, a safety valve and a gas outlet valve. A photograph of the experimental

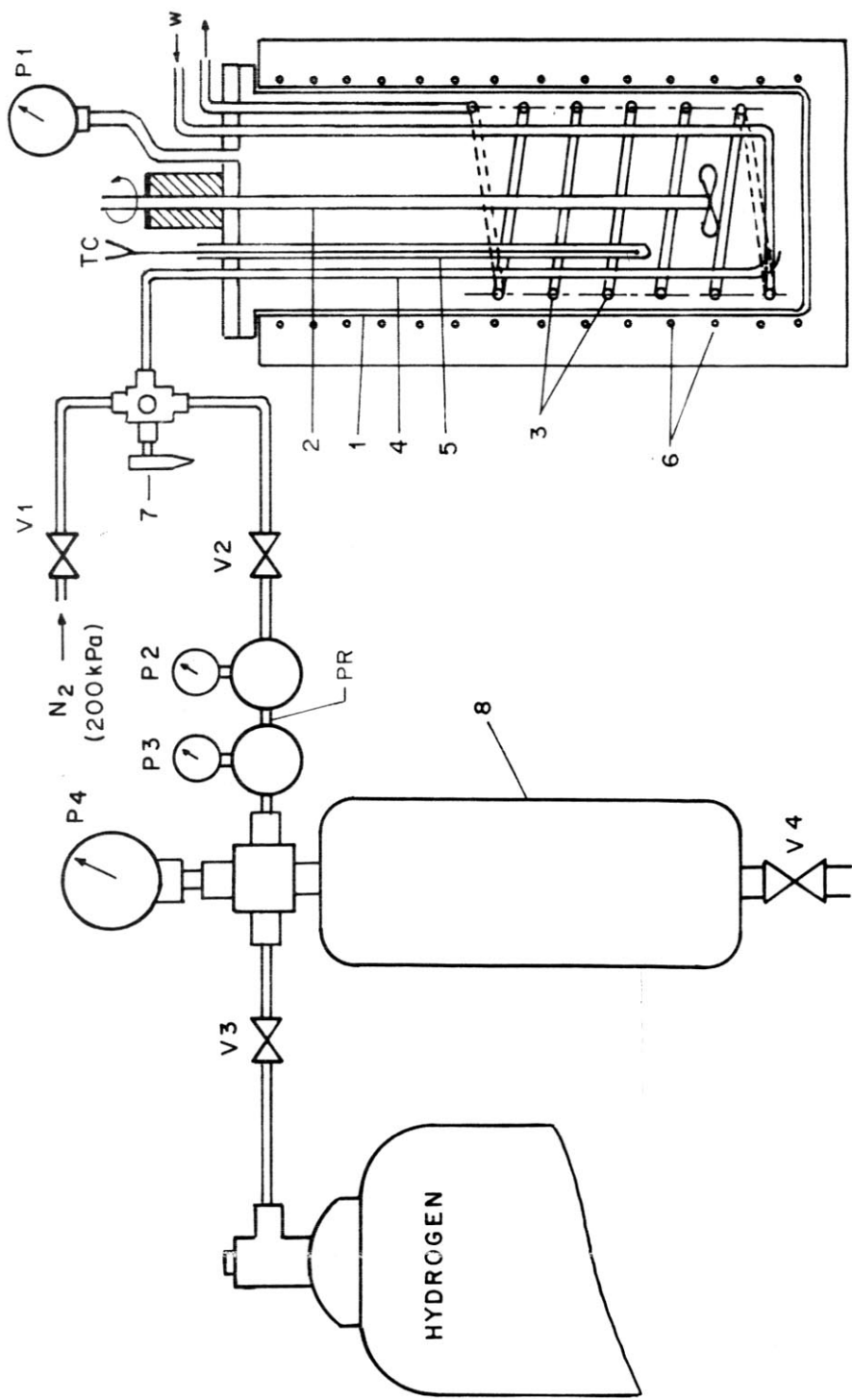


FIG. 3.1.1. EXPERIMENTAL SET-UP FOR THE HYDROGENATION OF O-NITROPHENOL

- 1 - HIGH PRESSURE PARR AUTOCLAVE (i.d.=10cm ; height= 26.7cm , capacity= 2 dm³),
- 2 - STIRRER , 3-COOLING COIL (coil dia. = 9.0 cm ; no. of coils = 2 ; tube id = 0.4 cm),
- 4 - H₂ - INLET TUBE , 5 - THERMOWELL , 6 - HEATING ELEMENTS , 7- THREE WAY BALL VALVE ,
- 8 - INTERMEDIATE PRESSURE VESSEL (capacity= 1.27 dm³), P - PRESSURE GAUGE ,
- V - NEEDLE VALVE , TC - THERMOCOUPLE , PR - TWO STAGE PRESSURE REGULATOR

assembly for the hydrogenation reaction is shown in Fig. 3.1.2.

The reactor temperature could be maintained at a desired constant value by using a temperature controller and removing the heat of the exothermic hydrogenation reaction by circulating water at the temperature: 1-2 K lower than the reaction temperature through the cooling coils immersed in the reaction mixture. The reaction temperature could be controlled within ± 0.3 K. The hydrogen pressure in the reactor could be maintained at a constant value with the help of the two stage pressure regulator (Fig.3.1.1).

The experimental procedure followed for carrying out the hydrogenation reaction is given below.

A 1.0 dm^3 of reaction mixture consisting of *o*-nitrophenol, the catalyst and solvent (or reaction medium) is introduced in the reactor and it was made leak proof. The reactor was then first flushed with N_2 at atmospheric pressure to remove the air in the reactor and then it was pressured with N_2 to check the leakage. After confirming that there is no gas leakage, the reactor was flushed with H_2 at atmospheric pressure by passing about 10 dm^3 of H_2 in the absence of stirring to drive off the N_2 in the reactor. After this is done, reactor gas outlet valve is closed and a desired reaction temperature is attained. The H_2 pressure in the reactor was then increased from the atmospheric pressure to a desired value and the reaction was allowed to proceed at a constant H_2 pressure by starting the stirring. The progress of the reaction was followed by measuring the fall in the pressure of H_2 in the intermediate vessel as a function of time. It may be noted that the reaction was carried out at a constant H_2 pressure. The consumption of H_2 in the hydrogenation reaction, as a function of

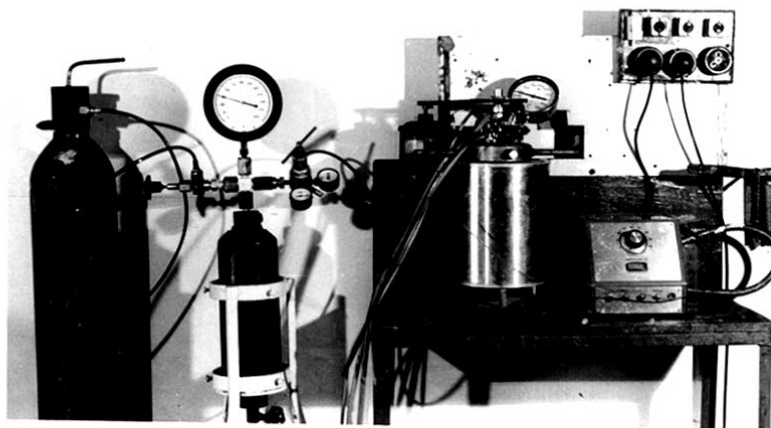


FIG. 3-1-2. A PHOTOGRAPH OF THE EXPERIMENTAL REACTOR ASSEMBLY FOR THE HYDROGENATION REACTION

time, was estimated from the change in the H_2 pressure in the intermediate vessel and also knowing the volume of the intermediate vessel, H_2 compressibility factor and the temperature of the gas.

The fractional conversion of ONP to OAP or the concentration of ONP in the reaction mixture as a function of time was estimated from the reaction stoichiometry.

The H_2 pressure in the intermediate vessel before the start of the reaction was always kept to be about 3500 kPa, so that at any stage of the reaction, the pressure in the intermediate vessel was much higher than the pressure in the reactor.

The material balance between the H_2 consumed in the reaction and the H_2 required as per the conversion of ONP to OAP (measured independently by chemical analysis of the reaction mixture) was found to be very good.

3.1.5 MEASUREMENT OF ADSORPTION OF REACTION SPECIES

Single component adsorption of *o*-nitrophenol (ONP), *o*-aminophenol (OAP) and water from their respective solution in methanol and also simultaneous two component (or binary) adsorption of ONP and OAP from their mixture in methanol on the Pd-carbon (4.62 wt % Pd) have been measured experimentally at the temperatures (278-308 K) at which the catalytic hydrogenation reaction occurs. The detailed experimental procedures for the single and two component adsorption are given below.

Methanol has high vapour pressure at the higher adsorption temperature (308 K) and hence the adsorption tube provided with teflon stopper

and injection port arrangement (as shown in Fig. 3.1.3) was used for the measurement of the adsorption.

3.1.5.1 Single Component Adsorption

A known weight (0.5-1.5 g) of the Pd-C catalyst (particle size 30 μm) was introduced in each of the eight adsorption tubes mounted on a stand kept immersed in a constant temperature water bath. The catalyst in the adsorption tubes was equilibrated with 25 cm^3 of the solution of an adsorbate in methanol at different concentrations for a period of 6 hr, which was found to be more than sufficient to establish the adsorption equilibrium. During this period, the solution with the catalyst was shaken manually at the interval of 5 min inside the water bath. The catalyst was allowed to settle and the liquid samples were taken out with a syringe for the chemical analysis.

The amount of the solute adsorbed on the catalyst was obtained from the initial and final (at equilibrium) concentration of the adsorbate in the solution using the relation,

$$q = V (C_i - C_e) / W \quad (8)$$

where

- q = amount of solute adsorbed, mmol.g^{-1}
- V = volume of the solution, cm^3
- C_i = initial concentrations adsorbate, mmol.cm^{-3}
- C_e = equilibrium concentration of adsorbate, mmol.cm^{-3}
- W = weight of the catalyst, g .

The analysis of ONP and OAP in their methanol solution was done

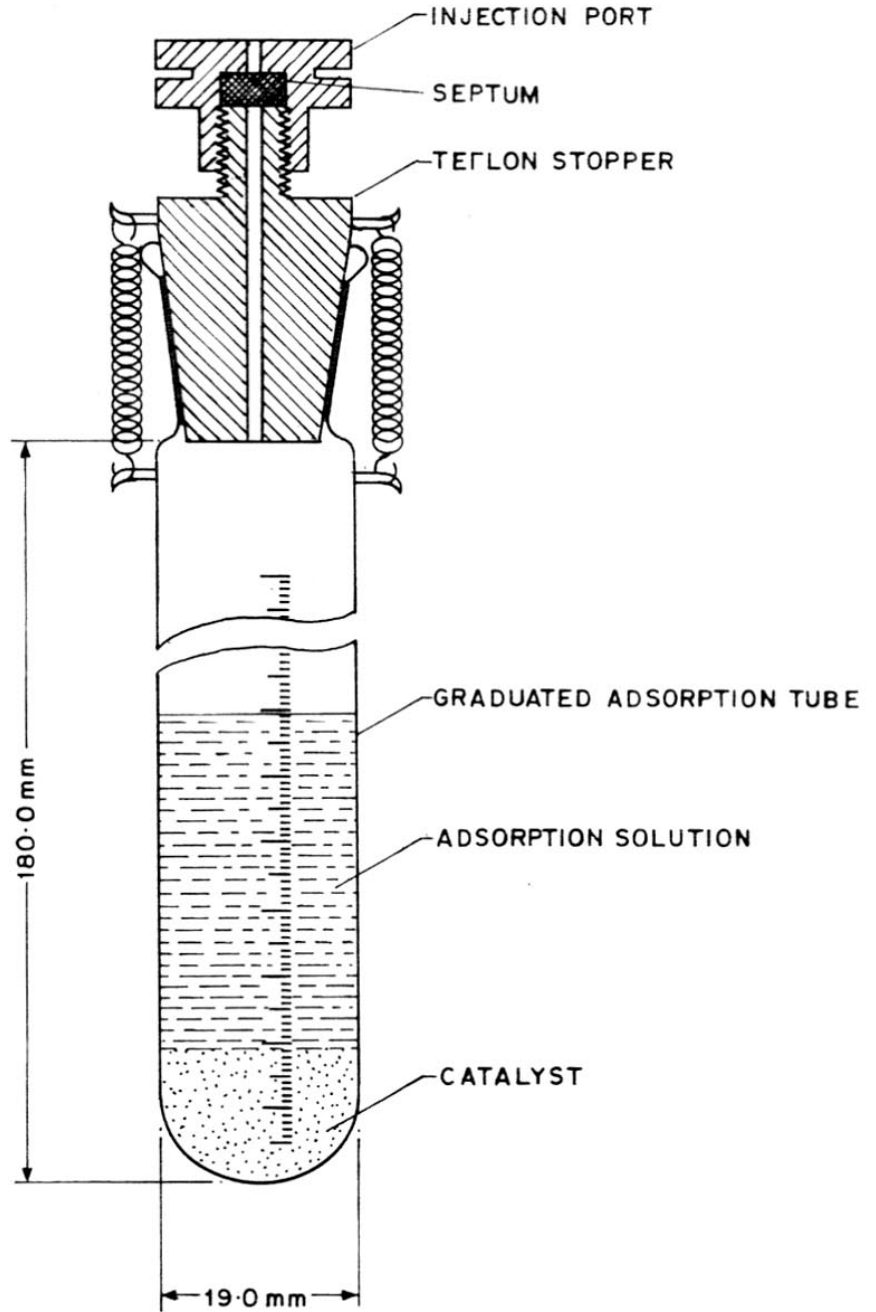


FIG. 3.1.3 ADSORPTION TUBE

by gas-liquid chromatography using SE 30 (5%) on chromosorb-W using nitrogen as the carrier gas ($25 \text{ cm}^3 \cdot \text{min}^{-1}$). A Perkin-Elmer (Sigma 3B) gas chromatograph fitted with a flame-ionization detector was used for this purpose. The column temperature was programmed from 398 (initial period: 8 min) to 423 K at a heating rate of 30 K min^{-1} .

The analysis for water in methanol was performed by the Karl Fisher method (2).

Experimental data for the adsorption of water from methanol at different concentrations were determined only at 308 K; whereas, the adsorption data for ONP and OAP at different concentrations were obtained at 278, 293 and 308 K.

In all the above adsorption experiments, the temperature could be controlled within 0.1 K.

3.1.5.2 Simultaneous Adsorption

In order to measure the simultaneous binary adsorption of ONP and OAP from their mixture in methanol on the catalyst, the experimental procedure followed was very similar to that described earlier for the single component adsorption except that in the binary adsorption measurement, the catalyst was equilibrated with the methanol solution containing equimolar ONP and OAP (i.e. initial concentration of ONP = initial concentration of OAP). The concentrations of ONP and OAP at the equilibrium were determined by the GC analysis. The amount of ONP and OAP adsorbed simultaneously at their different equilibrium concentrations was evaluated from the knowledge of their initial and final (at the adsorption equilibrium) concentrations using Eqn. 8.

The binary adsorption of ONP and OAP was measured at 278, 293 and 308 K. The initial concentration of ONP and OAP taken together in the two component system was varied from 0.06 to 0.36 mmol.cm⁻³.

3.1.6 MEASUREMENT OF GAS-LIQUID MASS TRANSFER COEFFICIENT

The gas-liquid mass transfer coefficient ($k_L a$) for the absorption of hydrogen in methanol (which is the reaction medium for the hydrogenation reaction) in the hydrogenation reactor was determined in the absence of the hydrogenation reaction but nearly at the same hydrodynamic conditions at which the hydrogenation reaction was carried out by measuring the kinetics of absorption of H₂ in methanol at 303 K. The H₂ absorption kinetic data at different stirring speeds using three (twisted) blade stirrer were measured using the volumetric apparatus shown in Fig. 3.1.4.

The volumetric apparatus was kept ready for the measurements as follows. The level of the mercury in the gas burette was brought to level A by connecting the gas burette for hydrogen bypass with the stopcock S₂ and lowering the mercury reservoir. The stopcock S₃ was closed, side tube and the gas burette was flushed with hydrogen and the stopcock S₂ was closed. The apparatus was then connected to H₂-inlet of the hydrogenation reactor.

A known volume of methanol (1.0 dm³) was introduced in the reactor and the reactor temperature was maintained at 303 K by passing water at 303 K through the cooling coils of the reactor. The reactor was then evacuated and H₂ was introduced in the reactor at atmospheric pressure. During the evacuation, which was for a very short duration, the methanol was stirred. Whereas at the time of introduction of H₂ in the evacuated

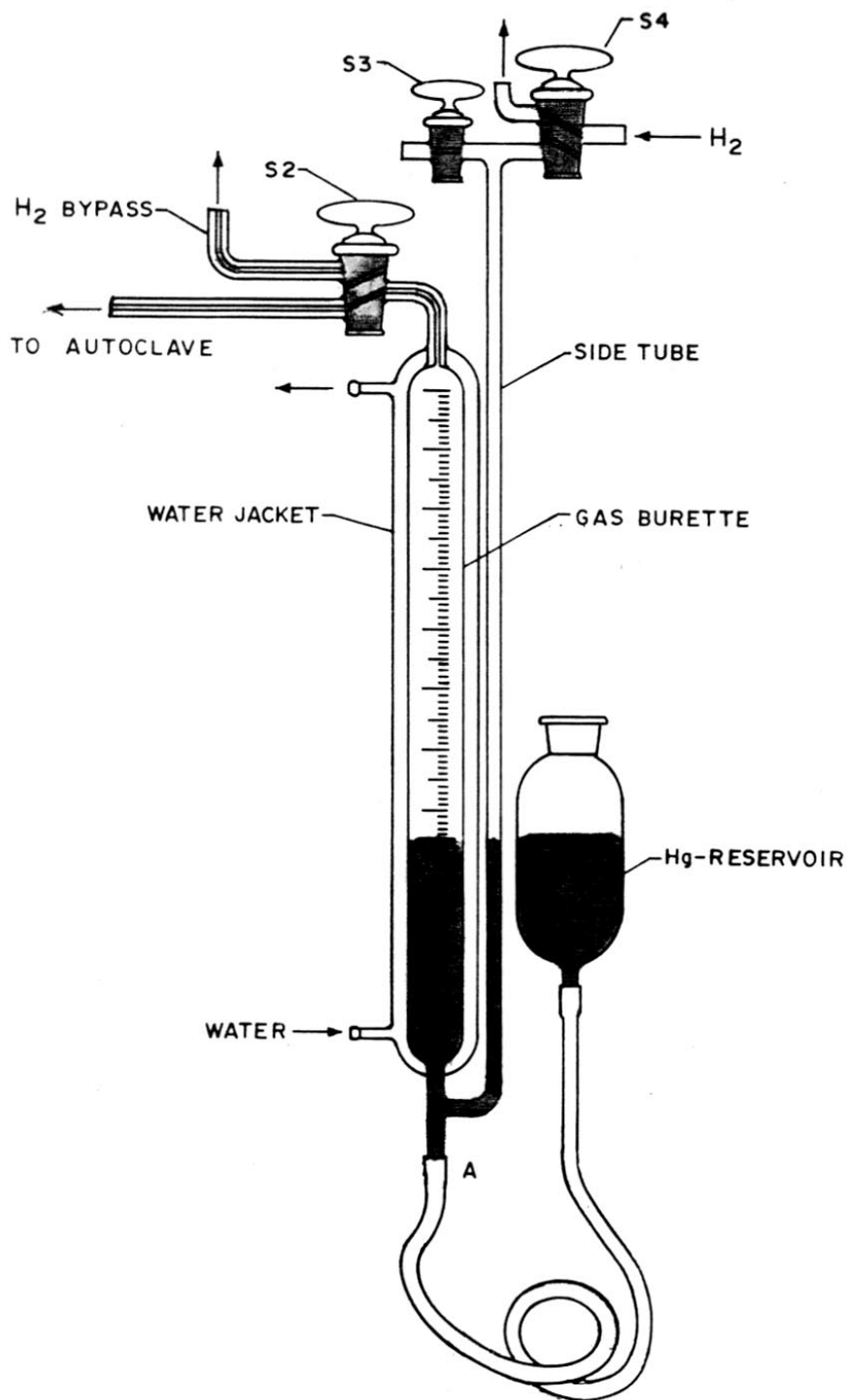


FIG. 3-1-4. VOLUMETRIC APPARATUS FOR MEASURING RATES OF ABSORPTION OF HYDROGEN IN METHANOL IN THE HYDROGENATION REACTOR

reactor, the stirring was stopped. This evacuation - H_2 introduction cycle was repeated for 3-4 times to remove the air from the reactor. After this was done, the reactor was connected to the volumetric apparatus by properly positioning the stopcock S_2 . The stopcock S_3 was opened and the mercury reservoir was raised until the mercury entered in the gas burette. The pressure in the system, which was slightly above the atmospheric pressure, was adjusted to the atmospheric pressure by a momentary opening and closing the reactor gas outlet valve. After doing this, the zero reading on the gas burette was recorded by bringing mercury in both the gas burette and the side tube to the same level by raising or lowering the mercury reservoir.

The absorption of H_2 in methanol was allowed to take place by starting the stirring (in the absence of stirring the H_2 absorption rate was insignificant). The volume of H_2 absorbed as a function of time was measured at atmospheric pressure by constantly adjusting mercury in both the gas burette and the side tube to the same level. The gas absorption data was collected until there was no further absorption of H_2 .

The fractional absorption for (or dissolution) of H_2 (α) at a particular time was estimated as,

$$\alpha = \frac{\text{Amount of } H_2 \text{ absorbed}}{\text{Amount of } H_2 \text{ absorbed at equilibrium}} \quad (9)$$

The data on the fractional absorption of H_2 as a function of time was obtained at different stirring speeds (260-1000 rpm).

REFERENCES

1. Choudhary, V.R. and Vaidya, S.H., *Research and Industry*, 26 (1981), 1.
2. Vogel, A.I., 'Elementary Practical Organic Chemistry', Longmans, Geen and Co., London, New York, Toronto (1968).

CHAPTER-3.2

CHAPTER-3.2

EFFECT OF CONCENTRATION OF Pd IN Pd-CARBON AND SOLVENT ON THE HYDROGENATION OF σ -NITROPHENOL

3.2.1 EFFECT OF CONCENTRATION OF Pd IN Pd-CARBON

In order to find the influence of concentration of Pd in the Pd-carbon catalyst on its catalytic activity in the liquid phase hydrogenation of ONP to OAP, the hydrogenation activity of the Pd-carbon (particle size: 30 μ m) with different concentrations of Pd (0.2-4.62 wt % Pd) was measured in the agitated three phase reactor (Fig. 3.1.1) at the following reaction conditions.

Reaction medium	:	Methanol
Volume of reaction mixture	:	1.0 dm ³
Initial concentration of ONP	:	0.36 mol.dm ⁻³
Catalyst loading	:	1.0 g.dm ⁻³
Reaction temperature	:	308 K
H ₂ -pressure	:	2136 kPa
Stirring speed	:	980 rpm

The results of the hydrogenation activity test for the catalysts containing Pd at the different concentrations are shown in Fig. 3.2.1. The scanning electron microphotographs of the Pd-carbon catalysts are presented in Fig. 3.2.2.

The results in Fig. 3.2.1 reveal that the hydrogenation rate is very strongly influenced by the concentration of Pd in the carbon supported

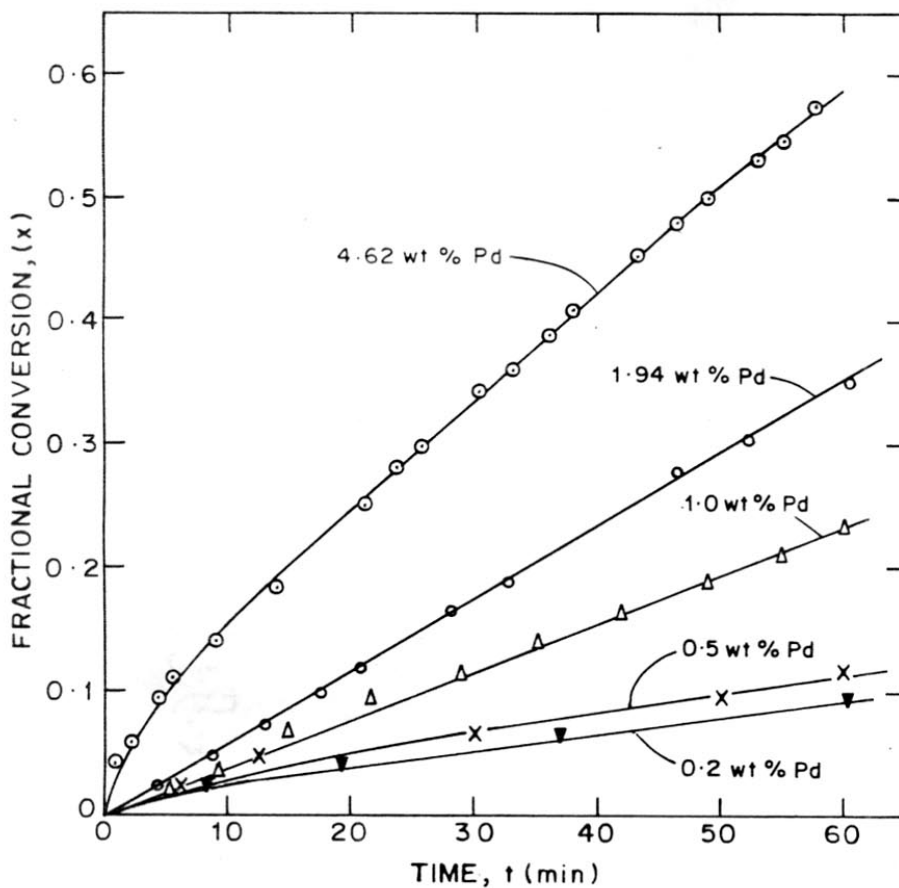


FIG. 3.2.1. EFFECT OF CONCENTRATION OF Pd IN Pd-CARBON ON ITS CATALYTIC ACTIVITY IN THE HYDROGENATION REACTION

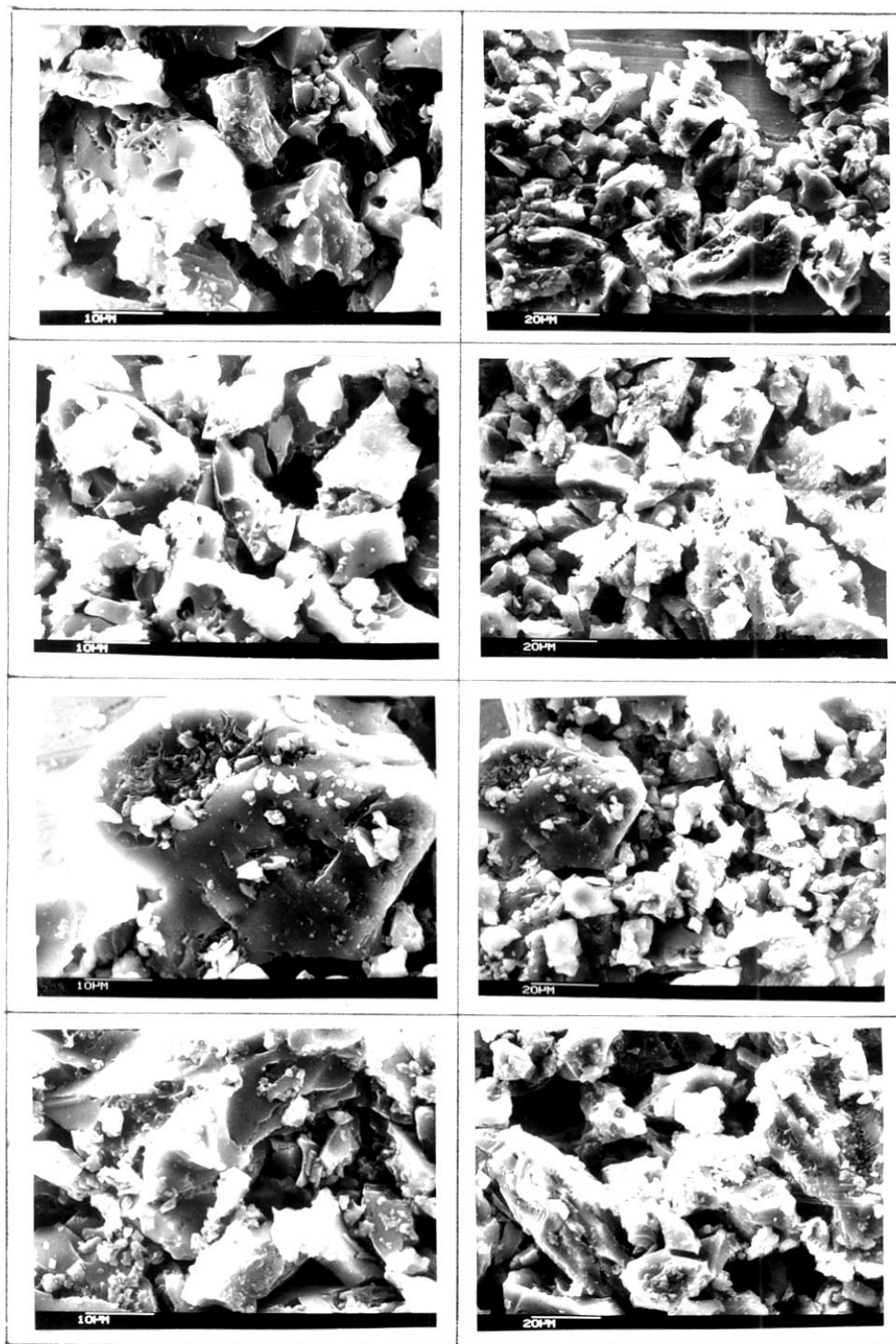


FIG. 3-2-2. SCANNING ELECTRON MICROPHOTOGRAPHS OF Pd-C CATALYST WITH DIFFERENT CONCENTRATION OF Pd

palladium catalysts; it is increased with the increase in the concentration of Pd in the catalyst. The increased catalytic activity is expected to be due to an increase in the hydrogenation active sites on the catalyst with the increase in its Pd-content. The scanning electron micrographs (Fig. 3.2.2) show that the coverage of the carbon surface with the Pd crystallites is increased with the increase in the Pd-content of the catalyst. However, since the surface area of the Pd and its dispersion in the catalysts could not be determined in the present study, no firm conclusion can be drawn regarding the dependence of the hydrogenation activity on the crystal size and surface area of Pd.

3.2.2 EFFECT OF SOLVENT ON THE HYDROGENATION

Solvents can have profound effects on both the rate and the selectivity of hydrogenation (1). Rates can be influenced markedly both by an intrinsic property of the solvent and by impurities in it. Many solvents, including alcohols, esters, ethers, carboxylic acid, hydrocarbons, amines, water, etc. have been used in the liquid-phase hydrogenation, but the effectiveness of the solvents varies with both the catalyst and substrate. The only way of choosing the best solvent is to try experimentally the suitability of all the solvents that can possibly be used. Influence of solvent on a large number of heterogeneously catalysed liquid phase hydrogenations has been much discussed (1-7).

The solvent plays different roles (1) in the solid catalysed liquid phase hydrogenation processes. (a) It can serve as a diluent to lessen the probability of interaction between molecules of reactive intermediates; (b) It can serve as a reactant to trap intermediates and thereby prevent their further hydrogenation; (c) It can prevent the product from precipitating

on to the catalyst and deactivating it; or (d) It can provide a medium in which a specific reaction and/or product stereochemistry is favoured. In many of these cases the observed effects are due to the solvating ability of the solvent or its reactivity, dielectric constant or acidity. Such cases are generally understood and the specific properties responsible are usually easily determined.

One aspect of the solvent effect in heterogeneously catalyzed reactions which has not been readily determinable is the nature of the solvent/catalyst interaction and also the effect of the solvent/catalyst interaction on the outcome of the reaction. In the present investigation, the hydrogenation of ONP to OAP on the Pd-carbon (4.62 wt % Pd) using methanol, ethanol and *n*-propanol as a reaction medium was carried out at the reaction conditions given below and the solvent/catalyst interaction was studied by measuring the heat of immersion of the catalyst in the alcohols at 303 K.

Reaction conditions

Catalyst	:	Pd-carbon (4.62 wt % Pd)
Catalyst particle size	:	30 μm
Reaction medium	:	Methanol, ethanol or <i>n</i> -propanol
Volume of reaction mixture	:	1.0 dm^3
Initial concentration of ONP	:	0.36 $\text{mol}\cdot\text{dm}^{-3}$
Catalyst loading	:	1.0 $\text{g}\cdot\text{dm}^{-3}$
Reaction temperature	:	308 K
H_2 -pressure	:	2136 kPa
Stirring speed	:	980 rpm

The conversion data on the hydrogenation in the different alcohols are presented in Fig. 3.2.3. The results show a very significant effect of solvent on the rate of the hydrogenation reaction. Among the alcohols used as the reaction medium, methanol is found to be the best solvent for the reaction. The order of preference of the alcohols for the reaction medium is found to be as follows:

Methanol > Ethanol > n-Propanol

In case of the hydrogenation of *p*-nitrotoluene on Raney-Ni, the same order of preference of the alcohols was found (7).

At the reaction conditions employed in the most liquid-solid catalytic processes, both the reaction species and solvent are adsorbed on the catalyst surface and the extent of the adsorption of the either of the two depends (8) strongly on their interactions with the catalyst and the solvent-solute properties (e.g. miscibility, solubility, relative polarity or dipole moments, molecular weights, etc.). The decrease in the hydrogenation rate with the increase in the molecular weight of alcohol is expected to be due to an increase in the relative adsorption of the solvent on the catalyst.

Solvent strongly affects the adsorption of reaction species on the catalyst and also competes with them for the adsorption, thus ultimately affecting the reaction rate. Due to the complex nature of solvent/catalyst and solvent/solute interactions, a priori choice of a suitable solvent for a particular reaction can not be done.

In all the further studies, methanol is used as the reaction medium as it has been found to be the best solvent among the C_1 - C_3 alcohols for the hydrogenation reaction.

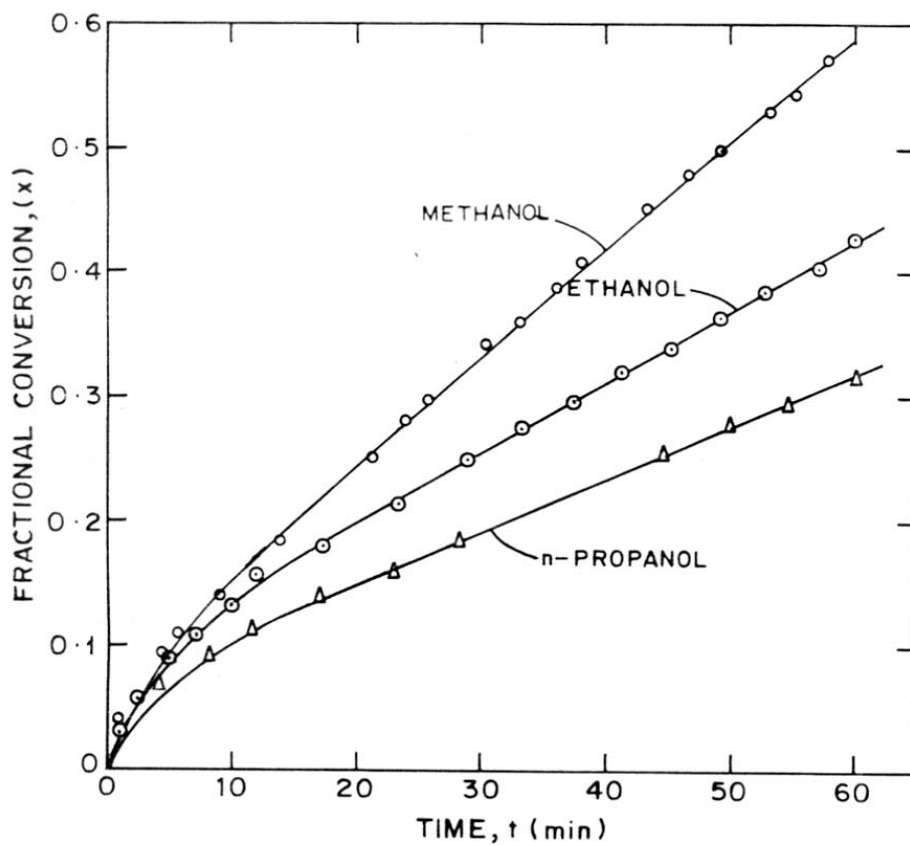


FIG. 3.2.3. EFFECT ON SOLVENT ON THE HYDROGENATION OF *o*-NITROPHENOL ON THE Pd-C CATALYST

The solvent/catalyst interaction in the present case was investigated in terms of the heat of immersion of the Pd-carbon catalyst in the alcohols at 303 K. The heat of immersion data are given below.

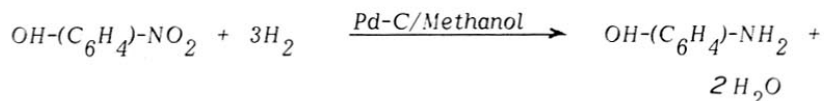
Solvent	:	Methanol	Ethanol	n-Propanol
Heat of immersion ($J.g^{-1}$)	:	63.0	68.0	80.0
Dipole moment (D)	:	1.63	1.66	1.71

The heat of immersion data was obtained using the calorimeter described elsewhere (9). The amount of catalyst and alcohols used in the measurement was 0.40 g and 80 g respectively. The heat of immersion of the catalyst increases with the increase in the molecular weight of alcohol. A comparison of the catalytic activity and the heat of immersion data shows that the catalytic activity is decreased with the increase in the energy of interaction between the solvent and the catalyst. This is very consistent with the fact that a stronger adsorption or interaction of solvent with catalyst results in a decrease in the catalytic activity. It may also be noted that the heat of immersion data is quite consistent with the dipole moment of the alcohols.

REFERENCES

1. Rylender, P.N., in 'Catalysis in Organic Synthesis', W.H. Jones, Ed., Academic Press, New York, N.Y. (1980), p. 155.
2. Baltzly, R.J., *Org. Chem.* 41 (1976) 920.
3. Cervený, L., Vostry, B. and Ruzika, V., *Collect Czech. Chem. Commun.* 46 (1981) 2676.
4. Koopman, P.G.J., Buurmana, H.M.A., Kieboom, A.P.G. and van Bekkam, H., *Recl. Trav. Chim. Pays-Bus*, 100 (1981) 156.
5. Augustine, R.L., Nocito, V., van Pappen, J., Warner, R. and Yaghmaie, E., in 'Catalysis in Organic Synthesis', Jones, W.H., Ed., Academic Press, New York (1980) p. 173.
6. Rylender, P.N., in 'Catalysis in Organic Synthesis', W.H. Jones, Ed., Academic press, New York, N.Y. (1978).
7. Choudhary, V.R. and Chaudhari, S.K., *Trans. Indian Inst. Chem. Engg.* (in press).
8. Kipling, J.J., in 'Adsorption from Solution of Non-electrolytes' Academic Press Inc., New York, 1965, p. 90.
9. Pradhan, S.D. and Pathak, G., *Proc. Indian Acad. Sci. (Chem. Sci.)*, 89 (1980).

CHAPTER-3.3

CHAPTER-3.3INFLUENCE OF MASS TRANSFER ON THE HYDROGENATION
OF o-NITROPHENOL ON Pd-CARBON3.3.1 REACTION MODEL

(1)

A most general model showing concentration profiles of the reactants for the above catalytic gas-liquid-solid reaction is presented in Fig. 3.3.1.

The hydrogenation reaction occurs in the following successive steps.

- (i) Transfer of hydrogen from the gas-liquid interface to the bulk liquid by diffusion through the gas-liquid film.
- (ii) Mixing of the transferred hydrogen in the bulk liquid containing the other reactant (ONP dissolved in methanol).
- (iii) Transfer of the reactants (i.e. dissolved H_2 and ONP) from the bulk liquid to the external surface² of the catalyst particle by diffusion through the liquid-solid film surrounding the particle.
- (iv) Diffusion of the reactants from the external surface to the internal surface through the pores of the catalyst.
- (v) Adsorption of reactants on the catalyst surface.
- (vi) Surface reaction between the adsorbed reactants.
- (vii) Desorption of product(s) from the catalyst surface.
- (viii) Diffusion of product(s) to the external surface through the pores of the catalyst.
- (ix) Transfer of the products from the external surface of the catalyst to the bulk liquid by the diffusion through

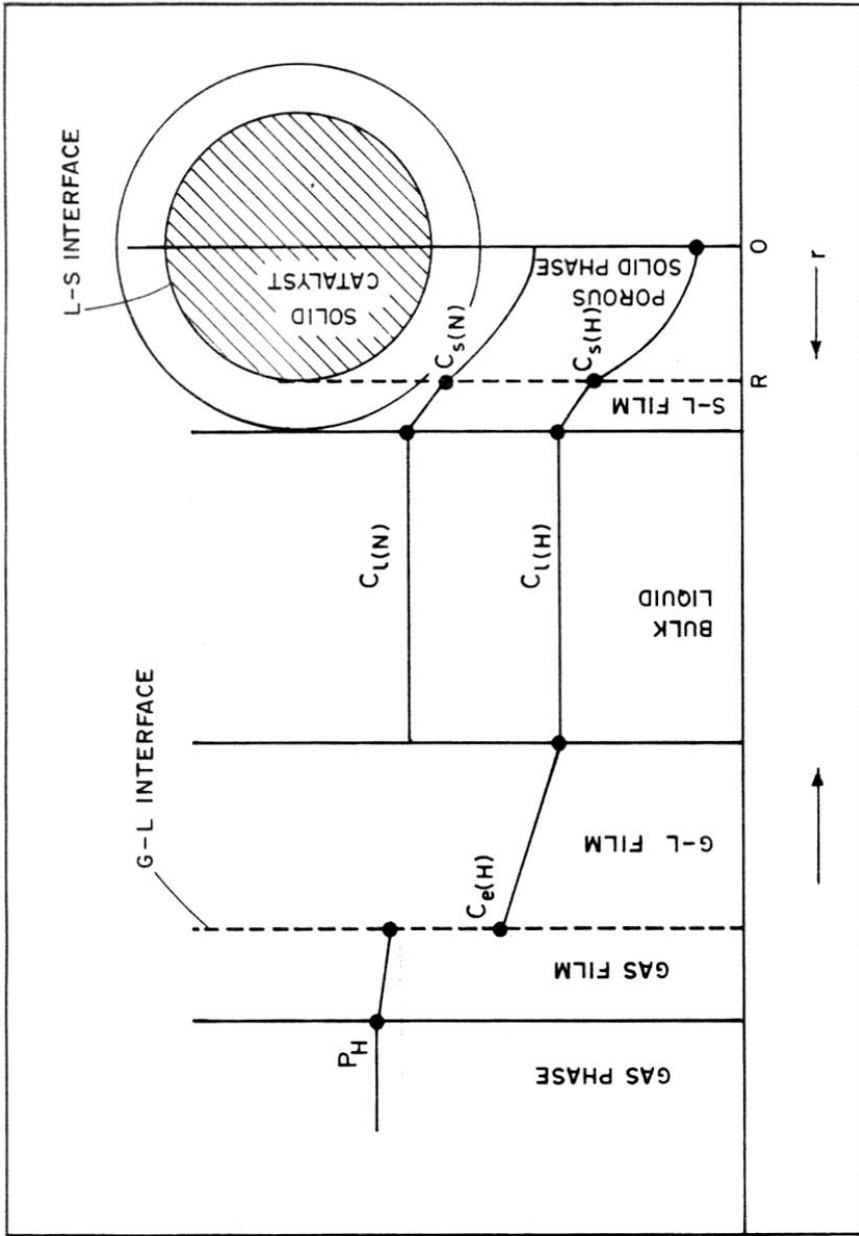


FIG. 3.3.1. A GENERAL MODEL SHOWING CONCENTRATION PROFILE FOR THE HYDROGENATION OF ONP IN THREE PHASE SLURRY REACTOR (H=HYDROGEN, N=0-NITROPHENOL)

the solid-liquid film.

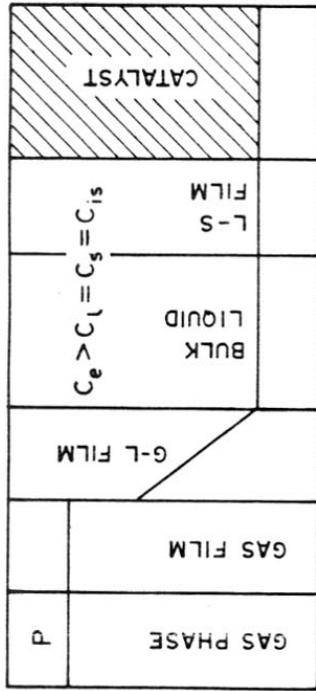
(x) *Mixing of the products in the bulk liquid.*

The steps (iv) to (vii) (i.e. pore diffusion and reaction) occur simultaneously. The processes involving adsorption of reactants, surface reaction and desorption of products are considered to be due to chemical phenomenon occurring in the catalytic process. Other processes involving mass transfer (i.e. gas-liquid film, liquid-solid film and pore diffusion of reactants and products) are due to physical phenomena. The concentration profiles for different controlling mechanisms for gas-solid-liquid reaction are shown in Fig. 3.3.2. In order to obtain the intrinsic rate parameters of any catalytic process, the kinetic data must be collected in the chemical control regime. This can be achieved by eliminating the effects due to accompanying mass and heat transfer processes by choosing suitable process conditions (viz. catalyst particle size, stirring speed, catalyst loading, initial reactants concentration, temperature, etc.) for the reaction in the three phase slurry reactor.

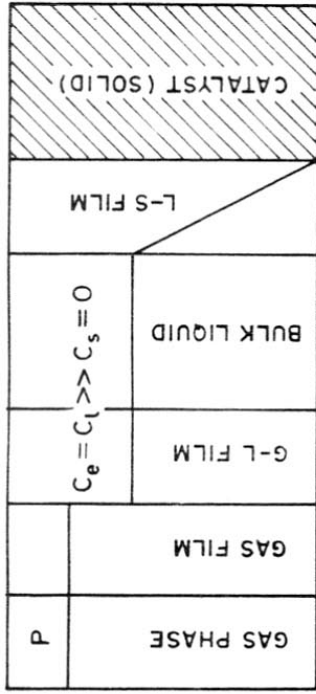
The present work was undertaken with the objective of studying the effects of gas-liquid, liquid-solid and intraparticle mass transfer processes on the hydrogenation of o-nitrophenol on the Pd-carbon (4.62 wt % Pd). The properties of the catalyst are given in Table-3.3.1.

3.3.2 SUSPENSION OF CATALYST PARTICLES

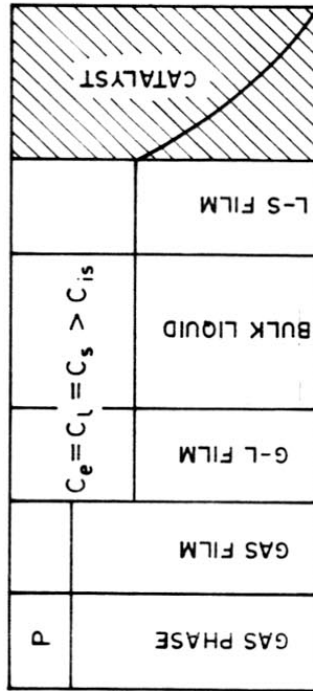
All the solid particles must be suspended in the reaction medium for maximum utilisation of the catalyst in the three phase reactor. To ensure this, a certain minimum degree of agitation is required. According to Zweitering (1), a suspension can be considered complete if no particle



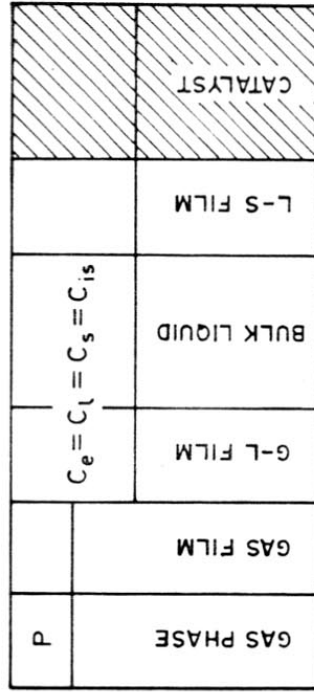
(a) GAS-LIQUID MASS TRANSFER CONTROL



(b) LIQUID-SOLID MASS TRANSFER CONTROL



(c) INTRAPARTICLE MASS TRANSFER
(OR PORE DIFFUSION) CONTROL



(d) SURFACE REACTION (OR CHEMICAL)
CONTROL

FIG. 3.3.2. CONCENTRATION PROFILES FOR DIFFERENT CONTROLLING MECHANISMS
FOR GAS-SOLID-LIQUID REACTION

TABLE-3.3.1

PROPERTIES OF THE Pd-CARBON CATALYST

Concentration of palladium	:	4.62 wt % Pd
Particle diameter (d_p)	:	30, 45, 90 and 165 m
Specific surface area (S)	:	616 m ² .g ⁻¹
Solid phase density (ρ_s)	:	1.87 g.cm ³
Particle density (ρ_p)	:	0.84 g.cm ³
Pore volume (P_v)	:	0.65 cm ³ .g ⁻¹
Porosity (ϵ)	:	0.55
Average pore radius * (r_p)	:	2.1 nm

* Estimated using the expression : $r_p = 2 P_v / S$

remains at the bottom of the reactor for longer than 1 or 2 seconds. The minimum stirrer speed (N_m) required for complete suspension can be estimated by the following correlation (1) :

$$N_m = \frac{\beta d_p^{0.2} \mu_l^{0.1} G^{0.45} (\rho_p - \rho_l)^{0.45} (w/\rho_l)^{0.13}}{\rho_l^{0.55} d_I^{0.85}} \quad (2)$$

The value of β was estimated to be 4.8 by the procedure outlined in the above reference. In the present case, the value of N_m for the catalyst of different particle sizes is estimated to be as follows.

Particle size ($d_p \times 10^4$) cm	:	30	165
Catalyst loading (w) g.dm ⁻³	:	1.0	1.0
N_m (rpm)	:	72	101

Thus, above a stirring speed of 100 rpm, a complete suspension of the catalyst particles, as large as 165 μ m, is achieved.

3.3.3 GAS-LIQUID MASS TRANSFER

3.3.3.1 Gas-Liquid Mass Transfer Coefficient ($k_L \cdot a$)

The gas-liquid (G-L) mass transfer coefficient ($k_L \cdot a$) was measured in the reactor by measuring the rates of absorption of H_2 in methanol at different stirring speeds, at nearly the same hydrodynamic conditions.

The experimental data on the absorption of H_2 is presented in Appendix-3.3.1. The variation of fractional absorption (α) of H_2 in methanol (at 303 K) with time at different stirring speeds is shown in Fig. 3.3.3.

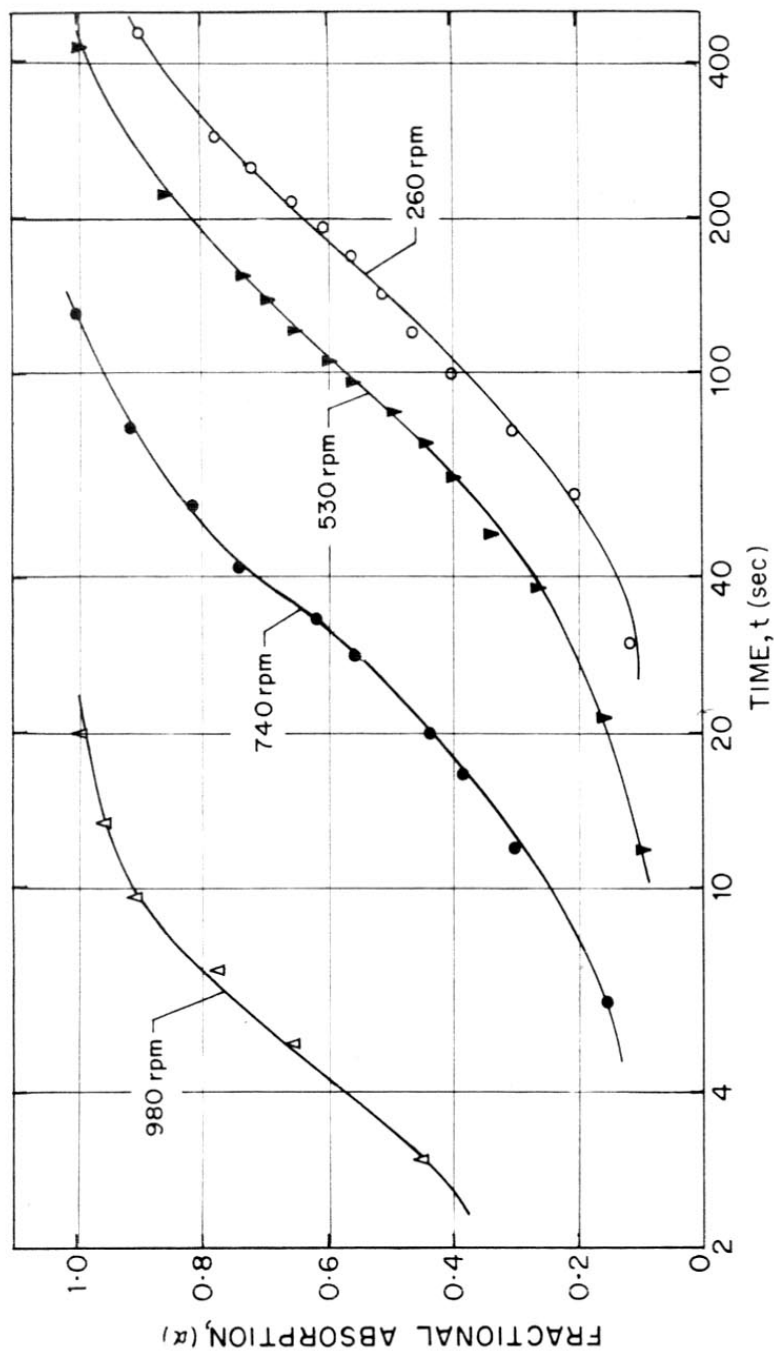


FIG. 3.3.3: VARIATION OF FRACTIONAL ABSORPTION OF H₂ IN METHANOL (at 303 K) WITH TIME AT DIFFERENT STIRRING SPEEDS.

The mass transfer coefficients ($k_L \cdot a$) can be obtained from the relation,

$$d \alpha / dt = k_L \cdot a (1 - \alpha) \quad (3)$$

or

$$[- \log (1 - \alpha) = (k_L \cdot a / 2.303) \cdot t]$$

The values of $k_L \cdot a$ [obtained from the slopes of the linear plots of $-\log (1 - \alpha)$ vs t , shown in Fig. 3.3.4] are given in Table-3.3.2. The variation of $k_L \cdot a$ with stirring speed is shown in Fig. 3.3.5.

The sharp increase in the $k_L \cdot a$ at the higher stirring speed is expected to be mostly due to sucking of the gas in the liquid resulting in higher dispersion of gas bubbles in liquid and hence increasing the total gas bubble area, a . This may also be due to higher turbulence produced at the higher stirring speeds.

Comparison between the G-L mass transfer rate and the reaction rate

Rate of mass transfer of H_2 from the gas phase to the bulk liquid is given by,

$$N_{(G-L)} = k_L \cdot a [C_{e(H)} - C_{l(H)}] \quad (4)$$

If the reaction rate were completely controlled by the gas-liquid mass transfer, $C_{l(H)}$ would approach zero and the observed rate would be,

$$\begin{aligned} N_{(G-L)} &= k_L \cdot a C_{e(H)} \quad (5) \\ &= 0.88 \text{ mol} \cdot \text{min}^{-1} \cdot \text{dm}^{-3} \end{aligned}$$

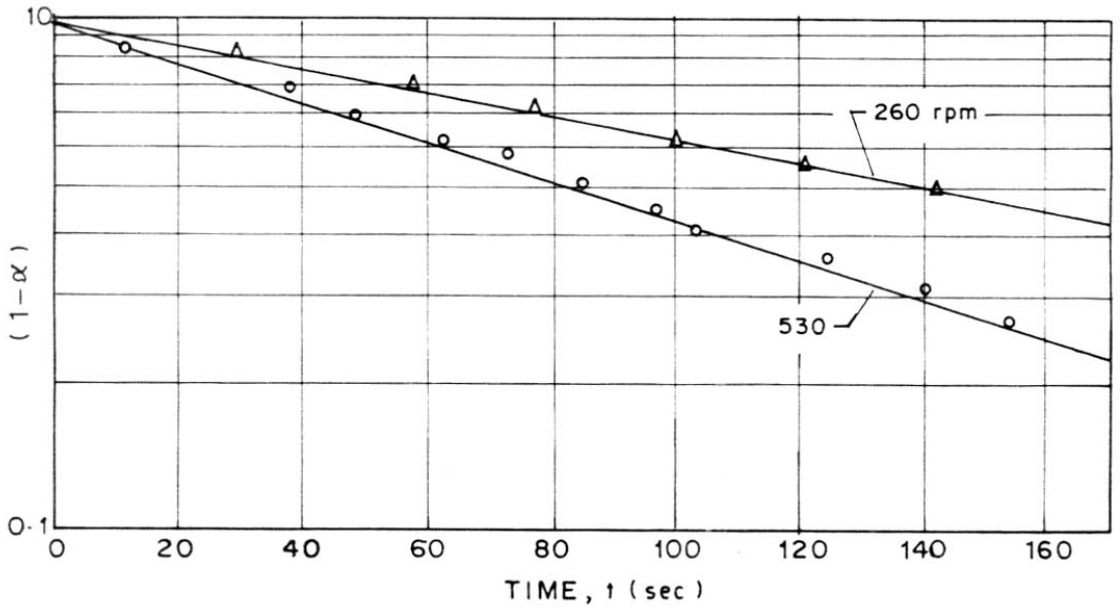
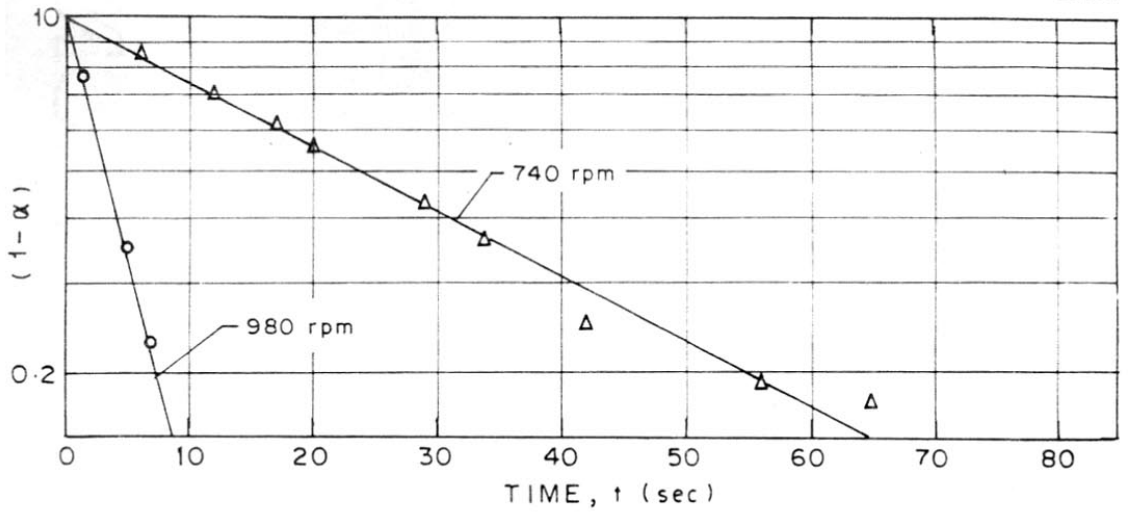


FIG. 3.3.4. PLOTS OF $\text{LOG}(1-\alpha)$ vs. t FOR THE ABSORPTION OF H_2 IN METHANOL (AT 303K) ACCORDING TO Eqn. 3.

TABLE-3.3.2GAS-LIQUID MASS TRANSFER COEFFICIENTS ($k_L \cdot a$)
AT DIFFERENT STIRRING SPEEDS

Temperature : 303 K

<u>Stirring speed</u>	<u>$k_L \cdot a$ (min^{-1})</u>
260	0.31
530	0.52
740	1.52
980	13.74

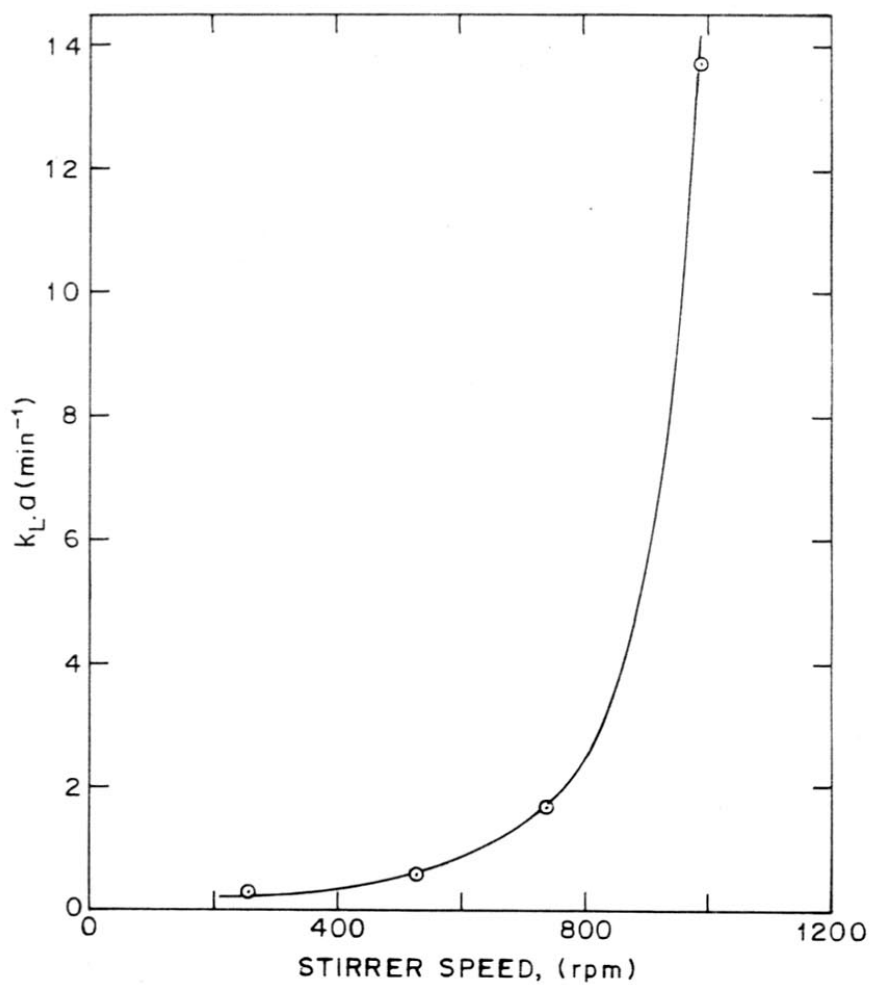


FIG. 3.3.5. DEPENDENCE OF GAS-LIQUID MASS TRANSFER COEFFICIENT ($k_L a$) ON STIRRING SPEED

$$[k_L \cdot a = 13.7 \text{ min}^{-1} \text{ at } 980 \text{ rpm and } C_{e(H)} = 0.064 \text{ mol.dm}^{-3}]$$

The maximum observed rate of H_2 consumed in the kinetic experiments [at 328 K and $C_H = 0.064 \text{ mol.dm}^{-3}$] is $0.047 \text{ mol.dm}^{-3} \cdot \text{min}^{-1}$, and hence,

$$\frac{\text{Rate of G-L mass transfer of } H_2 [N_{(G-L)}]}{\text{Maximum rate of } H_2 \text{ consumed in the reaction}} = 19$$

Thus the rate of H_2 mass transfer is very much higher than the maximum rate of the H_2 consumption observed in the hydrogenation process. This shows that the effect of G-L mass transfer on the reaction is insignificant.

3.3.3.2 Effect of Stirring Speed

The influence of G-L mass transfer on a gas-liquid reaction could also be investigated by studying the reaction at different stirring speeds. This is also done in the present study. The hydrogenation reaction for this purpose was carried out at different stirring speeds (260-1290 rpm) at the following reaction conditions,

Catalyst particle size	:	30 μm
Volume of reaction mixture	:	1.0 dm^3
Initial concentration of ONP	:	0.36 mol.dm^{-3}
Catalyst loading	:	0.5 g.dm^{-3}
Reaction temperature	:	328 K
H_2 -pressure	:	1476 kPa

The experimental conversion data for the hydrogenation at the different stirring speeds are presented in Appendix-3.3.2. The conversion

of ONP in the hydrogenation as a function of time at different stirring speeds is plotted in Fig. 3.3.6. It may be noted that the data at the stirring speed of 850, 980 and 1290 rpm fall almost on the same conversion curve.

The initial rates of the hydrogenation observed at the different stirring speeds are given in Table-3.3.3. The initial reaction rate (r_0) is obtained from the slope of the fractional conversion (x) vs time (t) plot at the zero reaction time, as follows:

$$r_0 = (\text{slope of } x \text{ vs } t \text{ plot at } t = 0) \times (\text{initial concn. of ONP}) \quad (6)$$

The variation of the conversion of ONP at different reaction times and the initial reaction rate with the stirring speed, shown in Figs. 3.3.7 and 3.3.8, respectively, reveals that, at and above a stirring speed at 850 rpm, the reaction is not affected by the stirring speed. This also indicates that, when a stirring speed of ≥ 850 rpm is used in the reaction, it is not influenced by the gas-liquid (and also by liquid-solid) mass transfer.

3.3.3.3 Effect of Catalyst Loading

The reaction rate in the absence of the G-L mass transfer effect is expected to be proportional to the catalyst loading in the slurry phase hydrogenation process. The effect of G-L mass transfer on the reaction could therefore be investigated by carrying out the reaction at different catalyst loadings. In the present case the hydrogenation reaction is carried out at different catalyst loadings ($0.05 - 1.0 \text{ g.dm}^{-3}$) at the following reaction conditions.

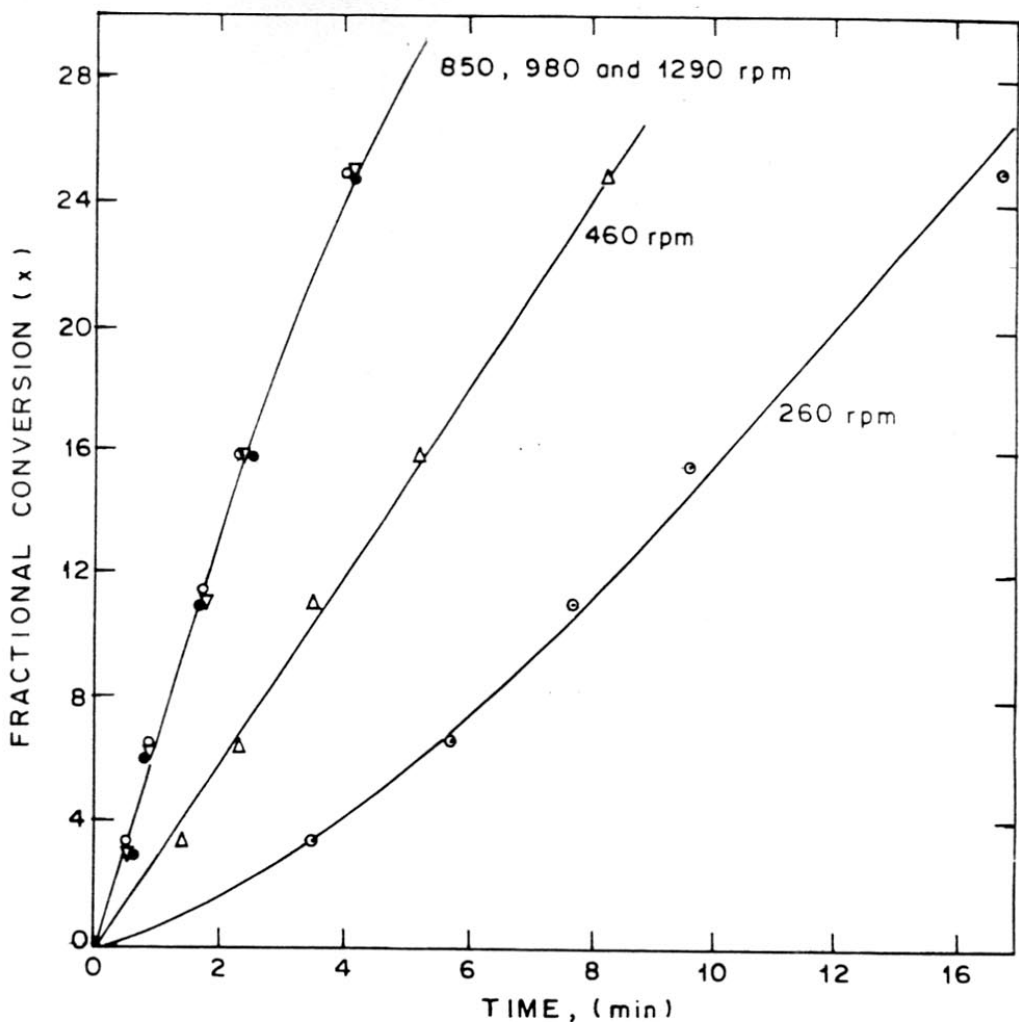


FIG. 3.3.6. EFFECT OF STIRRING SPEED ON THE HYDROGENATION OF *o*-NITROPHENOL AT 328 K (INITIAL CONCENTRATION OF *o*-NITROPHENOL = $0.36 \text{ mol. dm}^{-3}$; CATALYST PARTICLE SIZE = $30 \mu\text{m}$; CATALYST LOADING = 0.5 g. dm^{-3} ; H_2 -PRESSURE = 1476 kPa)

TABLE-3.3.3

INITIAL RATE (r_o) DATA FOR THE HYDROGENATION OF
o-NITROPHENOL IN METHANOL (AT 328 K) AT DIFFERENT
STIRRING SPEEDS

Stirring speed (rpm)	Initial rate, $r_o \times 10^3$ (mol. dm ⁻³ . min ⁻¹)
260	4.6
460	15.9
850	25.0
980	24.9
1290	25.0

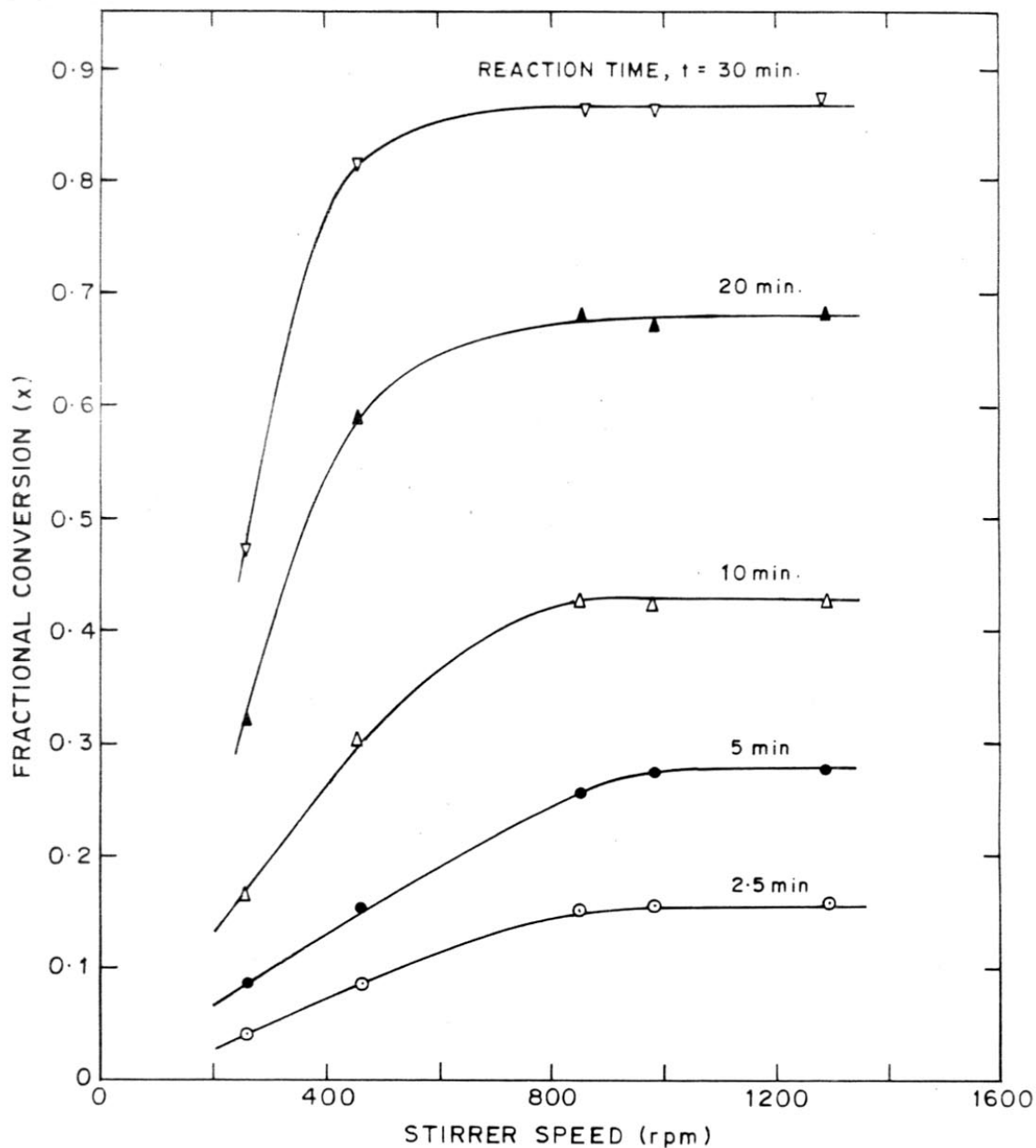


FIG. 3-3-7. DEPENDENCE OF FRACTIONAL CONVERSION OF *o*-NITROPHENOL (x) ON STIRRER SPEED AT DIFFERENT REACTION TIME

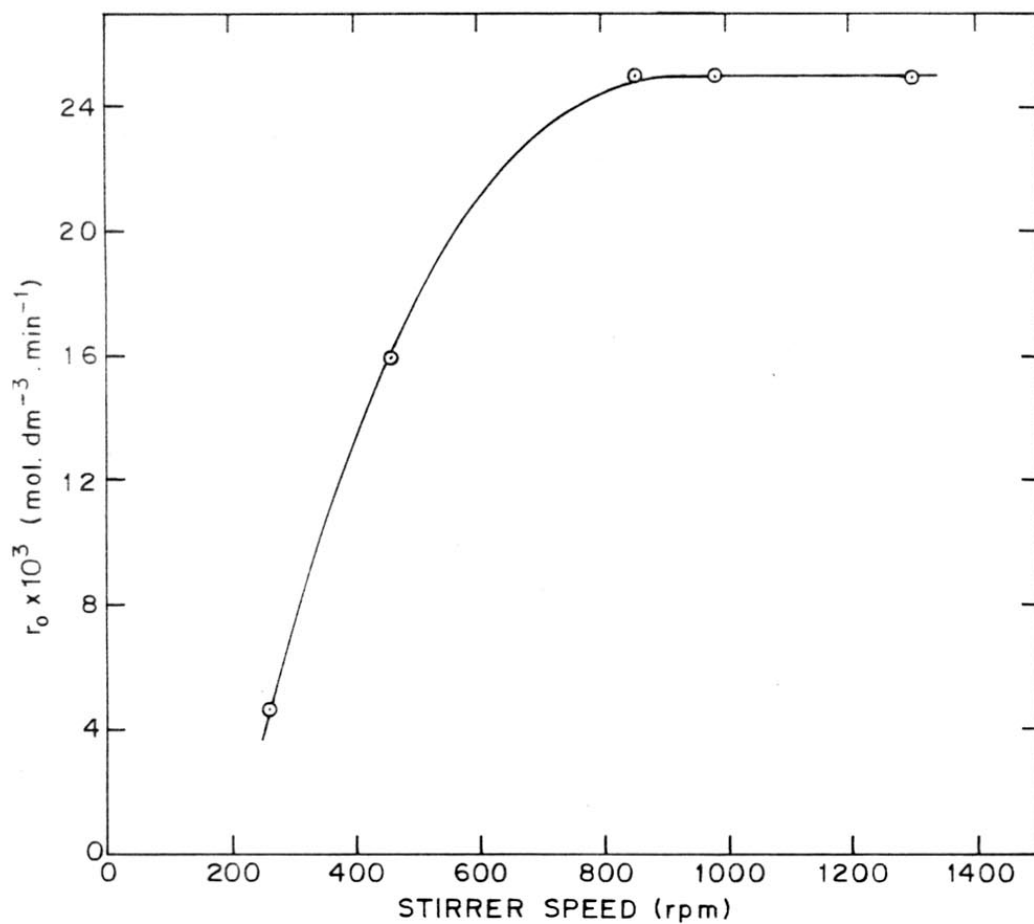


FIG. 3-3-8. VARIATION OF THE INITIAL RATE OF THE HYDROGENATION (AT 328 K) WITH THE STIRRING SPEED

Catalyst particle size	:	30 μm
Volume of reaction mixture	:	1.0 dm^3
Initial concentration of ONP	:	0.36 $\text{mol}\cdot\text{dm}^{-3}$
Reaction temperature	:	328 K
H_2 -pressure	:	1476 kPa
Stirring speed	:	980 rpm

The experimental conversion data for the hydrogenation at the different catalyst loadings are presented in Appendix-3.3.3. The conversion vs time plots for the hydrogenation at the different catalyst loadings are shown in Fig. 3.3.9 and the initial rate data are given in Table-3.3.4.

The linear r_0 vs w plot (which passes through the origin), shown in Fig. 3.3.10, indicates that the reaction rate is directly proportional to the catalyst loading and, therefore, at the above reaction conditions the reaction is not at all influenced by the G-L mass transfer.

3.3.4 LIQUID-SOLID MASS TRANSFER

3.3.4.1 Liquid Solid (L-S) Mass Transfer Coefficient (k_s)

Brian and Hales (2,3) have suggested the following correlation for the L-S mass transfer for solid particles suspended in liquid.

$$(N_{Sh})^2 = 4 + 1.21 (N_{Pe})^{2/3} \quad (7)$$

where N_{Sh} is the Sherwood number ($k_s \cdot d_p / D_{lm}$) and N_{Pe} , the Peclet number. The Peclet number for the terminal or settling velocity (U) for the catalyst particles is given by

$$N_{Pe}^* = d_p \cdot U / D_{lm} \quad (8)$$

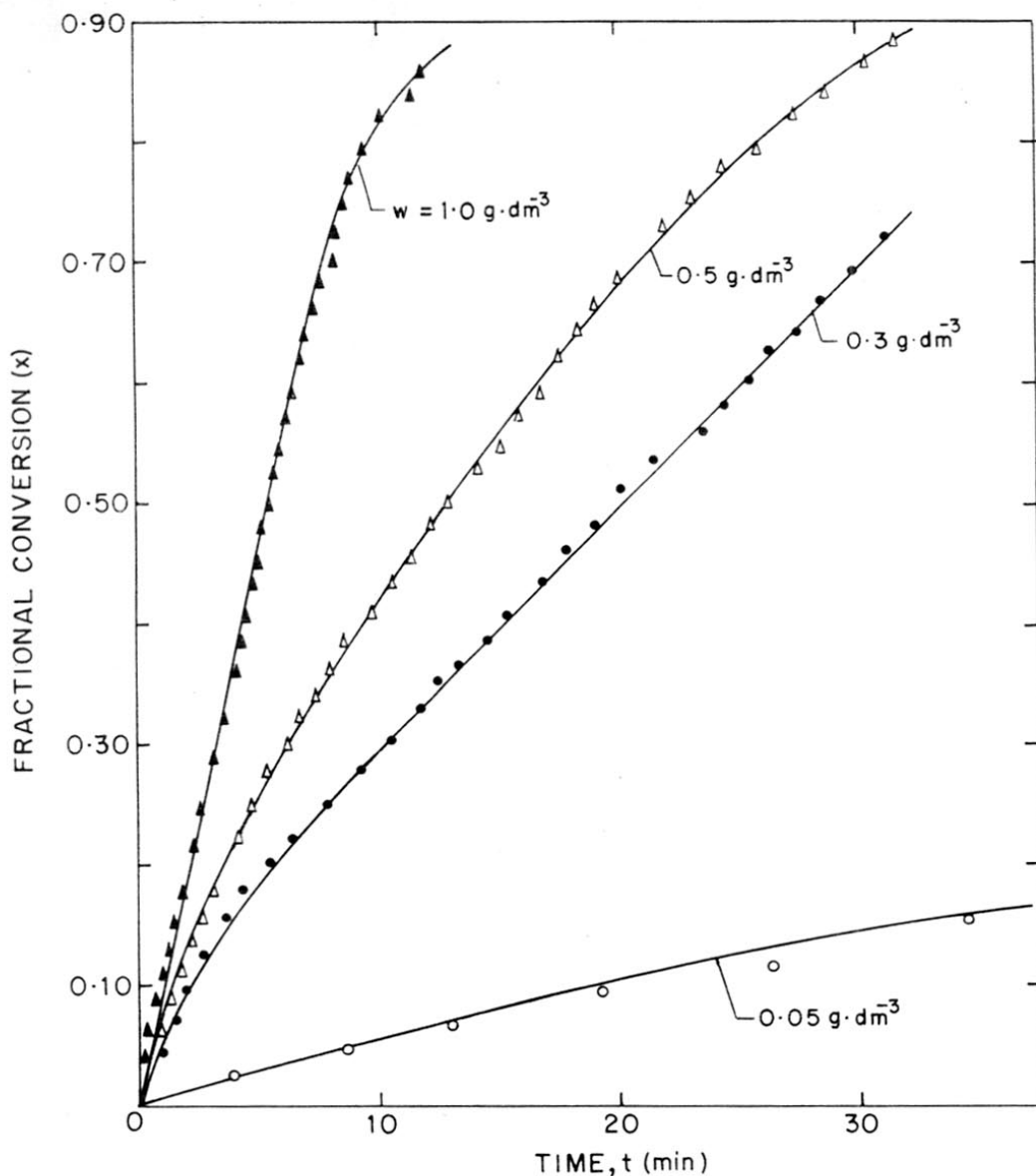


FIG.3.3.9: x vs. t PLOTS FOR THE HYDROGENATION (at 328K) AT DIFFERENT CATALYST LOADINGS (w)
 [INITIAL CONCENTRATION OF ONP = $0.36 \text{ mol} \cdot \text{dm}^{-3}$; CATALYST PARTICAL SIZE : $30 \mu\text{m}$; STIRRING SPEED : 980 rpm AND H_2 PRESSURE : 1476 kPa]

TABLE-3.3.4

INITIAL RATE DATA FOR THE HYDROGENATION OF
o-NITROPHENOL AT DIFFERENT CATALYST LOADINGS (AT 328 K)

Catalyst loading, w (g.dm^{-3})	Initial rate, (r_0) $\times 10^3$ ($\text{mol.dm}^{-3}.\text{min}^{-1}$)
0.05	2.5
0.30	15.0
0.50	24.9
1.00	47.0

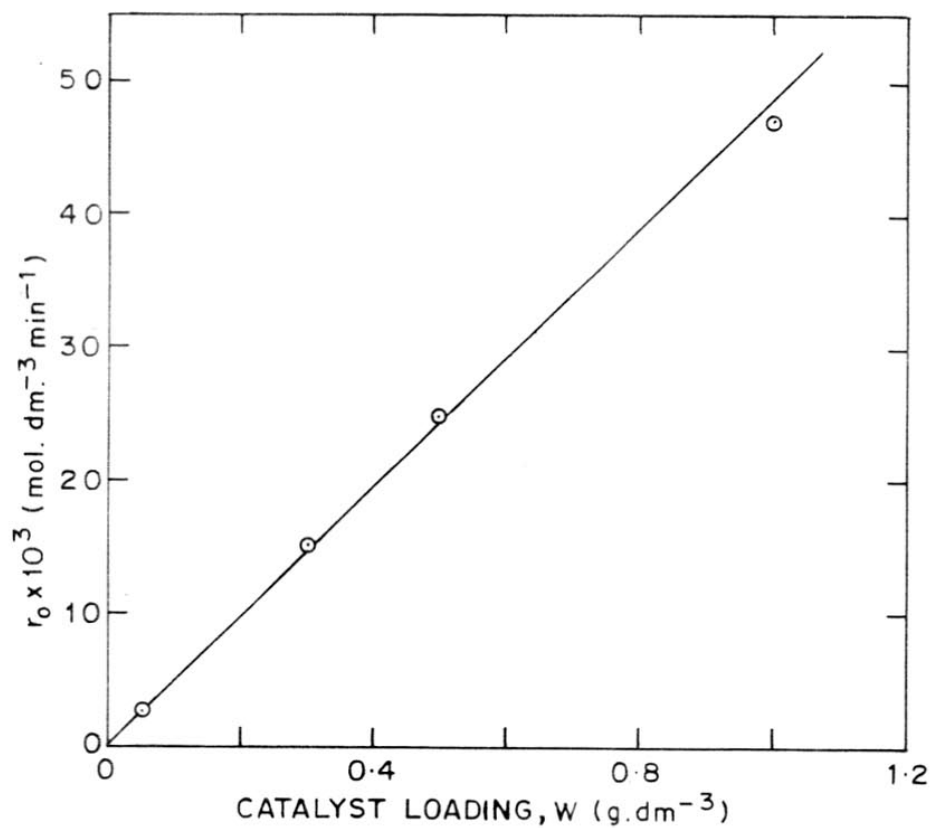


FIG. 3 3 10. A PLOT OF CATALYST LOADING (W) vs. INITIAL REACTION RATE (r_0) FOR THE HYDROGENATION AT 328 K

where U is the terminal velocity of solid particles, given by Stokes' law:

$$U = G \cdot d_p^2 (\rho_p - \rho_l) / (18 \mu_l) \quad (9)$$

The values of liquid-solid mass transfer coefficient, k_s can be obtained from the Eqns. 7-9.

The values of bulk diffusion coefficients (D_{lm}) for H_2 -methanol and ONP-methanol at different temperatures are presented in Table-3.3.5. The values of D_{lm} were estimated using the Wilke-Chang expression (4):

$$D_{lm} = \frac{7.4 \times 10^{-8} (X_M)^{0.5}}{\mu V_l^{0.6}} \quad (10)$$

(i) Estimation of k_s for H_2 [$(k_s)_H$]

$$U = \frac{G \cdot d_p (\rho_p - \rho_l)}{18 \mu_l} = \frac{981 \times (0.0030)^2 (0.84 - 0.75)}{18 \times (0.005)}$$

$$= 0.0088 \text{ (cm.sec}^{-1}\text{)}$$

$$(N^*_{Pe})_H = \frac{d_p U}{(D_{lm})_H} = \frac{0.0030 \times 0.0088}{11.092 \times 10^{-5}}$$

$$= 0.024$$

$$(N_{Sh})_H = [4 + 1.21 (N^*_{Pe})^{2/3}]^{1/2} = 2.03$$

$$(k_s)_H = \frac{(N_{Sh}) (D_{lm})_H}{d_p} = \frac{2.03 \times 11.1 \times 10^{-5}}{0.003}$$

$$= 0.075 \text{ cm.sec}^{-1}$$

TABLE-3.3.5

VALUES OF DIFFUSION COEFFICIENTS (D_{lm}) FOR o-NITROPHENOL AND HYDROGEN IN METHANOL AT DIFFERENT TEMPERATURES

<i>Diffusion system</i>	<i>Temp. (K)</i>	$D_{lm}^* \times 10^5$ ($\text{cm}^2 \cdot \text{sec}^{-1}$)
ONP-methanol	293	1.621
	308	1.904
	318	2.217
	328	3.071
H_2 -methanol	293	5.858
	308	6.878
	318	8.008
	328	11.092

* Estimated using the Wilke-Chang expression (Eqn. 10).

(ii) Estimation of k_s for o-nitrophenol $[(k_s)_N]$

$$U = 0.0088 \text{ (cm.sec}^{-1}\text{)}$$

$$(N_{Pe}^*)_{ONP} = \frac{d_p U}{(D_{lm})_{ONP}} = \frac{0.0030 \times 0.0088}{3.071 \times 10^{-5}}$$

$$= 0.86$$

$$(N_{Sh})_{ONP} = [4 + 1.21 (N_{Pe}^*)_{ONP}^{2/3}]^{1/2}$$

$$= 2.26$$

$$(k_s)_{ONP} = \frac{N_{Sh} (D_{lm})_{ONP}}{d_p} = \frac{2.26 \times 3.071 \times 10^{-5}}{0.0030}$$

$$= 0.023 \text{ cm.sec}^{-1}$$

Comparison between the observed maximum reaction rate and the maximum rate of liquid-solid mass transfer

The observed maximum rate of H_2 -consumption in the ONP hydrogenation [at 328 K, $C_H = 0.064 \text{ mol.dm}^{-3}$ and initial concentration of ONP = 0.36 mol.dm^{-3}] were as follows:

$$r_H \text{ (maximum) observed} = 0.048 \text{ (mol.dm}^{-3}\text{.min}^{-1}\text{)}$$

$$r_{(ONP)} \text{ (maximum) observed} = 0.016 \text{ (mol.dm}^{-3}\text{.min}^{-1}\text{)}$$

If the reaction were completely controlled by the L-S mass transfer, the rate of reaction would be,

$$N_{(L-S)} = k_s \cdot a_p \cdot C_l$$

where

$$a_p = \frac{6 w}{\rho_p d_p} = \frac{6 \times 0.3 \times 10^{-3}}{0.849 \times 0.0030} = 0.715 \text{ cm}^2\text{.cm}^{-3}$$

and

$$(C_l)_H = 0.064 \text{ mol.dm}^{-3} \text{ and } (C_l)_H = 0.36 \text{ mol.dm}^{-3}$$

For the case of the reaction being completely controlled by the L-S mass transfer of hydrogen or ONP,

$$\begin{aligned} [N_{(L-S)}]_H &= (0.075 \times 60) (0.715) (0.064) \\ &= 0.21 \text{ mol.dm}^{-3} \cdot \text{min}^{-1} \end{aligned}$$

$$\begin{aligned} [N_{L-S}]_{ONP} &= (0.023 \times 60) (0.715) (0.36) \\ &= 0.36 \text{ mol.dm}^{-3} \cdot \text{min}^{-1} \end{aligned}$$

Thus

$$[N_{(L-S)}]_H / r_H \text{ (maximum) observed} = 4.4$$

$$[N_{(L-S)}]_N / r_{ONP} \text{ (maximum) observed} = 22.5$$

A comparison of the observed maximum reaction rate for the consumption of hydrogen and for the conversion of ONP with the corresponding maximum rates of liquid-solid mass transfer shows that the latter are much higher (4.4 times for hydrogen and 23 times for ONP at 328 K) than the former indicating that the liquid-solid mass transfer effect on the reaction rate is not very significant. The actual values of k_s are expected to be much higher than those obtained above because of the stirring. The calculations given above are just indicative of the fact that the liquid-solid mass transfer effect on the reaction is not very significant.

The levelling of the effect of stirring speed above 850 rpm on the reaction rate (Figs. 33.7 and 3.3.8) has also indicated that the hydrogenation reaction, when carried out at the stirring speed of ≥ 850 rpm, is not influenced by the L-S mass transfer.

3.3.4.2 Effect of Catalyst Particle Size

If the reaction were controlled by the liquid-solid mass transfer, the reaction rate would vary with the particle size of the catalyst as the external surface area of a particle is inversely proportional to the particle diameter.

Therefore, the effect of the catalyst particle size on the hydrogenation reaction was investigated at the following reaction conditions;

Volume of reaction mixture	:	1.0 dm ³
Initial concentration of ONP	:	0.36 mol.dm ⁻³
Catalyst loading	:	0.3 or 0.5 g.dm ⁻³
Reaction temperature	:	varied from 308 to 328 K
H ₂ -pressure	:	1476 kPa
Stirring speed	:	980 rpm
Catalyst particle size	:	varied from 30 to 165 μm

The experimental conversion data on the hydrogenation using the catalyst of different particle sizes are presented in Appendix-3.3.4. The x vs t curves for the hydrogenation using the catalyst of the different particle sizes at 308, 318 and 328 K are shown in Figs. 3.3.11, 3.3.12 and 3.3.13, respectively. The dependence of the initial reaction rate per gram of the catalyst (r_0/w) on the catalyst particle size at the different temperatures is shown in Fig. 3.3.14.

Figure 3.3.14 shows that at all the temperatures, the reaction rate increases with the decrease in the catalyst particle size from 165 to 45 μm and thereafter remains unaffected by the further decrease in the particle size. This indicates that at the catalyst particle size of

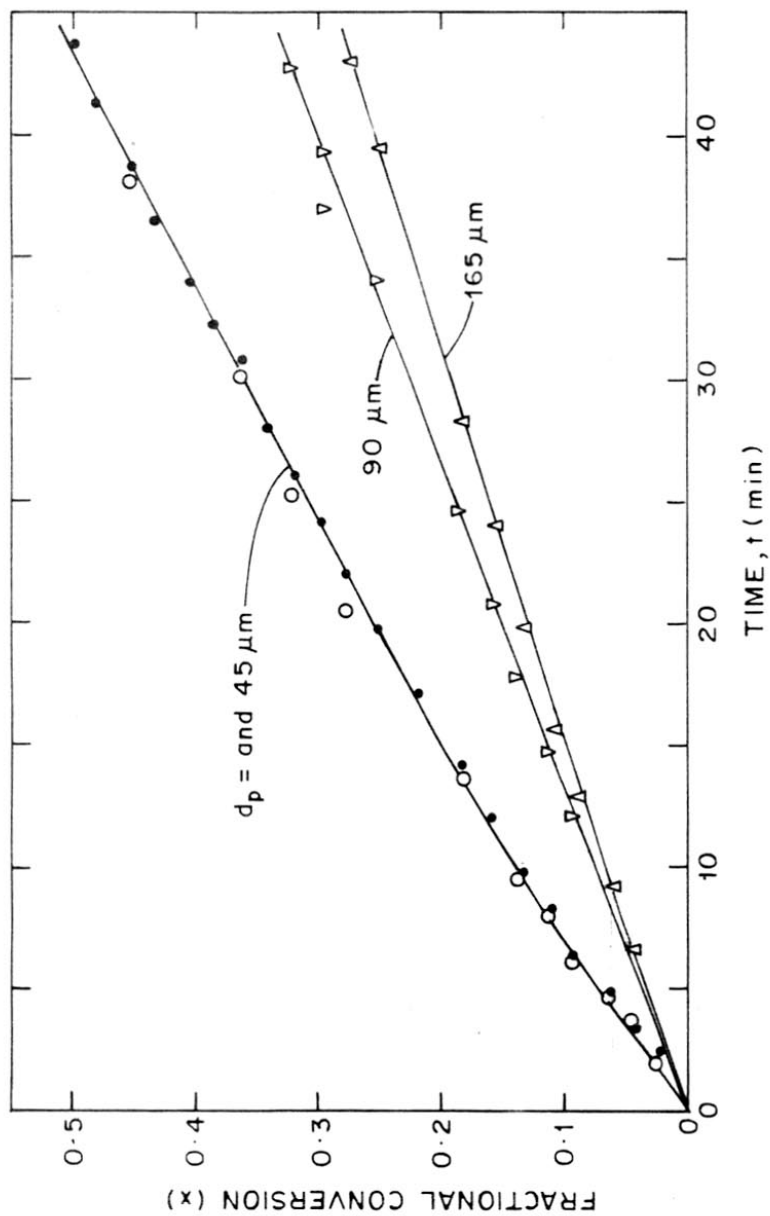


FIG. 3.3.11. x AND t CURVES FOR THE HYDROGENATION ON THE CATALYST OF DIFFERENT PARTICLE SIZES (d_p) AT 308 K [INITIAL CONCENTRATION OF ONP = $0.36 \text{ mol. dm}^{-3}$, H_2 PRESSURE = 1476 kPa , CATALYST LOADING = 0.59 dm^{-3} , STIRRER = 980 rpm]

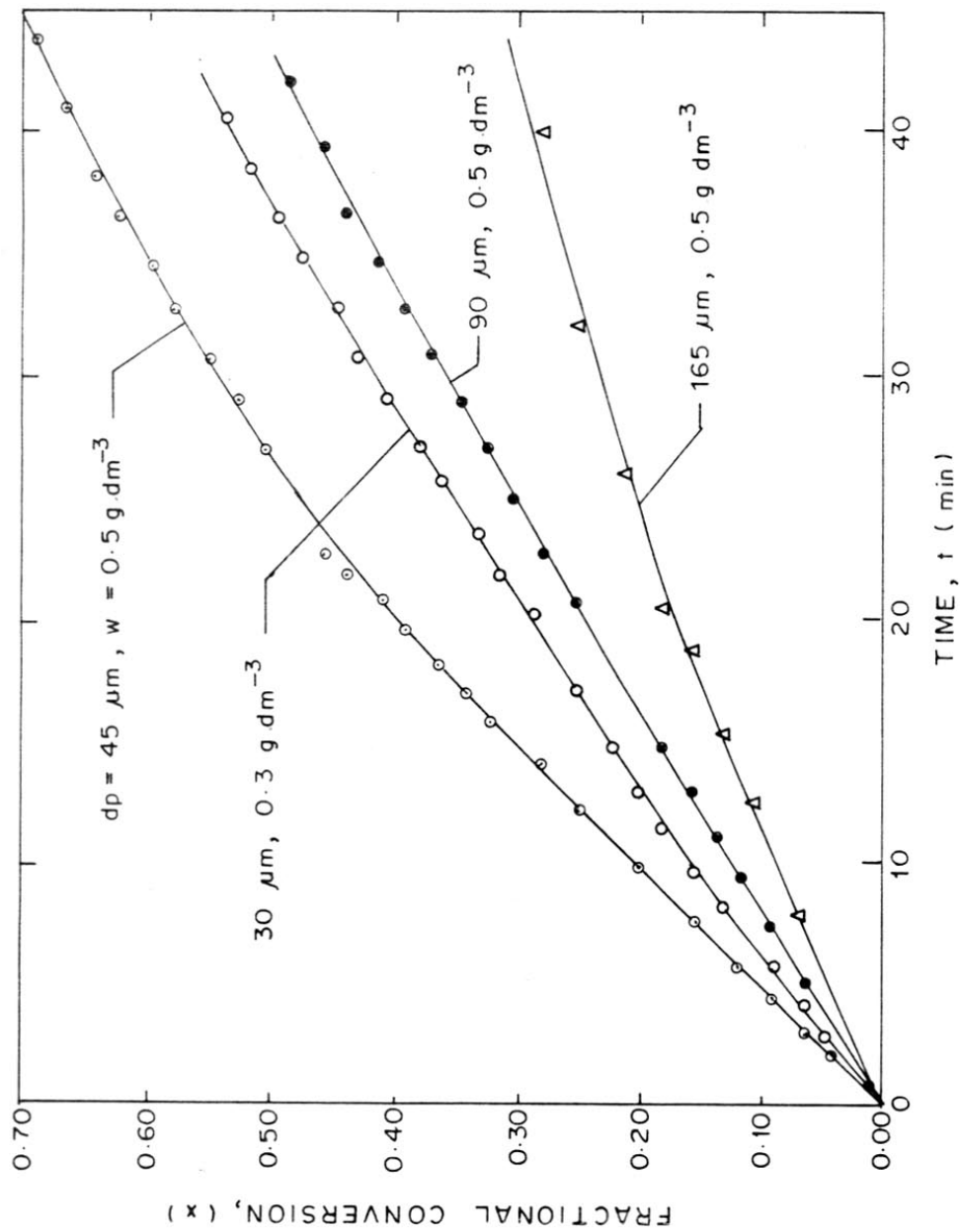


FIG. 3-3-12. x vs. t PLOTS FOR THE HYDROGENATION ON THE CATALYST OF DIFFERENT PARTICLE SIZES (d_p) AT 318 K (INITIAL CONCENTRATION OF ONP = 0.36 mol dm⁻³, H₂-PRESSURE = 1476 kPa, STIRRING SPEED = 980 rpm)

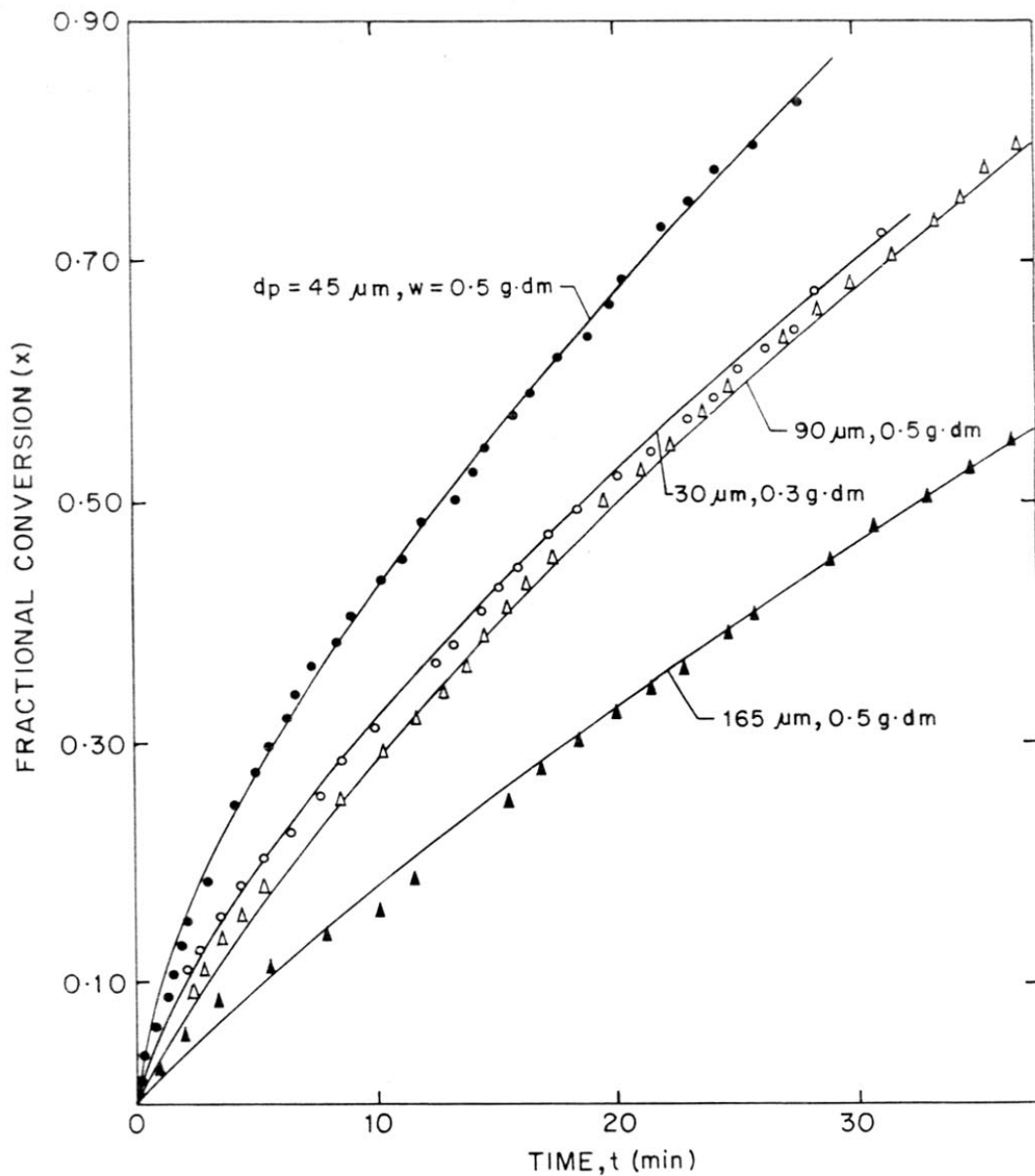


FIG.3-3-13: x vs. t PLOT FOR THE HYDROGENATION ON THE CATALYST OF DIFFERENT PARTICLE SIZES (d_p) AT 328 K (INITIAL CONCENTRATION OF ONP = $0.36 \text{ mol}\cdot\text{dm}^{-3}$; H_2 PRESSURE = 1476 kPa AND STIRRING SPEED = 980 rpm)

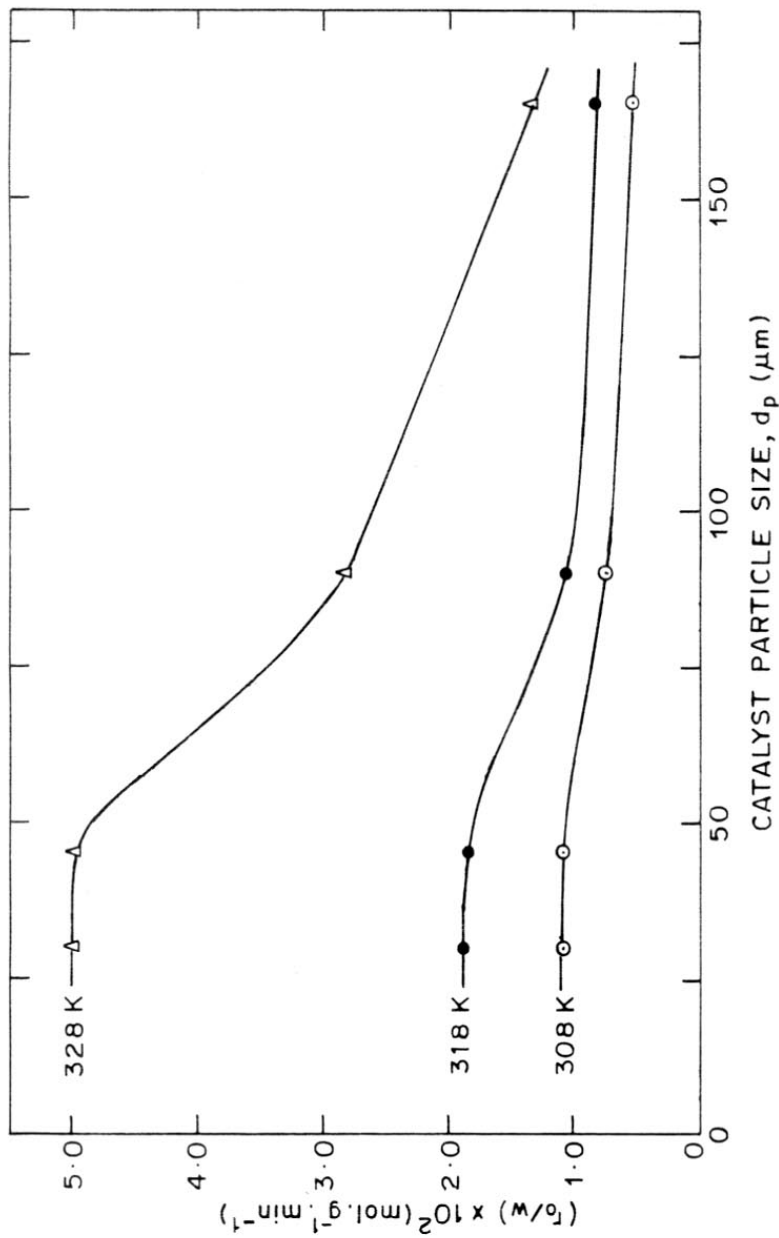


FIG. 3.3.14. VARIATION OF THE INITIAL REACTION RATE OF (r_0/w) OF THE HYDROGENATION WITH THE CATALYST PARTICLE SIZE (d_p) AT DIFFERENT TEMPERATURES

45 μm , the hydrogenation reaction even at 328 K is not controlled by the L-S mass transfer.

3.3.5 INTRAPARTICLE MASS TRANSFER

The intraparticle (or pore diffusional) mass transfer in any porous solid catalysed reaction can be very well investigated by studying the effect of particle size of the catalyst on the reaction rate under the identical conditions. This has been done in the present case and the results showing the effect of the catalyst particle size on the reaction rate in the hydrogenation process at different temperatures (308-328 K) have been shown in Fig. 3.3.14.

It is very clear from Fig. 3.3.14 that below the catalyst particle size of 45 μm the hydrogenation reaction even at 328 K is not affected by the intraparticle mass transfer.

The influence of intraparticle mass transfer on the catalytic reaction is generally expressed quantitatively in terms of the catalyst effectiveness factor.

The catalyst effectiveness factor (η) can be defined as the ratio of the observed reaction rate to the intrinsic reaction rate (i.e. the reaction rate uncontaminated by the intraparticle mass transfer effect).

For the endothermic and moderately exothermic reactions, the maximum value of η is 1. However, in case of highly exothermic reactions, η can have value much higher than 1.

Figure 3.3.15 shows the variation of the catalyst effectiveness factor (η) in the hydrogenation at 328 K on the catalyst particle size. It may be noted that the η increases with the decrease in the particle

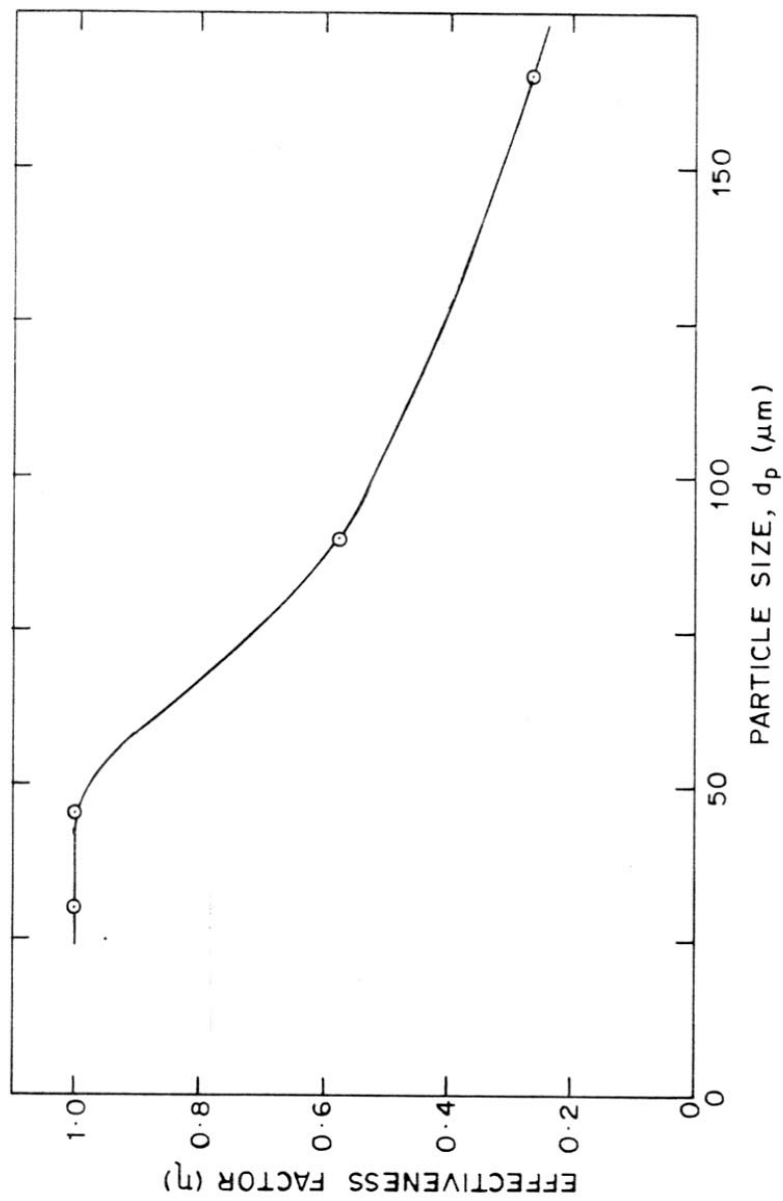


FIG. 3.3.15. DEPENDENCE OF THE CATALYST EFFECTIVENESS FACTOR (η) ON THE PARTICLE SIZE FOR THE HYDROGENATION AT 328 K

size from 165 to 45 μm , approaches to a value 1 at the catalyst particle size of 45 μm and thereafter unaffected by the further decrease in the catalyst particle size. For $\eta = 1$, the catalyst is fully utilised in the reaction and there is no influence of intraparticle mass transfer on the reaction.

The values of η for the catalyst of particle size 165 μm at the different temperatures are given in Table-3.3.7. The variation of η of the catalyst (particle size: 165 μm) with the reaction temperature is shown in Fig. 3.3.16. It may be noted that the catalyst effectiveness factor decreases with the increase in the reaction temperature, the decrease being more pronounced at the higher temperature. This is expected because of the higher activation energy of the reaction as compared to that of the intraparticle diffusion.

3.3.6 EFFECTIVE DIFFUSIVITY OF CATALYST (MEASURED DURING CATALYSIS)

The knowledge of effective intraparticle diffusiveness of reactants and products in porous catalysts is required for predicting the effects of intraparticle mass transfer on the reaction rate and also in the design of catalytic reactors. The effective intraparticle diffusivity could be measured during catalysis from experimental rate data obtained at various particle sizes of the catalyst in the absence of G-L and L-S mass transfer effects) and making use of $\eta - \Phi_s$ relations. It can be measured in the absence of catalytic reaction by the dynamic Wicke-Kellenbach method (5) and the dynamic tracer methods (6,7). However, it is desirable to determine the effective intraparticle diffusivity experimentally during catalysis by the reaction method (i.e. carrying out the reaction using the catalyst of different particle sizes) because of the following reasons. In any catalytic

TABLE-3.3.6

INITIAL RATE DATA FOR THE HYDROGENATION OF *o*-NITROPHENOL
ON THE CATALYST OF DIFFERENT PARTICLE SIZES AND AT DIFFERENT
TEMPERATURES

Temperature (K)	Catalyst loading, w ($\text{g}\cdot\text{dm}^{-3}$)	Catalyst particle size, (d_p) (μm)	Initial rate, (r_o) $\times 10^2$ ($\text{mol}\cdot\text{dm}^{-3}\cdot\text{min}^{-1}$)	Initial rate (r_o/w) $\times 10^2$ ($\text{mol}\cdot\text{g}^{-1}\cdot\text{min}^{-1}$)
308	0.5	30	0.54	1.08
	0.5	45	0.55	1.10
	0.5	90	0.27	0.54
	0.5	165	0.25	0.50
318	0.3	30	0.57	1.90
	0.5	45	0.94	1.88
	0.5	90	0.53	1.06
	0.5	165	0.42	0.84
328	0.3	30	1.50	5.00
	0.5	45	2.49	4.98
	0.5	90	1.42	2.84
	0.5	165	0.68	1.36

TABLE-3.3.7

VALUES OF EFFECTIVENESS FACTOR (η) AND THIELE MODULUS (Φ_s)
FOR THE HYDROGENATION ON THE Pd-CARBON (PARTICLE SIZE:165 μ m)
AT DIFFERENT TEMPERATURES

Catalyst particle radius (R)	:	0.0083 cm			
Catalyst particle density (ρ_p)	:	0.84 g.cm ⁻³			
Concentration of ONP (C_s)	:	0.36 x 10 ⁻³ mol.cm ⁻³			
Temp. (K)	$(r_o/w) \times 10^3$ (mol.g ⁻¹ .min ⁻¹)		Effectiveness factor (η)	Thiele modulus (Φ_s)	$r_A \times 10^5$ ($r_o \rho_p / 60 w$) (mol.cm ⁻³ .sec ⁻¹)
	Observed	Intrinsic			
308	5.0	10.8	0.46	8.5	7.0
318	8.4	19.0	0.44	9.0	11.8
328	13.6	50.0	0.27	13.6	19.04

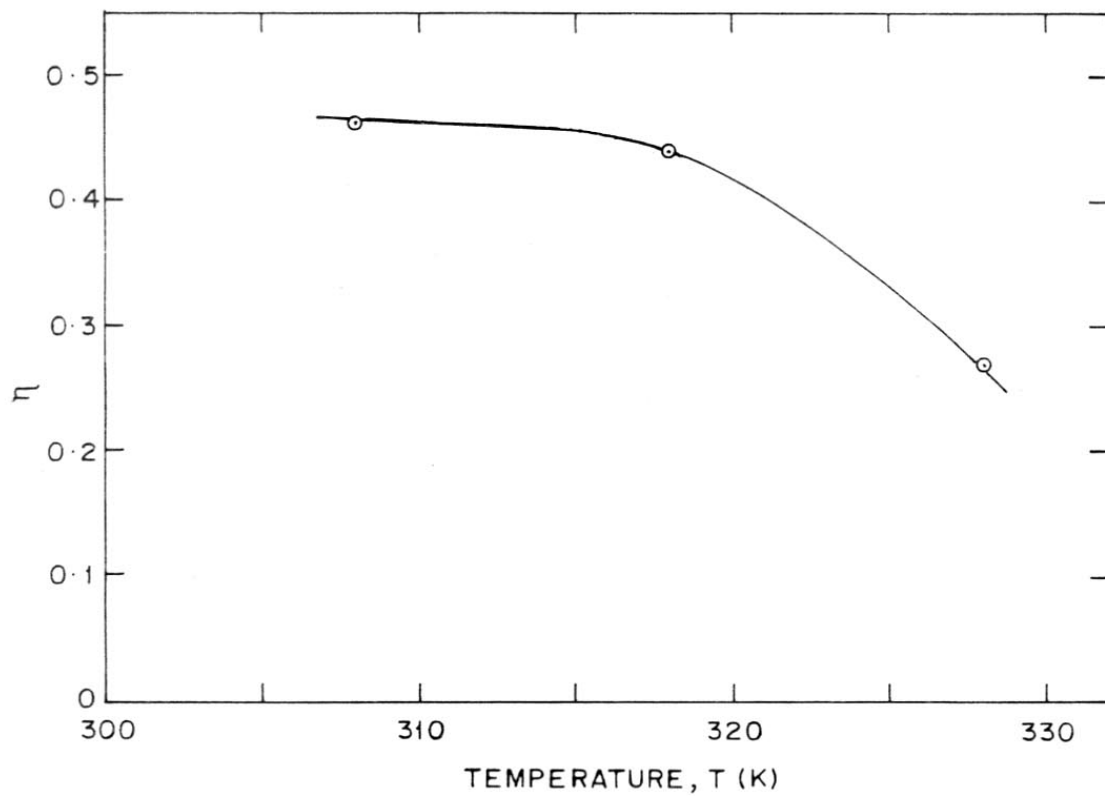


FIG. 3-3-16. VARIATION OF η OF THE Pd-CARBON (PARTICLE SIZE : 165 μm) WITH THE REACTION TEMPERATURE

gas-liquid-solid reaction, the total mass flux in the porous catalyst is due to the simultaneous occurrence of bulk diffusion in the liquid filled pores, adsorption on the pore walls and diffusion in the adsorb layer on the catalyst surface. It is retarded by adsorption and enhanced by surface diffusion. The adsorption from liquid phase on solid surface is very complex phenomenon as compared to the adsorption of gas on solid because of solvent/solute and solvent/catalyst interactions. Therefore, the values of effective diffusivities obtained by the other methods may be quite different from the true effective intraparticle diffusivity displayed in the catalytic reaction.

In the present case, the effective intraparticle diffusivity of *o*-nitrophenol in the Pd-carbon (4.62 wt %) at 308-328 K was determined during catalysis from the experimental rate data on the hydrogenation reaction (Table-3.3.6), obtained using the catalyst of different particle sizes (30-165 μm).

A comparison of the maximum G-L mass transfer, L-S mass transfer and observed reaction rates at the maximum temperature (328 K) of the study (Table-3.3.8) has indicated that the hydrogenation reaction on the catalyst of the different particle sizes at 308-328 K is not controlled or influenced by the G-L or L-S mass transfer processes. Thus the data could be used for the evaluation of the effective intraparticle diffusion coefficient of ONP in the catalyst.

The effective diffusivity (D_e) of the catalyst was evaluated from the catalyst effectiveness factor data (Table-3.3.7) using the following relation (8):

$$D_e = \frac{R^2 r_A}{\sigma_s^2 C_s \eta} \quad (11)$$

TABLE-3.3.8

COMPARISON OF THE MAXIMUM G-L MASS TRANSFER, L-S MASS TRANSFER AND OBSERVED REACTION RATES FOR THE HYDROGENATION ON THE CATALYST OF DIFFERENT PARTICLE SIZES AT 328 K

Catalyst particle size, d_p (μm)	Max. rate of G-L mass transfer, $N_{(G-L)}^3$ ($mol.dm^{-3}.min^{-1}$)	Max. rate of L-S mass transfer, $N_{(L-S)}^3$ ($mol.dm^{-3}.min^{-1}$)	Rate of reaction, ($mol.dm^{-3}.min^{-1}$)	
			$(r_o)_H$	$(r_o)_{ONP}$
30	0.86	0.36	0.045	0.015
45	0.86	0.30	0.075	0.025
90	0.86	0.11	0.042	0.014
165	0.86	0.052	0.021	0.007

The value of the Thiele modulus (ϕ_s) was obtained from the η vs ϕ_s plot (for a zero order reaction) given elsewhere (8). The reaction is assumed to be a zero order with respect to the ONP concentration because the analysis of the initial reaction rate data (discussed) in the Chapter-3.5 indicated that the reaction rate is independent of the concentration of ONP at $C_{ONP} = 0.25 \text{ mol.dm}^{-3}$ (the initial concentration of ONP in the present experiments is 0.36 mol.dm^{-3}).

The values of the effective diffusivity (D_e) of the catalyst for ONP along with the values of the bulk diffusion coefficient (D_{lm}) for ONP-methanol system and the catalyst tortuosity factor (τ) at the different temperatures are given in Table-3.3.9. The tortuosity factor was evaluated by the relation,

$$D_e = \frac{D_{lm} \epsilon}{\tau} \quad (12)$$

The catalyst tortuosity factor [$\tau = 22.9$ (av.)] estimated by the above relation is quite high. A commonly observed value of τ for porous solids is less than six (8). The high value in the present case indicates that the diffusion of ONP in the Pd-carbon [which has a high surface area ($616 \text{ m}^2.\text{g}^{-1}$)] is strongly influenced by the adsorption of ONP on the catalyst. It may be noted that the adsorption of ONP on the catalyst (at $C_{ONP} = 0.36 \text{ mol.cm}^{-3}$) has been found to be quite high (2.15 mmol.g^{-1} at 308 K) (Chapter-3.4).

The temperature dependence of the D_e can be expressed by the following Arrhenius type equation,

TABLE-3.3.9

VALUES OF EFFECTIVE DIFFUSIVITY (D_e), BULK DIFFUSION COEFFICIENT (D_{lm}) AND TORTUOSITY FACTOR (τ) FOR THE DIFFUSION OF o-NITROPHENOL AT DIFFERENT TEMPERATURES

Temperature (K)	$D_e \times 10^7$ ($\text{cm}^2 \cdot \text{sec}^{-1}$)	$D_{lm} \times 10^7$ ($\text{cm}^2 \cdot \text{sec}^{-1}$)	Tortuosity factor, τ
308	4.0	190.4	26.2
318	6.3	221.7	19.4
328	7.3	307.1	23.1

Parameters of Eqn. 13

Activation energy (E)	:	28.9 $\text{kJ} \cdot \text{mol}^{-1}$
Constant (D_o)	:	0.03 $\text{cm}^2 \cdot \text{sec}^{-1}$

$$D_e = D_o \text{ Exp } (-E / R_g T) \quad (13)$$

or

$$\log D_e = \log D_o - (E / 2.303) (1/T)$$

The $\log D_e$ vs $1/T$ plot, according to the above expression is shown in Fig. 3.3.17. The value of activation energy (E) for the diffusion of ONP in the catalyst and of the constant, D_o of the Eqn. 13 is found to be 28.9 kJ.mol^{-1} and $0.03 \text{ cm}^2.\text{sec}^{-1}$, respectively.

The effective diffusivity of the catalyst can thus be expressed by the following expression:

$$D_e = 0.03 \text{ Exp } (3455 / T) \quad (14)$$

The activation energy for the diffusion is somewhat on the higher side. This indicates that the diffusion in the catalyst (which contains micro pores, average pore radius 2.1 nm) is activated one and this is mostly due to the influence of strong adsorption of ONP on the catalyst and the surface diffusion in the adsorbed layer.

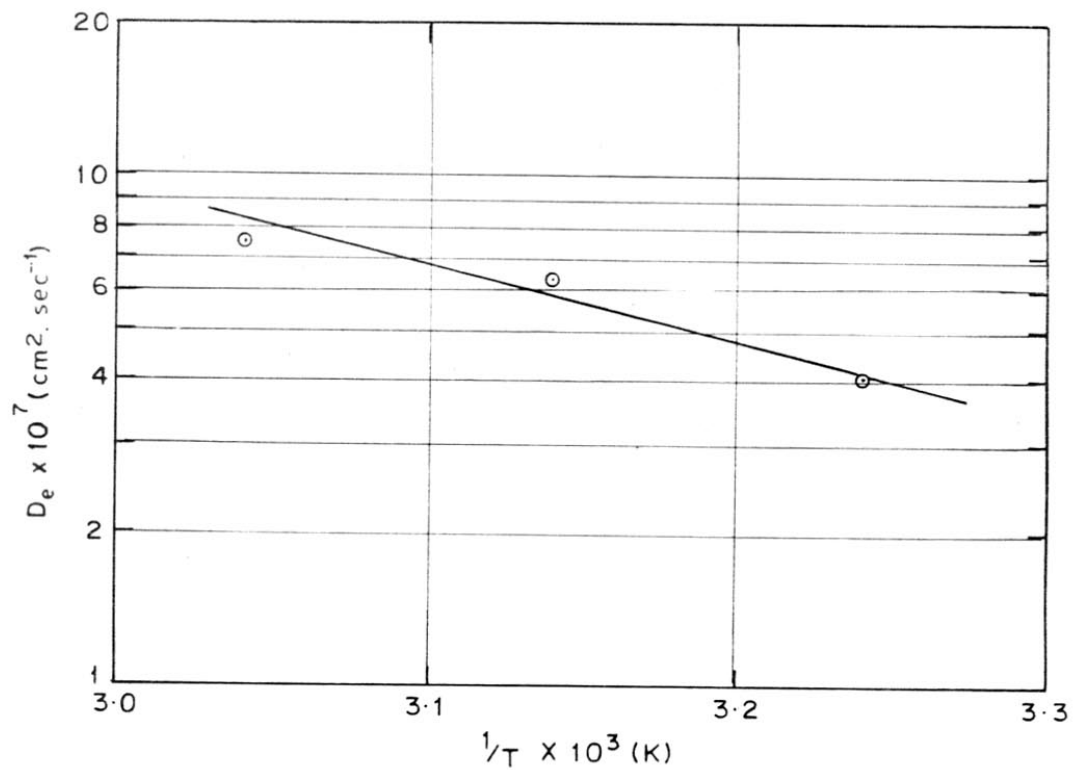


FIG. 3.3.17. TEMPERATURE DEPENDENCE OF THE EFFECTIVE DIFFUSIVITY (D_e) OF *o*-NITROPHENOL IN THE Pd-CARBON

NOMENCLATURE

a_p	external surface area of catalyst [$\text{cm}^2 \cdot \text{cm}^{-3}$ (slurry)]
C_e	equilibrium concentration at G-L interface ($\text{mol} \cdot \text{dm}^{-3}$)
C_H	concentration of H_2 ($\text{mol} \cdot \text{dm}^{-3}$)
C_l	concentration in bulk liquid ($\text{mol} \cdot \text{dm}^{-3}$)
C_N	concentration of ONP ($\text{mol} \cdot \text{dm}^{-3}$)
C_s	concentration at external surface of the catalyst ($\text{mol} \cdot \text{dm}^{-3}$)
C_{si}	concentration at internal surface of the catalyst ($\text{mol} \cdot \text{dm}^{-3}$)
d_I	diameter of stirrer (cm)
d_p	particle size of the catalyst (cm)
D_e	effective diffusivity ($\text{cm}^2 \cdot \text{sec}^{-1}$)
D_o	constant of Eqn. ($\text{cm}^2 \cdot \text{sec}^{-1}$)
D_{lm}	diffusion coefficient of the diffusing species in the liquid ($\text{cm}^2 \cdot \text{sec}^{-1}$)
E	activation energy for the diffusion ($\text{J} \cdot \text{mol}^{-1}$)
G	acceleration due to gravity ($\text{cm} \cdot \text{sec}^{-2}$)
k_s	liquid-solid mass transfer coefficient ($\text{cm} \cdot \text{sec}^{-1}$)
$k_{L,a}$	gas-liquid mass transfer coefficient (min^{-1})
M	molecular weight of solvent
N_m	minimum stirrer speed (rpm)
N_{Pe}	Peclet number
N_{Pe}^*	Peclet number for free-settling particle

N_{Sh}	Sherwood number
$N_{(G-L)}$	rate of gas-liquid mass transfer ($\text{mol.dm}^{-3}.\text{min}^{-1}$)
$N_{(L-S)}$	rate of liquid-solid mass transfer ($\text{mol.dm}^{-3}.\text{min}^{-1}$)
r_A	reaction rate [mol.cm^{-3} (catalyst particle). sec^{-1}]
r_o	initial rate of the reaction [mol.dm^{-3} (slurry). min^{-1}]
R	particle radius (cm)
R_g	gas constant ($\text{J.mol}^{-1}.\text{K}^{-1}$)
T	temperature (K)
t	time (min)
U	terminal velocity of small sphere (cm.sec^{-1})
w	catalyst loading (g.dm^{-3})
x	fractional conversion
X	an empirical association parameter of the solvent (for methanol $X = 1.9$).

Greek letters

α	fractional absorption
β	constant of Eqn. 2
ρ_l	liquid density (g.cm^{-3})
ρ_p	particle density (g.cm^{-3})
ρ_s	solid phase density (g.cm^{-3})
ϵ	porosity
η	catalyst effectiveness factor

μ	<i>viscosity of solution (poise)</i>
μ_l	<i>viscosity of liquid ($\text{g.cm}^{-1}.\text{sec}^{-1}$)</i>
Φ_s	<i>Thiele modulus (Eqn. 11)</i>
τ	<i>tortuosity factor</i>

Subscripts

<i>H</i>	<i>hydrogen</i>
<i>N</i>	<i>o-nitrophenol</i>

REFERENCES

1. Zweitering, T.N., *Chem. Engg. Sci.*, 8 (1968) 244.
2. Brian, P.L.T. and Hakes, H.R., *A.I.Ch.E.J.*, 15 (1969) 419.
3. Brian, P.L.T., Hales, H.B. and T.K. Sherwood, *A.I.Ch.E.J.*, 15, (1969) 727.
4. Wilke, C.R. and Chang, *A.I.Ch.E.J.*, 1 (1955) 264.
5. Shibaye, H. and Uraguchi, Y., *J. Chem. Engg. (Japan)* 10 (1977) 446.
6. Ramachandran, P.A. and Smith, J.M., *Ind. Eng. Chem. Fundam.*, 17 (1978b) 148.
7. Furusawa, T. and Suziki, M., *J. Chem. Eng. (Japan)* 8 (1975) 119.
8. Satterfield, C.N., 'Mass Transfer in Heterogeneous Catalysts', M.I.T. Press, Cambridge (1970).

CHAPTER-3.4

CHAPTER-3.4

ADSORPTION OF REACTION SPECIES ON Pd-CARBON FOR
LIQUID PHASE HYDROGENATION OF o-NITROPHENOL

3.4.1 INTRODUCTION

In any solid catalysed process, adsorption of reactants (or at least one reactant) on the catalyst, reaction between adsorbed reactants [or reaction between at least one adsorbed reactant and other reactant(s) in the bulk phase] and desorption of product(s) occur in successive steps. The overall catalytic process (in the absence of mass transfer resistances) is controlled by one of the steps or a combination of the steps. The adsorption of reaction species plays a vital role in the catalytic process. Hence, in order to understand the catalytic process and its controlling mechanism, it is necessary to investigate the adsorption of reaction species at the catalytic conditions (or at least at the temperatures at which the catalytic reaction occurs).

To the best of the investigator's knowledge no study on adsorption of o-nitrophenol, o-aminophenol and water on Pd-carbon has been reported so far. The literature on the adsorption of H_2 on Pd-carbon is summarised below.

Dus (1) has observed three different forms of H_2 deposit on Pd, first - atomic electronegative polarised $\bar{\beta}$ form, second - atomic electro-positive polarised β^+ form and third - reversibly adsorbed positively polarised molecular α form. Gentsch et al. (2) measured isosteric heat of hydrogen adsorption on atomically dispersed Pd on a high purity carbon film and dispersed Pd. The heat of adsorption ($-\Delta H$) which was dependent on H_2 coverage, was estimated to be 22-26 kcal.mol⁻¹.

Zakumbaeva et al. (3) have investigated the effect of catalyst preparation method, Pd concentration on carbon and temperature on the adsorption of H_2 from solution on Pd-carbon (2 to 20 wt % Pd) and also determined the ratio of dissolved to adsorbed hydrogen.

Aldag and Schmidt (4) studied the adsorption and absorption of hydrogen on palladium wires using flash filament desorption for hydrogen pressures less than 10^{-7} torr; the saturation coverage at 200 K and 300 K were 0.95 H/Pd and 0.39 H/Pd, respectively. The steps at these coverages correspond only to hydrogen adsorbed on palladium surface. The binding energies for the observed three adsorb states, β_1 , β_2 and β_3 with apparent second order desorption kinetics were found to be about 22, 25 and 35 kcal.mol⁻¹, respectively. However, at 100 K a new state, α , which corresponds to solution of H_2 in the palladium wire was observed. The initial heat of H_2 adsorption on palladium film and supported Pd was found to be about 26 kcal.mol⁻¹ (5,6).

In the present investigation, the single and multicomponent adsorption of the reaction species (particularly *o*-nitrophenol, *o*-aminophenol and water) for the hydrogenation of *o*-nitrophenol on Pd-carbon (4.62 wt % Pd) (which is used in the kinetic studies in the hydrogenation) from methanol at the catalytic reaction conditions (temperature: 278-308 K) have been studied.

The experimental procedures for measuring the single and multicomponent adsorption of the reaction species on the catalyst from their methanol solution are described earlier (Section-3.1.5).

3.4.2 SINGLE COMPONENT ADSORPTION

Experimental data on the adsorption of *o*-nitrophenol (ONP), *o*-aminophenol (OAP) and water from their respective methanol solution were collected covering the following adsorption variables.

<u>Adsorbate</u>	<u>Temperature (K)</u>	<u>Equilibrium concentration (mmol.cm⁻³)</u>
<i>o</i> -Nitrophenol	278-308	0.0-0.70
<i>o</i> -Aminophenol	278-308	0.0-0.34
Water	308	0.0-2.00

The use of concentration of ONP and OAP in the adsorption higher than that mentioned above was not possible because of the limitation imposed by the solubility of these compounds in methanol [solubility of ONP in methanol at 278 K $\approx 1.0 \text{ mmol.cm}^{-3}$; solubility of OAP in methanol $\approx 0.4 \text{ mmol.cm}^{-3}$ at 278 K and 0.5 mmol.cm^{-3} at 293 K]. It was also not possible to collect precise adsorption data at the temperatures above 308 K because of the high vapour pressure of methanol at the higher temperatures.

3.4.2.1 Adsorption Isotherms

The results of the adsorption of ONP, OAP and water from methanol on the Pd-carbon are presented in Tables-3.4.1, 3.4.2 and 3.4.3, respectively. The isotherms of the adsorption of these reaction species on the catalyst are shown in Figs. 3.4.1-3.4.3.

It may be noted that, according to the classification of isotherms for adsorption from solution suggested by Giles et al. (7), the isotherms of ONP, OAP and water (Figs. 3.4.1-3.4.3) are of type L1.

TABLE-3.4.1

DATA ON THE ADSORPTION OF *o*-NITROPHENOL ON THE Pd-C

Temperature (K)	Equilibrium concentration of ONP, C_N (mmol.cm^{-3})	Amount of ONP adsorbed, q_N (mmol.g^{-1})
278	0.681	4.890
	0.543	4.500
	0.370	4.110
	0.232	3.400
	0.188	3.160
	0.076	0.180
	0.020	0.980
	0.008	0.526
293	0.540	3.61
	0.298	3.07
	0.242	2.71
	0.195	2.61
	0.128	2.40
	0.08	1.93
	0.024	0.85
	0.010	0.48
308	0.708	2.37
	0.552	2.27
	0.312	2.11
	0.252	1.88
	0.140	1.69
	0.093	1.22
	0.032	0.66
	0.014	0.37

TABLE-3.4.2

DATA ON ADSORPTION OF *o*-AMINOPHENOL ON THE Pd-C

Temperature (K)	Equilibrium concentration of OAP, C_A ($\text{mmol}\cdot\text{cm}^{-3}$)	Amount of OAP adsorbed, q_A ($\text{mmol}\cdot\text{g}^{-1}$)
278	0.330	2.60
	0.230	2.44
	0.140	2.09
	0.113	1.93
	0.086	1.69
	0.068	1.26
	0.036	1.21
	0.011	0.50
293	0.332	2.20
	0.264	1.95
	0.190	1.66
	0.150	1.50
	0.122	1.34
	0.094	1.18
	0.072	0.99
	0.045	0.73
308	0.340	1.16
	0.274	1.11
	0.199	1.04
	0.128	0.86
	0.100	0.81
	0.072	0.75
	0.046	0.60
	0.012	0.41

TABLE-3.4.3

DATA ON THE ADSORPTION OF WATER ON THE Pd-C

Temperature (K)	Equilibrium concentration of water, C_W (mmol.cm^{-3})	Amount of water adsorbed, q_W (mmol.g^{-1})
308	1.95	2.08
	1.16	1.66
	0.77	1.24
	0.62	1.10
	0.46	0.85
	0.31	0.71
	0.15	0.38

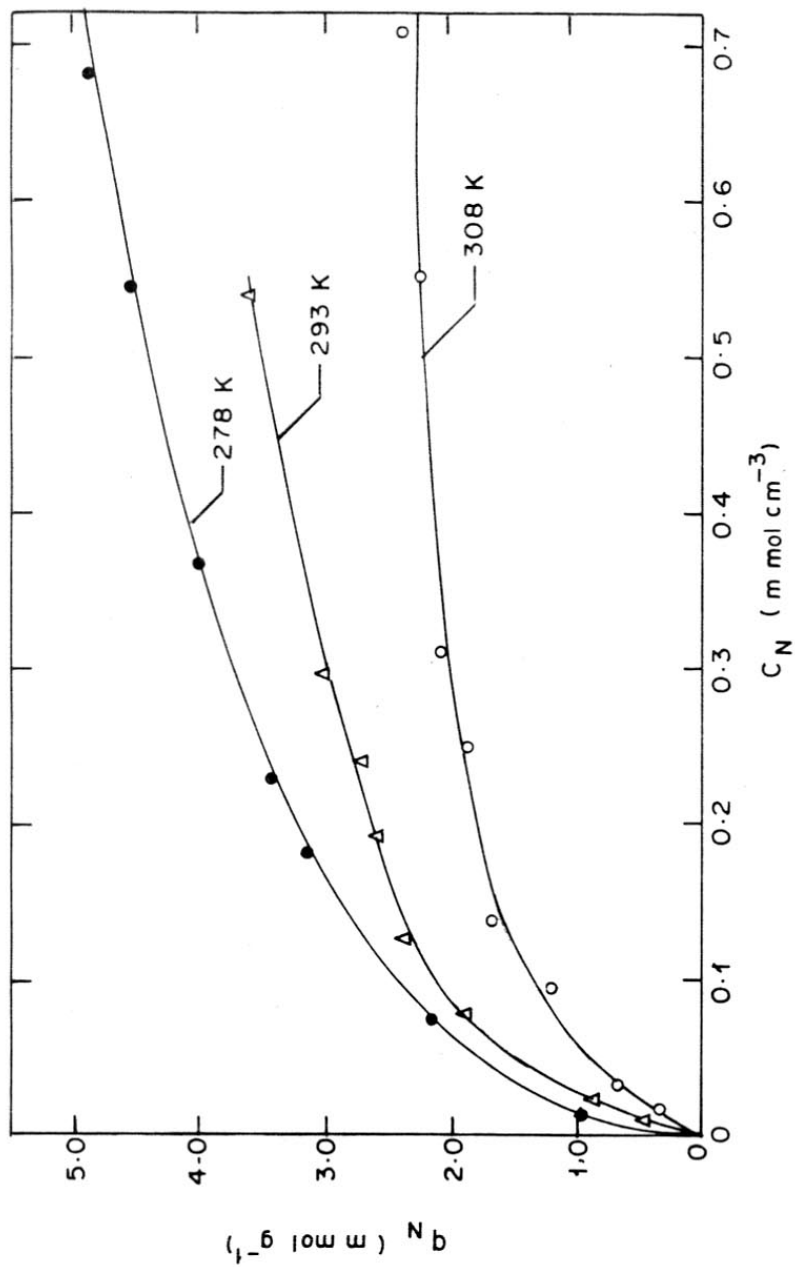


FIG. 3.4.1. ISOTHERMS OF ADSORPTION OF ONP ON THE Pd-C FROM ONP-METHANOL SYSTEM AT DIFFERENT TEMPERATURES

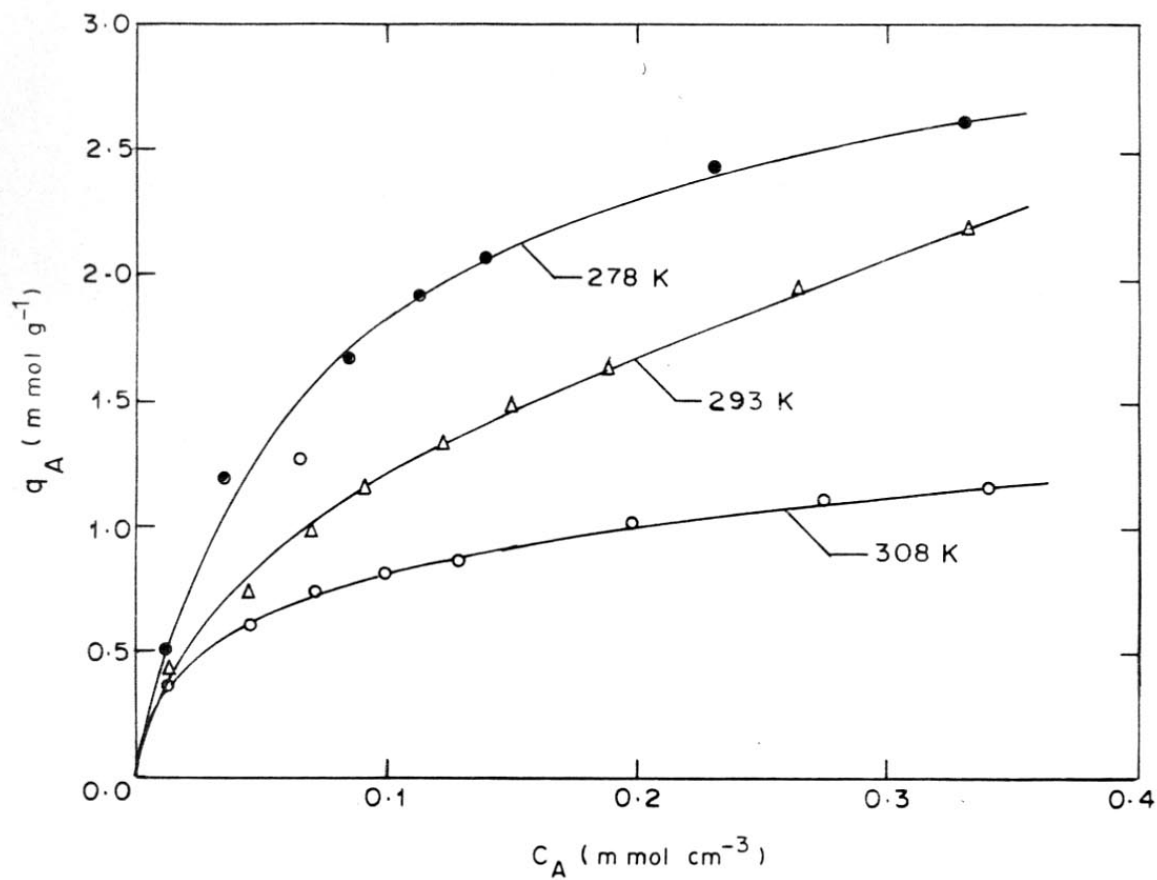


FIG. 3.4.2. ISOTHERMS OF ADSORPTION OF OAP ON THE Pd-C FROM OAP-METHANOL SYSTEM AT DIFFERENT TEMPERATURES

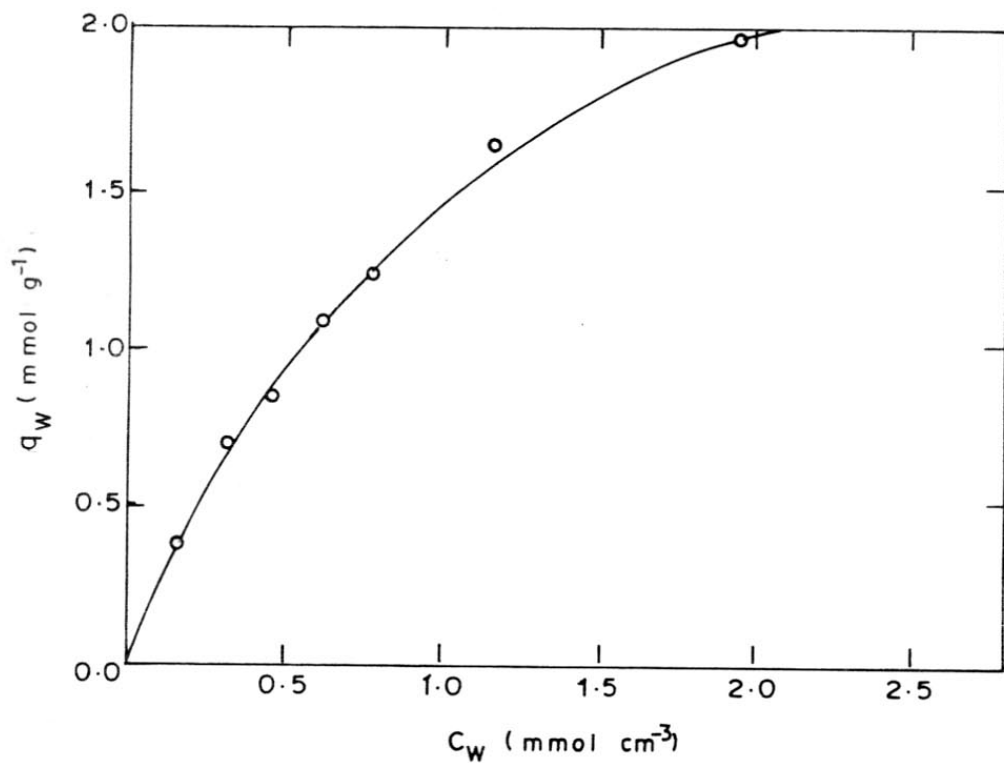


FIG. 3.4.3. ISOTHERM OF ADSORPTION OF WATER FROM METHANOL ON THE Pd-C AT 308 K

In all the cases, the adsorption increases continuously with the increase in the equilibrium concentration of adsorbate. A comparison of the adsorption data for the three reaction species indicates that their adsorption on the Pd-C catalyst occurs in the following order:

ONP > OAP >> Water .

3.4.2.2 Fitting of Adsorption Data

Efforts were made to fit the adsorption data for ONP, OAP and water to the following Langmuir and Freundlich adsorption equations.

Langmuir equation

$$q = q_m \frac{K C}{1 + K C} \quad (1)$$

or

$$C/q = [1 / (q_m K)] + (1 / q_m) C$$

where, q is the amount adsorbed; q_m , the monolayer adsorption capacity of the adsorbent or catalyst; K , the adsorption equilibrium constant; and C , the equilibrium concentration of the adsorbate.

Freundlich equation

$$q = k C^n \quad (2)$$

or

$$\log q = \log k + n \log C$$

where, k is the adsorption constant; and n , the exponent.

Adsorption of o-nitrophenol

The C_N/q_N vs C_N plots according to the Langmuir equation (Eqn. 1) for the adsorption of o-nitrophenol at the different temperatures are shown in Fig. 3.4.4. The plots are linear and this indicates a good fit of the adsorption data at all the temperatures to the Langmuir equation. The values of the adsorption parameters (q_m and K) obtained from Eqn. 1, are given in Table 3.4.4.

When the ONP adsorption data are plotted according to the Freundlich equation (Eqn. 2), $\log q_N$ vs $\log C_N$ (Fig. 3.4.5) plots showed a break for the adsorption at all the temperatures. This indicates that the adsorption of ONP does not follow the Freundlich isotherm.

Adsorption of o-aminophenol

Figure 3.4.6 reveals that the data for the adsorption of OAP (except that at the very low OAP concentrations at 293 and 308 K) give a good fit to the Langmuir equation, thus indicating that the adsorption follows Langmuir isotherm. The values of the Langmuir parameters (q_m and K) for the adsorption of OAP are included in Table-3.4.4.

Figure 3.4.7 indicates that the OAP adsorption data at 293 and 308 K also give a good fit to the Freundlich equation. The adsorption data at 278 K however show a break in the Freundlich plot (Fig. 3.4.7), thus indicating that the adsorption of OAP at 278 K does not follow the Freundlich isotherm. The values of the Freundlich parameters (k and n) for the adsorption at 293 and 308 K are presented in Table-3.4.5.

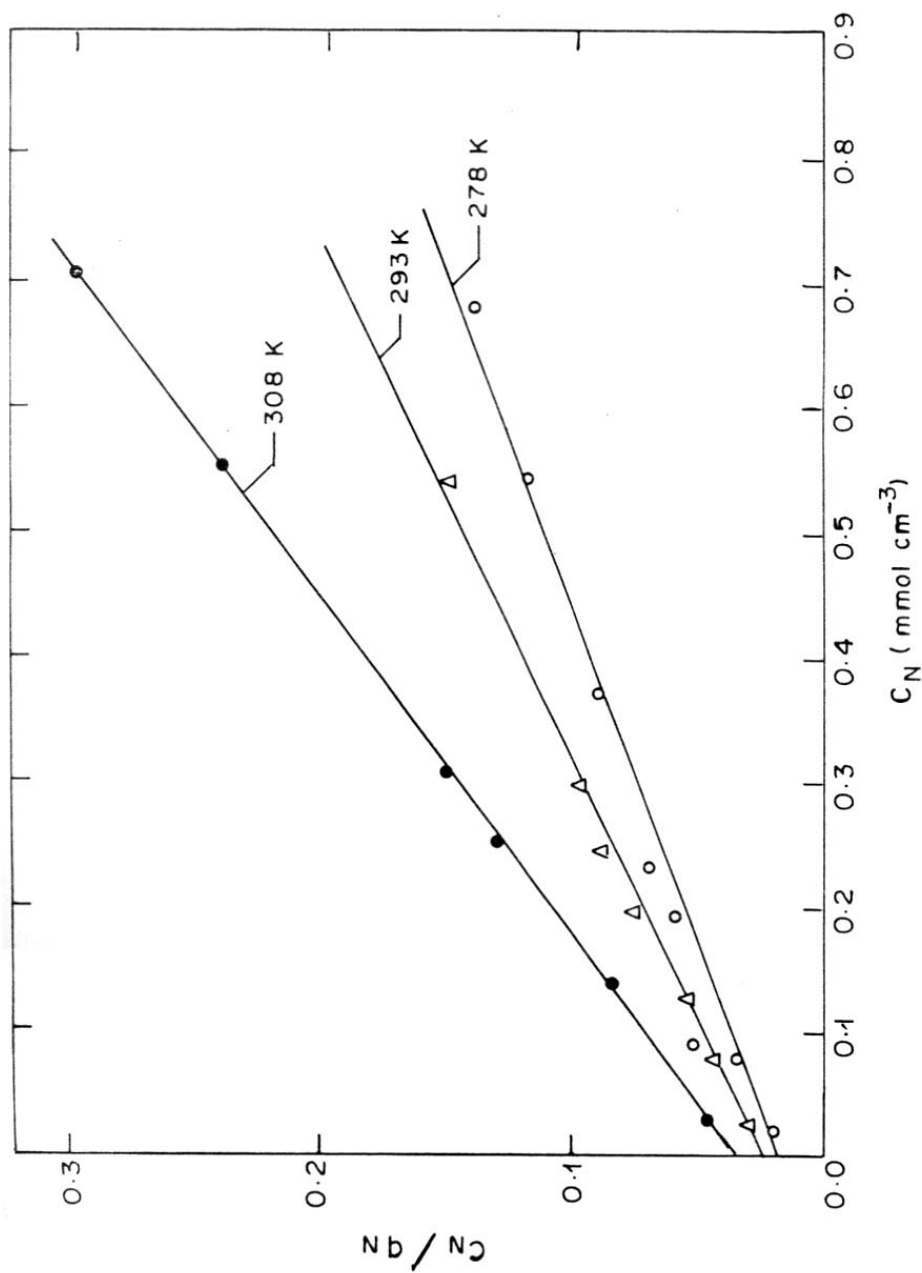


FIG. 3.4.4. LANGMUIR PLOTS (C_N / q_N vs C_N) ACCORDING TO EQN. 1 FOR THE ADSORPTION OF o-NITROPHENOL

TABLE-3.4.4

PARAMETERS (q_m and K) OF EQN. 1 FOR THE SINGLE COMPONENT
 ADSORPTION OF ONP, OAP AND WATER FROM METHANOL ON THE PD-CARBON

Adsorbate	Temperature (K)	q_m (mmol.g ⁻¹)	K (cm ³ .mmol ⁻¹)
ONP	278	5.33	9.28
	293	4.15	9.63
	308	2.69	11.01
OAP	278	2.94	19.60
	293	2.94	7.55
	308	1.38	14.49
Water	308	3.41	0.82

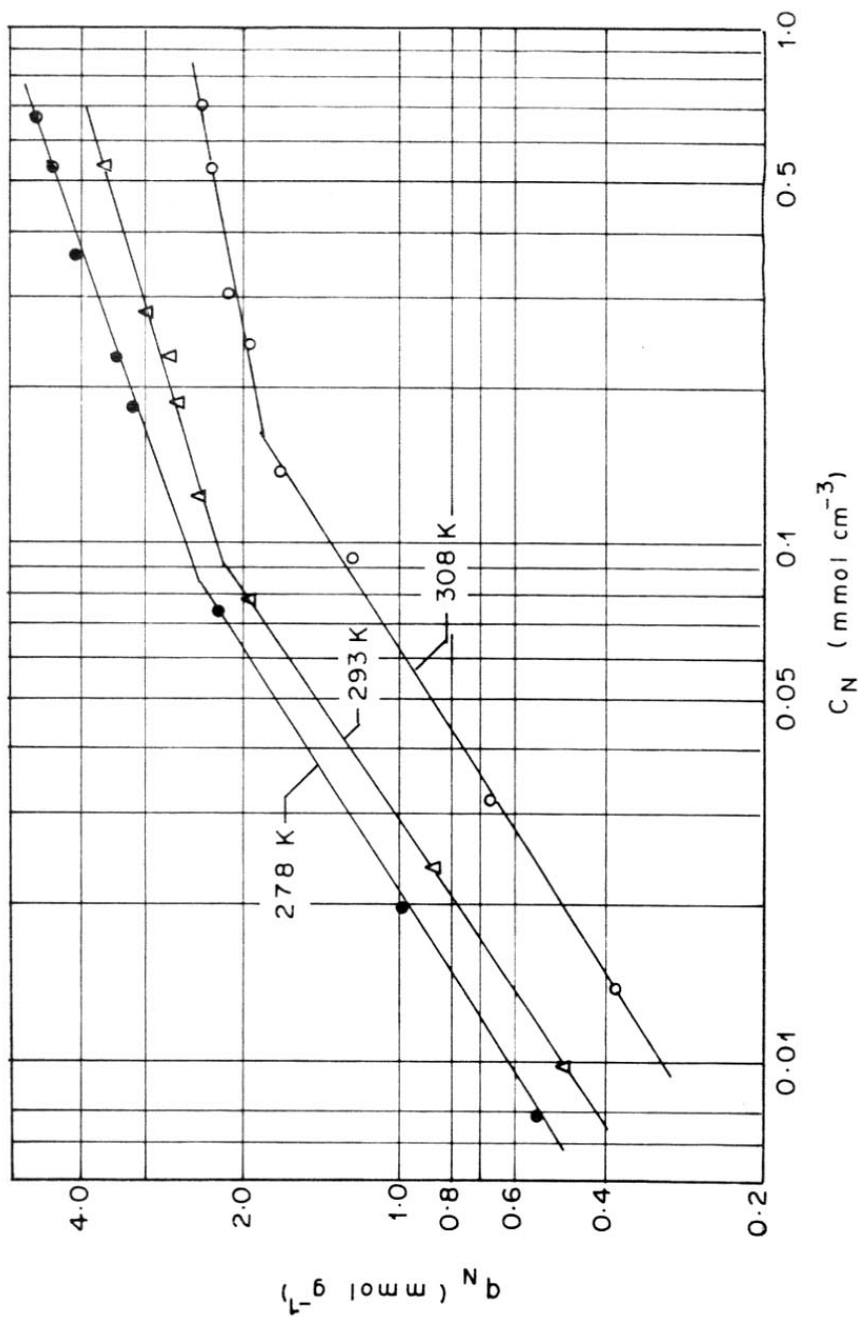


FIG. 3.4.5. FREUNDLICH PLOTS (ACCORDING TO EQN. 2) FOR THE ADSORPTION OF *o*-NITROPHENOL FROM METHANOL ON Pd-CARBON AT DIFFERENT TEMPERATURES

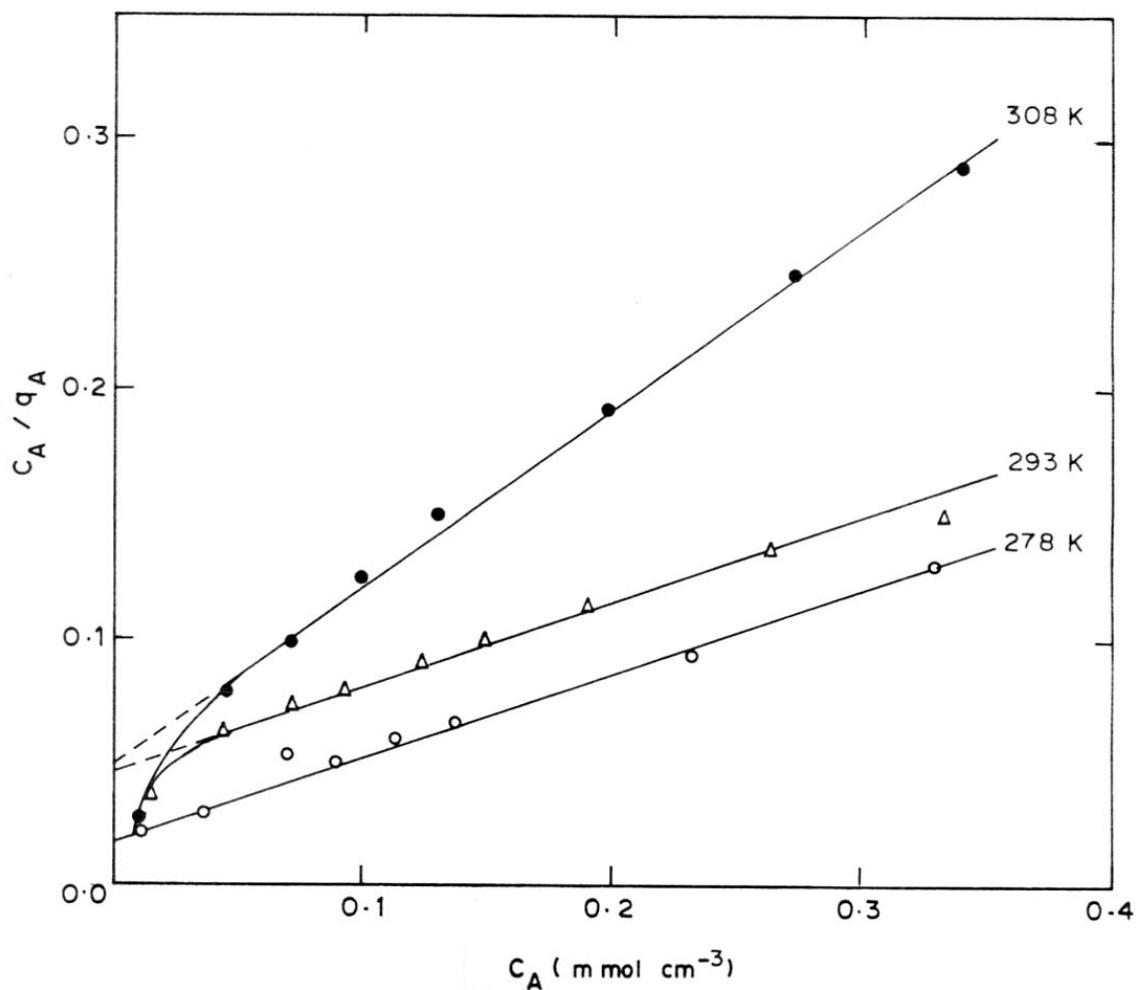


FIG. 3.4.6. LANGMUIR PLOTS (C_A/q_A vs. C_A) ACCORDING TO EQN. 1. FOR THE ADSORPTION OF o-AMINOPHENOL

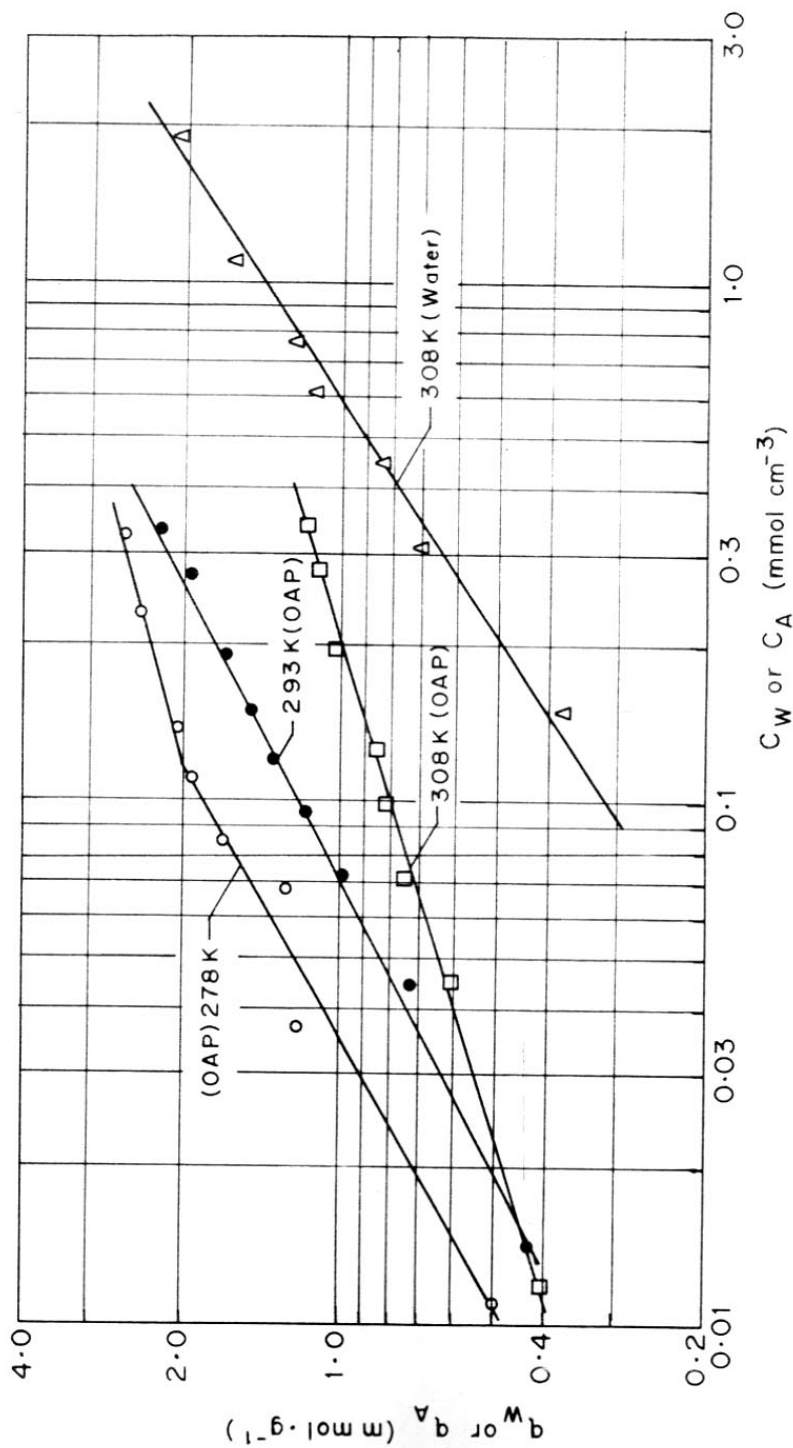


FIG. 3.4.7. FREUNDLICH PLOTS (ACCORDING TO Eqn.2) FOR THE ADSORPTION OF o-AMINOPHENOL AND WATER FROM METHANOL ON Pd-CARBON AT DIFFERENT TEMPERATURES

TABLE-3.4.5

FREUNDLICH PARAMETERS (k AND n) FOR THE ADSORPTION OF
OAP AND WATER FROM METHANOL ON Pd-CARBON

Adsorbate	Temperature (K)	k ($\text{cm}^{3n} \cdot \text{mmol}^{1-n} \cdot \text{g}^{-1}$)	n
OPA	293	4.02	0.52
	308	1.63	0.31
Water	308	1.41	0.65

Adsorption of water

The linear Langmuir and Freundlich plots in Figs. 3.4.8 and 3.4.7, respectively, for the adsorption of water at 308 K show that the adsorption follows both the Langmuir and Freundlich isotherms. The values of the Langmuir and Freundlich parameters for the adsorption of water are included in Tables-3.4.4 and 3.4.5, respectively.

3.4.3 TWO COMPONENT ADSORPTION

The data on the binary adsorption of *o*-nitrophenol and *o*-aminophenol from their mixture in methanol on the Pd-carbon at 278-308 K are given in Table-3.4.6. In the measurement of binary adsorption of ONP and OAP, an equimolar mixture of ONP and OAP in methanol (volume of solution: about 25 cm³) was used at the start of the adsorption.

The individual isotherms of adsorption of ONP and OAP from their mixtures in methanol are shown in Figs. 3.4.9 and 3.4.10, respectively. For a purpose of comparison, the single component adsorption data for ONP and OAP are also included in Figs. 3.4.9 and 3.4.10, respectively. The binary adsorption data are represented by the solid lines, whereas the single component adsorption data by the dotted lines.

A comparison between the binary adsorption and the single component adsorption very clearly shows that the adsorption of ONP is affected (or decreased) very significantly because of the presence of OAP and vice-versa.

Since the single component adsorption of ONP and OAP could be described by the Langmuir equation, it is expected that the binary adsorption of ONP and OAP would also follow the Langmuir equation for

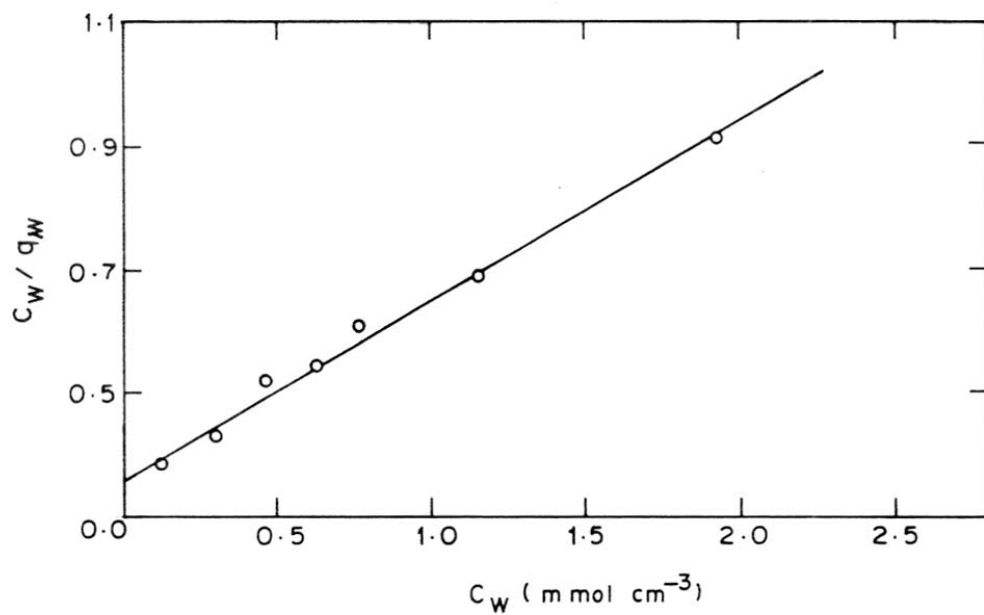


FIG. 3.4.8. LANGMUIR PLOTS (C_W / q_W vs. C_W) ACCORDING TO EQN. 1. FOR THE ADSORPTION OF WATER

TABLE-3.4.6

DATA ON THE BINARY ADSORPTION OF ONP AND OAP ON THE Pd-C
FROM ONP-OAP-METHANOL SYSTEM

Temperature (K)	Equilibrium concentration, C		Amount adsorbed, q	
	C_N (mmol.cm ⁻³)	C_A (mmol.cm ⁻³)	q_N (mmol. g ⁻¹)	q_A (mmol.g ⁻¹)
278	0.128	0.13	1.40	1.3
	0.087	0.095	1.36	0.96
	0.054	0.059	1.09	0.86
	0.030	0.032	0.75	0.66
	0.007	0.004	0.35	0.19
293	0.162	0.172	1.35	0.89
	0.128	0.136	1.22	0.86
	0.092	0.096	1.01	0.82
	0.058	0.060	0.86	0.76
	0.005	0.005	0.22	0.09
308	0.158	0.170	1.30	0.74
	0.126	0.135	1.13	0.71
	0.058	0.06	0.74	0.64
	0.032	0.033	0.58	0.53
	0.003	0.01	0.10	0.17

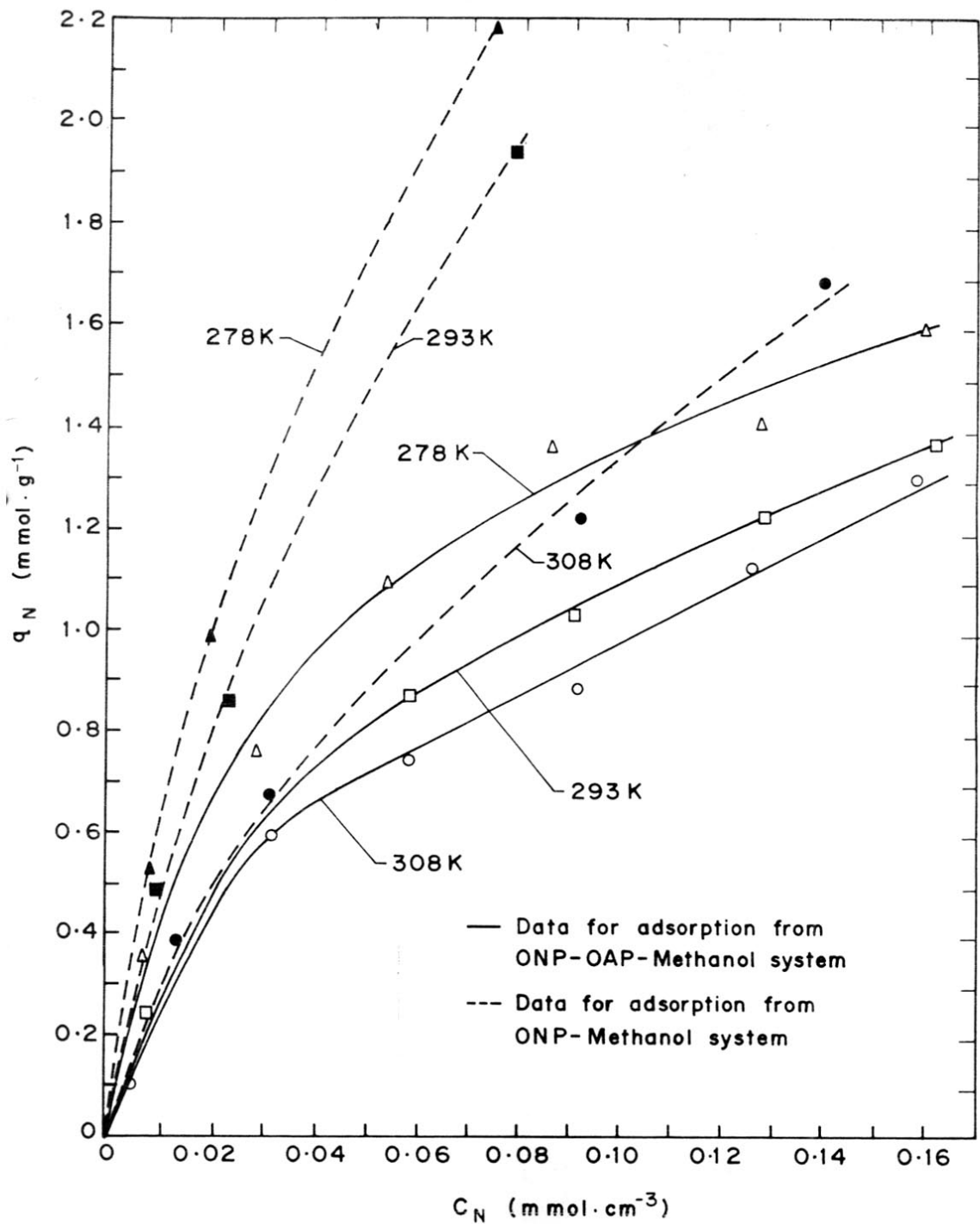


FIG. 3.4.9. ISOTHERMS OF ADSORPTION OF ONP FROM ONP-OAP-METHANOL SYSTEM AT DIFFERENT TEMPERATURE

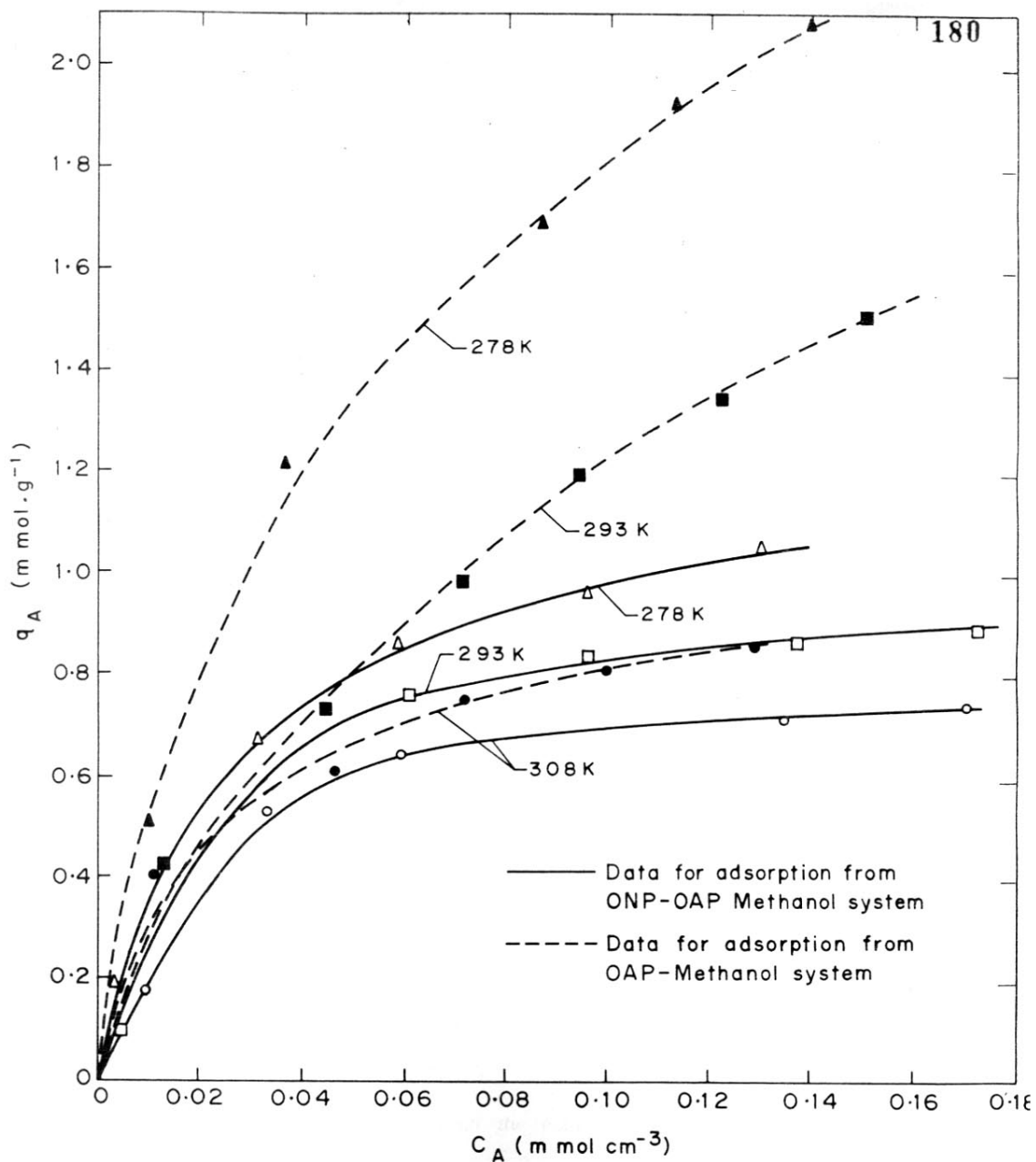


FIG. 3.4.10. ISOTHERMS OF ADSORPTION OF **OAP** FROM **OAP-ONP-METHANOL** SYSTEM AT DIFFERENT TEMPERATURES

the case of multicomponent adsorption. The binary adsorption data are therefore fitted to the following Langmuir equations.

$$q_N = q_m [(K_N C_N) / (1 + K_N C_N + K_A C_A)] \quad (3)$$

or

$$q_N = q_m \alpha$$

and

$$q_A = q_m [(K_A C_A) / (1 + K_A C_A + K_N C_N)] \quad (4)$$

or

$$q_A = q_m \beta$$

where, the suffix N and A represent *o*-nitrophenol and *o*-aminophenol, respectively.

According to the Langmuir theory of adsorption, the adsorption equilibrium constant is expected to be the same for single and multicomponent adsorption. Therefore, the values of K_N and K_A obtained from the single component adsorption of ONP and OAP, respectively, are used in Eqns. 3 and 4 and q_N vs α and q_A vs β plots were obtained (as shown in Figs. 3.4.11 and 3.4.12, respectively). The values of q_m (obtained from the slopes of the linear plots in Figs. 3.4.11 and 3.4.12) for the adsorption of ONP and OAP from their mixtures in methanol, along with the values of K_N and K_A are given in Table-3.4.7.

A comparison between the estimated (from Eqns. 3 and 4) and experimental q_N and q_A , shown in Fig. 3.4.13, indicates a fairly good fit of the binary adsorption data to the Langmuir equations (Eqns. 3 and 4).

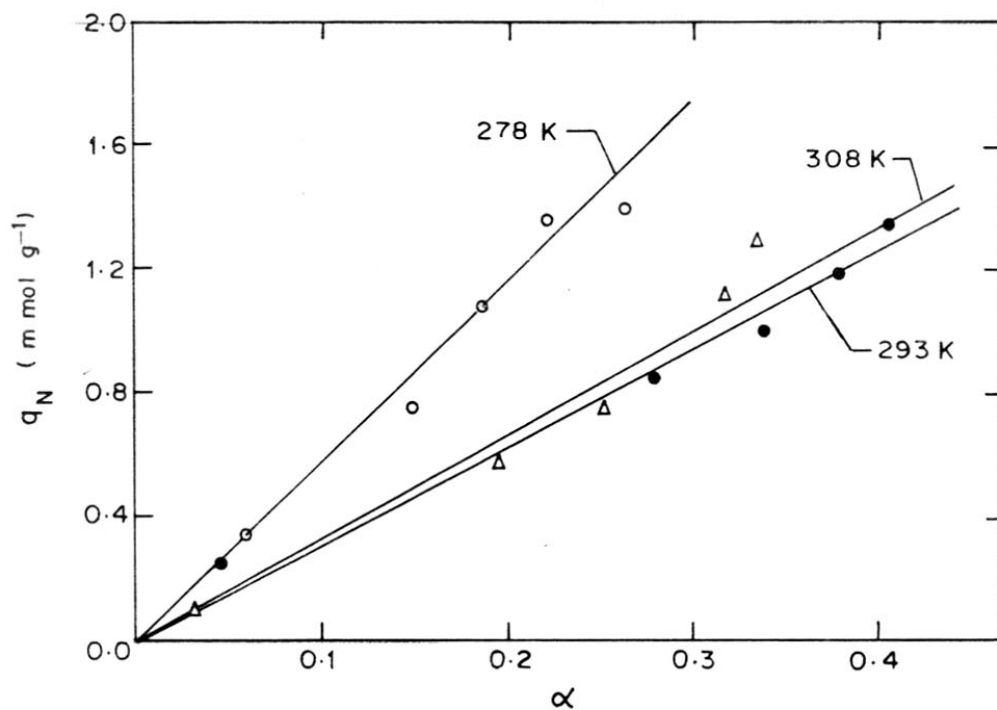


FIG. 3.4.11. A PLOT OF q_N vs. α ACCORDING TO EQN. 3. FOR THE ADSORPTION OF ONP FROM THE ONP-OAP-METHANOL SYSTEM

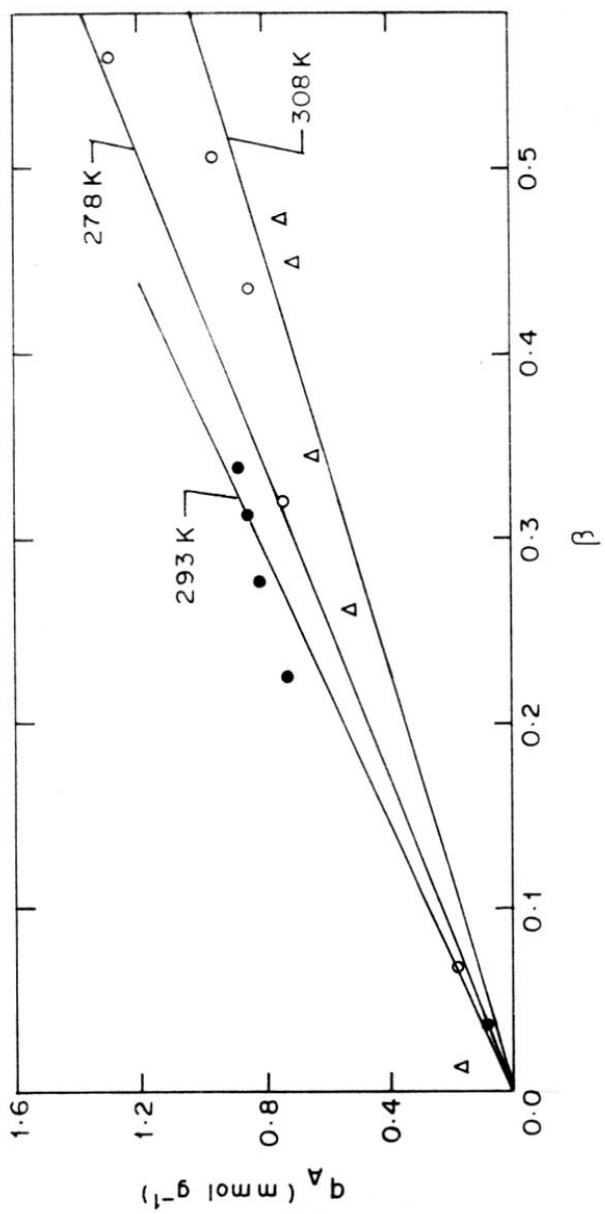


FIG. 3.4.12. A PLOT OF q_A vs β ACCORDING TO EQN. 4. FOR THE ADSORPTION OF OAP FROM THE ONP - OAP - METHANOL SYSTEM

TABLE-3.4.7

PARAMETERS (q_m AND K) OF EQNS. 3 AND 4 FOR THE TWO COMPONENT ADSORPTION OF ONP AND OAP FROM ONP-OAP-METHANOL SYSTEM ON THE Pd-CARBON

Adsorbate	Temperature (K)	q_m (mmol.g^{-1})	K_N ($\text{cm}^3.\text{mmol}^{-1}$)	K_A ($\text{cm}^3.\text{mmol}^{-1}$)
ONP	278	5.8	9.28	19.60
	293	3.2	9.63	7.55
	308	3.35	11.01	14.49
OAP	278	2.4	9.28	19.60
	293	2.75	9.63	7.55
	308	1.80	11.01	14.49

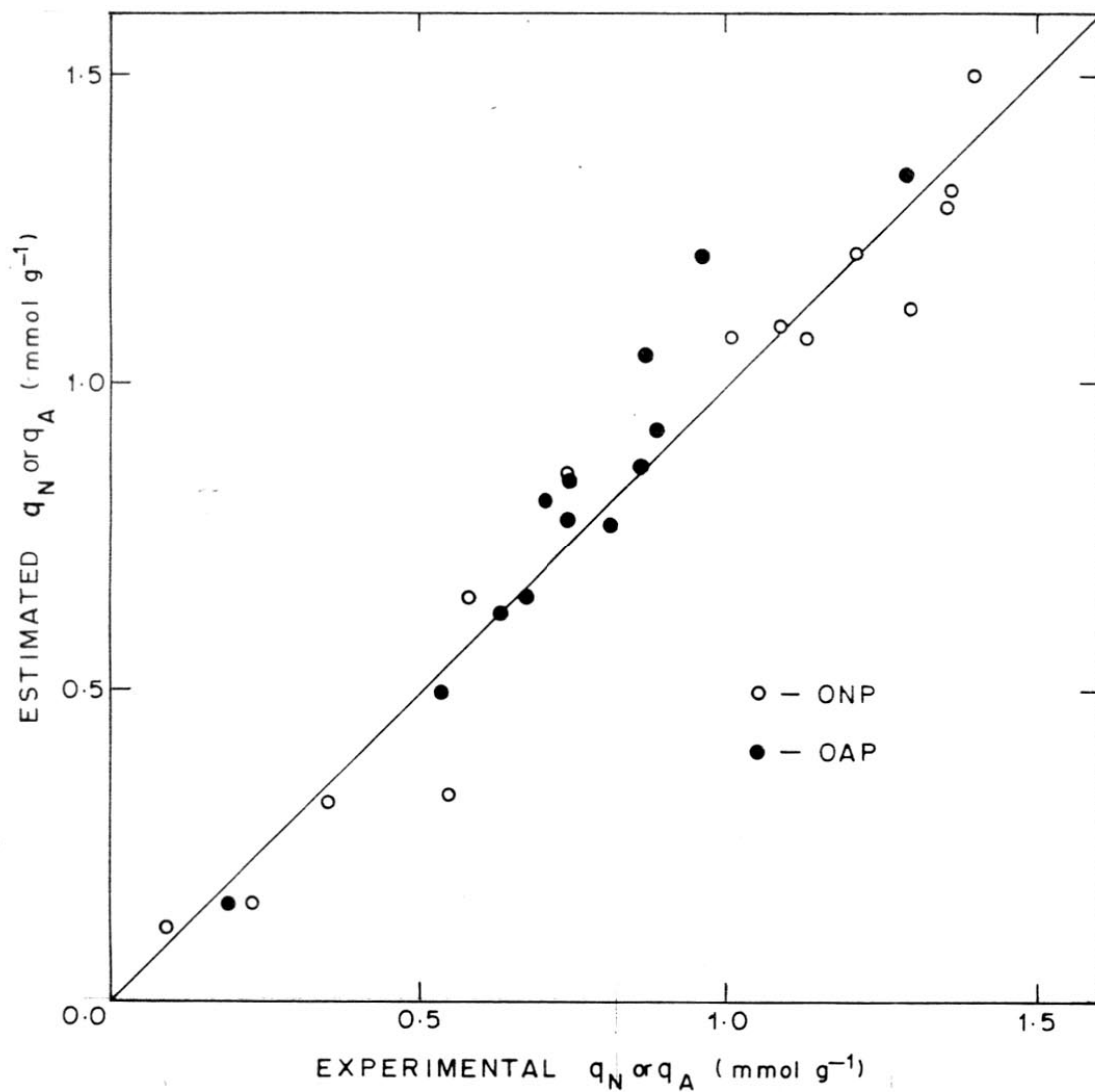


FIG. 3.4.13. A PLOT OF ESTIMATED (FROM EQNS. 3 AND 4) vs. EXPERIMENTAL VALUES OF q_N AND q_A IN THE BINARY ADSORPTION OF ONP AND OAP FROM THE ONA-OAP-METHANOL SYSTEM

In order to obtain a better fit of the experimental data, efforts were also made to fit the binary adsorption data to the following Langmuir-Freundlich equation,

$$q_N = q_m (K_N C_N^{n_N}) / (1 + K_N C_N^{n_N} + K_A C_A^{n_A}) \quad (5)$$

and

$$q_A = q_m K_A C_A^{n_A} / (1 + K_A C_A^{n_A} + K_N C_N^{n_N}) \quad (6)$$

The values of q_m were taken as the same as those obtained from Eqns. 3 and 4, and the values of K_N , K_A , n_N and n_A were determined by a non-linear analysis on the computer [(SN-23 (PDP-11 Equivalent))]. The optimised values of the parameters (K_N , K_A , n_N and n_A) of Eqns. 5 and 6 along with the values of q_m are given in Table-3.4.8. The estimated (from Eqns. 5 and 6) and experimental values of q_n and q_A are compared in Fig. 3.4.14.

A comparison of the results in Figs. 3.4.13 with those in Fig. 3.4.14 indicates that, as compared to the Langmuir equations (Eqns. 3 and 4), the Langmuir-Freundlich equations (Eqns. 5 and 6) give a better fit to the binary adsorption data.

3.4.4 INFLUENCE OF SOLVENT ON THE ADSORPTION

Adsorption from solution on a solid surface is, in general, a complex phenomenon (8) because of the competition between the adsorption of the solute and that of the solvent on the solid surface. The polarity of molecules plays an important role in the adsorption. In case of adsorption from dilute solutions, as in the present case, adsorption of solute can occur

TABLE-3.4.8

PARAMETERS (q_m , K , n) OF EQNS. 5 AND 6 FOR THE TWO COMPONENT ADSORPTION OF ONP AND OAP

Adsorbate	Temp. (K)	q_m (mmol.g ⁻¹)	K_N (cm ³ .mmol ⁻¹)	K_A (cm ³ .mmol ⁻¹)	n_N	n_A
ONP	278	5.80	7.4	15.4	0.97	1.00
	293	3.20	7.2	7.3	0.89	1.00
	308	3.35	7.0	5.3	0.99	1.00
OAP	278	2.40	3.8	12.8	0.51	0.85
	293	2.75	3.1	2.7	0.94	0.69
	308	1.80	1.2	2.3	1.00	0.55

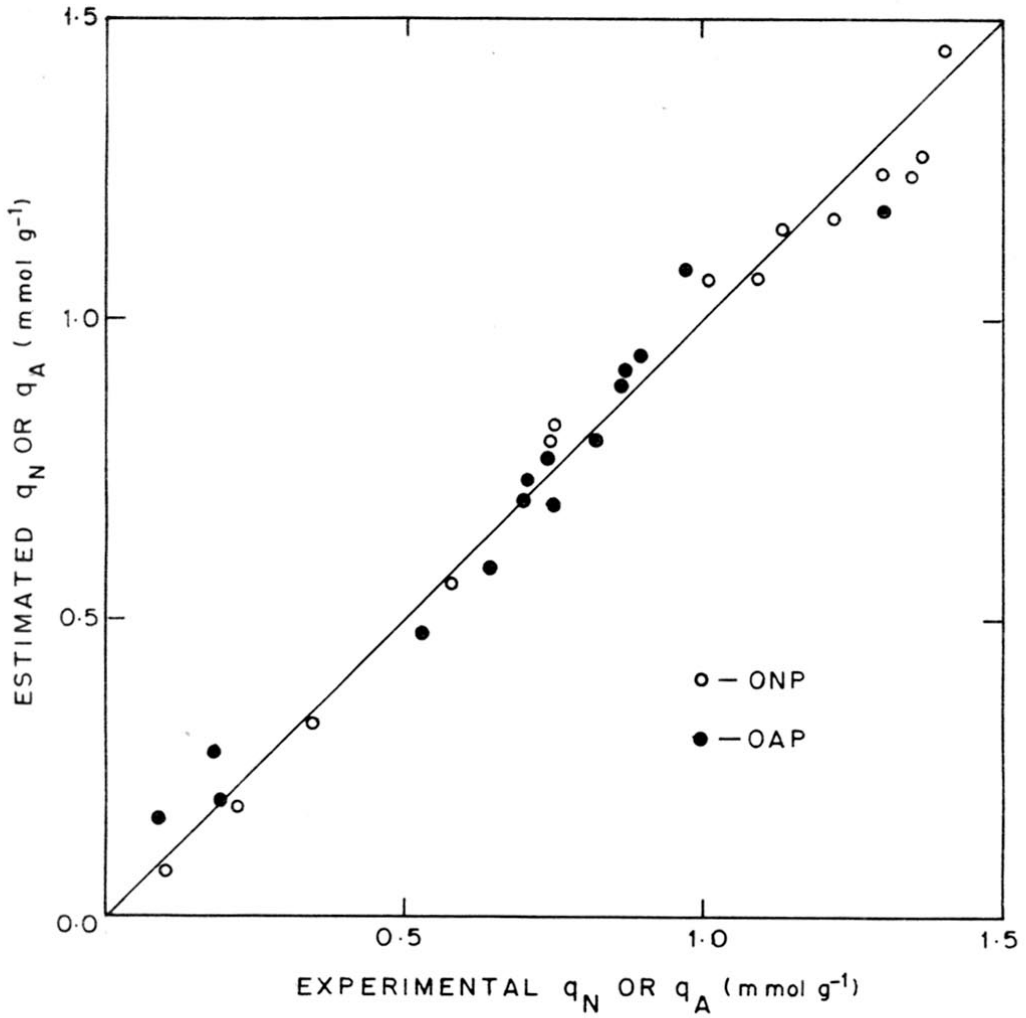


FIG. 3.4.14. A PLOT OF ESTIMATED (FROM EQNS. 5 AND 6) vs. EXPERIMENTAL VALUES OF q_N AND q_A IN THE BINARY ADSORPTION OF ONP AND OAP FROM THE ONP-OAP-METHANOL SYSTEM

to an appreciable extent only if its polarity is much higher than that of the solvent. If this is not so, the adsorption of the solvent is expected to occur in preference to that of the solute as the concentration of the solvent is very high compared to that of the solute. In the present case, the dipole moment of the various reaction species is in the following order:

o-Nitrophenol (3.13D) > *o*-Aminophenol [2.7D (predicted value, Ref.9)]
 > Water (1.71 D) > Methanol (1.63 D) and the adsorption data (Figs. 3.4.1-3.4.3) is quite consistent with this.

According to the classification of isotherms (7,8), the isotherms of the adsorption of all the reaction species are of type L1 and the limit of saturation is not attained in any case. The value of q_m was found to vary with temperature of the adsorption (Table-3.4.4 and 3.4.7). Also the adsorption equilibrium constant (K) for both the reaction species (ONP and OAP) does not show an expected trend with the increase in temperature (generally, K should decrease with the increase in temperature). All these facts indicate that either the adsorption of the reaction species does not strictly follow the Langmuir isotherm or the solvent (i.e. methanol), which is at a very high concentration (about 24 mmol.cm^{-3}) as compared to that of the reaction species, strongly influences the adsorption. The heat of immersion of the catalyst in methanol at 303 K was found to be 63 J.g^{-1} . This indicates that the solvent/catalyst interactions are fairly strong. Recently, Augustine et al. (10) have observed that methanol is readily adsorbed on active Pd catalysts resulting in the blockage of active sites and also in the conversion of original active sites into unreactive sites. The observed unexpected trend in the adsorption (i.e. the observed variation of q_m and K with temperature) is, therefore, attributed most probably to the adsorption of methanol, occurring simultaneously with the adsorption of reaction species.

REFERENCES

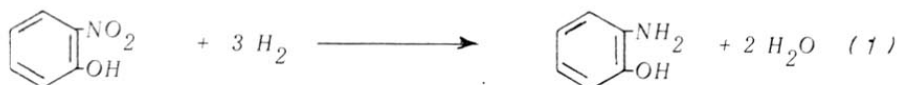
1. Dus, R., *J. Catal.*, 42 (1976) 334.
2. Gentsch, H., Guillen, N. and Koepp, M., *Z. Phys. Chem. (Frankfort am Main)* 82 (1972) 49.
3. Zakumbseva, G.D., Zahargna, N.A., Toktabaera, N.F. and Masalk, N.V., *Kinet. Katal.* 18 (1977) 1007.
4. Aldag, A.W., Schmidt, L.D., *J. Catal.*, 22 (1971) 260.
5. Beeck, O., *Discuss. Faraday Soc.* 8 (1950) 118.
6. Schuit, G.S.A. and Van Rejjen, L.S., *Advn. Catal. Relat. Subj.*, 10 (1958) 242.
7. Giles, C.H., Mac Evan, H., Nakhwa, S.N. and Smith, D.J., *J. Chem. Soc.* (1960) 3973.
8. Kipling, J.J., 'Adsorption from Solutions of Non-electrolytes', Academic Press, London, 1965, p. 90.
9. Owen, A.J., *Tetrahydron*, 25 (1969) 3693.
10. Augustine, R.L., Warner, R.W. and Melnick, M.J., *J. Org. Chem.*, 49 (1984) 4853.

CHAPTER-3.5

CHAPTER-3.5

KINETICS OF HYDROGENATION OF o-NITROPHENOL ON
Pd-CARBON IN THREE PHASE STIRRED REACTOR

The hydrogenation of o-nitrophenol to o-aminophenol proceeds according to the following reaction scheme:



The reaction is exothermic and irreversible. The heat of the hydrogenation reaction (ΔH) at 298 K is estimated to be about -460 kJ.mol^{-1} .

In the present investigation, the hydrogenation reaction is carried out in the three phase stirred (slurry) reactor (Fig. 3.1.1) on the Pd-carbon (4.62 wt % Pd) catalyst using methanol as a reaction medium for the purpose of obtaining kinetic data in the chemical control regime and a kinetic rate model (based on the Langmuir adsorption theory) for the reaction is developed.

3.5.1 KINETIC DATA

The kinetic data on the hydrogenation reaction were obtained at the following conditions.

Catalyst	:	Pd-carbon (4.62 wt % Pd)
Catalyst particle size	:	30 μm
Reaction medium (or solvent)	:	methanol
Volume of reaction mixture	:	1.0 dm^3
Initial concentration of ONP	:	0.072 - 0.36 mol.dm^{-3}

Catalyst loading	:	0.3 or 0.5 g.dm ⁻³
H ₂ -pressure	:	445-1463 kPa
Stirring speed	:	980 rpm
Reaction temperature	:	293-328 K

The properties of the catalyst have already been given in Table 3.3.1.

In Chapter-3.3, it has already been shown that the hydrogenation reaction (when carried out at the above conditions) is not influenced by any of the mass transfer processes (viz. gas-liquid, liquid-solid, and intra-particle mass transfer) occurring simultaneously with the reaction. The kinetic data thus obtained could therefore be used for developing a kinetic model which can form a basis for the rational design of reactor for the hydrogenation process.

The kinetic data on the reaction showing the variation of the concentrations of *o*-nitrophenol, *o*-aminophenol and water with the reaction time at the different temperatures and H₂-pressures are presented in Appendices-3.5.1-3.5.4.

The *o*-nitrophenol concentration (C_N) - reaction time (t) data obtained in every kinetic run, were fitted to the following polynomial equation:

$$C_N = A_1 + A_2t + A_3t^2 + A_4t^3 + A_5t^4 + A_6t^5 \quad (2)$$

The values of the polynomial coefficients (A₁, A₂, A₃, A₄, A₅ and A₆) for the kinetic data obtained in the different kinetic runs are presented in Appendix-3.5.5. The values of the coefficients were obtained by the linear least square analysis.

The reaction rates ($-dC_N/dt$) were obtained by differentiating the above equation, as follows.

$$-dC_N/dt = A_2 + 2A_3 t + 3A_4 t^2 + 4A_5 t^3 + 5A_6 t^4 \quad (3)$$

The reaction rate data are included in Appendices-3.5.1-3.5.4.

The analysis of the kinetic data and the kinetic modelling have been done on a SN23 (PDP-11 Equivalent) computer.

3.5.2 ANALYSIS OF INITIAL RATE DATA

The initial reaction rate (i.e. the rate of zero reaction time) data on the hydrogenation at different temperatures, H_2 -concentrations and initial concentrations of *o*-nitrophenol are given in Table-3.5.1.

3.5.2.1 Order of Reaction w.r.t. *o*-Nitrophenol Concentration

The ONP concentration (C_N) dependence of the initial reaction rate of the hydrogenation at different temperatures is shown in Fig. 3.5.1. The results indicate that the reaction is independent of the ONP concentration (i.e. it is zero order w.r.t. the concentration of ONP) at the higher concentrations (i.e. at $C_N > 0.25 \text{ mol.dm}^{-3}$).

The power law rate model for the reaction can be expressed as,

$$r_o/w = k (C_N)^n (C_H)^m \quad (4)$$

where, r_o is the initial rate of the reaction; C_N , the concentration of ONP; C_H , the concentration of hydrogen; k , the reaction rate constant; n and m , the reaction orders with respect to ONP and hydrogen

TABLE-3.5.1

INITIAL RATE DATA FOR THE HYDROGENATION

Temperature (K)	P_{H_2} (kPa)	C_H (mol.dm ⁻³)	C_N (mol.dm ⁻³)	$(r_o/w) \times 10^2$ (mol.g ⁻¹ .min ⁻¹)
1	2	3	4	5

Data at constant ONP concentration

293	1463	0.051	0.36	0.48
	1050	0.036	0.36	0.44
	776	0.027	0.36	0.32
	500	0.017	0.36	0.28
308	1448	0.055	0.36	1.08
	1035	0.039	0.36	1.00
	760	0.029	0.36	0.72
	486	0.018	0.36	0.56
318	1432	0.058	0.36	1.93
	1619	0.042	0.36	1.43
	744	0.030	0.36	1.13
	469	0.019	0.36	0.008
328	1407	0.059	0.36	5.00
	995	0.042	0.36	2.70
	720	0.031	0.36	1.80
	445	0.019	0.36	1.13

Data at constant total pressure

293	1463	0.0512	0.360	0.48
	1463	0.0512	0.250	0.48
	1463	0.0523	0.144	0.44
	1463	0.0526	0.072	0.30

.....

Table-3.5.1 contd.

1	2	3	4	5
308	1448	0.0550	0.36	1.08
	1448	0.0564	0.251	1.05
	1448	0.0572	0.149	0.64
	1448	0.0579	0.072	0.50
318	1432	0.0587	0.360	1.93
	1432	0.0615	0.251	1.93
	1432	0.0644	0.443	1.63
	1432	0.0658	0.072	0.93
328	1407	0.0597	0.360	5.00
	1407	0.0640	0.251	5.20
	1407	0.0682	0.143	4.50
	1407	0.0714	0.072	2.67

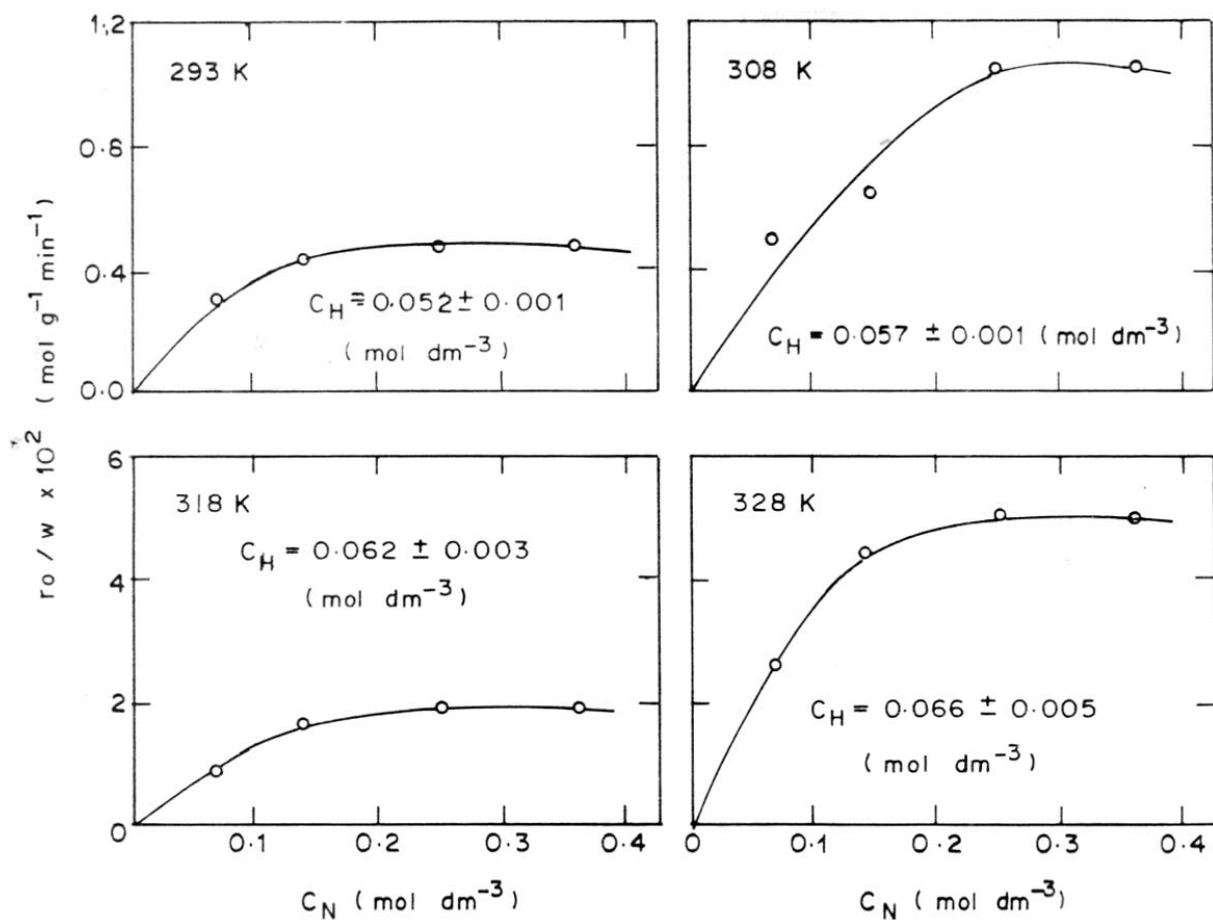


FIG. 3.5.1. DEPENDENCE OF THE INITIAL REACTION RATE (r_0/w) ON THE CONCENTRATION OF ONP (C_N) AT A NEARLY CONSTANT H_2 CONCENTRATION (C_H) IN THE HYDROGENATION OF DIFFERENT TEMPERATURES

concentration, respectively. Since the concentration of hydrogen was almost the same for the data collected at the particular temperature (Table-3.5.1 and Fig. 3.5.1), the reaction order with respect to ONP concentration (n) could be obtained from the slope of the linear $\log (r_o/w)$ vs $\log C_N$ plots, shown in Fig. 3.5.2. The values of n for $C_N < 0.25 \text{ mol.dm}^{-3}$ at the different temperatures are presented in Table-3.5.2. The average order of the reaction w.r.t. ONP concentration has been found to be 0.54.

3.5.2.2 Order of Reaction w.r.t. H_2 -Concentration

The dependence of the initial reaction rate on the H_2 concentration at the constant ONP concentration ($C_N = 0.36 \text{ mol.dm}^{-3}$) at the different temperatures is shown in Fig. 3.5.3. The initial reaction rate increases continuously with the increase in the H_2 -concentration.

The reaction order (m) w.r.t. the H_2 -concentration was determined from the slopes of the linear $\log (r_o/w)$ vs $\log C_H$ plots, shown in Fig. 3.5.4, and the values of m at the different temperatures are included in Table-3.5.2. It is interesting to note that the order of reaction (m) increases with the increase in the temperature.

3.5.2.3 Activation Energy of the Reaction

Because of the fact that the concentration of ONP, while collecting the data given in Fig. 3.5.3, was kept constant ($C_N = 0.36 \text{ mol.dm}^{-3}$) at all the temperatures (293-328 K), the Eqn. 3 in this case reduces to,

$$r_o/w = k_a C_H^m \quad (5)$$

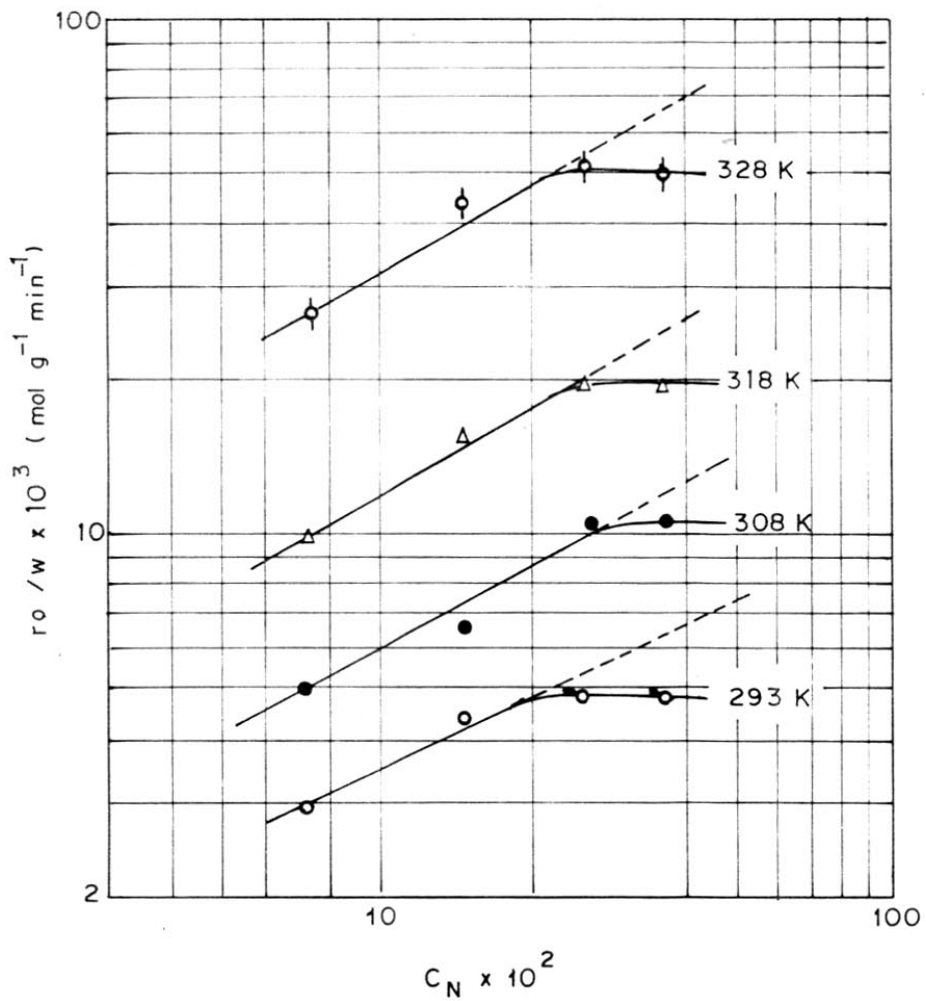


FIG. 3.5.2. LOG (r_o/w) vs. LOG C_N PLOTS FOR THE HYDROGENATION AT DIFFERENT TEMPERATURES

TABLE-3.5.2

ORDER OF THE HYDROGENATION REACTION

Temperature (K)	Order of reaction	
	w.r.t. ONP concentration (n)*	w.r.t. H_2 concentration (m)
293	0.50	0.54
308	0.55	0.64
318	0.56	0.77
328	0.56	1.00

* Valid upto ONP concentration of 0.25 mol.dm^{-3} . Above this concentration, the reaction is zero order w.r.t. the ONP concentration

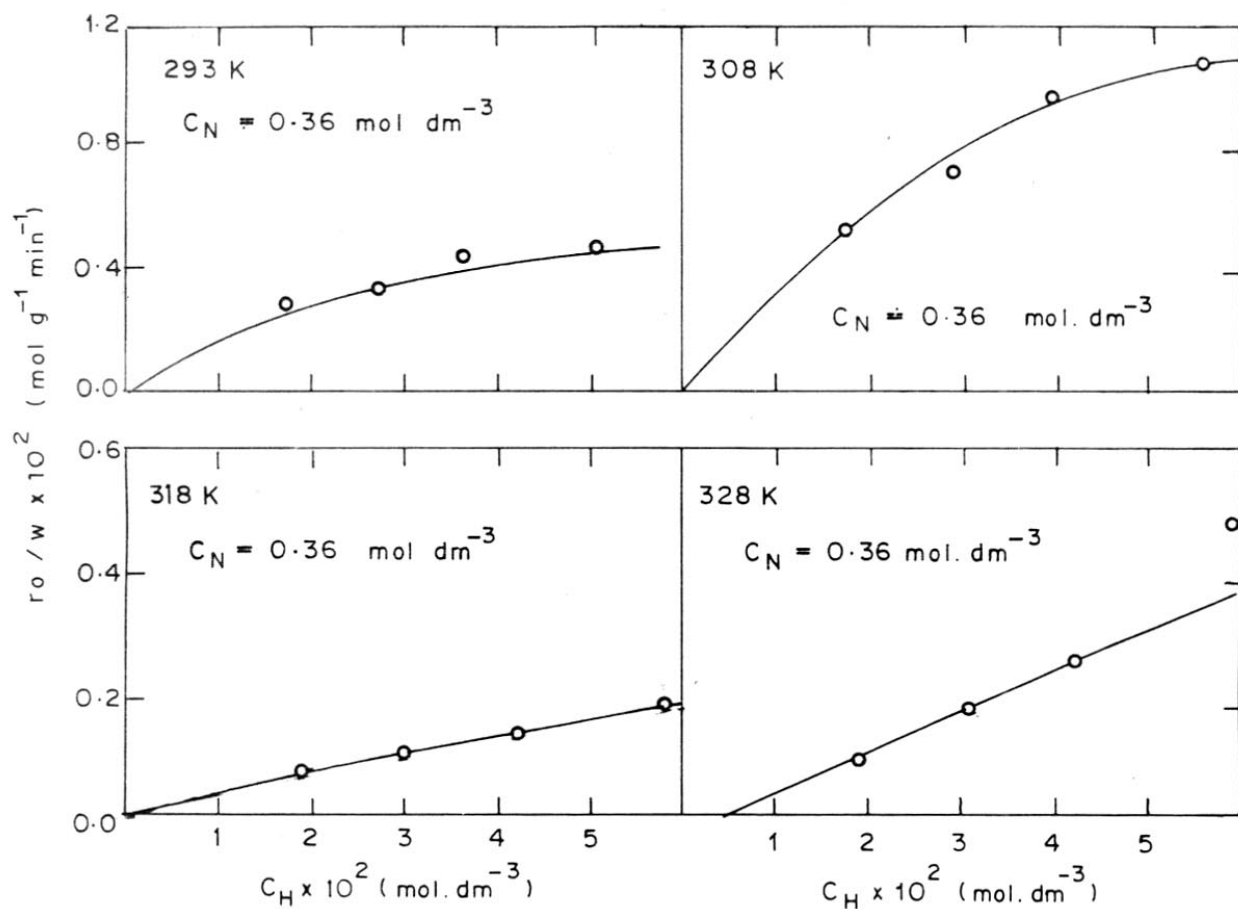


FIG. 3.5.3. DEPENDENCE OF THE INITIAL REACTION RATE (r_0/w) ON THE H_2 -CONCENTRATION (C_H) AT CONSTANT ONP CONCENTRATION (C_N) IN THE HYDROGENATION AT DIFFERENT TEMPERATURES

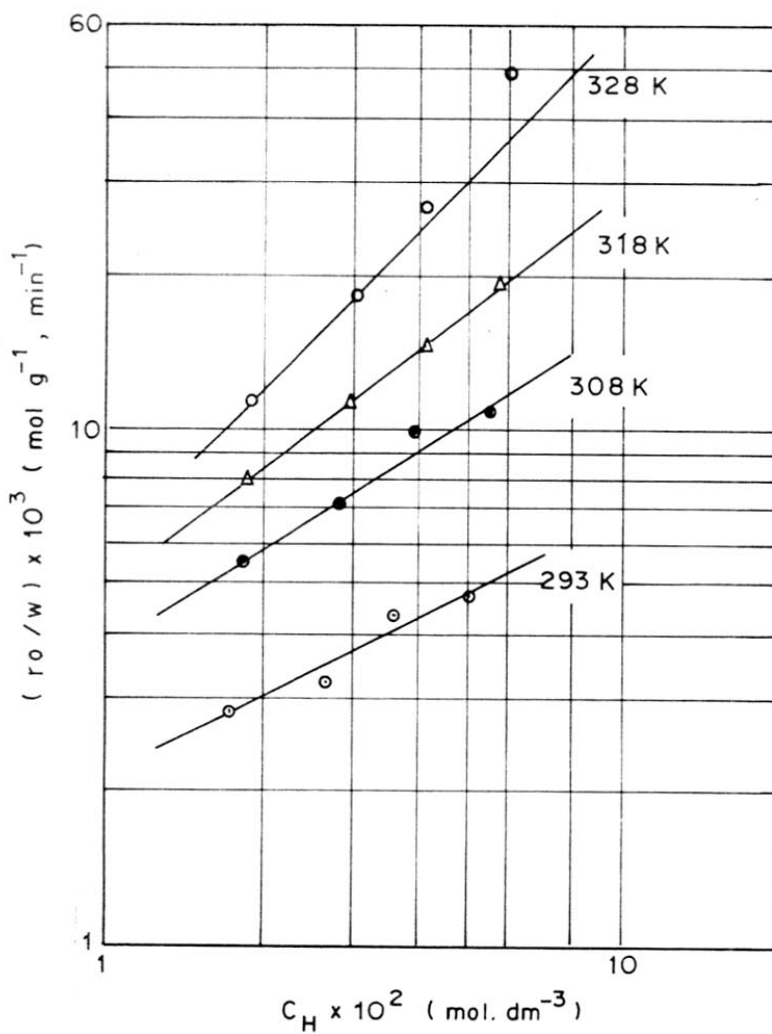


FIG. 3.5.4. LOG (r_o/w) vs. LOG C_H PLOTS FOR THE HYDROGENATION AT DIFFERENT TEMPERATURES

where, k_a is the apparent reaction rate constant (which includes the ONP concentration term). The values of k_a at the different temperatures are given in Table-3.5.3.

The temperature dependence of the apparent reaction rate constant (k_a) can be expressed by the Arrhenius equation,

$$k_a = A \text{ Exp } [- E / RT] \quad (6)$$

or

$$\log k_a = \log A - (E/2.303 R) (1/T)$$

where, E is the activation energy of the reaction; A , the frequency factor; R , the gas constants; and T , the temperature.

The Arrhenius plot [$\log k_a$ vs $1/T$] for the reaction is shown in Fig. 3.5.5. The activation energy of the reaction, obtained from the slope of the linear Arrhenius plot is found to be 70.2 kJ.mol^{-1} .

It may be noted that the order of reaction can be very conveniently determined by the analysis of initial rate data, particularly, when the reaction rate is influenced by the products of the reaction. In the present case, the preliminary study has indicated a very significant influence of OAP on the reaction rate. However, the effect of water on the reaction rate was found to be very small.

TABLE-3.5.3

APPARENT REACTION RATE CONSTANT (k_a) AND ACTIVATION ENERGY FOR THE HYDROGENATION

Temperature (K)	k_a [$\text{mol}^{1-m} \cdot \text{dm}^3 \cdot \text{g}^{-1} \cdot \text{min}^{-1}$]
293	0.024
308	0.075
318	0.182
328	0.600

Activation energy (E) = 70.17 $\text{kJ} \cdot \text{mol}^{-1}$

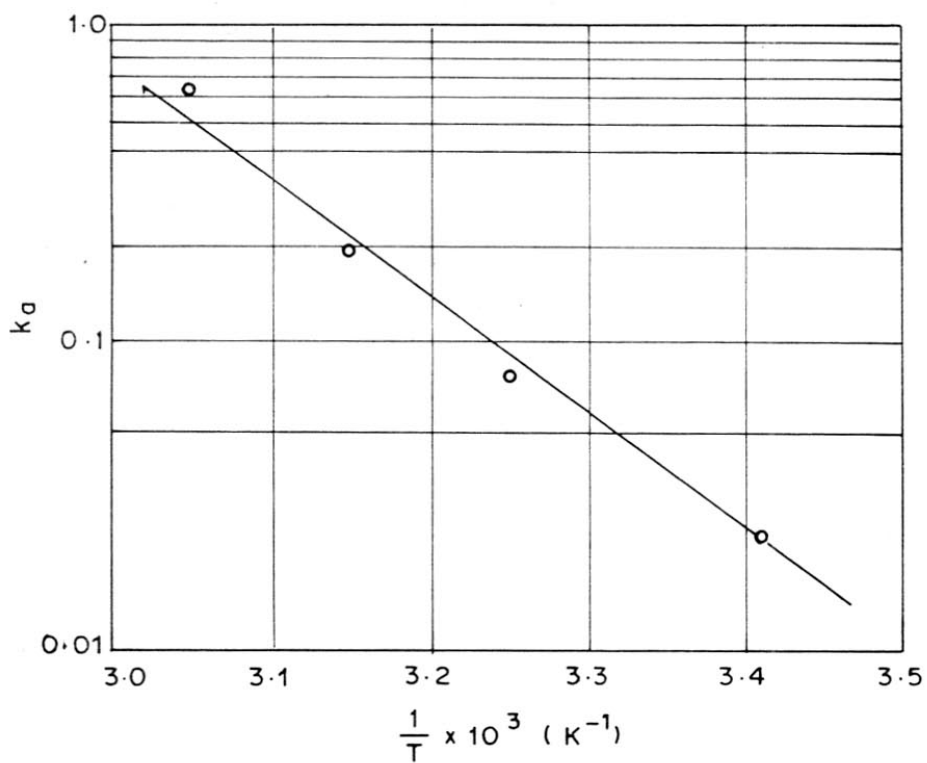


FIG. 3.5.5. TEMPERATURE DEPENDENCE OF THE APPARENT REACTION RATE CONSTANT (k_a) FOR THE HYDROGENATION

3.5.3 HETEROGENEOUS MODELLING OF THE HYDROGENATION REACTION

The mathematical modelling of the chemical controlling catalytic process involving adsorption of reactants, surface reaction between adsorbed reactants and desorption of products can be done by two methods - one, by empirical power law analysis (homogeneous models); and second, by semi-theoretical mechanistic rate models (heterogeneous models) based on the theory of adsorption. Though the empirical power law models fit a given set of data as well or some times even better (based on a residual sum of squares) than the mechanistic heterogeneous rate models, the latter have the advantage that their semi-theoretical basis permits safer extrapolation.

Efforts were made to fit the kinetic data (Appendices-3.5.1-3.5.4) to the power law model (similar to that given in Eqn. 3) but without success.

3.5.3.1 Hougen-Watson (or Langmuir-Hinshelwood) Models

A major breakthrough in the study of solid catalysed reactions was obtained by Hougen and Watson (1) about thirty five years ago when they introduced the Langmuir-Hinshelwood theory for the analysis of their kinetic data and developed rate models for the various cases of chemical controlling mechanisms. These rate models are now commonly known as the Hougen-Watson (H-W) models. These are based on the Langmuir-Hinshelwood adsorption theory, and hence have the same basic assumptions regarding adsorption phenomena, such as-

- i) only one type of active centers are present on the catalyst surface;

- ii) the heat of adsorption is constant with respect to surface coverage (i.e. there is no interaction between adsorbed molecules);
- iii) the adsorption results in the formation of monomolecular layer of adsorbate; and
- iv) the catalyst has uniform adsorption capacity.

The Hougen-Watson approach is based on the assumption that one of the elementary steps (viz. adsorption of one of the reactants, surface reaction, or desorption of one of the products) offers the controlling resistance in the overall reaction process. The possibility of dissociation of one or more of the reactants or products and the fact that some of them may not be adsorbed are also included in the Hougen-Watson analysis. As such these models seem to have the advantage of flexibility in fitting a given set of data.

3.5.3.2 Plausible Hougen-Watson Models for the Hydrogenation of o-Nitrophenol

The elementary steps involved in the hydrogenation reaction, along with their rate expressions for different mechanisms of adsorption of the reaction species (viz. single site adsorption with molecularly adsorbed reaction species, single site adsorption with atomically adsorbed H_2 and molecularly adsorbed other reaction species, and dual site adsorption with molecularly adsorbed reaction species) are presented in Tables-3.5.4-3.5.6.

The Hougen-Watson models based on the assumption that only one step out of the five elementary steps (adsorption of ONP, adsorption of H_2 , surface reaction between adsorbed ONP and H_2 , desorption of OAP and desorption of water) is controlling, the other four steps being in equilibrium, are derived for the adsorption of ONP controlling, adsorption of

TABLE-3.5.4

ELEMENTARY STEPS INVOLVED IN THE HYDROGENATION OF *o*-NITROPHENOL - SINGLE SITE ADSORPTION AND MOLECULARLY ADSORBED ALL THE REACTION SPECIES

Sr.No.	Controlling mechanism	Elementary steps	Rate of elementary step
1	2	3	4
1.	Adsorption of ONP controlling	$N+s \xrightleftharpoons[k'_1]{k_1} Ns$	$r = k_1 (C_N \Theta_V - \Theta_N / K_N) \quad (7)$ $(K_N = k_1 / k'_1)$
2.	Adsorption of H_2 controlling	$H_2 + s \xrightleftharpoons[k'_2]{k_2} H_2s$	$r = k_2 (C_H \Theta_V - \Theta_H / K_{H_2}) \quad (8)$ $(K_{H_2} = k_2 / k'_2)$
3.	Surface reaction controlling	$Ns + 3H_2 \xrightleftharpoons[k'_3]{k_3} As + 2(Ws) + s$	$r = k_3 [\Theta_N \Theta_H^3 - (k'_3 \Theta_A \Theta_W^2 \Theta_V) / K_I] \quad (9)$ $(K = k_3 / k'_3)$
4.	Desorption of <i>o</i> -aminophenol controlling	$As \xrightleftharpoons[k_4]{k'_4} A + s$	$r = k'_4 (\Theta_A / K_A - C_A \Theta_V) \quad (10)$ $(K_A = k_4 / k'_4)$

.....

Table-3.5.4 contd.

1	2	3	4
5.	Desorption of water controlling	$Ws \xrightleftharpoons[k_5]{k'_5} W + s$	$r = k_5 (\theta_W / K_W - C_W \theta_V)$ $(K_W = k_5 / k'_5)$ <p style="text-align: right;">(11)</p>
N	=	<i>o</i> -Nitrophenol	
A	=	<i>o</i> -Aminophenol	
W	=	water	
s	=	adsorption site	
θ	=	fractional surface coverage	
C_N	=	concentration of <i>o</i> -nitrophenol	
C_H	=	concentration of hydrogen	
C_A	=	concentration of <i>o</i> -aminophenol and	
C_W	=	concentration of water	

TABLE-3.5.5

ELEMENTARY STEPS INVOLVED IN THE HYDROGENATION OF *o*-NITROPHENOL - SINGLE SITE AND ATOMICALLY ADSORBED H₂ (ONP, OAP AND WATER ADSORBED MOLECULARLY)

Sr.No.	Controlling mechanism	Elementary step	Rate of elementary step
1.	Adsorption of ONP controlling	$N + s \xrightleftharpoons[k'_1]{k_1} Ns$	$r = k_1 [C_N \theta_V - \theta_N / K_N] \quad (12)$ $(K_N = k_1 / k'_1)$
2.	Adsorption of hydrogen controlling	$H_2 + 2s \xrightleftharpoons[k'_2]{k_2} 2Hs$	$r = k_2 [C_H \theta_V^2 - \theta_H^2 / K_H] \quad (13)$ $(K_H = k_2 / k'_2)$
3.	Surface reaction controlling	$6Hs + Ns \xrightleftharpoons[k'_3]{k_3} As + 2Ws + 4s$	$r = k_3 [\theta_H^6 \theta_N - (\theta_A \theta_W^2 \theta_V^4) / K] \quad (14)$ $(K = k_3 / k'_3)$
4.	Desorption of OAP controlling	$As \xrightleftharpoons[k_4]{k'_4} A + s$	$r = k_4 [\theta_A / K_A - C_A \theta_V] \quad (15)$ $(K_A = k_4 / k'_4)$
5.	Desorption of water controlling	$Ws \xrightleftharpoons[k_5]{k'_5} W + s$	$r = k_5 [\theta_W / K_W - C_W \theta_V] \quad (16)$ $(K_W = k_5 / k'_5)$

TABLE-3.5.6

ELEMENTARY STEPS INVOLVED IN THE HYDROGENATION OF o-NITROPHENOL - DUAL SITE* AND MOLECULARLY ADSORBED ALL THE REACTION SPECIES

Sr.No.	Controlling mechanism	Elementary step	Rate of elementary step
1.	Adsorption of ONP controlling	$N + s \xrightleftharpoons[k'_1]{k_1} Ns$	$r = k_1(C_N \theta_V - \theta_N/K_N) \quad (17)$ $(K_N = k_1/k'_1)$
2.	Adsorption of H ₂ controlling	$H_2 + s' \xrightleftharpoons[k'_2]{k_2} H_2s'$	$r = k_2 [C_H (1 - \theta_H) - \theta_H/K_{H_2}] \quad (18)$ $(K_{H_2} = k_2/k'_2)$
3.	Surface reaction controlling	$Ns + 3H_2s' + 2s \xrightleftharpoons[k'_3]{k_3} As + 2Ws + 3s'$	$r = k_3 [\theta_V^2 \theta_N \theta_H^3 - \theta_A \theta_W^2 (1 - \theta_H^3)/K] \quad (19)$ $(K = k_3/k'_3)$

.....

Table-3.5.6 contd.

1	2	3	4
4.	Desorption of OAP controlling	$As \xrightleftharpoons[k_4]{k'_4} A + s$	$r = k_4 (\theta_A/K_A - C_A \theta_V)$ $(K_A = k_4/k'_4)$ (20)
5.	Desorption of water controlling	$Ws \xrightleftharpoons[k_5]{k'_5} W + s$	$r = k_5 (\theta_W/K_W - C_W \theta_V)$ $(K_W = k_5/k'_5)$ (21)

* H_2 adsorbed on the sites (s') different from those (s) involved in the adsorption of ONP, OAP and water

H_2 controlling and surface reaction controlling mechanisms from the basic principles of the Langmuir adsorption theory. The desired H-W models for the hydrogenation reaction are presented in Table-3.5.7.

The derivation of the rate model for the case of surface reaction controlling (single site - molecular adsorption of the reaction species) is illustrated in Appendix-3.5.6.

The models based on the desorption of OAP or water controlling mechanism are not considered in the present case because of the following reason. The rate models desired for this case were very complicated because of the appearance of the reaction equilibrium constant (K), which has a very high value ($K = 1.4 \times 10^{73}$) in the numerator of terms in the model and these terms could not be eliminated. Also, the adsorption of the reaction species on the catalyst under reaction conditions (Chapter-3.4) has indicated that the adsorption of the different reaction species occurs in the following order:

o -nitrophenol > o -aminophenol > water

The adsorption of hydrogen on Pd-catalysts has also been reported to be very strong. The hydrogenation reaction is, therefore, expected to be controlled mostly by the adsorption of one of the reactants (i.e. ONP or H_2) or the surface reaction between the adsorbed reactants. All the reaction species were found to be adsorbed at the reaction conditions. Therefore, models describing one or more reaction species not adsorbed are not considered.

TABLE-3.5.7

PLAUSIBLE H-W MODELS FOR THE DIFFERENT CONTROLLING MECHANISMS FOR THE HYDROGENATION OF o-NITROPHENOL

Sr.No.	Controlling mechanism	Rate model	Model no.
1	2	3	4
I. Single-site-all the reaction species adsorbed molecularly			
1.	Adsorption of ONP controlling	$r = \frac{k_1 C_N}{(1 + K_{H_2} C_H + K_A C_A + K_W C_W)}$	(22) I
2.	Adsorption of H ₂ controlling	$r = \frac{k_2 C_H}{(1 + K_N C_N + K_A C_A + K_W C_W)}$	(23) II
3.	Surface reaction controlling	$r = \frac{k_3 K_N K^3 H_2 C_N C^3}{(1 + K_N C_N + K_{H_2} C_H + K_A C_A + K_W C_W)^4}$	(24) III
II. Single site-atomically adsorbed H₂ and molecularly adsorbed ONP, OAP and water			
4.	Adsorption of ONP controlling	$r = \frac{k_1 C_N}{(1 + \sqrt{K_H C_H} + K_A C_A + K_W C_W)}$	(25) IV

.....

Table-3.5.7 contd.

I	2	3	4
5.	Adsorption of H_2 controlling	$r =$	$\frac{k_2 C_H}{(1 + K_N C_N + K_A C_A + K_W C_W)^2} \quad (26)$ <p style="text-align: right;">V</p>
6.	Surface reaction controlling	$r =$	$\frac{k_3 K_N K_H^3 C_N C_H^3}{(1 + \sqrt{K_H C_H} + K_N C_N + K_A C_A + K_W C_W)^7} \quad (27)$ <p style="text-align: right;">VI</p>
<p>III. <u>Dual site - all the reaction species adsorbed molecularly (H_2 adsorbed on different sites from those involved in the adsorption of ONP, OAP and water)</u></p>			
7.	Adsorption of ONP controlling	$r =$	$\frac{k_1 C_N}{(1 + K_A C_A + K_W C_W)} \quad (28)$ <p style="text-align: right;">VII</p>
8.	Surface reaction controlling	$r =$	$\frac{k_3 K_N K_H^3 C_N C_H^3}{(1 + K_{H_2} C_H)^3 (1 + K_N C_N + K_A C_A + K_W C_W)^3} \quad (29)$ <p style="text-align: right;">VIII</p>

3.5.3.3 Estimation of Model Parameters

Parameters of the H-W models (Table-3.5.7) were estimated by non-linear analysis using Marquardt's algorithm (2,3). The Fortran 77 code for the algorithm is listed in Appendix-3.5.7. All the computations (numerical work) was carried out on SN23 (PDP-11 Equivalent) computer.

The parameters of the different H-W models, estimated by fitting the rate data (Appendix-3.5.1-3.5.4) to them are presented in Table-3.5.8. While fitting the rate data, the reaction rate (r) is defined as,

$$r = (-d C_N / dt) / w$$

where, C_N is the concentration of ONP; and w , the catalyst loading.

3.5.3.4 Choice of Model for the Hydrogenation

Among the H-W models (Table-3.5.8), models I, II, IV, V, VI and VII are rejected because of the fact that their some of the model parameters are negative and also their variances were found to be quite high as compared to the other two models (i.e. models of III and VIII).

The residual sum of squares (R.S.S.) and variance (σ^2) of models III and VIII (which have all the parameters positive) are presented in Table-3.5.9. The residual sum of squares (R.S.S.) and a variance (σ^2) of model are defined as follows:

$$\text{R.S.S.} = \sum [r_{(\text{observed})} - r_{(\text{estimated})}]^2$$

$$\text{and } \sigma^2 = \frac{\sum [r_{(\text{observed})} - r_{(\text{estimated})}]^2}{q - 1}$$

TABLE-3.5.8

PARAMETERS OF THE H-W MODELS BASED ON DIFFERENT CONTROLLING MECHANISM OF THE HYDROGENATION REACTION

Model	Controlling mechanism	Temp. (K)	Model parameters				
			k_1, k_2 or k_3	K_N ($\text{dm}^3 \cdot \text{mol}$)	K_H ($\text{dm}^3 \cdot \text{mol}^{-1}$)	K_A ($\text{dm}^3 \cdot \text{mol}^{-1}$)	K_W ($\text{dm}^3 \cdot \text{mol}^{-1}$)
1	2	3	4	5	6	7	8
A. <u>Single site all the reaction species adsorbed molecularly</u>							
(I)	Adsorption of ONP controlling (all the reaction species adsorbed)	293 308 318 328	5.85×10^{-3} 1.50×10^{-2} 2.3×10^{-2} 3.6×10^{-2}	- - - -	-12.27 -10.02 -10.46 -12.92	1.02 -0.018 -16.93 -38.65	-0.62 0.023 8.08 19.81
(II)	Adsorption of H_2 controlling (all the reaction species adsorbed)	293 308 318 328	5.60×10^{-2} 7.45×10^{-2} 0.14 0.4159	-1.21 -1.93 -1.70 -1.32	- - - -	1.67 -0.51 -35.47 5.50	-0.63 -0.21 17.43 -1.03
(III)	Surface reaction controlling (all the reaction species adsorbed)	293 308 318 328	0.0408 0.1162 0.2008 0.5363	44.01 19.18 23.50 14.93	551 314 297 118	18.88 7.85 6.47 6.35	9.9×10^{-6} 4.9×10^{-6} 40×10^{-6} 3.5×10^{-6}

TABLE-3.5.8 contd.

	1	2	3	4	5	6	7	8
B. <u>Single site - atomically adsorb H₂</u>								
(IV) Adsorption of ONP controlling (molecularly adsorbed ONP, OAP and water)	293 308 318 328		0.0034 0.0094 0.0197 0.0136	- - - -	-6.70 -1.30 -1.07 -0.7569	-12.68 -9.86 -7.73 -12.32	0.35 -0.12 -5.64 7.50	-0.28 -0.27 2.45 -4.00
(V) Adsorption of H ₂ controlling (molecularly adsorbed ONP, OAP and water)	293 308 318 328		0.055 0.0686 0.1377 0.3972	- - - -	- - - -	- - - -	0.96 -0.24 -28.84 5.29	-0.36 -0.15 14.24 -1.89
(VI) Surface reaction controlling (molecularly adsorbed ONP, OAP and water)	293 308 318 328		1.34x10 ⁴ 1.88x10 ⁴ 2.29x10 ⁵ 7.05x10 ³	4718 907 27907 75	14.22 4.41 36.47 2.37	6.91 4.08 -227.05 19.36	-0.35 -1.51 119.41 -9.13	

.....

Table-3.5.8 contd.

1	2	3	4	5	6	7	8
C. <u>Dual site: all the reaction species adsorbed molecularly</u> (H ₂ adsorbed on different sites)							
(VII)	Adsorption of ONP controlling	293	0.00801	-	-	1.69	-0.24
		308	0.1598	-	-	4.73	-1.62
		318	0.2443	-	-	-102.0	51.29
		328	0.5928	-	-	13.17	-3.45
(VIII)	Surface reaction controlling	293	0.0448	2.62	140	0.99	1.0x10 ⁻⁶
		308	0.1055	1.31	121	0.21	71x10 ⁻⁶
		318	0.1386	2.52	223	0.51	51x10 ⁻⁶
		328	0.4576	2.92	79	1.9	9.19x10 ⁻⁵

TABLE-3.5.9

RESIDUAL SUM OF SQUARES (R.S.S.) AND VARIANCE (σ^2) OF THE MODELS HAVING ALL THEIR PARAMETERS POSITIVE

Model	293K	308K	R.S.S.	318K	328K	293K	308K	318K	328K
							σ^2		
III.	4.34×10^{-5}	1.67×10^{-4}	2.74×10^{-3}	4.66×10^{-3}	3.781×10^{-7}	1.132×10^{-6}	1.635×10^{-5}	2.648×10^{-5}	
VIII.	3.44×10^{-3}	8.32×10^{-4}	4.92×10^{-2}	0.31	2.997×10^{-5}	5.625×10^{-6}	2.551×10^{-4}	7.753×10^{-3}	

where, q is the number of data points. The model which has the minimum residual sum of squares (or variance) is considered to be the most probable model among the rival models. A comparison of the R.S.S. or variance of the two models (models III and VIII) indicates that the model III (Eqn. 24) gives the best fit to the data for the hydrogenation reaction.

Figure 3.5.6 shows a comparison of the estimated reaction rates from model III (Eqn. 24) with the observed reaction rates. The results indicate that the rate data are fitted fairly well to the rate model.

3.5.3.5 Temperature Dependence of Model Parameters

The values of parameters (k_3 , K_N , K_H , K_A and K_W) of model III at the different temperatures are given in Table-3.5.10.

The temperature dependence of the surface reaction rate constant (k_3), expressed by the Arrhenius equation (Eqn. 6), is shown in Fig. 3.5.7. The values of activation energy (E) and frequency factor (A) for the hydrogenation reaction are estimated to be 63.5 kJ.mol^{-1} and $5.27 \text{ mol.g}^{-1}.\text{min}^{-1}$, respectively. Thus, the temperature dependence of k_3 can be expressed by the following equation:

$$k_3 = 5.27 \text{ Exp} (- 63500/RT) \quad (30)$$

The temperature dependence of the adsorption equilibrium constants (K_N , K_H , K_A and K_W) obtained from the rate model (model III) can be expressed by the relation,

$$K_N, K_M, K_W \text{ or } K_A = \beta \text{ Exp} [- \Delta H/RT] \quad (31)$$

or

$$\log (K_N, K_H, K_W \text{ or } K_A) = \log \beta - (\Delta H/2.303 R) (1/T)$$

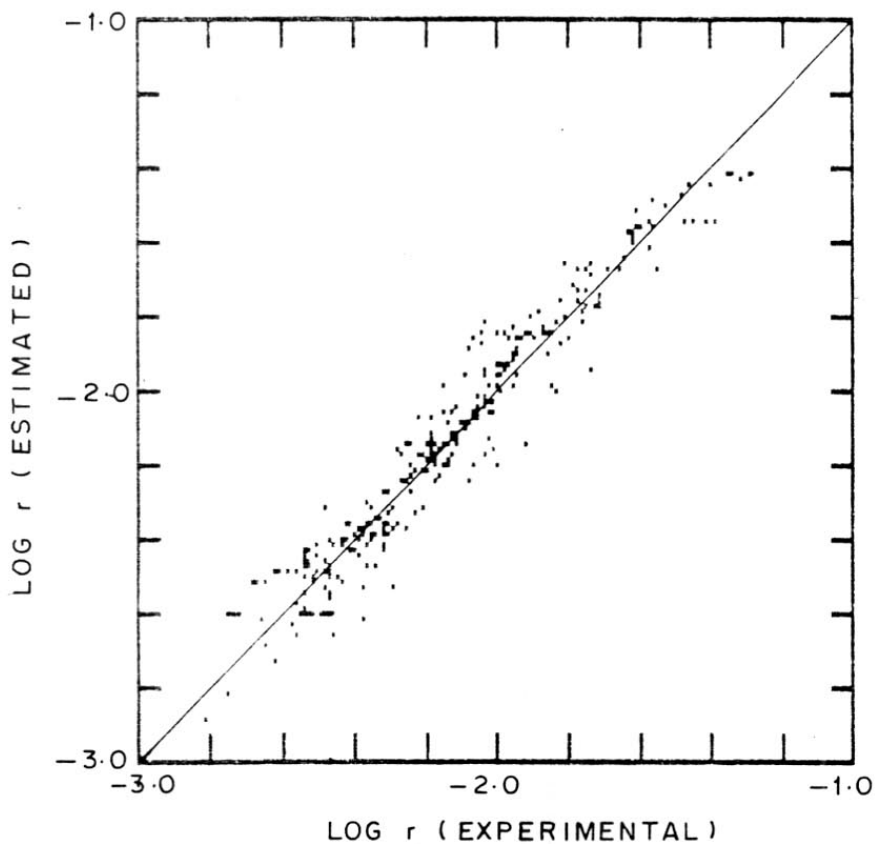


FIG. 3.5.6. COMPARISON OF THE ESTIMATED REACTION RATES (FROM MODEL III) WITH THE OBSERVED REACTION RATES

TABLE-3.5.10

PARAMETERS OF THE MOST PLAUSIBLE MODEL (MODEL III) FOR THE HYDROGENATION REACTION

Temp. (K)	k_3 ($\text{mol}\cdot\text{g}^{-1}\cdot\text{min}^{-1}$)	K_{N_3} ($\text{dm}^3\cdot\text{min}^{-1}$)	K_{H_2} ($\text{dm}^3\cdot\text{mol}^{-1}$)	K_A ($\text{dm}^3\cdot\text{mol}^{-1}$)	$K_W \times 10^6$ ($\text{dm}^3\cdot\text{mol}^{-1}$)
293	0.0408	44.01	551	18.88	9.9
308	0.1162	19.18	314	7.85	4.9
318	0.2008	23.50	297	6.47	4.0
328	0.5363	14.93	118	6.35	3.50

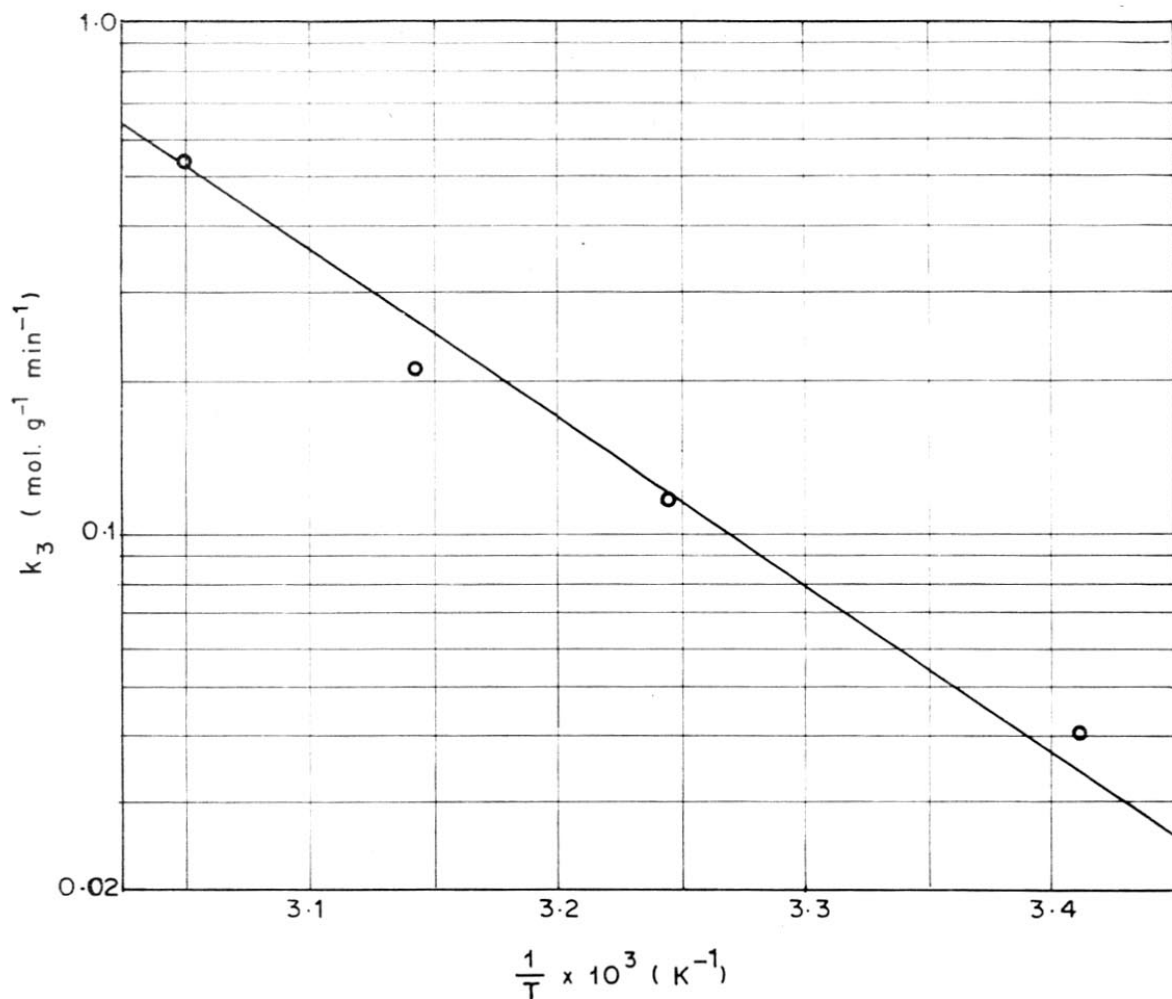


FIG. 3.5.7. TEMPERATURE DEPENDENCE OF THE SURFACE REACTION RATE CONSTANT (k_3) (MODEL III) FOR THE HYDROGENATION REACTION

The temperature dependence of the adsorption constants, according to Eqn. 31, is shown in Fig. 3.5.8. The values of heat of adsorption (ΔH) estimated for the adsorption of ONP, H_2 , OAP and water on the catalyst are as follows:

Reaction species	ONP	H_2	OAP	Water
$-\Delta H$ (kJ.mol ⁻¹)	25.9	28.7	21.0	19.3

The negative values of ΔH indicate that the adsorption for all the cases is exothermic.

3.5.3.5 Fitting of the Initial Rate Data to Model III

For fitting the initial rate data (Table-3.5.1) to model III, Eqn. 24 reduces to,

$$r_o / w = \frac{K_3 K_N K_{H_2}^3 C_N C_H^3}{(1 + K_N C_N + K_{H_2} C_H)^4} \quad (32)$$

The initial rate data are fitted to the above equation and the rate parameters along with the variance of the above rate model are presented in Table-3.5.11. A comparison of the variance of the rate model (Eqn. 32) with that of model III (Eqn. 24) indicates that the initial rate data are fitted quite well to the model (Eqn. 32).

The temperature dependence of the surface reaction rate constant, k_3 (obtained by the initial rate analysis) is shown in Fig. 3.5.9. The value of the activation energy (E) and the frequency factor (A) in this case is estimated to be 68.9 kJ.mol⁻¹ and 9.62 mol.g⁻¹.min⁻¹, respectively. It

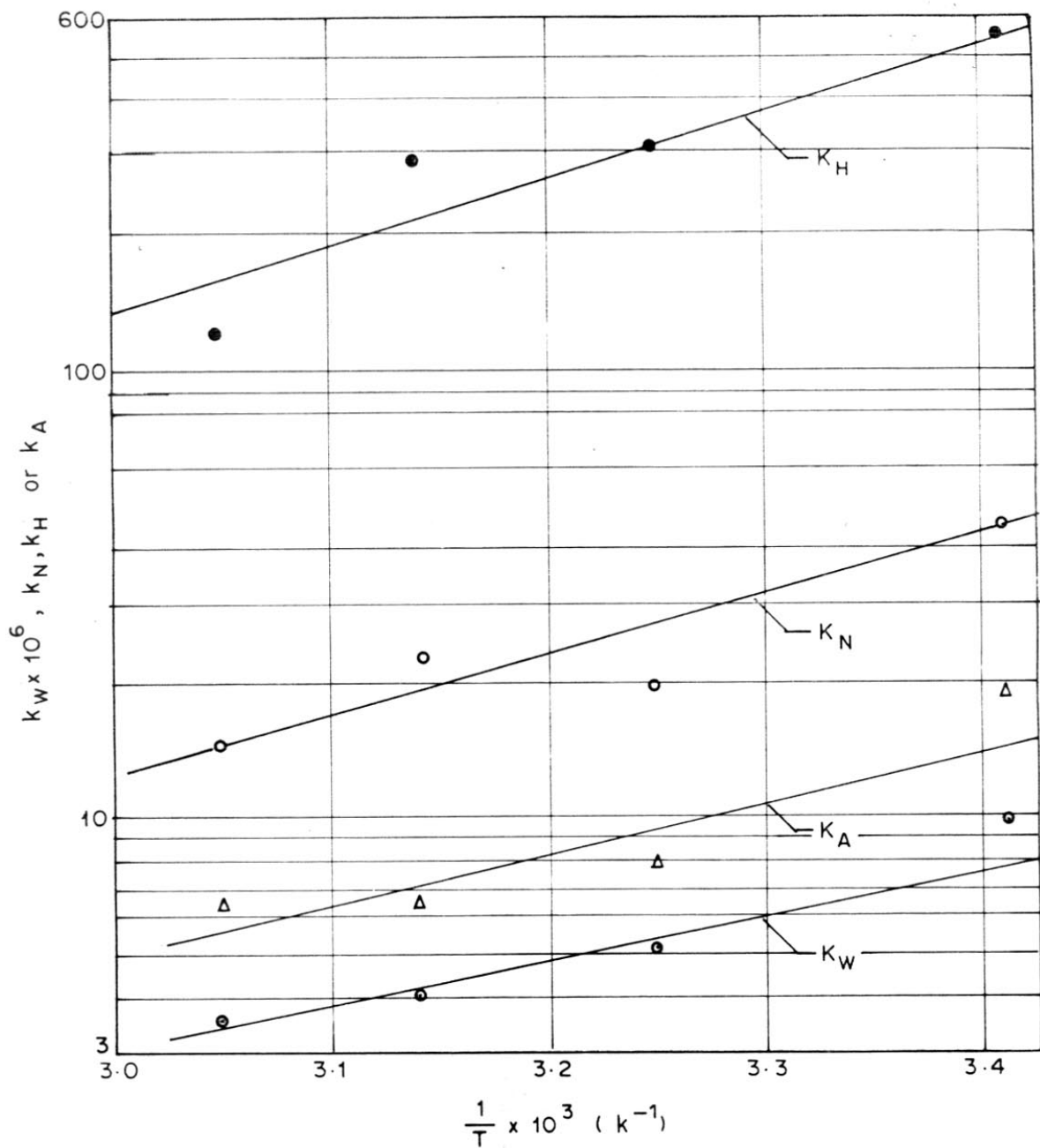


FIG. 3.5.8. TEMPERATURE DEPENDENCE OF THE ADSORPTION EQUILIBRIUM CONSTANTS K_N, K_H, K_A AND K_W (OBTAINED FROM MODEL III)

TABLE-3.5.11

RATE PARAMETERS OF MODEL III FITTED TO THE INITIAL RATE DATA

Temp. (K)	k_3 ($\text{mol.g}^{-1}.\text{min}^{-1}$)	K_N ($\text{dm}^3.\text{mol}^{-1}$)	K_{H_2} ($\text{dm}^3.\text{mol}^{-1}$)	σ^2
293	0.054	27.3	417	2.7×10^{-8}
308	0.162	5.6	133	7.3×10^{-7}
318	0.337	5.3	82	5.4×10^{-6}
328	0.810	5.0	65	6.6×10^{-5}

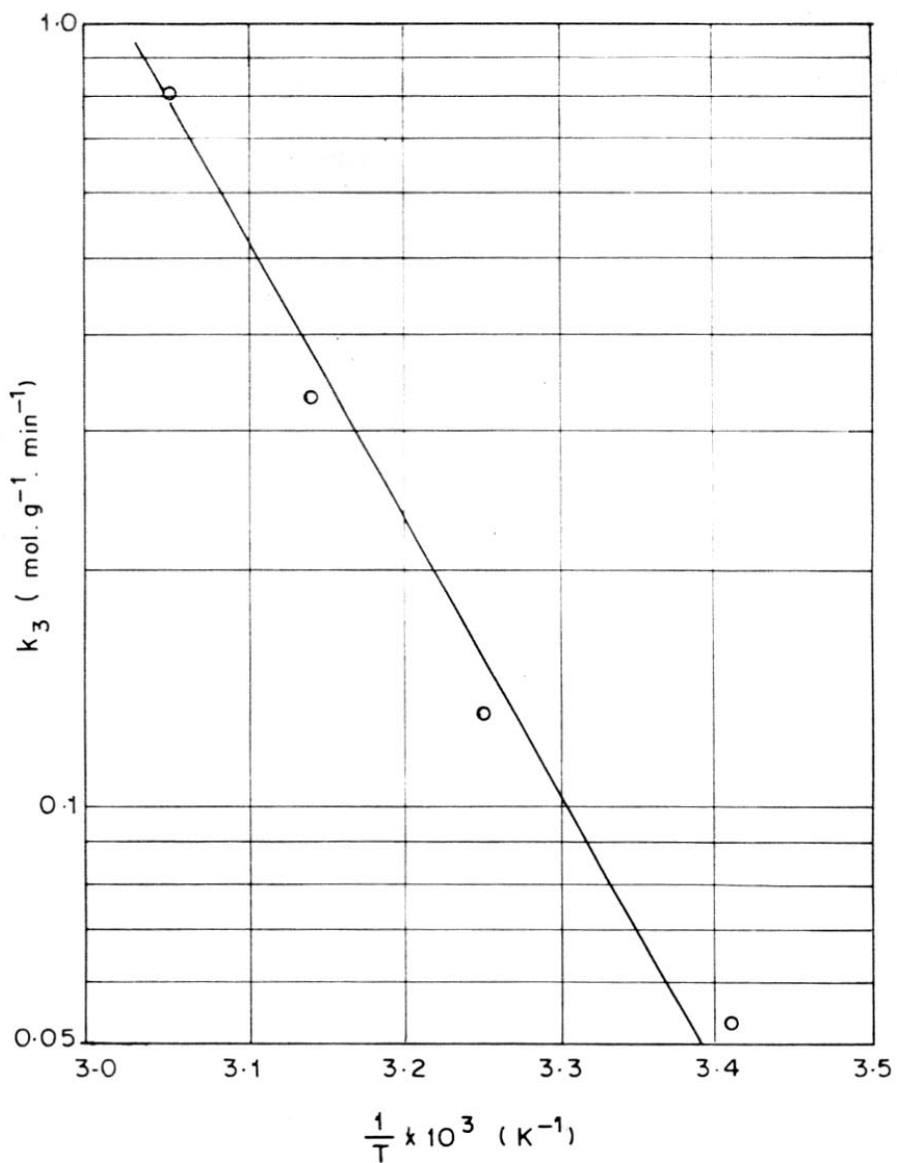


FIG. 3.5.9. TEMPERATURE DEPENDENCE OF SURFACE REACTION RATE CONSTANT k_3 (OBTAINED FROM MODEL III BY FITTING THE INITIAL RATE DATA)

may be noted that this value of activation energy is very close to that (70.2 kJ.mol^{-1}) obtained from the power law analysis of the initial rate data. However, the value of the activation energy (63.5 kJ.mol^{-1}) obtained from the heterogeneous modelling (model III) using all the kinetic data is somewhat lower than the one obtained from the initial rate data analysis.

REFERENCES

1. Hougen, O.A. and Watson, K.M., 'Chemical Process Principles', Vol. III, Kinetics and Catalysis', John Wiley & Sons, Inc. New York, (1947).
2. Marquardt, D.W., 'Least Squares Estimation of Non-Linear Parameters' IBM SHARE Library Program No. 3094 Exhibit B.
3. Witzheimer, W.W., Ph.D. Thesis, Univ. Pennsylvania (1969).

NOMENCLATURE

A_1, A_2, A_3	constants of Eqn. 2
A_4, A_5, A_6	constants of Eqn. 2
C_N	concentration of ONP (mol.dm^{-3})
C_H	concentration of hydrogen (mol.dm^{-3})
C_A	concentration of OAP (mol.dm^{-3})
C_W	concentration of water (mol.dm^{-3})
E	activation energy (J.mol^{-1})
k	specific reaction rate constant ($\text{mol.g}^{-1}.\text{min}^{-1}$)
k_a	apparent reaction rate constant ($\text{mol}^{1-m}.\text{dm}^{3m}.\text{g}^{-1}.\text{min}^{-1}$)
K_N	ONP adsorption equilibrium constant ($\text{dm}^3.\text{mol}^{-1}$)
K_{H_2}	H_2 adsorption equilibrium constant ($\text{dm}^3.\text{mol}^{-1}$)
K_A	OAP adsorption equilibrium constant ($\text{dm}^3.\text{mol}^{-1}$)
K_W	water adsorption equilibrium constant ($\text{dm}^3.\text{mol}^{-1}$)
m	order of reaction w.r.t. H_2
n	order of reaction w.r.t. ONP
q	number of data
R	gas constant ($\text{J.mol}^{-1}.\text{K}^{-1}$)
r	reaction rate ($\text{mol.dm}^{-3}(\text{slurry})\text{min}^{-1}$)
r_o	initial rate of the reaction ($\text{mol.dm}^{-3}.\text{min}^{-1}$)
w	weight of the catalyst (g)
ΔH	heat of adsorption (kJ.mol^{-1})
σ^2	variance

CHAPTER-3.6

CHAPTER-3.6

POISONING OF Pd-CARBON IN SLURRY PHASE HYDROGENATION OF o-NITROPHENOL

3.6.1 INTRODUCTION

Palladium supported on an activated carbon is a commonly used catalyst in liquid phase hydrogenation of aromatic nitro compounds to aromatic amines (1). Catalytic activity of palladium in liquid phase hydrogenation processes is known to be inhibited by heavy metals and their compounds, and halogen and sulphur containing compounds, when present in small amounts (2). Though these inhibiting or poisoning effects are known since many decades, the poisoning of supported palladium catalyst, particularly, in liquid phase hydrogenation processes has not been thoroughly investigated.

Only few studies concerning the poisoning of Pd in liquid phase hydrogenations have been reported. Zwicky and Gut (3) studied the influence of poisoning by *o*-thiocresol on the performance of a suspended Pd-carbon for the liquid phase hydrogenation of *o*-cresol and observed that the poison is very strongly adsorbed and there is practically no interaction between poison and substrate on the remaining catalyst surface. Fuji and Bailar (4) investigated the poisoning effects of Group-V (N,P,As,Sb and Bi) triphenyl compounds on the selective hydrogenation with Pd-carbon and observed that the poisoning effects is not only a simple blocking of the active sites of the catalyst but also the nature of the active sites is changed depending on the nature of poison. The lead poisoning was found to impart selectivity in the hydrogenation of olefins on Pd-carbon due to the creation of new active sites.

Williams and Baron (5) observed that lead adsorbed on Pd surface is drawn from the surface to the bulk phase of Pd, thus poison gets desorbed and accumulated in the bulk phase of Pd. The penetration of sulphur in the bulk phase of Pd in the sulphur poisoning has also been studied (6).

The poisoning of Pd catalyst in automobile exhaust catalysis by Pd, P and S compounds has been thoroughly investigated (7,8). In automobile exhaust catalysis, Pd is found to be more poison sensitive than Pt.

The present investigation was undertaken with the objective of studying the poisoning effect of potent inhibitors such as thiophene, dichloroethane, Zn-, Pb- and Hg(II)-acetates and Hg(II)-chloride in the liquid phase hydrogenation of o-nitrophenol in a three phase slurry reactor at commercial process conditions.

3.6.2 EXPERIMENTAL

3.6.2.1 Pd-Carbon Catalyst

Pd-carbon (4.1% Pd) catalyst was used in the poisoning studies. The specific surface area, particle density, porosity and particle size of the Pd-carbon catalyst were $582 \text{ m}^2 \cdot \text{g}^{-1}$, $0.82 \text{ g} \cdot \text{cm}^{-3}$, 0.55 and $30 \mu\text{m}$, respectively.

3.6.2.2 Catalyst poisoning

The catalyst poisoning in the hydrogenation was carried out in the agitated three phase high pressure reactor system shown in Fig. 3.1.1 (Chapter-3.1). The progress of the reaction was followed by measuring the uptake of hydrogen as a function of reaction time at a constant H_2 -pressure in the reactor. The experimental conditions for the hydrogenation

were as follows.

Reaction medium	:	methanol
Volume of reaction mixture	:	1.0 dm ³
Initial concentration of o-nitrophenol	:	0.36 mol.dm ⁻³
Catalyst loading	:	0.5 g.dm ⁻³
Reaction temperature	:	308 K
H ₂ -pressure	:	1508 kPa
Stirring speed	:	980 rpm
Reaction time	:	1.0 hr

The poison concentration in the reaction mixture was varied from 0 to 5000 g.m⁻³ for thiophene, dichloroethane and zinc and lead acetates and from 0 to 500 g.m⁻³ for mercuric acetate and chloride.

In order to find the influence of gas-liquid, liquid-solid and intra-particle mass transfer effects on the hydrogenation process, additional experimental data in absence of poison were collected at different stirring speeds and using the catalyst of smaller particle size (15 μm).

3.6.3 RESULTS AND DISCUSSIONS

The results of the variation in the stirring speed in absence of poisoning indicated that the hydrogenation rate remains almost constant above a stirring speed of 500 rpm. The change in the particle size of the catalyst from 30 to 15 μm has also not resulted a significant change in the rate of hydrogenation. These results have clearly indicated that the hydrogenation reaction, when carried out at the above mentioned conditions (employed for studying the catalyst poisoning) occurs essentially

in the chemical control regime and not at all influenced by any mass transfer process. The absence of mass transfer effect on the hydrogenation process is further confirmed by the fact that the hydrogenation rate is very significantly decreased due to the catalyst poisoning by the various catalyst inhibitors employed in the present study, and that the decrease in the reaction rate depends strongly on the nature and concentration of poison, as discussed below.

The experimental data on the poisoned catalyst at different poison concentrations for the hydrogenation reaction are given in Appendix-3.6.1. The hydrogenation activity curves [fractional conversion (x) versus reaction time (t)] for the catalyst poisoned by various catalyst inhibitors at their different concentrations are presented in Fig. 3.6.1. The variation of catalyst activity (measured in terms of initial reaction rate) for the hydrogenation process with the poison concentration for the different poisons is shown in Fig. 3.6.2. The initial rate data on the poisoned catalyst are given in Table-3.6.1.

The results in Fig. 3.6.2 indicate that thiophene, dichloroethane, Hg(II)-acetate and chloride and Zn- and Pb-acetates are potent poisons for the hydrogenation on Pd-carbon catalyst. Among these poisons, Hg(II)-acetate is the most potent poison for the catalyst. At the Hg(II)-acetate concentration of 500 g.m^{-3} , the catalyst was found to be completely deactivated.

It is interesting to note from Fig. 3.6.2 that, in the case of poisoning by thiophene, dichloroethane and Pb-acetate the catalyst activity initially decreases and then levels off with the increase in the poison concentration;

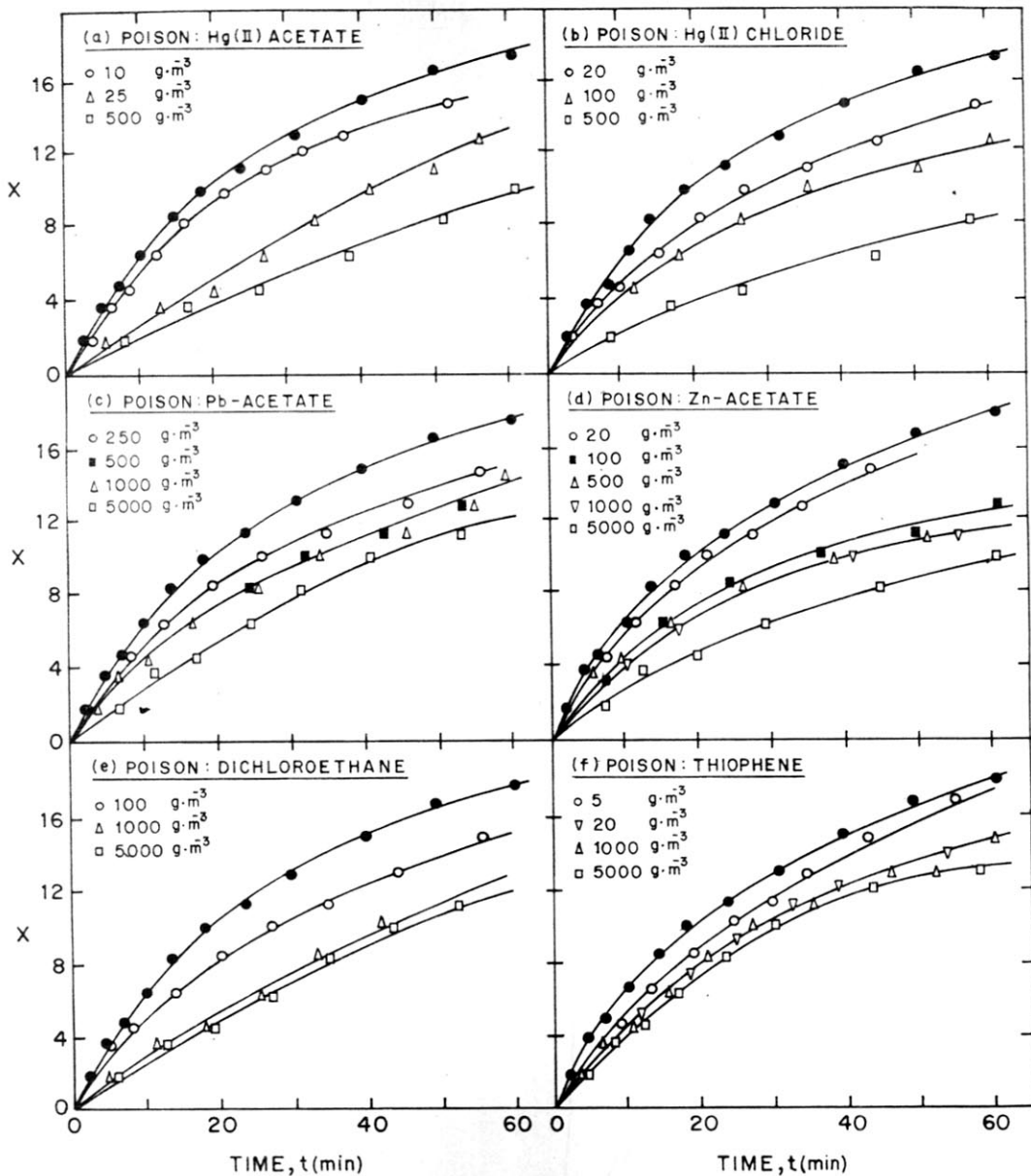


FIG. 3-6-1. HYDROGENATION ACTIVITY PLOTS [FRACTIONAL CONVERSION (x) vs. t] FOR THE POISONING OF Pd-CARBON WITH DIFFERENT POISONS AT THEIR DIFFERENT CONCENTRATIONS. (● - WITHOUT POISON)

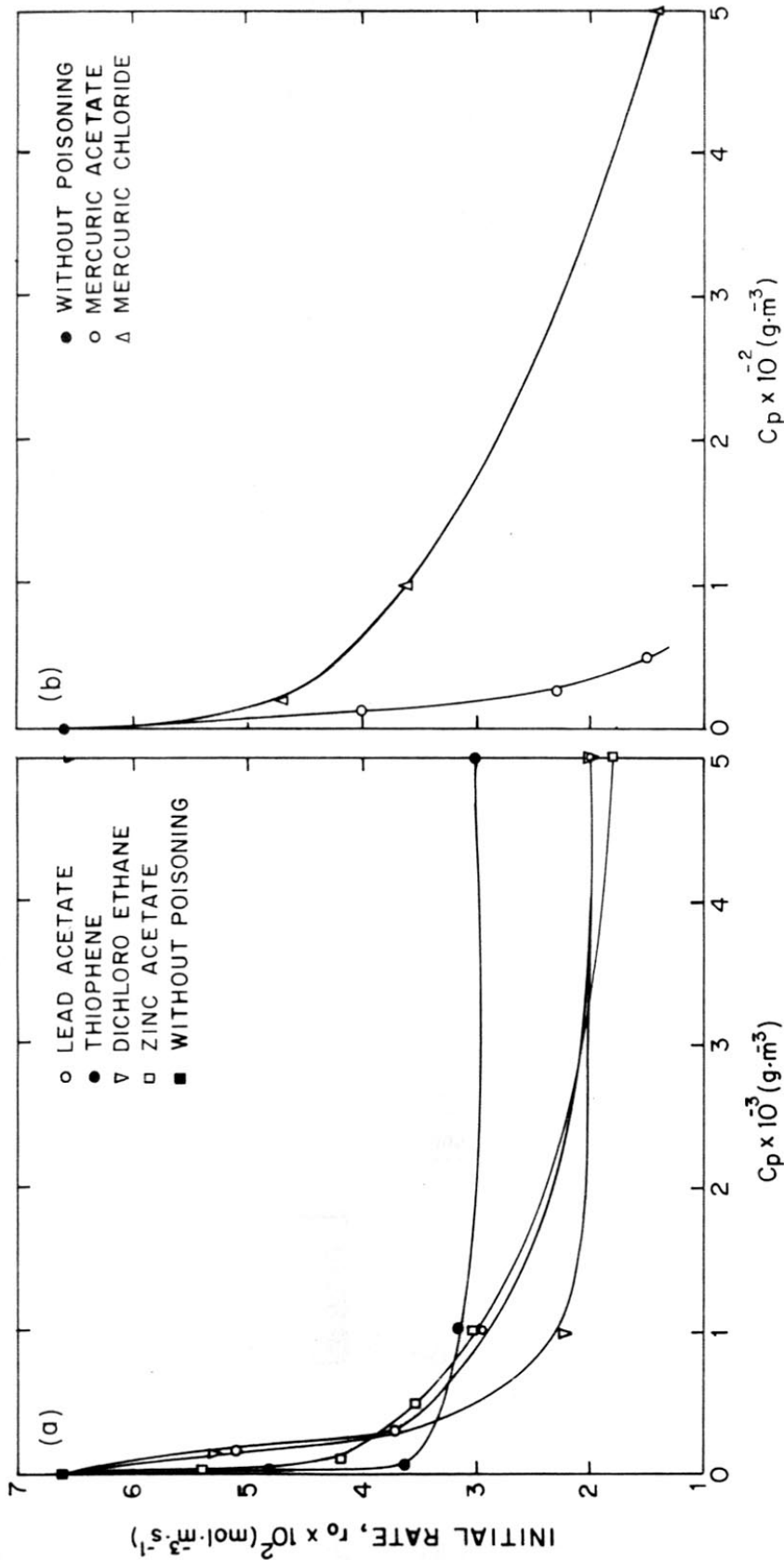


FIG. 3.6-2. VARIATION OF INITIAL REACTION RATE (r_0) OF THE HYDROGENATION WITH POISON CONCENTRATION (C_p) FOR DIFFERENT POISONS

TABLE-3.6.1

INITIAL REACTION RATE DATA FOR THE HYDROGENATION OF ORTHO-NITRO PHENOL ON THE Pd-CARBON POISONED WITH SULPHUR, CHLORO- AND HEAVY METAL COMPOUNDS AT DIFFERENT CONCENTRATIONS

Poison	Concentration of poison ($\text{g}\cdot\text{m}^{-3}$)	Initial reaction rate $r_0 \times 10^2$ ($\text{mol}\cdot\text{m}^{-3}\cdot\text{s}^{-1}$)
Without poison	-	6.6
Thiophene	5	4.8
	20	3.7
	1000	3.1
	5000	3.0
Dichloroethane	100	5.3
	1000	2.4
	5000	1.78
Mercuric chloride	20	4.7
	100	3.6
	500	1.4
Mercuric acetate	10	4.0
	25	2.3
	50	1.5
Lead acetate	150	5.1
	500	3.7
	1000	3.0
	5000	2.0
Zinc acetate	20	5.4
	100	4.2
	500	3.5
	1000	3.2
	5000	1.8

whereas, in the case of the poisoning by Hg(II)-acetate and chlorides and zinc-acetate, the catalyst activity decreases with the increase in poison concentration and the decrease is exponential.

Poisoning by thiophene, dichloroethane and Pb-acetate

The catalyst activity in this typical case of poisoning could be related to the poison concentration by the expression,

$$\frac{r_o - r_p}{r_o r_p} = \beta \frac{\alpha C_p}{1 + \alpha C_p} \quad (1)$$

or

$$\frac{r_o r_p}{r_o - r_p} = \frac{1}{\beta} + \frac{1}{\alpha\beta} \left(\frac{1}{C_p} \right) \quad (2)$$

where r_o and r_p are the initial hydrogenation rates in the absence and presence of the poison, respectively; C_p , the concentration of the poison; and α and β , the poisoning constants.

The $r_o r_p / (r_o - r_p)$ vs $1/C_p$ plots showing a very good fit of the poisoning data for the above poisons to Eqn. (1) are shown in Fig. 3.6.3.

At a very high poison concentration Eqn. (1) reduces to

$$\frac{r_o - r_p}{r_o r_p} = \beta \quad (3)$$

Thus (which is the difference between the reciprocals of r_p , corresponding to a very high poison concentration, and r_o) signifies the maximum possible decrease in the catalyst activity due to poisoning.

The values of the poisoning parameters (α and β) alongwith the lowest possible catalytic activity of the poisoned catalyst expressed as

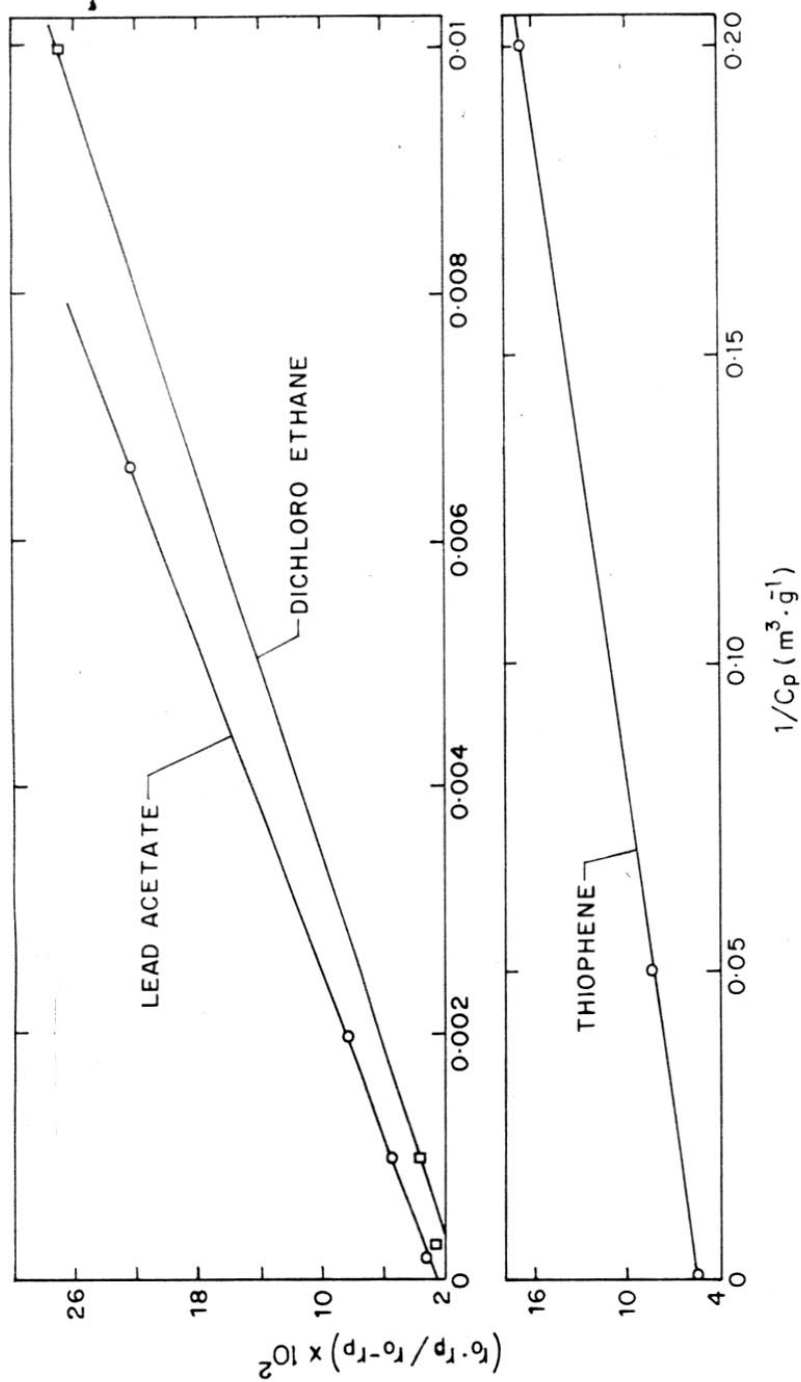


FIG. 3-6-3. $r_0 \cdot r_p / (r_0 - r_p)$ vs. $1/C_p$ PLOTS ACCORDING TO Eqn.2 FOR THE POISONING BY THIOPHENE, DICHLOROETHANE AND LEAD ACETATE

r_p^*/r_o^* (where $r_p^* = r_p$ at a very high poison concentration, obtained from Eqn. 3) for the thiophene, Pb-acetate and dichloroethane poisoning are presented in Table-3.6.2.

Poisoning by Hg(II)-acetate and chloride and Zn-acetate

In the case of Hg(II)-acetate and chloride and Zn-acetate poisoning, the catalyst activity (which is found to decrease continuously with the poison concentration) could be related by the expression,

$$r_p = r_o (1 - \alpha' C_p^n) \quad (4)$$

or

$$\left(1 - \frac{r_p}{r_o}\right) = \alpha' C_p^n \quad (5)$$

where α' and n are constants. The plots of $\log(1 - r_p/r_o)$ vs $\log C_p$, showing a good fit of the poisoning data for the above poisons to Eqn. 4, are presented in Fig. 3.6.4. The values of the poisoning parameters (α' and n) of Eqn. 4 for the poisons are included in Table-3.6.2.

It may be noted that the catalyst activity of Raney-Ni in the hydrogenation of *o*-nitrotoluene (9) could be related to the poison concentration by the equation similar to Eqn. (1) for the poisoning by thiophene, dichloroethane and Pb- and Zn-acetates and by the equation similar to Eqn. (4) for the poisoning by Hg(II)-acetate and chloride.

The decrease in the catalyst activity in the hydrogenation with the increase in the poison concentration (Fig. 3.6.2) is expected mostly due to the increase blockage of the active sites on the catalyst surface by the strong adsorption of poison molecules. However, the levelling of

TABLE-3.6.2

POISONING PARAMETERS

Poison	α		β	r_p^* / r_o
	$(m^3 \cdot g^{-1})$	$(m^3 \cdot mol^{-1})$	$(m^3 \cdot s \cdot mol^{-1})$	
Thiophene	9.9×10^{-2}	8.320	17.2	0.47
Pb-acetate	8.1×10^{-4}	0.240	41.7	0.25
Dichloroethane	5.5×10^{-4}	0.054	71.4	0.16

	α'		
	$(m^{3n} \cdot g^{-n})$	$(m^{3n} \cdot mol^{-n})$	n
Hg(II)-acetate	0.14	1.59	0.43
Hg(II)-chloride	0.12	0.64	0.30
Zn-acetate	0.11	0.33	0.22

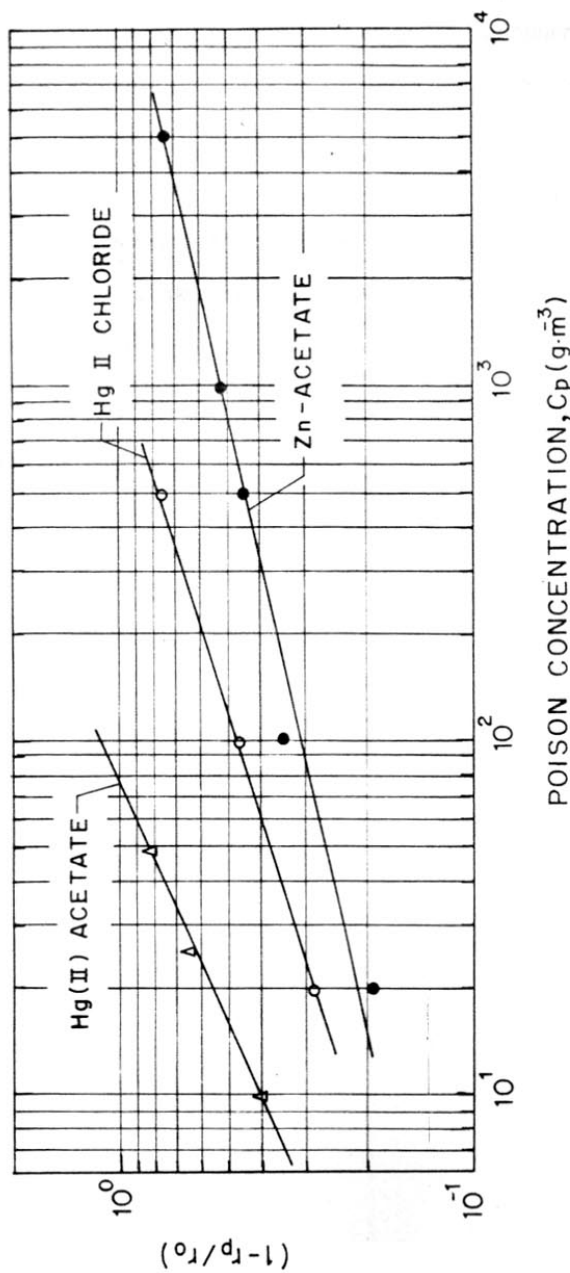


FIG. 3.6.4. $\text{LOG}(1-r_p/r_0)$ vs. $\text{LOG } C_p$ PLOTS ACCORDING TO Eqn. 5 FOR THE POISONING BY MERCURIC ACETATE AND MERCURIC CHLORIDE AND ZINC ACETATE

the catalyst activity in the poisoning by thiophene, dichloroethane and Pb-acetate indicates that sites of different strengths are present on the catalyst surface. At the lower concentrations of poison, the strong sites are blocked and after the strong sites are occupied a further increase in the poison concentration results only a small decrease in the catalytic activity as the weaker active sites available on the catalyst surface are not blocked permanently by the adsorbed poison.

In the case of Hg(II) acetate and chloride poisoning, the catalytic activity vanishes above a certain concentration of poison. This indicates that these poisons are strongly adsorbed even on the weaker sites, resulting in a complete deactivation of the catalyst at the higher poison concentrations.

REFERENCES

1. Stratz, A.M., 'Catalysis of Organic Reactions' Ed. Kosak, J.R., Marcel Dekker, Inc. 1984, p. 335 (Chemical Industries Vol. 18, Ed. H. Heinemann).
2. Freitelder, M., 'Practical Catalytic Hydrogenation' John Wiley and Sons, Inc. New York, 1971, p. 23.
3. Zwicky, J.J. and Gut, G., Chem. Eng. Science, 33 (1978) 1363.
4. Fuji, Y. and Bailar, J.C., J. Catal., 52 (1978) 342.
5. Williams, F.L. and Baron, K., J. Catal. 40 (1975) 108.
6. Tasi, J., Agarwal, P.K., Foley, J.M., Katzer, J.R. and Monogue, W.H., J. Catal. 61 (1980) 192.
7. Shelef, M., Offo, K. and Offo, N.V., Adv. Catal., 27 (1978) 311.
8. Hegedas, L.L. and Gumbleton, J.J., Chemtech. 10 (1980) 630.
9. Choudhary, V.R. and Chaudhari, S.K., React. Kinet. Catal. Lett., 29(1) 153 (1985).

APPENDICES

APPENDIX-1HEAT OF FORMATION OF o-AMINOPHENOL

The heat of formation (ΔH_f) o-aminophenol at 298K has been estimated by the group contribution method reported by Franklin.

In o-aminophenol ($\text{OH}-(\text{C}_6\text{H}_4)-\text{NH}_2$) has four (CH), two (C), one phenolic ($-\text{OH}$) and one ($-\text{NH}_2$) group. The heat of formation associated with each group at 298K is given in the following table.

Group	$(\Delta H_f)_{298\text{K}}$ (kcal.mol ⁻¹)	Number of groups in OAP
CH	3.30	4
C	5.57	2
$-\text{OH}(\text{phenolic})$	-46.9	1
$-\text{NH}_2$	2.8	1

The heat of formation of OAP at 298K is :

$$\begin{aligned} \Delta H_{f(\text{OAP})} &= 4 \times (3.30) + 2 (5.57) + 1 (-46.9) + 1 (2.8) \\ &= -19.76 \text{ kcal.mol}^{-1} \\ &= -82.59 \text{ kJ.mol}^{-1} . \end{aligned}$$

APPENDIX-2

FREE ENERGY OF FORMATION OF o-NITROPHENOL (ONP) AND o-AMINO-PHENOL (OAP)

The free energy of formation (ΔG_f) of o-nitrophenol and o-aminophenol has been estimated by the method suggested by van Krevelen*. The values of constants are given in the following table.

Group	Group contribution for Free Energy of Formation		Number of groups	
	A	B x 10 ²	ONP	OAP
CH-	3.047	0.615	4	4
C	4.675	1.15	2	2
-OH	-41.56	1.28	1	1
-NO ₂	-9.0	3.70	1	-
-NH ₂	2.82	2.71	-	1

* van Krevelen suggested that the (ΔG_f) can be correlated as a linear function of temperature as follows.

$$\Delta G_f = A + B T$$

The constants are additive functions of the atomic groups comprising the molecule. The sum of 'A' values for ONP is (-29.022) and for OAP is (-17.202), the values of 'B' for ONP is (0.0974) and for OAP is (0.0875). The values for the free energy of formation at 298K are estimated as 0.003 kcal.mol⁻¹ for ONP, 8.873 kcal.mol⁻¹ for OAP.

APPENDIX-2.1

CATALYTIC ACTIVITY OF RANEY NICKEL CATALYSTS PREPARED AT DIFFERENT CONDITIONS FOR HYDROGENATION OF o-NITROPHENOL TO o-AMINOPHENOL

Volume of the reaction mixture : $1000 \pm 5 \text{ cm}^3$
 Temperature of reaction : 308 K
 Hydrogen pressure : 1508 kPa
 Stirring speed : 980 rpm
 Initial concentration of ONP : $0.36 \text{ mmol.cm}^{-3}$
 Catalyst loading : $(1.03 \pm 0.02) \times 10^{-3} \text{ g.cm}^{-3}$

Catalyst	Fractional conversion (x) at different reaction periods									
	Reaction period (min)									
	20	40	60	80	100	120	140	160	180	
I	2	3	4	5	6	7	8	9	10	
RN1	0.147	0.275	0.380	0.470	0.550	0.616	0.675	-	-	-
RN2	0.046	0.128	0.243	0.263	0.349	0.378	0.456	0.526	0.551	
RN3	0.0401	0.057	0.083	0.119	0.163	0.172	0.183	0.195	0.223	
RN4	0.061	0.106	0.135	0.176	0.213	0.245	0.254	-	0.332	
RN5	0.087	0.225	0.313	0.430	0.486	0.554	0.667	0.713	0.845	
RN6	0.144	0.337	0.535	0.703	0.843	0.899	0.919	-	-	
RN7	0.183	0.339	0.489	0.606	0.686	0.780	0.905	0.949	-	
RN8	0.171	0.353	0.431	0.539	0.597	0.704	0.791	0.830	0.913	
RN9	0.075	0.137	0.220	0.287	0.346	0.413	0.500	0.546	0.633	

.....

Appendix-2.1 contd.

	1	2	3	4	5	6	7	8	9	10
RN10	0.129	0.274	0.407	0.500	0.592	0.682	0.784	0.863	0.907	0.907
RN11	-	-	0.20	-	-	0.424	-	-	-	0.633
RN12	0.185	0.358	0.551	0.670	0.893	0.905	0.913	-	-	-
RN13	0.233	0.515	0.763	0.929	0.435	0.938	0.942	-	-	-
RN14	0.056	0.125	0.176	0.226	0.279	0.344	0.352	0.420	0.430	0.430
RN15	0.095	0.194	0.273	0.351	0.417	0.461	0.533	0.540	0.710	0.710
RN16	0.073	0.141	0.199	0.246	0.319	0.360	0.409	0.445	0.478	0.478
RN17	0.231	0.371	0.405	0.579	0.666	0.762	0.754	0.837	0.875	0.875
RN18	0.13	0.262	0.312	0.432	0.494	0.574	0.632	0.709	0.771	0.771
RN19	0.025	0.060	0.087	0.109	-	-	-	-	-	-
RN20	0.087	0.236	0.332	0.421	0.508	0.577	0.673	-	-	-
RN21	0.034	0.078	0.126	-	0.163	0.170	0.214	-	-	0.255
RN22	0.030	0.077	0.080	0.114	0.178	0.210	0.242	0.271	0.271	0.245

APPENDIX-2.2

CATALYTIC ACTIVITY OF RANEY NICKEL (RN1) STORED UNDER DIFFERENT CONDITIONS FOR HYDRO-
 GENATION OF *o*-NITROPHENOL TO *o*-AMINOPHENOL

Volume of reaction mixture : $1000 \pm \text{cm}^3$
 Temperature of reaction : 308 K
 Hydrogen pressure : 1508 kPa
 Stirring speed : 980 rpm
 Initial concentration of ONP : $0.36 \text{ mmol.cm}^{-3}$
 Catalyst loading : $(1.03 \pm 0.02) \times 10^{-3} \text{ g.cm}^{-3}$

Catalyst *	Fractional conversion (x) at different reaction periods									
	Reaction period (min)									
	20	40	60	80	100	120	140	160	180	
1	2	3	4	5	6	7	8	9	10	
RN1(1)	0.147	0.275	0.380	0.470	0.550	0.616	0.675	-	-	-
RN1(2)	0.141	0.251	0.363	0.532	0.653	0.750	0.790	0.940	0.979	
RN1(3)	0.185	0.369	0.549	0.680	0.842	0.865	-	-	-	
RN1(4)	0.251	0.456	0.595	-	0.813	0.408	-	-	-	
RN1(5)	0.119	0.284	0.442	0.578	0.705	0.815	0.964	-	-	
RN1(6)	0.061	0.181	0.276	0.314	0.428	0.500	0.609	0.625	0.685	
RN1(7)	0.156	0.299	0.459	0.599	0.715	0.920	0.965	-	-	
RN1(8)	0.115	0.275	0.424	0.545	0.657	0.684	0.819	0.918	0.940	

Appendix-2.2 contd.

<u>1</u>	<u>2</u>	<u>3</u>	<u>4</u>	<u>5</u>	<u>6</u>	<u>7</u>	<u>8</u>	<u>9</u>	<u>10</u>
RNI(9)	0.118	0.232	0.348	0.413	0.543	0.593	0.713	0.764	0.882
RNI(10)	0.078	0.161	0.255	0.329	0.416	0.476	0.561	0.629	0.693
RNI(11)	0.051	0.082	0.125	0.176	0.193	0.207	0.243	0.266	0.294
RNI(12)	0.029	0.158	0.210	0.255	0.273	0.298	0.365	-	0.460
RNI(13)	0.111	0.183	0.287	0.359	0.406	0.505	0.520	0.607	0.664
RNI(14)	0.062	0.090	0.133	0.153	0.173	0.223	0.231	0.239	0.255
RNI(15)	0.003	0.020	0.031	0.038	0.049	0.053	0.076	0.079	0.103
RNI(16)	0.060	0.123	0.183	0.207	0.239	0.280	0.346	0.407	0.439
RNI(17)	0.028	0.070	0.130	0.147	0.173	0.229	0.250	0.310	0.341

APPENDIX-3.3.1

EXPERIMENTAL DATA ON ABSORPTION OF H_2 IN METHANOL AT DIFFERENT STIRRING SPEEDS

Temperature : 303 K
 Total pressure : 715 torr

	260 rpm		530 rpm		740 rpm		980 rpm	
	t (sec)	α	t (sec)	α	t (sec)	α	t (sec)	α
30		0.12	12	0.10	6	0.15	1.4	0.23
58		0.21	39	0.26	12	0.50	5.0	0.65
78		0.31	49	0.35	17	0.38	7.0	0.77
100		0.40	63	0.41	20	0.44	9.6	0.91
121		0.46	74	0.43	25	0.46	13.7	0.96
143		0.52	85	0.51	29	0.56		
170		0.56	97	0.57	34	0.62		
193		0.61	103	0.61	42	0.74		
219		0.65	125	0.65	56	0.81		
244		0.71	141	0.70	79.5	0.91		
255		0.72	154	0.74				
283		0.76	222	0.86				
350		0.84						
468		0.90						

APPENDIX-3.3.2

EXPERIMENTAL DATA ON THE HYDROGENATION OF *o*-NITROPHENOL AT DIFFERENT STIRRING SPEEDS

Volume of reaction mixture	:	1000 ± 0.5 cm ³
Initial concentration of ONP	:	0.36 mol.dm ⁻³
Catalyst loading	:	0.5 g.dm ⁻³
Temperature	:	328 K
Pressure	:	1476 kPa
Catalyst size	:	30 μm

Stirring speed, rpm	Time required, t (min)									
	conversion (%)									
	2.78	6.45	11.12	15.73	25.02	34.27	43.53	52.82	62.07	70.41
260	3.50	5.75	7.66	9.66	14.75	21.75	27.16	33.0	39.0	45.0
460	1.50	2.33	3.50	5.23	8.16	12.50	-	18.50	21.25	24.66
850	0.06	-	1.82	2.55	4.26	7.00	10.75	14.23	17.75	21.66
980	0.05	0.83	1.83	2.43	4.16	6.81	10.65	14.18	17.76	-
1290	0.05	0.82	1.84	2.45	4.14	6.85	-	14.20	17.75	-

APPENDIX-3.3.3

EXPERIMENTAL DATA ON THE HYDROGENATION OF *o*-NITROPHENOL AT DIFFERENT CATALYST LOADINGS
AT 328 K

Volume of reaction mixture : $1000 \pm 0.5 \text{ cm}^3$
 Initial concentration of ONP : 0.36 mol.dm^{-3}
 Particle size of catalyst : $30 \mu\text{m}$
 Temperature : 328 K
 Pressure : 1476 kPa
 Stirring speed : 980 rpm

Time required, t (min)

Catalyst loading ₃ (g. dm ⁻³)	Time required, t (min)										
	2.78	6.45	11.12	15.73	25.02	34.27	38.92	48.17	57.43	66.72	75.06
0.05	4.0	13.0	26.50	44.0	-	-	-	-	-	-	-
0.30	-	0.91	2.08	3.66	8.00	-	14.12	18.08	24.16	28.10	-
0.50	0.06	0.66	2.00	3.1	5.3	6.58	6.83	11.11	17.00	18.75	22.0
1.00	0.05	0.46	1.13	1.76	2.83	3.86	4.36	5.36	6.41	7.50	8.75

APPENDIX-3.3.4

EXPERIMENTAL DATA ON THE HYDROGENATION OF *o*-NITROPHENOL ON Pd-CARBON WITH DIFFERENT PARTICLE SIZES AT DIFFERENT TEMPERATURES

Volume of reaction mixture : $1000 \pm 0.5 \text{ cm}^3$
 H_2 -pressure : 1476 kPa
 Stirring speed : 980 rpm

Time required, t (min)

Conversion (%)

Temp. (K)	Catalyst loading, w (g.dm ⁻³)	Particle size (μm)	Conversion (%)													
			2.78	6.45	11.12	18.34	32.41	40.75	45.39	54.65	63.94					
308	0.5	30	2.00	4.58	8.03	13.50	25.66	-	38.16	-	-	-	-	-	-	-
	0.5	45	2.06	4.55	8.00	14.03	26.00	34.16	38.15	48.50	60.00	-	-	-	-	-
	0.5	90	2.50	9.25	14.75	24.50	42.50	42.75	-	-	-	-	-	-	-	-
	0.5	165	2.50	9.25	15.75	28.00	50.08	-	-	-	-	-	-	-	-	-
318	0.3	30	1.40	4.00	-	11.25	22.70	29.0	33.60	41.00	51.73	-	-	-	-	-
	0.5	90	-	-	9.33	14.75	27.11	34.75	39.50	52.66	59.23	-	-	-	-	-
	0.5	165	1.16	5.00	12.50	20.33	42.75	51.75	-	-	-	-	-	-	-	-
328	0.3	30	-	0.91	2.08	4.50	-	14.66	16.73	22.25	27.08	-	-	-	-	-
	0.5	45	0.05	0.83	1.83	3.33	6.66	9.23	11.42	14.75	19.0	-	-	-	-	-
	0.5	90	0.33	1.83	2.83	5.16	11.92	15.42	17.16	22.50	27.33	-	-	-	-	-
	0.5	165	0.41	2.16	5.75	11.75	20.08	26.50	28.88	-	43.25	-	-	-	-	-

APPENDIX-3.5.1

RATE DATA FOR THE HYDROGENATION OF *o*-NITROPHENOL AT 293 KCatalyst loading (w) = 0.5 g.l^{-1} , $(-dn/dt = -dC/dt)$

Time (t) (min)	Reaction Rate $(-dn/dt) \times 10^2$ $\text{mol. l}^{-1}\text{min}^{-1}$	Conc. Of ONP (C_N) mol. l^{-1}	Conc. Of OAP (C_A) mol. l^{-1}	Conc. Of Water (C_W) mol. l^{-1}	Conc. Of H (C_H) mol. l^{-1}
0.00	0.24000	0.36150	0.00000	0.00000	0.0512
4.50	0.24000	0.34910	0.01237	0.02474	0.0512
7.33	0.24090	0.34180	0.01963	0.03926	0.0512
10.00	0.23860	0.33530	0.02615	0.05230	0.0512
13.50	0.22530	0.32720	0.03426	0.06852	0.0512
17.50	0.21210	0.31850	0.04300	0.08600	0.0512
21.66	0.20030	0.30990	0.05157	0.10310	0.0512
22.08	0.19920	0.30910	0.05241	0.10480	0.0512
29.25	0.18310	0.29540	0.06609	0.13220	0.0512
32.50	0.17710	0.28950	0.07194	0.14390	0.0512
37.66	0.16900	0.28060	0.08087	0.16170	0.0512
48.33	0.15660	0.26330	0.09819	0.19640	0.0512
49.50	0.15550	0.26140	0.10000	0.20000	0.0512
52.75	0.15270	0.25640	0.10500	0.21010	0.0512
58.33	0.14880	0.24800	0.11340	0.22690	0.0512
64.00	0.14580	0.23970	0.12180	0.24360	0.0512
70.00	0.14370	0.23100	0.13050	0.26090	0.0512
75.00	0.14300	0.22380	0.13760	0.27530	0.0512
82.25	0.14370	0.21350	0.14800	0.29600	0.0512
86.00	0.14520	0.20800	0.15340	0.30680	0.0512
92.11	0.14950	0.19910	0.16240	0.32480	0.0512
98.33	0.15700	0.18950	0.17190	0.34390	0.0512
104.00	0.16720	0.18040	0.18110	0.36220	0.0512
108.80	0.17870	0.17220	0.18930	0.37860	0.0512
110.50	0.18370	0.16900	0.19250	0.38490	0.0512
117.00	0.20660	0.15630	0.20510	0.41020	0.0512
0.00	0.23630	0.25230	0.00000	0.00000	0.0512
4.16	0.23080	0.24260	0.00972	0.01943	0.0512
7.33	0.22650	0.23530	0.01696	0.03393	0.0512
10.00	0.22280	0.22930	0.02296	0.04593	0.0512
13.75	0.21740	0.22110	0.03122	0.06744	0.0512
18.66	0.21000	0.21060	0.04172	0.08343	0.0512
22.00	0.20470	0.20370	0.04864	0.09728	0.0512
26.66	0.19670	0.19430	0.05800	0.11600	0.0512
30.33	0.19050	0.18720	0.06511	0.13020	0.0512
34.00	0.18390	0.18030	0.07198	0.14400	0.0512
39.00	0.17480	0.17140	0.08095	0.16190	0.0512
44.66	0.16460	0.16180	0.09055	0.18110	0.0512
49.33	0.15660	0.15430	0.09805	0.19610	0.0512
53.66	0.14970	0.14760	0.10470	0.20940	0.0512

Time (t) (min)	Reaction Rate $(-dn/dt) \times 10^2$ mol. l ⁻¹ min ⁻¹	Conc. Of ONP (C _N) mol. l ⁻¹	Conc. Of OAP (C _A) mol. l ⁻¹	Conc. Of Water (C _W) mol. l ⁻¹	Conc. Of H ₂ (C _H) mol. l ⁻¹
59.00	0.14240	0.13980	0.11250	0.22500	0.0512
64.50	0.13690	0.13220	0.12010	0.24030	0.0512
93.00	0.17300	0.09133	0.16100	0.32200	0.0512
98.00	0.19740	0.08210	0.17020	0.34040	0.0512
0.00	0.22060	0.14420	0.00000	0.00000	0.0523
4.16	0.22040	0.13490	0.00928	0.01856	0.0523
7.33	0.22090	0.12780	0.01635	0.32700	0.0523
10.16	0.21420	0.12160	0.02251	0.04503	0.0523
15.16	0.19770	0.11130	0.03283	0.06563	0.0523
19.16	0.18320	0.10370	0.04044	0.08089	0.0523
23.33	0.16900	0.09638	0.04778	0.09556	0.0523
29.50	0.15260	0.08649	0.05767	0.11530	0.0523
35.00	0.14340	0.07837	0.06579	0.13160	0.0523
40.00	0.13830	0.07134	0.07282	0.14560	0.0523
46.00	0.13210	0.06321	0.08095	0.16190	0.0523
53.66	0.11150	0.05373	0.09043	0.18090	0.0523
0.00	0.15000	0.07200	0.00000	0.00000	0.0526
8.75	0.14620	0.06433	0.00748	0.01496	0.0526
13.75	0.14340	0.05696	0.01484	0.02969	0.0526
20.00	0.14340	0.04755	0.02425	0.04850	0.0526
26.33	0.11750	0.03926	0.03255	0.06509	0.0526
34.00	0.08802	0.03145	0.04035	0.08071	0.0526
41.00	0.07766	0.02577	0.04603	0.09206	0.0526
0.00	0.21550	0.36000	0.00000	0.00000	0.0360
4.50	0.17080	0.35140	0.00860	0.01725	0.0360
9.75	0.13870	0.34340	0.01666	0.03333	0.0360
15.50	0.12260	0.33590	0.02409	0.04819	0.0360
21.33	0.12050	0.32890	0.03112	0.06225	0.0360
27.75	0.12860	0.32090	0.03908	0.07816	0.0360
33.75	0.14070	0.31290	0.04714	0.09429	0.0360
40.75	0.15500	0.30250	0.05750	0.11500	0.0360
47.75	0.16520	0.29130	0.06874	0.13750	0.0360
51.66	0.16800	0.28480	0.07527	0.15050	0.0360
54.00	0.16850	0.28080	0.07921	0.15840	0.0360
59.00	0.16660	0.27240	0.08760	0.17520	0.0360
63.00	0.16210	0.26580	0.09418	0.18840	0.0360
68.00	0.15330	0.25790	0.10210	0.20420	0.0360
72.00	0.14430	0.25200	0.10800	0.21610	0.0360
92.00	0.10350	0.22730	0.13270	0.26540	0.0360
96.00	0.10610	0.22300	0.13700	0.27400	0.0360
99.75	0.11310	0.21960	0.14040	0.28080	0.0360
105.80	0.14260	0.21210	0.14790	0.29590	0.0360
112.60	0.21050	0.20020	0.15980	0.31960	0.0360
117.70	0.29120	0.18770	0.17240	0.34470	0.0360
0.00	0.16000	0.35990	0.00000	0.00000	0.0270
6.16	0.16000	0.35200	0.00790	0.01580	0.0270
12.00	0.16000	0.34360	0.01632	0.03265	0.0270
17.00	0.15030	0.33610	0.02380	0.04761	0.0270
22.66	0.14890	0.32760	0.03228	0.06457	0.0270
28.50	0.14620	0.31900	0.04090	0.08181	0.0270

Time (t) (min)	Reaction Rate $(-dn/dt) \times 10^2$ mol. l ⁻¹ min ⁻¹	Conc. Of ONP (C _N) mol. l ⁻¹	Conc. Of OAP (C _A) mol. l ⁻¹	Conc. Of Water (C _W) mol. l ⁻¹	Conc. Of H (C _H) mol. l ⁻¹
38.16	0.14440	0.30500	0.05489	0.10980	0.0270
47.75	0.14950	0.29100	0.06892	0.13780	0.0270
51.75	0.15350	0.28490	0.07498	0.15000	0.0270
54.50	0.15680	0.28060	0.07925	0.15850	0.0270
60.00	0.16330	0.27180	0.08805	0.17610	0.0270
66.00	0.16850	0.26190	0.09802	0.19600	0.0270
68.00	0.16930	0.25820	0.10170	0.20330	0.0270
75.00	0.16500	0.24670	0.11320	0.22630	0.0270
80.16	0.15150	0.23850	0.12140	0.24280	0.0270
86.50	0.11680	0.22990	0.13000	0.26000	0.0270
96.00	0.10980	0.22320	0.13670	0.27340	0.0270
0.00	0.15400	0.35970	0.00000	0.00000	0.0270
5.66	0.15420	0.35000	0.00970	0.01952	0.0270
12.05	0.12440	0.34110	0.01859	0.03718	0.0270
17.00	0.10930	0.33540	0.02435	0.04870	0.0270
26.66	0.09370	0.32570	0.03403	0.06806	0.0270
36.33	0.08930	0.31690	0.04282	0.08564	0.0270
55.00	0.09000	0.30020	0.05953	0.11910	0.0270
64.00	0.08970	0.29210	0.06762	0.13520	0.0270
73.00	0.08900	0.28400	0.07567	0.15130	0.0270
81.00	0.09010	0.27690	0.08281	0.16560	0.0270
90.00	0.09710	0.26850	0.09117	0.18230	0.0270
97.00	0.11050	0.26130	0.09839	0.19680	0.0270
105.00	0.13930	0.25150	0.10830	0.21650	0.0270
110.00	0.16740	0.24380	0.11590	0.23180	0.0270

APPENDIX-3.5.2

RATE DATA FOR THE HYDROGENATION OF *o*-NITROPHENOL AT 308 KCatalyst loading (w) = 0.5 g.l⁻¹, ($-dn/dt = -dC/dt$)

Time (t) (min)	Reaction Rate ($-dn/dt$) x 10 ² mol. l ⁻¹ min ⁻¹	Conc. Of ONP (C _N) mol. l ⁻¹	Conc. Of OAP (C _A) mol. l ⁻¹	Conc. Of Water (C _W) mol. l ⁻¹	Conc. Of H ⁺ (C _H) mol. l ⁻¹
0.00	0.54110	0.35970	0.00000	0.00000	0.0550
2.00	0.54010	0.34990	0.00980	0.01960	0.0550
3.33	0.54000	0.34300	0.01670	0.03340	0.0550
4.58	0.54000	0.33640	0.02330	0.04660	0.0550
6.10	0.53680	0.32790	0.03180	0.06360	0.0550
7.83	0.52950	0.31960	0.04070	0.08140	0.0550
9.50	0.51480	0.31030	0.04940	0.09880	0.0550
13.50	0.46340	0.29060	0.06910	0.13820	0.0550
20.50	0.37800	0.26140	0.09830	0.19660	0.0550
25.16	0.35370	0.24450	0.11520	0.23040	0.0550
30.00	0.35860	0.22740	0.13230	0.26460	0.0550
38.16	0.37220	0.19710	0.16260	0.32520	0.0550
48.00	0.08889	0.16960	0.19010	0.38020	0.0550
0.00	0.54350	0.25290	0.00000	0.00000	0.0564
2.25	0.53220	0.24060	0.01232	0.02463	0.0564
3.33	0.57890	0.23490	0.01794	0.03598	0.0564
4.66	0.50370	0.22810	0.02479	0.04958	0.0564
6.25	0.48720	0.22020	0.03267	0.06533	0.0564
7.41	0.47610	0.21960	0.03825	0.07651	0.0564
9.50	0.45790	0.20490	0.04801	0.09602	0.0564
11.50	0.44210	0.19590	0.05701	0.11400	0.0564
13.66	0.42630	0.18650	0.06638	0.13280	0.0564
15.50	0.41370	0.17880	0.07411	0.14820	0.0564
17.66	0.39930	0.17000	0.08289	0.16580	0.0564
19.92	0.38450	0.16110	0.09175	0.18350	0.0564
21.50	0.37410	0.15510	0.09774	0.19550	0.0564
24.16	0.35640	0.14540	0.10750	0.21490	0.0564
26.16	0.34280	0.13840	0.11450	0.22890	0.0564
27.75	0.33170	0.13310	0.11980	0.23960	0.0564
30.25	0.31380	0.12500	0.12790	0.25580	0.0564
33.50	0.28990	0.11520	0.13770	0.21540	0.0564
36.50	0.26750	0.10680	0.14610	0.29210	0.0564
40.00	0.24220	0.09790	0.15500	0.30990	0.0564
43.75	0.21750	0.08930	0.16360	0.32720	0.0564
50.33	0.18800	0.07609	0.17680	0.35360	0.0564
57.33	0.19440	0.06301	0.18990	0.37970	0.0564
58.66	0.20220	0.06038	0.19250	0.38500	0.0564
63.50	0.25470	0.04948	0.20340	0.40680	0.0564
66.50	0.31030	0.04106	0.21180	0.42360	0.0564
0.00	0.32490	0.14900	0.00000	0.00000	0.0572

Time (t) (min)	Reaction Rate $(-dn/dt) \times 10^2$ mol. l ⁻¹ min ⁻¹	Conc. Of ONP (C _N) mol. l ⁻¹	Conc. Of OAP (C _A) mol. l ⁻¹	Conc. Of Water (C _W) mol. l ⁻¹	Conc. Of H ⁺ (C _H) mol. l ⁻¹
4.00	0.32320	0.13580	0.08240	0.01648	0.0572
6.83	0.32280	0.12760	0.01642	0.03284	0.0572
9.16	0.32740	0.12010	0.02388	0.04775	0.0572
11.50	0.32160	0.11240	0.03160	0.06320	0.0572
14.00	0.32220	0.10420	0.03978	0.07956	0.0572
16.33	0.30680	0.09680	0.04712	0.09424	0.0572
19.75	0.27690	0.08689	0.05712	0.11420	0.0572
22.50	0.25080	0.07964	0.06437	0.12870	0.0572
25.75	0.22180	0.07197	0.07204	0.14410	0.0572
29.75	0.19340	0.06370	0.08031	0.16060	0.0572
34.50	0.17320	0.05505	0.08896	0.17790	0.0572
38.00	0.16690	0.04912	0.09390	0.18980	0.0572
43.16	0.16310	0.04060	0.10340	0.20680	0.0572
50.00	0.13680	0.03006	0.11400	0.22790	0.0572
58.00	0.01589	0.02390	0.12010	0.24020	0.0572
0.00	0.25000	0.07200	0.00000	0.00000	0.0579
4.50	0.25400	0.06351	0.00892	0.01698	0.0579
7.00	0.26440	0.05694	0.01506	0.03011	0.0579
10.00	0.23950	0.04932	0.02268	0.04535	0.0579
17.00	0.17090	0.03531	0.03669	0.07339	0.0579
22.00	0.16810	0.03361	0.03839	0.07677	0.0579
28.50	0.17640	0.02681	0.04519	0.09038	0.0579
33.50	0.18130	0.01465	0.05735	0.11470	0.0579
0.00	0.54000	0.36130	0.00000	0.00000	0.0390
2.25	0.52970	0.34900	0.01230	0.02461	0.0390
3.75	0.50940	0.34120	0.02009	0.04019	0.0390
5.16	0.49220	0.33410	0.02715	0.05431	0.0390
7.00	0.47260	0.32520	0.03602	0.07205	0.0390
8.00	0.46310	0.32060	0.04070	0.08140	0.0390
10.33	0.44400	0.31000	0.05126	0.10250	0.0390
12.16	0.43160	0.30200	0.05927	0.11850	0.0390
13.75	0.42250	0.29520	0.06606	0.13210	0.0390
15.50	0.41410	0.28790	0.07338	0.14680	0.0390
17.75	0.40550	0.27870	0.08259	0.16520	0.0390
19.75	0.39950	0.27060	0.09064	0.18130	0.0390
21.75	0.39490	0.26270	0.09858	0.19720	0.0390
24.00	0.38090	0.25380	0.10740	0.21480	0.0390
26.75	0.38810	0.24510	0.11620	0.23240	0.0390
28.00	0.38630	0.23830	0.12300	0.24590	0.0390
30.33	0.38450	0.22930	0.13190	0.26390	0.0390
32.86	0.38280	0.21960	0.14160	0.28330	0.0390
33.00	0.38270	0.21910	0.14220	0.28440	0.0390
37.00	0.37980	0.20380	0.15740	0.31490	0.0390
39.75	0.37730	0.19340	0.16780	0.33570	0.0390
42.50	0.37390	0.18310	0.17820	0.35630	0.0390
44.00	0.37160	0.17750	0.18380	0.36750	0.0390
45.33	0.36930	0.17260	0.18870	0.37740	0.0390
48.16	0.36340	0.16220	0.19910	0.39810	0.0390
49.75	0.35950	0.15640	0.20480	0.40960	0.0390
52.00	0.35530	0.14840	0.21280	0.42570	0.0390

Time (t) (min)	Reaction Rate $(-dn/dt) \times 10^2$ mol. l ⁻¹ min ⁻¹	Conc. Of ONP (C _N) mol. l ⁻¹	Conc. Of OAP (C _A) mol. l ⁻¹	Conc. Of Water (C _W) mol. l ⁻¹	Conc. Of H ⁺ (C _H) mol. l ⁻¹
56.61	0.33770	0.13250	0.22880	0.45750	0.0390
58.75	0.32920	0.12530	0.23590	0.47180	0.0390
62.00	0.31520	0.11490	0.24640	0.49280	0.0390
64.33	0.30430	0.10760	0.25360	0.50720	0.0390
67.16	0.29050	0.09923	0.26200	0.52400	0.0390
70.00	0.27620	0.09118	0.27010	0.54010	0.0390
73.50	0.25870	0.08183	0.27940	0.55810	0.0390
76.83	0.24300	0.07347	0.28180	0.57560	0.0390
80.00	0.22970	0.06599	0.29530	0.59050	0.0390
83.50	0.21790	0.05817	0.30310	0.60020	0.0390
87.75	0.20970	0.04911	0.31210	0.62430	0.0390
90.00	0.20900	0.04440	0.31690	0.63370	0.0390
0.00	0.36480	0.35860	0.00000	0.00000	0.0290
2.26	0.35050	0.35050	0.00808	0.01616	0.0290
4.00	0.34010	0.34450	0.01409	0.02818	0.0290
6.16	0.32810	0.33730	0.02130	0.04261	0.0290
9.08	0.31330	0.32800	0.03066	0.06133	0.0290
12.33	0.29910	0.31800	0.04061	0.08122	0.0290
15.00	0.28910	0.31020	0.04846	0.09699	0.0290
18.00	0.27980	0.30160	0.05699	0.11400	0.0290
21.00	0.27240	0.29340	0.06526	0.13050	0.0290
23.75	0.26730	0.28590	0.07268	0.14540	0.0290
26.75	0.26350	0.27800	0.08064	0.16130	0.0290
29.75	0.26140	0.27010	0.08851	0.17700	0.0290
32.75	0.26090	0.26230	0.09634	0.19270	0.0290
35.66	0.26170	0.25470	0.10390	0.20790	0.0290
38.50	0.26360	0.24720	0.11140	0.22280	0.0290
42.00	0.26710	0.23790	0.12070	0.24140	0.0290
45.00	0.27080	0.22990	0.12870	0.25750	0.0290
48.00	0.27480	0.22170	0.13690	0.27390	0.0290
51.50	0.27940	0.21200	0.14660	0.29330	0.0290
54.33	0.28270	0.20400	0.15460	0.30920	0.0290
57.00	0.28540	0.19550	0.16310	0.32620	0.0290
77.00	0.24790	0.14090	0.21770	0.43530	0.0290
80.00	0.22770	0.13380	0.22480	0.44960	0.0290
86.33	0.16560	0.12120	0.23740	0.47480	0.0290
89.00	0.13030	0.11720	0.24140	0.48280	0.0290
0.00	0.28860	0.35940	0.00000	0.00000	0.0180
2.33	0.28120	0.35270	0.00664	0.01327	0.0180
5.00	0.27350	0.34530	0.01404	0.02808	0.0180
8.50	0.26460	0.33590	0.02345	0.04690	0.0180
11.75	0.25760	0.32740	0.03193	0.06387	0.0180
15.50	0.25110	0.31790	0.04147	0.08293	0.0180
18.33	0.24730	0.31080	0.04852	0.09703	0.0180
21.50	0.24400	0.30310	0.05630	0.11260	0.0180
24.66	0.24190	0.29540	0.06398	0.12800	0.0180
27.50	0.24080	0.28850	0.07083	0.14170	0.0180
31.00	0.24040	0.28010	0.07925	0.15850	0.0180
35.50	0.24130	0.26930	0.09008	0.18020	0.0180

Time (t) (min)	Reaction Rate $(-dn/dt) \times 10^2$ mol. l ⁻¹ min ⁻¹	Conc. Of ONP (C _N) mol. l ⁻¹	Conc. Of OAP (C _A) mol. l ⁻¹	Conc. Of Water (C _W) mol. l ⁻¹	Conc. Of H ⁺ (C _H) mol. l ⁻¹
51.16	0.25040	0.23080	0.12850	0.25700	0.0180
64.25	0.25170	0.19780	0.16150	0.32310	0.0180
67.00	0.24940	0.19090	0.16840	0.33690	0.0180
73.75	0.23750	0.17440	0.18490	0.36990	0.0180
77.33	0.22670	0.16610	0.19320	0.38650	0.0180
82.00	0.20690	0.15600	0.20340	0.40680	0.0180
85.75	0.18540	0.14860	0.21080	0.42160	0.0180
88.33	0.16740	0.14400	0.21530	0.43070	0.0180

APPENDIX-3.5.3

RATE DATA FOR THE HYDROGENATION OF *o*-NITROPHENOL AT 318 KCatalyst loading (w) = 0.3 g.l^{-1} , $(-dn/dt = -dC/dt)$

Time (t) (min)	Reaction Rate $(-dn/dt) \times 10^2$ mol. $\text{l}^{-1}\text{min}^{-1}$	Conc. Of ONP (C_N) mol. l^{-1}	Conc. Of OAP (C_A) mol. l^{-1}	Conc. Of Water (C_W) mol. l^{-1}	Conc. Of H (C_H) mol. l^{-1}
0.00	0.57950	0.35850	0.00000	0.00000	0.0580
0.75	0.57580	0.35420	0.00432	0.00867	0.0580
2.75	0.56540	0.34280	0.01574	0.03149	0.0580
4.00	0.55870	0.33580	0.02297	0.04554	0.0580
5.66	0.54950	0.32660	0.03197	0.06394	0.0580
8.00	0.53620	0.31390	0.04467	0.08934	0.0580
9.50	0.52760	0.30590	0.05265	0.10530	0.0580
11.25	0.51740	0.29670	0.06179	0.12360	0.0580
13.00	0.50720	0.28780	0.07076	0.14150	0.0580
14.75	0.49700	0.27900	0.07955	0.15910	0.0580
20.33	0.46510	0.25220	0.10640	0.21280	0.0580
21.83	0.45680	0.24520	0.11330	0.22660	0.0580
23.58	0.44730	0.23730	0.12120	0.24240	0.0580
25.66	0.43620	0.22810	0.13040	0.26080	0.0580
27.16	0.41930	0.21390	0.14470	0.28940	0.0580
29.00	0.41080	0.20660	0.15190	0.30390	0.0580
30.75	0.40140	0.19850	0.16010	0.32010	0.0580
32.75	0.39230	0.19050	0.16800	0.33600	0.0580
34.75	0.38460	0.18370	0.17480	0.34960	0.0580
36.50	0.37610	0.17610	0.18240	0.36480	0.0580
38.50	0.36730	0.16810	0.19040	0.38090	0.0580
40.66	0.35800	0.15960	0.19890	0.39780	0.0580
43.00	0.34830	0.15080	0.20770	0.41550	0.0580
45.50	0.33830	0.14170	0.21690	0.43370	0.0580
48.16	0.32880	0.13330	0.22520	0.45040	0.0580
50.66	0.32070	0.12640	0.23220	0.46430	0.0580
52.80	0.30910	0.11710	0.24150	0.48290	0.0580
55.75	0.29480	0.10680	0.25180	0.50350	0.0580
59.16	0.27940	0.09720	0.26130	0.52270	0.0580
62.50	0.26480	0.08949	0.26900	0.53810	0.0580
65.33	0.25680	0.08579	0.27280	0.54550	0.0580
66.75	0.23990	0.07895	0.27960	0.55920	0.0580
69.50	0.20280	0.06785	0.29070	0.58140	0.0580
75.50	0.19430	0.06586	0.29270	0.58540	0.0580
85.50	0.08050	0.05165	0.30690	0.61380	0.0580
0.00	0.58160	0.25100	0.00000	0.00000	0.0651
0.16	0.57880	0.24580	0.00093	0.00186	0.0651
1.50	0.55520	0.23820	0.00852	0.01705	0.0651
2.75	0.53360	0.23140	0.01533	0.03066	0.0651
4.25	0.50840	0.22360	0.02314	0.04629	0.0651

Time (t) (min)	Reaction Rate $(-dn/dt) \times 10^2$ mol. l ⁻¹ min ⁻¹	Conc. Of ONP (C _N) mol. l ⁻¹	Conc. Of OAP (C _A) mol. l ⁻¹	Conc. Of Water (C _W) mol. l ⁻¹	Conc. Of H (C _H) mol. l ⁻¹
6.41	0.47390	0.21300	0.03375	0.06750	0.0651
8.75	0.43920	0.20230	0.04442	0.08850	0.0651
11.50	0.40270	0.19070	0.05599	0.11200	0.0651
13.66	0.37780	0.18230	0.06441	0.12880	0.0651
15.33	0.36110	0.17610	0.07058	0.14120	0.0651
17.25	0.34470	0.16940	0.07735	0.15470	0.0651
19.33	0.33070	0.16240	0.08437	0.16870	0.0651
21.33	0.32100	0.15580	0.09088	0.18180	0.0651
23.75	0.31450	0.14820	0.09856	0.19710	0.0651
26.16	0.31980	0.13270	0.11400	0.22800	0.0651
28.66	0.33450	0.12340	0.12330	0.24660	0.0651
31.50	0.35940	0.11300	0.13370	0.26740	0.0651
34.50	0.38390	0.10500	0.14170	0.28340	0.0651
36.66	0.42240	0.09360	0.15310	0.30620	0.0651
39.50	0.47730	0.07901	0.16770	0.33540	0.0651
42.75	0.52830	0.06606	0.18070	0.36130	0.0651
45.33	0.54260	0.06247	0.18430	0.36850	0.0651
46.00	0.55910	0.05834	0.18840	0.37680	0.0651
46.75	0.57600	0.05408	0.19260	0.38530	0.0651
47.50	0.60550	0.04670	0.20000	0.40000	0.0651
48.75	0.65530	0.03410	0.21260	0.42520	0.0651
50.75	0.70160	0.02223	0.22450	0.44900	0.0651
52.50	0.74050	0.01206	0.23470	0.46930	0.0651
0.00	0.52140	0.14390	0.00000	0.00000	0.0644
1.50	0.51350	0.13620	0.00777	0.01554	0.0644
3.25	0.49720	0.12730	0.01662	0.03324	0.0644
4.50	0.48180	0.12120	0.02274	0.04549	0.0644
6.50	0.45250	0.11180	0.03209	0.06419	0.0644
8.50	0.41950	0.10310	0.04082	0.08164	0.0644
10.36	0.38710	0.09562	0.04832	0.09664	0.0644
12.50	0.34970	0.08774	0.05620	0.11240	0.0644
15.33	0.30290	0.07851	0.06543	0.13090	0.0644
18.00	0.26410	0.07095	0.07298	0.14600	0.0644
21.50	0.22370	0.06245	0.08148	0.16300	0.0644
25.16	0.19540	0.05483	0.08911	0.17820	0.0644
29.00	0.17910	0.04767	0.09626	0.19250	0.0644
33.33	0.16990	0.04013	0.10380	0.20760	0.0644
39.16	0.14780	0.03072	0.11320	0.22640	0.0644
45.50	0.05273	0.02376	0.12020	0.24040	0.0644
0.00	0.28350	0.07115	0.00000	0.00000	0.0658
2.50	0.28450	0.06572	0.00603	0.01206	0.0658
5.83	0.28160	0.05553	0.01622	0.03244	0.0658
8.50	0.28250	0.04753	0.02422	0.04843	0.0658
11.75	0.22480	0.03927	0.03248	0.06497	0.0658
15.16	0.17020	0.03259	0.03917	0.07833	0.0658
20.50	0.13940	0.02466	0.04709	0.09418	0.0658
26.50	0.16810	0.01554	0.05622	0.11240	0.0658
32.75	0.10110	0.00586	0.06589	0.13180	0.0658
0.00	0.43000	0.35920	0.00000	0.00000	0.0420
1.75	0.42910	0.35180	0.00736	0.01472	0.0420

Time (t) (min)	Reaction Rate $(-dn/dt) \times 10^2$ mol. l ⁻¹ min ⁻¹	Conc. Of ONP (C _N) mol. l ⁻¹	Conc. Of OAP (C _A) mol. l ⁻¹	Conc. Of Water (C _W) mol. l ⁻¹	Conc. Of H ⁺ (C _H) mol. l ⁻¹
5.00	0.42650	0.33800	0.02119	0.04237	0.0420
7.16	0.42490	0.32880	0.03039	0.06078	0.0420
9.33	0.42090	0.31960	0.03957	0.07914	0.0420
11.16	0.41610	0.31200	0.04723	0.09446	0.0420
13.50	0.40840	0.30230	0.05688	0.11380	0.0420
15.50	0.40100	0.29420	0.06497	0.12990	0.0420
17.25	0.39400	0.28730	0.07193	0.14390	0.0420
19.25	0.38590	0.29750	0.07973	0.15950	0.0420
21.75	0.37580	0.27000	0.08925	0.17850	0.0420
24.00	0.36720	0.26160	0.09761	0.19520	0.0420
26.10	0.35970	0.25400	0.10520	0.21050	0.0420
28.25	0.35290	0.24630	0.11290	0.22580	0.0420
30.33	0.34720	0.23900	0.12020	0.24040	0.0420
32.50	0.34230	0.23150	0.12770	0.25530	0.0420
35.16	0.33790	0.22250	0.13670	0.27340	0.0420
37.50	0.33550	0.21460	0.14460	0.28920	0.0420
40.00	0.33440	0.20630	0.15290	0.30590	0.0420
42.00	0.33570	0.19180	0.16740	0.33490	0.0420
44.33	0.33760	0.18450	0.17470	0.34950	0.0420
46.50	0.34040	0.17600	0.18320	0.36640	0.0420
49.00	0.34410	0.16570	0.19350	0.38700	0.0420
52.00	0.34720	0.15620	0.20300	0.40600	0.0420
54.75	0.34920	0.13670	0.22250	0.44440	0.0420
60.33	0.34220	0.12140	0.23780	0.47560	0.0420
64.75	0.33260	0.11270	0.24650	0.49300	0.0420
70.75	0.31140	0.10170	0.25750	0.51510	0.0420
73.33	0.28750	0.09393	0.26530	0.53060	0.0420
77.00	0.23900	0.08421	0.27500	0.55000	0.0420
0.00	0.34000	0.36110	0.00000	0.00000	0.0320
4.00	0.34060	0.35010	0.01103	0.02206	0.0320
7.00	0.34090	0.34140	0.01969	0.03939	0.0320
9.25	0.34050	0.33470	0.02638	0.05277	0.0320
11.50	0.34010	0.32790	0.03321	0.06642	0.0320
13.75	0.34040	0.32090	0.04015	0.08030	0.0320
16.33	0.34030	0.31290	0.04823	0.09647	0.0320
19.50	0.32920	0.30280	0.05830	0.11660	0.0320
22.50	0.32120	0.29480	0.06630	0.13260	0.0320
24.33	0.32210	0.28730	0.07380	0.14760	0.0320
26.50	0.32220	0.28030	0.08079	0.16160	0.0320
29.50	0.32130	0.27070	0.09044	0.18090	0.0320
31.50	0.32000	0.26420	0.09686	0.19370	0.0320
34.00	0.31760	0.25630	0.10480	0.20970	0.0320
36.75	0.31420	0.24760	0.11350	0.22700	0.0320
39.50	0.30990	0.23900	0.12210	0.24420	0.0320
42.50	0.30440	0.22980	0.13130	0.26260	0.0320
45.50	0.29810	0.22070	0.14040	0.28070	0.0320
48.33	0.29140	0.21240	0.14870	0.29740	0.0320
51.00	0.28470	0.20470	0.15640	0.31280	0.0320
53.75	0.27740	0.19700	0.16410	0.32830	0.0320

Time (t) (min)	Reaction Rate $(-dn/dt) \times 10^2$ mol. l ⁻¹ min ⁻¹	Conc. Of ONP (C _N) mol. l ⁻¹	Conc. Of OAP (C _A) mol. l ⁻¹	Conc. Of Water (C _W) mol. l ⁻¹	Conc. Of H ⁺ (C _H) mol. l ⁻¹
64.00	0.24810	0.17000	0.19110	0.38210	0.0320
74.50	0.21950	0.14550	0.21560	0.43120	0.0320
76.66	0.21430	0.14080	0.22030	0.44050	0.0320
78.75	0.20970	0.13640	0.22470	0.44940	0.0320
85.50	0.19810	0.12270	0.23840	0.47690	0.0320
88.75	0.19470	0.11630	0.24480	0.48960	0.0320
0.00	0.32960	0.35830	0.00000	0.00000	0.0190
1.75	0.31950	0.35260	0.00578	0.01135	0.0190
4.50	0.30840	0.34400	0.01430	0.02859	0.0190
6.83	0.30290	0.33690	0.02141	0.04282	0.0190
10.75	0.30040	0.32510	0.03321	0.06642	0.0190
13.33	0.30230	0.31730	0.04098	0.08196	0.0190
15.50	0.30570	0.31070	0.04757	0.09515	0.0190
18.16	0.31140	0.30250	0.05578	0.11160	0.0190
22.75	0.32380	0.28800	0.07635	0.14070	0.0190
28.50	0.34060	0.26890	0.08946	0.17890	0.0190
42.16	0.36570	0.22030	0.13810	0.27610	0.0190
45.50	0.36590	0.20800	0.15030	0.30060	0.0190
48.60	0.36380	0.19670	0.16160	0.32320	0.0190
53.33	0.35600	0.17970	0.17860	0.35730	0.0190
58.00	0.34340	0.16330	0.19500	0.39000	0.0190
65.50	0.31550	0.13860	0.21970	0.43950	0.0190
70.50	0.29440	0.12330	0.23500	0.47000	0.0190
75.33	0.27500	0.10960	0.24870	0.49750	0.0190
82.50	0.25450	0.09060	0.26760	0.53530	0.0190
85.16	0.25140	0.08396	0.27440	0.54870	0.0190

APPENDIX-3.5.4

RATE DATA FOR THE HYDROGENATION OF *o*-NITROPHENOL AT 328 KCatalyst loading (w) = 0.3 g.l⁻¹, (-dn/dt = -dC/dt)

Time (t) (min)	Reaction Rate (-dn/dt) x 10 ² mol. l ⁻¹ min ⁻¹	Conc. Of ONP (C _N) mol. l ⁻¹	Conc. Of OAP (C _A) mol. l ⁻¹	Conc. Of Water (C _W) mol. l ⁻¹	Conc. Of H (C _H) mol. l ⁻¹
0.00	1.50100	0.35260	0.00000	0.00000	0.0540
0.53	1.42300	0.35490	0.00775	0.01549	0.0540
0.91	1.37100	0.33960	0.01305	0.02610	0.0540
1.50	1.29500	0.33170	0.02091	0.04183	0.0540
2.08	1.22800	0.32440	0.02823	0.05645	0.0540
2.75	1.15700	0.31640	0.03621	0.07242	0.0540
3.66	1.07200	0.30630	0.04634	0.09268	0.0540
4.50	1.00500	0.29760	0.05506	0.11010	0.0540
5.50	0.93800	0.28790	0.06476	0.12950	0.0540
6.50	0.88300	0.27880	0.07386	0.14770	0.0540
8.00	0.82000	0.26600	0.08661	0.17320	0.0540
9.33	0.78100	0.25540	0.09724	0.19450	0.0540
10.50	0.75680	0.24640	0.10620	0.21250	0.0540
11.50	0.74240	0.23890	0.11370	0.22740	0.0540
12.63	0.73160	0.23060	0.12200	0.24410	0.0540
13.58	0.72590	0.22370	0.12900	0.25790	0.0540
14.66	0.72230	0.21590	0.13680	0.27360	0.0540
15.16	0.72130	0.21230	0.14040	0.28080	0.0540
16.16	0.72020	0.20500	0.14760	0.29520	0.0540
17.50	0.71940	0.19540	0.15720	0.31450	0.0540
18.66	0.71830	0.18710	0.16560	0.33120	0.0540
20.08	0.71510	0.17690	0.17580	0.35150	0.0540
21.75	0.70700	0.16500	0.18760	0.37530	0.0540
23.66	0.69020	0.15160	0.20100	0.40200	0.0540
24.66	0.67770	0.14470	0.20780	0.41570	0.0540
25.56	0.66410	0.13880	0.21390	0.42780	0.0540
26.50	0.64760	0.13260	0.22000	0.44010	0.0540
27.66	0.62380	0.12520	0.22740	0.45490	0.0540
28.50	0.60450	0.12010	0.23260	0.46520	0.0540
31.25	0.53000	0.10440	0.24820	0.49640	0.0540
33.83	0.44970	0.09177	0.26090	0.52170	0.0540
35.58	0.39390	0.08439	0.26830	0.53650	0.0540
37.66	0.33190	0.07686	0.27580	0.55160	0.0540
40.50	0.26800	0.06842	0.28420	0.56850	0.0540
43.16	0.24850	0.06166	0.29910	0.58200	0.0540
46.50	0.31530	0.05259	0.30010	0.60010	0.0540
48.66	0.43560	0.04461	0.30800	0.61610	0.0540
50.50	0.60030	0.03517	0.31750	0.63490	0.0540
0.00	1.55900	0.25100	0.00000	0.00000	0.0640
0.08	1.54200	0.24730	0.00129	0.00257	0.0640

Time (t) (min)	Reaction Rate $(-dn/dt) \times 10^2$ mol. l ⁻¹ min ⁻¹	Conc. Of ONP (C _N) mol. l ⁻¹	Conc. Of OAP (C _A) mol. l ⁻¹	Conc. Of Water (C _W) mol. l ⁻¹	Conc. Of H ⁺ (C _H) mol. l ⁻¹
0.68	1.43100	0.23840	0.01016	0.02031	0.0640
1.52	1.29500	0.22700	0.02159	0.04318	0.0640
2.33	1.18400	0.21700	0.03162	0.06223	0.0640
3.08	1.09600	0.20840	0.04016	0.08032	0.0640
3.75	1.03000	0.20130	0.04728	0.09455	0.0640
4.50	0.96710	0.19380	0.05476	0.10950	0.0640
5.33	0.90990	0.18610	0.06254	0.12510	0.0640
6.33	0.85580	0.17720	0.07136	0.14270	0.0640
7.41	0.81230	0.16820	0.08035	0.16070	0.0640
8.66	0.77690	0.15830	0.09027	0.18050	0.0640
9.58	0.75840	0.15130	0.09733	0.19470	0.0640
10.66	0.74210	0.14320	0.10540	0.21090	0.0640
11.75	0.71820	0.12730	0.12130	0.24250	0.0640
14.00	0.70550	0.11900	0.12960	0.25920	0.0640
15.00	0.69280	0.11200	0.13660	0.27320	0.0640
17.66	0.64410	0.09418	0.15440	0.30880	0.0640
19.00	0.60930	0.08577	0.16280	0.32570	0.0640
20.50	0.56190	0.07698	0.17160	0.34320	0.0640
22.00	0.50670	0.06895	0.17960	0.35930	0.0640
23.91	0.42890	0.06001	0.18860	0.37720	0.0640
25.16	0.37680	0.05497	0.19360	0.38720	0.0640
28.16	0.26840	0.04539	0.20320	0.40640	0.0640
32.16	0.24360	0.03583	0.21280	0.42550	0.0640
33.83	0.31160	0.03128	0.21730	0.43460	0.0640
36.50	0.57180	0.01996	0.22860	0.45730	0.0640
0.00	1.35300	0.14300	0.00000	0.00000	0.0682
0.08	1.33800	0.13920	0.00112	0.00223	0.0682
0.78	1.22700	0.13020	0.01005	0.02010	0.0682
1.66	1.10300	0.12000	0.02029	0.04058	0.0682
2.50	1.00100	0.11120	0.02912	0.05824	0.0682
3.50	0.89790	0.10170	0.03860	0.07720	0.0682
4.33	0.82460	0.09454	0.04574	0.09148	0.0682
5.50	0.73790	0.08592	0.05486	0.10970	0.0682
6.56	0.67280	0.07795	0.06233	0.12470	0.0682
7.45	0.62620	0.07218	0.06811	0.13620	0.0682
9.33	0.54510	0.06120	0.07909	0.15820	0.0682
11.00	0.48510	0.05260	0.08768	0.17540	0.0682
12.75	0.42950	0.44600	0.09568	0.19140	0.0682
14.75	0.36470	0.03634	0.10390	0.20790	0.0682
17.50	0.27980	0.02773	0.11260	0.22510	0.0682
20.75	0.17960	0.02030	0.12000	0.24000	0.0682
25.75	0.10560	0.01387	0.12640	0.25280	0.0682
31.00	0.36630	0.00379	0.13650	0.27300	0.0682
0.00	0.80630	0.07200	0.00000	0.00000	0.0714
1.66	0.80410	0.05850	0.01355	0.02709	0.0714
1.83	0.79550	0.05714	0.01491	0.02981	0.0714
2.75	0.73030	0.05010	0.02195	0.04389	0.0714
4.33	0.57940	0.03972	0.03232	0.06465	0.0714
6.50	0.38780	0.02935	0.04270	0.08540	0.0714
8.16	0.30250	0.02370	0.04834	0.09668	0.0714

Time (t) (min)	Reaction Rate $(-dn/dt) \times 10^2$ $\text{mol. l}^{-1} \text{min}^{-1}$	Conc. Of ONP (C_N) mol. l^{-1}	Conc. Of OAP (C_A) mol. l^{-1}	Conc. Of Water (C_W) mol. l^{-1}	Conc. Of H (C_H) mol. l^{-1}
15.70	0.04651	0.05921	0.06612	0.13220	0.0714
0.00	0.83460	0.35910	0.00000	0.00000	0.0420
0.83	0.78000	0.35240	0.00670	0.01339	0.0420
1.83	0.72220	0.34490	0.01420	0.02840	0.0420
3.00	0.66470	0.33680	0.02230	0.04461	0.0420
4.16	0.61750	0.32940	0.02973	0.05946	0.0420
5.83	0.56480	0.31950	0.03958	0.07916	0.0420
7.50	0.52770	0.31040	0.04868	0.09736	0.0420
9.21	0.50330	0.30160	0.05748	0.11500	0.0420
10.75	0.49090	0.29400	0.06512	0.13020	0.0420
12.33	0.48580	0.28630	0.07283	0.14570	0.0420
13.45	0.48590	0.28090	0.07827	0.15650	0.0420
15.33	0.49140	0.27170	0.08745	0.17490	0.0420
16.75	0.49850	0.26470	0.09447	0.18890	0.0420
18.25	0.50780	0.25710	0.10200	0.20400	0.0420
19.75	0.51770	0.24940	0.10970	0.21940	0.0420
21.50	0.52900	0.24030	0.11890	0.23770	0.0420
23.03	0.53770	0.23210	0.12700	0.25410	0.0420
24.66	0.54490	0.22330	0.13590	0.27170	0.0420
26.16	0.54910	0.21510	0.14410	0.28810	0.0420
27.75	0.55040	0.20630	0.15280	0.30560	0.0420
29.20	0.54860	0.19830	0.16080	0.32160	0.0420
30.91	0.54240	0.18900	0.17010	0.34020	0.0420
32.83	0.53020	0.17870	0.18040	0.36090	0.0420
38.25	0.46780	0.15150	0.20760	0.41530	0.0420
40.16	0.43810	0.14280	0.21630	0.43260	0.0420
43.66	0.37920	0.12850	0.23060	0.46120	0.0420
46.11	0.33910	0.11970	0.23940	0.47880	0.0420
48.83	0.30180	0.11100	0.24810	0.49620	0.0420
52.83	0.27630	0.09962	0.25950	0.51900	0.0420
54.75	0.28350	0.09428	0.26490	0.52970	0.0420
56.50	0.30510	0.08915	0.27000	0.54000	0.0420
59.75	0.39880	0.07798	0.28110	0.56230	0.0420
62.75	0.54680	0.06407	0.29510	0.59010	0.0420
63.75	0.61620	0.05826	0.30090	0.60170	0.0420
0.00	0.39180	0.35990	0.00000	0.00000	0.0310
2.33	0.35650	0.35120	0.00869	0.01737	0.0310
4.50	0.33670	0.34370	0.01619	0.03237	0.0310
6.30	0.32810	0.33780	0.02216	0.04432	0.0310
9.33	0.32560	0.32790	0.03203	0.06406	0.0310
12.16	0.33270	0.31860	0.04133	0.08266	0.0310
14.33	0.34160	0.31130	0.04864	0.09728	0.0310
16.75	0.35300	0.30290	0.05704	0.11410	0.0310
18.83	0.36260	0.29540	0.06449	0.12900	0.0310
20.75	0.37060	0.28840	0.07153	0.14310	0.0310
22.75	0.37710	0.28090	0.07901	0.15800	0.0310
25.00	0.38170	0.27240	0.08755	0.17510	0.0310
27.00	0.38280	0.26470	0.09520	0.19040	0.0310
29.50	0.38000	0.25520	0.10470	0.20950	0.0310

Time (t) (min)	Reaction Rate $(-dn/dt) \times 10^2$ mol. l ⁻¹ min ⁻¹	Conc. Of ONP (C _N) mol. l ⁻¹	Conc. Of OAP (C _A) mol. l ⁻¹	Conc. Of Water (C _W) mol. l ⁻¹	Conc. Of H (C _H) mol. l ⁻¹
33.75	0.36440	0.23930	0.12060	0.24120	0.0310
36.16	0.35000	0.23070	0.12920	0.25850	0.0310
38.50	0.33310	0.22270	0.13720	0.27440	0.0310
41.00	0.31300	0.21460	0.14530	0.29060	0.0310
43.00	0.29650	0.20850	0.15140	0.30280	0.0310
46.30	0.27120	0.19920	0.16080	0.32150	0.0310
49.75	0.25270	0.19020	0.16980	0.33950	0.0310
52.50	0.24870	0.18330	0.17660	0.35330	0.0310
55.50	0.26070	0.17570	0.18420	0.36840	0.0310
58.75	0.30050	0.16670	0.19330	0.38650	0.0310
0.00	0.31020	0.36010	0.00000	0.00000	0.0190
2.75	0.28270	0.35180	0.00826	0.01652	0.0190
5.75	0.25150	0.34380	0.01625	0.03250	0.0190
9.50	0.22330	0.33500	0.02512	0.05024	0.0190
13.00	0.20610	0.32750	0.03261	0.06522	0.0190
16.00	0.19690	0.32140	0.03865	0.07729	0.0190
21.50	0.19050	0.31080	0.04925	0.09849	0.0190
25.75	0.19190	0.30270	0.05736	0.11470	0.0190
29.33	0.19570	0.29580	0.06429	0.12860	0.0190
32.75	0.20050	0.28900	0.07106	0.14210	0.0190
37.00	0.20690	0.28040	0.07972	0.15940	0.0190
41.00	0.21230	0.27200	0.08810	0.17620	0.0190
45.00	0.21630	0.26340	0.09668	0.19340	0.0190
48.50	0.21830	0.25580	0.10430	0.20860	0.0190
52.00	0.21860	0.24810	0.11190	0.22390	0.0190
56.23	0.21650	0.23890	0.12120	0.24230	0.0190
60.50	0.21200	0.22980	0.13030	0.26060	0.0190
64.50	0.20590	0.22140	0.13870	0.27740	0.0190
68.50	0.19870	0.21330	0.14680	0.29350	0.0190
71.50	0.19310	0.20740	0.15270	0.30530	0.0190
76.33	0.18490	0.19830	0.16180	0.32350	0.0190
78.75	0.18190	0.19390	0.16620	0.33240	0.0190
82.50	0.17950	0.18710	0.17300	0.34590	0.0190
92.70	0.19770	0.16860	0.19150	0.38290	0.0190
95.53	0.21400	0.16240	0.19770	0.39540	0.0190
100.50	0.25610	0.15080	0.20930	0.41850	0.0190

APPENDIX-3.5.5

COEFFICIENTS OF THE POLYNOMIAL EQUATION = $C_N = A_1 + A_2t + A_3t^2 + A_4t^3 + A_5t^4 + A_6t^5$
 FITTED TO THE KINETIC DATA FOR THE HYDROGENATION AT DIFFERENT TEMPERATURES

P _{H₂} (kPa)	Conc. of ONP, C _N (mol.l ⁻¹)	Conc. of H ₂ , C _H (mol.l ⁻¹)	Coefficients of the polynomial equation (Eqn. 2)					
			A ₁	A ₂	A ₃	A ₄	A ₅	A ₆
1	2	3	4	5	6	7	8	9
<u>Temperature 293 K (w = 0.5 g.dm⁻³)</u>								
1463	0.360	0.0511	0.3615	-0.2873E-02	0.2888E-04	-0.3330E-06	0.2354E-08	-0.7853E-11
1050	0.360	0.036	0.3600	-0.2155E-02	0.5992E-04	-0.1615E-05	0.1706E-07	-0.6148E-10
776	0.360	0.027	0.3599	-0.1151E-02	0.2632E-04	0.8787E-06	-0.1246E-07	0.6097E-10
500	0.360	0.017	0.3597	-0.1929E-02	0.4015E-04	-0.7538E-06	0.6846E-08	-0.2413E-10
1463	0.250	0.0512	0.2523	-0.2363E-02	0.6540E-05	0.2677E-08	0.8142E-09	-0.8750E-11
1463	0.144	0.0523	0.1442	-0.2196E-02	-0.1401E-04	0.1473E-05	-0.3077E-07	0.2142E-09
1463	0.072	0.0526	0.0718	-0.9471E-04	-0.1200E-03	0.4278E-05	-0.5928E-07	0.2777E-09
<u>Temperature 308 K (w = 0.5 g.dm³)</u>								
1035	0.360	0.039	0.3613	-0.5649E-02	0.8444E-04	-0.1961E-05	0.2202E-07	-0.8596E-10
760	0.360	0.029	0.3586	-0.3648E-02	0.3275E-04	-0.2985E-06	-0.2386E-08	0.3295E-10
486	0.360	0.018	0.3594	-0.2886E-02	0.1650E-04	-0.1798E-06	-0.7799E-09	0.1530E-10

Appendix-3.5.5 contd.

1	2	3	4	5	6	7	8	9
1448	0.251	0.0564	0.2529	-0.5635E-02	0.7512E-04	-0.1787E-05	0.3581E-07	-0.2646E-09
1448	0.149	0.0572	0.1490	-0.1349E-02	-0.2150E-03	0.1005E-04	-0.1811E-06	0.1172E-08
1448	0.072	0.0579	0.0720	-0.8033E-03	-0.3542E-03	0.2931E-04	-0.9661E-06	0.1128E-07
<u>Temperature 318 K (w = 0.3 g.dm⁻³)</u>								
1432	0.360	0.0587	0.3585	-0.5795E-02	0.2470E-04	0.2623E-06	-0.6610E-08	0.4318E-10
1019	0.360	0.042	0.3592	-0.4177E-02	-0.1946E-04	0.1602E-05	-0.2905E-07	0.1669E-09
744	0.367	0.030	0.3611	-0.2673E-02	-0.2228E-04	0.3205E-06	-0.3829E-09	-0.5869E-11
469	0.360	0.019						
1432	0.251	0.0615	0.2467	-0.5816E-02	0.8915E-04	-0.3459E-06	-0.2235E-07	0.1778E-09
1432	0.143	0.0644	0.1439	-0.5214E-02	0.1553E-04	0.5130E-05	-0.1612E-06	0.1501E-08
1432	0.072	0.0658	0.0718	-0.1835E-02	-0.2946E-03	0.2763E-04	-0.9119E-06	0.1032E-07

.....

Appendix-3.5.5 contd.

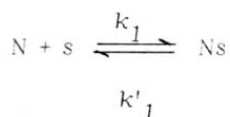
----- 1 ----- 2 ----- 3 ----- 4 ----- 5 ----- 6 ----- 7 ----- 8 ----- 9 -----

Temperature 328 K ($w = 0.3 \text{ g.dm}^{-3}$)

1407	0.36	0.059	0.3526	-0.1501E-01	0.7613E-03	-0.3577E-04	0.7897E-06	-0.6182E-08
995	0.36	0.042	0.3591	-0.8346E-02	0.3475E-03	-0.1542E-04	0.2888E-06	-0.1857E-08
720	0.36	0.031	0.3599	-0.3918E-02	0.9382E-04	-0.5509E-05	0.1170E-06	-0.8051E-09
445	0.36	0.019	0.3601	-0.3192E-02	0.7379E-04	-0.1886E-05	0.2045E-07	-0.7864E-10
1407	0.251	0.0640	0.2486	0.1559E-01	0.9982E-03	-0.6087E-04	0.1843E-05	-0.2008E-07
1407	0.143	0.0682	0.1403	-0.1353E-01	0.8586E-03	-0.4648E-04	0.1518E-05	-0.1956E-07
1407	0.072	0.0714	0.0720	-0.7963E-02	-0.3426E-03	0.1552E-03	-0.1293E-04	0.3443E-06

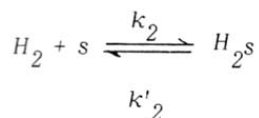
APPENDIX-3.5.6DERIVATION OF H-W MODEL FOR THE HYDROGENATION OF o-NITROPHENOL

For the single site adsorption and molecularly adsorbed reaction species, the elementary reaction steps involved in the overall hydrogenation reaction are as follows:

Adsorption of ONP controlling

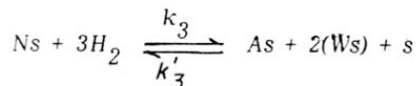
$$r_1 = k_1 (C_N \theta_V - \theta_N / K_N) \quad (1)$$

$$(K_N = k_1/k'_1)$$

Adsorption of H₂ controlling

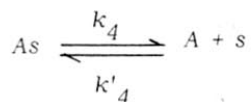
$$r_2 = k_2 (C_H \theta_V - \theta_H / K_{H_2}) \quad (2)$$

$$(K_{H_2} = k_2/k'_2)$$

Surface reaction controlling

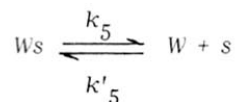
$$r_3 = k_3 [\theta_N \theta_H^3 - k'_3 \theta_A \theta_W^2 \theta_V / K] \quad (3)$$

$$K = \frac{k_3}{k'_3}$$

Desorption of o-aminophenol controlling

$$r_4 = k_4 (\theta_A / K_A - C_A \theta_V) \quad (4)$$

$$K_A = \frac{k_4}{k'_4}$$

Desorption of water controlling

$$r_5 = k_5 (\theta_W / K_W - C_W \theta_V) \quad (5)$$

$$K_W = \frac{k_5}{k'_5}$$

where, θ_V is the fraction of active sites unoccupied

$$(i.e. \theta_V = (1 - \theta_N - \theta_H - \theta_A - \theta_W))$$

for the case of surface reaction controlling,

$$r_1 = r_2 = r_4 = r_5 = 0 \quad (6)$$

because of the steps other than surface reaction are assumed to be in equilibrium. From the equilibrium steps the values of θ_N , θ_H , θ_A and θ_W are as follows.

$$\theta_N = K_N C_N \theta_V \quad (7)$$

$$\theta_H = K_{H_2} C_H \theta_V \quad (8)$$

$$\theta_A = K_A C_A \theta_V \quad (9)$$

$$\theta_W = k_W C_W \theta_V \quad (10)$$

$$\theta_V = \frac{1}{(1 + K_N C_N + K_H C_H + K_A C_A + K_W C_W)} \quad (11)$$

Substituting these values in Eqn. 3, we get,

$$r_3 = k_3 [K_N C_N \theta_V (K_{H_2} C_{H_2} \theta_V)^3 - K_A C_A \theta_V (K_W C_W \theta_V)^2 \theta_V / K]$$

Since, the equilibrium constant (K) for the reaction is very high ($K=1.4 \times 10^{73}$), the above rate expression reduces to,

$$r = k_3 (K_N K_{H_2}^3 C_N C_{H_2}^3) \theta_V^4$$

or

$$r = \frac{k_3 K_N K_{H_2}^3 C_N C_{H_2}^3}{(1 + K_N C_N + K_{H_2} C_{H_2} + K_A C_A + K_W C_W)^4}$$

```
C      THIS IS AN OPTIMIZATION PROGRAMME USING MARQUARDT'S ALGORITHM
      DIMENSION P(1000), A(10,10), AC(10,10), X1(200), X2(200)
      DIMENSION B(10), Z(200), Y(200), BV(10), BMIN(10), BMAX(10), X3(200)
      DIMENSION X4(200)
      EXTERNAL FUNC
      COMMON X1, X2, X3, X4
      CHARACTER ASS*25
1      TYPE*, 'GIVE ME DATAFILE NAME'
      ACCEPT 112, ASS
112     FORMAT(A25)
C      KK IS THE NO OF UNKNOWNNS
      KK=5
C      READ IN WEIGHT OF THE CATALYST AND NO OF DATA POINTS
      OPEN(UNIT=2, FILE=ASS, STATUS='OLD')
      READ(2, *) WCAT, NN
      DO 111 I=1, NN
C      READS DATA FROM A FILE AND CONVERTS TO PROPER UNITS
      READ(2, *) Y(I), X2(I), X3(I), X4(I), X1(I)
111     Y(I)=Y(I)*0.01/WCAT
      CLOSE(2)
C      READ IN INITIAL GUESSES, MINIMUM AND MAXIMUM LIMITS
      OPEN(UNIT=2, FILE='P2.DAT', STATUS='OLD')
      READ(2, *) (B(J), J=1, KK)
      READ(2, *) (BMIN(J), J=1, KK)
      READ(2, *) (BMAX(J), J=1, KK)
      CLOSE(2)
C      OPENS FILE FOR HARD COPY
      OPEN(UNIT=2, FILE='SANE10.RES', STATUS='NEW')
      WRITE(2, *) 'NN, KK', NN, KK
      WRITE(2, *) 'B(J)', (B(J), J=1, KK)
      WRITE(2, *) 'BMIN(J)', (BMIN(J), J=1, KK)
      WRITE(2, *) 'BMAX(J)', (BMAX(J), J=1, KK)
      FNU=0.0
      FLA=0.0
      TAU=0.0
      EPS=0.0
      PHMIN=0.0
      I=0
      KD=KK
      FV=0.0
      DO 100 J=1, KK
100     BV(J)=1.
      CONTINUE
      ICON=KK
      ITER=0
200     WRITE(2, *) 'BSOLVE REGRESSION ALGORITHM'
      CALL BSOLVE(KK, B, NN, Z, Y, PH, FNU, FLA, TAU, EPS
/      , PHMIN, I, ICON, FV, DV, BV, BMIN, BMAX, P, FUNC,
/      DERIV, KD, A, AC, GAMM)
      ITER=ITER+1
      IF (ICON) 10, 300, 200
10     IF (ICON+1) 20, 60, 200
20     IF (ICON+2) 30, 70, 200
30     IF (ICON+3) 40, 80, 200
40     IF (ICON+4) 50, 90, 200
```



```

50      GO TO 95
60      WRITE(2,*) 'NO FUNCTION IMPROVEMENT POSSIBLE'
        GO TO 300
70      WRITE(2,*) 'MORE UNKNOWN THAN FUNCTION'
        GO TO 300
80      WRITE(2,*) 'TOTAL VARIABLE ARE ZERO'
        GO TO 300
90      WRITE(2,*) 'CORRECTIONS SATISFY CONVERGENCE REQUIREMENTS BUT
/      LAMDA FACTOR(FLA) STILL LARGE'
        GO TO 300
95      WRITE(2,*) 'THIS IS NOT POSSIBLE'
        GO TO 300
300     WRITE(2,*) ' SOLUTIONS OF THE EQUATIONS(COEFFICIENTS)'
        WRITE(2,*) '-----00-----'
        DO 400 J=1, KK
        WRITE(2,*) J, B(J)
        WRITE(2,*) '-----00-----'
        WRITE(2,*) 'H2 CONCENTRATION=', CH, 'WT OF THE CATALYST=', WCAT
        WRITE(2,*) 'NO OF POINTS=', NN
        GO TO 1
1000    STOP
        END

SUBROUTINE FUNC (KK, B, NN, Z, FV)
DIMENSION X1(200), X2(200), X3(200), X4(200), Z(200), B(10)
COMMON X1, X2, X3, X4
DO 100 JJ=1, NN
Z1=B(1)*X2(JJ)*X1(JJ)**3.
Z2=1.+(B(2)*X2(JJ)+(B(3)*X1(JJ)+(B(4)*X3(JJ)+B(5)*X4(JJ))
Z(JJ)=Z1/(Z2**4.)
100    CONTINUE
        RETURN
        END

SUBROUTINE BSOLVE(KK, B, NN, Z, Y, PH, FNU, FLA, TAU, EPS, PHMIN
/      , I, ICON, FV, DV, BV, BMIN, BMAX, P, FUNC, DERIV, KD, A, AC, GAMM)
DIMENSION B(10), Z(200), Y(200), BV(10), BMIN(10), BMAX(10)
DIMENSION P(1000), A(10,10), AC(10,10), X(200), FV(10), DV(10)
K=KK
N=NN
KP1=K+1
KP2=KP1+1
KBI1=K*N
KBI2=KBI1+K
KZI=KBI2+K
IF(FNU .LE. 0.) FNU=10.
IF(FLA .LE. 0) FLA=0.01
IF(TAU .LE. 0.) TAU=0.001
IF(EPS .LE. 0) EPS=0.00002
IF(PHMIN .LE. 0.) PHMIN=0.
120    KE=0
130    DO 160 I1=1, K
140    IF( BV(I1) .NE. 0.) KE=KE+1
        IF(KE .GT. 0) GO TO 170
162    ICON=-3

```

```

163 GO TO 2120
170 IF (N .GE. KE) GO TO 500
180 ICON=-2
190 GO TO 2120
500 I1=1
530 IF ( I .GT.0) GO TO 1530
550 DO 560 J1=1,K
      J2=KBI1+J1
      P(J2) = B(J1)
      J3=KBI2+J1
560 P(J3)=ABS(B(J1))+ 1.0E-02
      GO TO 1030
590 IF ( PHMIN .GT.PH .AND. I.GT.1) GO TO 625
      DO 620 J1=1,K
      N1=(J1-1)*N
      IF ( BV(J1)) 601,620,605
601 CALL DERIV (K,B,N,Z,P(N1+1),FV,DV,J1,JTEST)
      IF (JTEST .NE. (-1)) GO TO 620
      BV(J1)=1.0
605 DO 606 J2=1,K
      J3=KBI1+J2
606 P(J3)=B(J2)
      J3=KBI1+J1
      J4=KBI2+J1
      DEN=0.001*AMAX1(P(J4),ABS(P(J3)))
      IF (P(J3) +DEN .LE. BMAX(J1)) GO TO 55
          P(J3)=P(J3)-DEN
          DEN=-DEN
      GO TO 56
55 P(J3)=P(J3)+DEN
56 CALL FUNC (K,P(KBI1+1),N,P(N1+1),FV)
      DO 610 J2=1,N
      JB=J2+N1
610 P(JB) =(P(JB)- Z(J2))/DEN
620 CONTINUE
C SET UP CORRECTION EQUATIONS
625 DO 725 J1=1,K
      N1=(J1-1)*N
      A(J1,KP1)=0.
      IF (BV(J1)) 630,692,630
630 DO 640 J2=1,N
      N2=N1+J2
640 A(J1,KP1)=A(J1,KP1)
      + P(N2)*(Y(J2)-Z(J2))
650 DO 680 J2=1,K
660 A(J1,J2)=0.0
665 N2=(J2-1)*N
670 DO 680 J3=1,N
672 N3=N1+J3
674 N4=N2+J3
680 A(J1,J2)=A(J1,J2)+P(N3)*P(N4)
      IF(A(J1,J1) .GT. 1.E-20) GO TO 725
692 DO 694 J2=1,KP1
694 A(J1,J2)=0.0
695 A(J1,J1)=1.0

```

```

725   CONTINUE
      GN=0.
      DO 729 J1=1,K
729   GN=GN+A(J1,KP1)**2.
C     SCALE CORRECTION EQUATIONS
      DO 726 J1=1,K
726   A(J1,KP2)=SQRT(A(J1,J1))
      DO 727 J1=1,K
      A(J1,KP1) = A(J1,KP1)/A(J1,KP2)
      DO 727 J2 =1,K
727   A(J1,J2)= A(J1,J2)/(A(J1,KP2)*A(J2,KP2))
730   FL=FLA/FNU
      GO TO 810
800   FL=FNU*FL
810   DO 840 J1=1,K
820   DO 830 J2=1,KP1
830   AC(J1,J2)=A(J1,J2)
840   AC(J1,J1)=AC(J1,J1) +FL
C     SOLVE CORRECTION EQUATIONS
      DO 930 L1=1,K
      L2=L1+1
      DO 910 L3=L2,KP1
910   AC(L1,L3)=AC(L1,L3)/AC(L1,L1)
      DO 930 L3=1,K
      IF (L1-L3) 920,930,920
920   DO 925 L4=L2,KP1
925   AC(L3,L4)=AC(L3,L4)-AC(L1,L4)*AC(L3,L1)
930   CONTINUE
      DN=0.
      DG=0.0
      DO 1028 J1=1,K
      AC(J1,KP2)= AC(J1,KP1)/A(J1,KP2)
      J2=KBI1+J1
      P(J2)=AMAX1(BMIN(J1),AMIN1(BMAX(J1),B(J1)+AC(J1,KP2)))
      DG=DG+AC(J1,KP2)*A(J1,KP1)*A(J1,KP2)
      DN=DN+AC(J1,KP2)*AC(J1,KP2)
1028  AC(J1,KP2)=P(J2)-B(J1)
      COSG=DG/SQRT(DN*GN)
      JGAM=0
      IF (COSG) 1100,1110,1110
1100  JGAM=2
      COSG=-COSG
1110  CONTINUE
      COSG=AMIN1(COSG,1.0)
      GAMM=ARCCOS(COSG)*180./(3.14159265)
      IF (JGAM .GT.0) GAMM=180.-GAMM
1030  CALL FUNC (K,P(KBI1+1),N,P(KZI+1),FV)
1500  PHI=0.
      DO 1520 J1=1,N
      J2=KZI+J1
1520  PHI=PHI+(P(J2)-Y(J1))**2.
      IF (PHI .LT.1.E-10) GO TO 3000
      IF (I .GT. 0) GO TO 1540
1521  ICON=K
      GO TO 2110

```

```

1540 IF(PHI .GE. PH) GO TO 1530
C   EPSILON TEST
1200 ICON=0
      DO 1220 J1=1,K
      J2=KBI1+J1
1220 IF (ABS(AC(J1,KP2))/(TAU+ABS
/   (P(J2))) .GT. EPS )ICON=ICON+1
      IF(ICON .EQ. 0) GO TO 1400
C   GAMMA LAMBDA TEST
      IF(FL .GT. 1.0 .AND. GAMM .GT. 90.00)ICON=-1
      GO TO 2105
C   GAMMA EPSILON TEST
1400 IF(FL .GT. 1.0 .AND. GAMM .LE. 45.0) ICON=-4
      GO TO 2105
1530 IF(I1-2) 1531,1531,2310
1531 I1=I1+1
      GO TO (530,590,800),I1
2310 IF (FL .LT. 1.E+8) GO TO 800
1320 ICON=-1
2105 FLA=FL
      DO 2091 J2=1,K
      J3=KBI1+J2
2091 B(J2)=P(J3)
2110 DO 2050 J2=1,N
      J3=KZI+J2
2050 Z(J2)=P(J3)
      PH=PHI
      I=I+1
2120 RETURN
3000 ICON=0
      GO TO 2105
      END

```

```

FUNCTION ARCOS(Z)
X=Z
KEY=0
IF(X .LT. (-1.)) X=-1.
IF(X .GT. 1.) X=1.
IF(X .GE. (-1.) .AND. X .LT. 0.) KEY=1
IF(X .LT. 0.) X=ABS(X)
IF(X .EQ. 0.) GO TO 10
ARCOS=ATAN (SQRT(1.-X*X)/X)
IF( KEY .EQ.1) ARCOS=3.14159265-ARCOS
GO TO 999
10  ARCOS=1.5707963
999  RETURN
      END

```

APPENDIX-3.6.J

EXPERIMENTAL DATA FOR THE POISONING OF Pd-CARBON IN THE HYDROGENATION OF o-NITROPHENOL

Reaction conditions

Reaction medium	:	methanol
Initial concentration of o-nitrophenol	:	0.36 mol.dm ⁻³
Reaction temperature	:	308 K
Stirring speed	:	980 rpm
Volume of reaction mixture	:	1.0 dm ³
Catalyst loading	:	0.5 g.dm ⁻³
H ₂ -pressure	:	1508 kPa
Reaction time	:	1.0 hr

Poison	Concn. of poison (g.m ⁻³)	Time t (min) required for the conversion of o-nitrophenol												
		3	4	5	6	7	8	9	10	11	12	13		
Without poison	-	2.10	4.75	7.50	10.50	13.66	17.83	23.50	30.50	39.50	49.0	60		
Thiophene	5	2.16	4.83	9.00	13.50	19.16	24.83	29.66	34.26	42.50	53.93	-		
	20	2.66	4.90	10.66	15.10	19.92	26.75	34.65	49.95	63.00	-			
	100	3.33	6.50	11.08	15.50	20.33	27.00	46.13	52.75	66.00	-			
	5000	4.20	8.06	12.00	17.00	22.80	29.92	48.10	57.75	-				
Mercuric acetate	10	2.66	5.16	7.75	11.56	14.73	20.50	26.50	37.00	51.30	-			
	25	4.50	12.00	19.50	26.03	32.83	40.33	49.00	55.20	-				
	50	7.23	15.66	25.36	37.73	50.66	60.00	-	-	-				

Appendix-3.6.1 contd..

1	2	3	4	5	6	7	8	9	10	11	12	13
Lead acetate	150	2.25	4.93	8.00	12.58	19.25	25.90	34.61	45.55	55.58	-	-
	500	3.18	6.06	10.63	16.50	24.00	32.00	42.00	53.33	-	-	-
	1000	3.28	6.33	10.83	17.45	25.00	33.16	45.00	55.50	-	-	-
	5000	6.16	11.18	17.33	24.48	31.00	40.33	52.50	-	-	-	-
Zinc acetate	20	2.18	4.75	7.50	11.38	16.10	20.63	27.00	34.03	42.98	-	-
	100	2.25	4.98	8.36	15.30	24.33	36.08	49.12	60.00	-	-	-
	500	2.33	5.30	9.33	16.30	25.66	38.00	51.00	-	-	-	-
	1000	2.35	5.45	10.00	17.01	26.10	41.00	55.00	-	-	-	-
	5000	6.83	12.40	19.58	28.83	44.73	60.00	-	-	-	-	-
Mercuric chloride	20	2.25	5.03	8.75	14.66	19.83	24.95	34.58	44.33	56.72	-	-
	100	2.75	6.16	11.11	17.42	25.33	34.50	49.66	59.3	-	-	-
	500	7.95	16.10	25.66	43.66	57.00	-	-	-	-	-	-
Dichloro ethane	100	2.36	5.06	8.25	13.83	20.20	26.68	34.50	44.25	55.50	-	-
	1000	5.00	11.33	18.66	25.45	33.66	41.92	51.00	-	-	-	-
	5000	5.50	12.33	19.16	26.66	34.75	43.00	52.33	-	-	-	-